FAKULTA STAVEBNÍ ČVUT V PRAZE

DIPLOMOVÁ PRÁCE

Návrh zavěšeného mostu přes Vltavu v Praze z Hlediska postupu výstavby

Design of a cable-stayed bridge over Vltava River in Prague with respect to construction stages.

Vypracoval:	*Bc. Yazan Amri*
Studijní program:	*Stavební inženýrství*
Studijní obor:	*Konstrukce a dopravní stavby*
Vedoucí diplomové práce:	*Ing. Michal Drahorád, Ph. D*

Praha, 2022

ČESKÉ VYSOKÉ UČENÍ TECHNICKÉ V PRAZE
Fakulta stavební
Thákurova 7, 166 29 Praha 6

ZADÁNÍ DIPLOMOVÉ PRÁCE

I. OSOBNÍ A STUDIJNÍ ÚDAJE

Příjmení: Amri Jméno: Yazan Osobní číslo: 494154

Zadávající katedra: K133 - Katedra betonových a zděných konstrukcí

Studijní program: Stavební inženýrství

Studijní obor: Konstrukce a dopravní stavby

II. ÚDAJE K DIPLOMOVÉ PRÁCI

Název diplomové práce: Návrh zavěšeného mostu přes Vltavu v Praze z hlediska postupu výstavby

Název diplomové práce anglicky: Design of cable stayed bridge over Vltava river in Prague with respect to construction sequence

Pokyny pro vypracování:
- Předběžný návrh nosné konstrukce mostu a spodní stavby v definitivním stavu
- Podrobná analýza postupu výstavby

Seznam doporučené literatury:

Jméno vedoucího diplomové práce: Michal Drahorád

Datum zadání diplomové práce: 24. 9. 2021 Termín odevzdání diplomové práce: 3. 1. 2022

Údaj uveďte v souladu s datem v časovém plánu příslušného ak. roku

Podpis vedoucího práce Podpis vedoucího katedry

III. PŘEVZETÍ ZADÁNÍ

Beru na vědomí, že jsem povinen vypracovat diplomovou práci samostatně, bez cizí pomoci, s výjimkou poskytnutých konzultací. Seznam použité literatury, jiných pramenů a jmen konzultantů je nutné uvést v diplomové práci a při citování postupovat v souladu s metodickou příručkou ČVUT „Jak psát vysokoškolské závěrečné práce" a metodickým pokynem ČVUT „O dodržování etických principů při přípravě vysokoškolských závěrečných prací".

Datum převzetí zadání Podpis studenta(ky)

Čestné prohlášení

Prohlašuji, že jsem předloženou práci vypracoval samostatně a že jsem uvedl veškeré použité informační zdroje v souladu s Metodickým pokynem o etické přípravě vysokoškolských závěrečných prací.

……

Yazan Amri

V Praze dne

Abstract

This thesis deals with the design of a proposed bridge over the Vltava and will connect the two-city sides, the bridge will carry two tram tracks and two pedestrian lanes. The proposal is a three-span cable-stayed bridge. The superstructure has been designed at the serviceability and ultimate limit states.

Key words

Tramway bridge, cable-stayed bridge, bridge design, concrete structure, prestressed concrete, time-dependent analysis

---

Anotace

Tato práce se zabývá návrhem mostu přes Vltavu a propojí obě městské strany, most ponese dvě tramvajové koleje a dva pruhy pro pěší. Návrh je třípolový zavěšený most. Nosná konstrukce je navržena v mezních stavech použitelnosti a únosnosti.

Klíčová slova

Tramvajový most, zavěšený most, návrh mostu, betonová konstrukce, předpjatý beton, časově závislá analýza

Special Thanks

At the beginning I would like to thank the supervise of my master thesis Ing. Michal Drahorád, Ph.D. for the priceless support, advises and special kindness

Contents

1 Introduction

This work deals with the analysis and design of a proposed cable-stayed bridge (Dvorecký most v Praze) with respect to construction stages, a detailed design for bridge deck regarding construction stage analysis, and preliminary design of pylon, pier, and pier cap will be considered in this thesis.

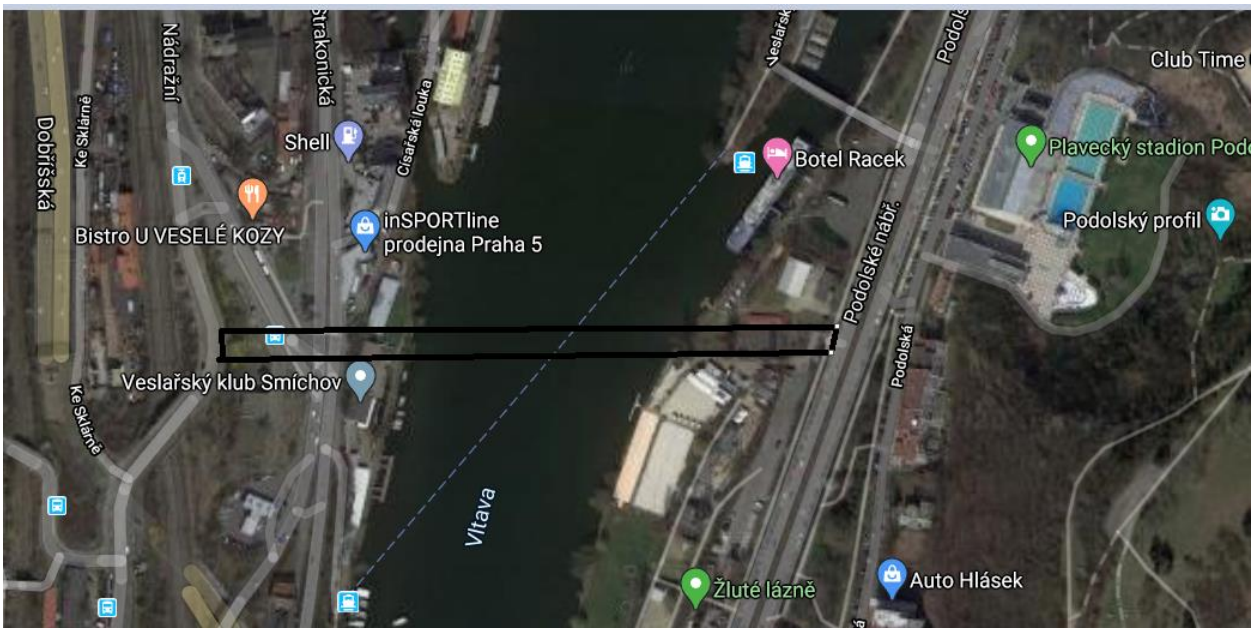

1.1 Bridge parameter Bridge design restraint

Bridge span: 360 m

Pedestrian and bicycle lane must be on a bridge

The bridge has been designed for tramway operation

1.2 Bridge design restraint

The width of the navigation area is 80 m

The height of the navigation area is 7,0 m

The maximum navigation level is 188.40 m

The flood level Q2002 is 193.05

2 Cable-stayed bridge

2.1 Main parts

A typical cable-stayed bridge, as shown in Figures 1, consists of a continuous girder, stay cables, two pylons, and two end piers. The span between two pylons is called the main span. The main span length is a key design parameter of cable-stayed bridges. [1]

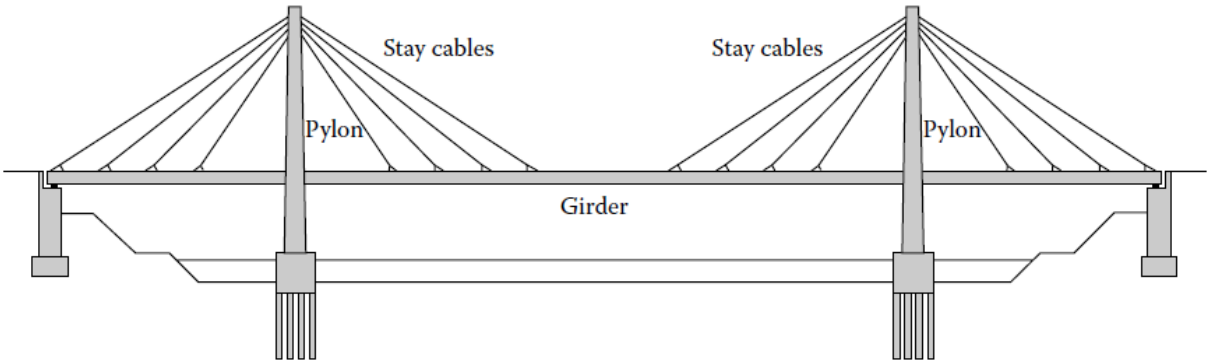

Figure 1 Main parts of cable-stayed bridge

2.2 Cable arrangements

2.2.1 Layout in the Longitudinal Direction

Cable-stayed bridges have at least one forestay and one backstay cable per tower. The forestays act like two piers omitted in the main span.

There are three basic cable arrangements in bridge elevation. With the fan arrangement, all cables join at the tower head. With the harp arrangement, all cables run parallel and are anchored over the height of the tower. The true fan arrangement cannot be realized practically. [1]
In such way an intermediate cable arrangement between harp and fan is created, which should be as close as possible to the fan arrangement due to its economic advantages. The harp arrangement, however, is aesthetically advantageous because there are no visual intersections of the stay cables, even for two cable planes in a skew view. [1]
The cable-stay layouts are shown in the figure 2.

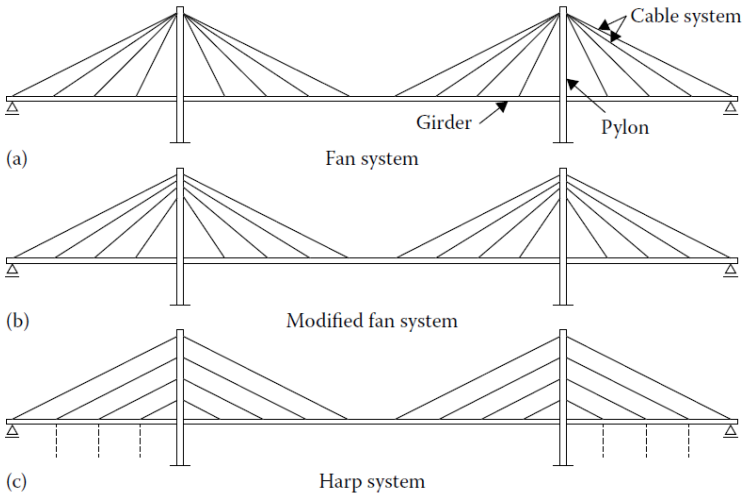

Figure 2 Type of cable stayed bridge based on cable arrangement [2]

2.2.2 Cable Spacing and Angle

The cable spacing for concrete segmental cable-stayed bridges typically ranges from 5 to 10 m. The angle between the cables and the main girder ranges from 25° to 65°, but not smaller than 22°.

2.2.3 Layout in the Transverse Direction

In the transverse direction, the stay cables can be arranged in one plane (see Fig. 10-8a), two planes (see Fig. 10-8b), or three and more planes as needed. Theoretically, the stay cables in one-plane arrangements do not have the capacity to resist torsion and the main girder must have greater torsion capacity. Most of the torsion can be resisted by the stay cables in a two-plane arrangement, and the cross sections of the main girder may have a smaller torsion capacity. [1]

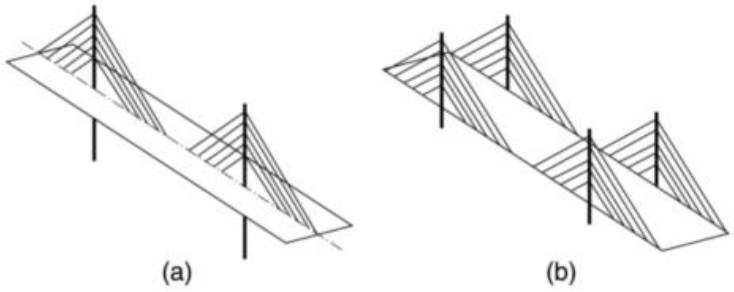

Figure 3 Typical Transverse Layout of Cables, (a) One Plane, (b) Two Planes [1]

2.3 Cable stiffness

The stiffness of cable-stayed bridges is governed by the stiffness of the stay cables, which is reduced by the cable sag, as given in the formula by Ernst [1]

$$A_s E_{eff} = \frac{A_s E_0}{1 + \frac{\gamma^2 l_k^2 E_0}{12 \sigma^3}}$$

As =Cable Steel Area
E0 =Modulus of Elasticity for straight Cables
E, eff =E-Modulus of Cable with Sag
γ = Specific Weight of Cable including Corrosion Protection
lk =Horizontal Length of Cable
σ =Tensile Stress in Cable

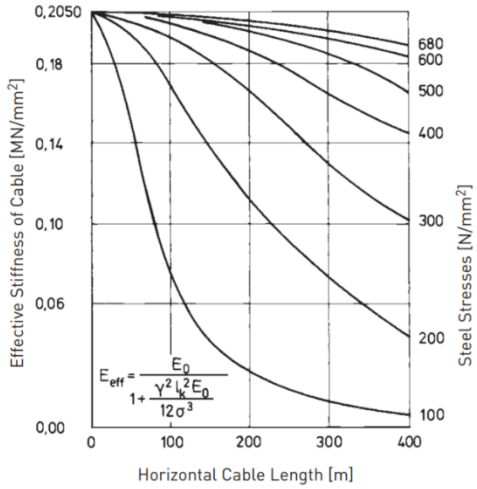

Figure 4 Relation between E, effective of cables, span lengths and [1]

The influence of the various parameters on the cable stiffness is shown in Fig. 3.

2.4 Geometry

2.4.1 Main span/Side span ration

The ratio of the main span to side span plays a critical role for cable-stayed bridges, the length of a side span can be approximated to about 40 % of the main span for a concrete beam under road traffic loads. however, for a steel bridge with railway loading, this ratio may be reduced to 30 %.

The critical factor for the span ratio is the stress in the backstay cables. This cable plays a significant role since it has the maximum variation of stresses. For the cable size required for the biggest backstay force with live load in the main span. [1]

2.4.2 Pylon heights

Hight of the pylon reduces the required amount of cable steel and the compression forces in the bridge beam by increasing the degree of inclination up to a cable inclination of 45°. However, increase the costs for the towers themselves. Optimizations indicate that tower heights of about 0.2 of the main span above deck achieve minimum costs for the whole bridge, Fig. 5 [1]

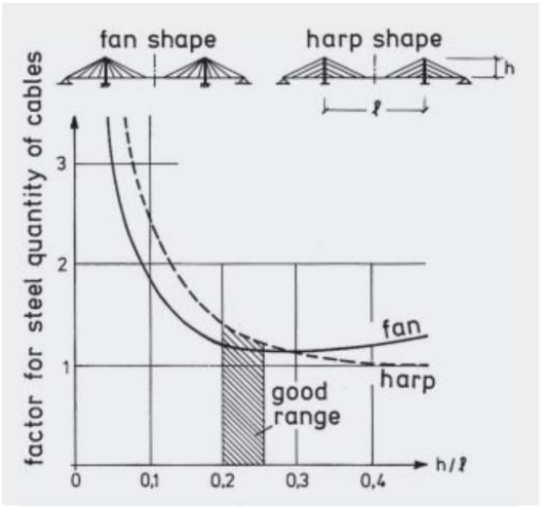

Figure 5 Relationship between tower height and amount of cable steel [1]

2.5 Articulation of bridge

The longitudinal support conditions for the girder of cable-stayed bridges have to be chosen carefully since they affect the changes in lengths due to temperature, shrinkage, and creep in addition to longitudinal forces such as braking, wind, and earthquake. A Summary of different types of longitudinal support is shown and described below. [1]

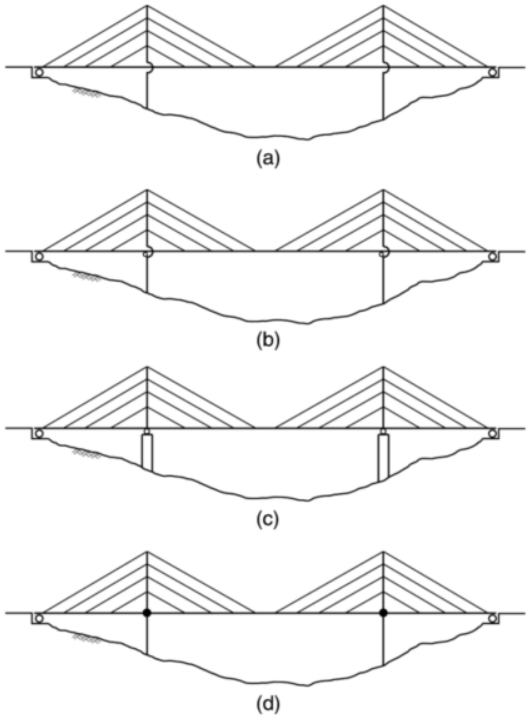

Figure 6 Systems of Conventional Cable-Stayed Bridges, (a) Floating System, (b) Semi-Floating (c) Pylon-Beam System, (d) T-Frame System. [3]

2.5.1 *Floating* System

In a floating system, the main girder is completely supported by the stay cables and the end abutments. The pylons are rigidly connected to the piers. There are no connections between the main girder and the pylons. This system is used for bridges with span lengths greater than 400 m and has the following advantages and disadvantages: [3]

Advantages

a. Removes the negative moment at the locations of the pylons in the beam.

b. Allowing the movement of the beam due to effects of temperature changes, shrinkage, and creep of concrete.

c. The variation of the moment in the main beam in the longitudinal direction is comparatively small and uniform.

d. the ability of the superstructure to move longitudinally lead to absorbing large earthquake loads.

Disadvantages
a. The need for the temporarily fixed connection during the cantilever construction method between the main beam.
b. removing the temporary fixed support may cause longitudinal movement of the main girder Because of the effect of inevitable unbalanced forces experienced during construction. [3]

2.5.2 Semi-Floating System

The difference between this system and the floating system is the existence of additional vertical support at each of the pylon locations.

This system can be approximated to a continuous beam with a three-span supported on some spring supports which represent the cables. Compared to the floating system, it possesses the following advantages and disadvantages:

Advantages

a. the resistance of the beam to the deformations induced by live loads is much higher due to vertical supports.

b. Can have similar advantages to the floating system if the vertical supports on the pylons are

designed as vertically adjustable or as spring supports.

Disadvantages

a. the existence of the negative moments at the locations of pylons in the main girder.

b. The effects of temperature, creep, and shrinkage will be higher when the pylon support restricts the horizontal movement. [3]

2.5.3 Pylon-Beam System

In the pylon-beam system, the pylons and the beam are fixedly connected. The entire structure consisting of girder, pylons, and cables is similar to a beam simply supported on the piers and abutments. The cables are like the external post-tensioning tendons in the continuous segmental bridges. This system has the following advantages and disadvantages:
Advantages
a. Significantly reduces the tensile force in the middle region of the main girder.
b. Significantly reduces the forces caused by temperature changes.
c. Comparatively simple for structural analysis.
Disadvantages
a. large displacement at the top of pylons may result due to the inclined deformation of the pylons when fully loaded at the midspan. This increases the defection at midspan and the the negative moment inside spans.
b. There are large reactions at the piers for long-span cable-stayed bridges, which may require high capacity supports and causes difficulty for future maintenance. [3]

2.5.4 Frame System

In the frame system, the piers, pylons, and main girder are rigidly connected. This system is often used in single-pylon cable-stayed bridges and has the following advantages and disadvantages:

Advantages

a. Eliminates high-capacity supports at the piers and facilitates maintenance.

b. Comparatively easy for construction.

c. Possesses higher stiffness resulting in a small defection of the main girder.

Disadvantages

a. High negative moment at the rigidly connected joints between the pylon and the main girder.

b. The piers may need to be designed comparatively flexible to reduce the temperature forces [3]

2.6 Tower shapes and number of cable planes

Since towers are mainly loaded by compression, concrete towers are more economical and, therefore, mainly used today. Only if extremely bad foundation conditions would require exceptionally long piles, are the lighter steel towers used today. [1]

2.6.1 Two outer cable planes

The beams of cable-stayed bridges should normally be supported at the outsides to restrain the rotational deformations most effectively. This requires two cable planes, supported by two tower legs, Fig. 7. For small and medium spans vertical tower legs may be used. To stiffen them transversely they can be connected with cross beams. For longer spans, the two-tower legs should lean towards one another above deck in an A-shape, which provides increased torsional rigidity to the beam and stiffens the towers for transverse loads. [1]

For bridge beams with a high clearance, the two foundations for a straight-A may be uneconomic. The two legs can then be pulled together underneath the beam to permit a common foundation. [1]

Type of sections used in two outer cable planes

- Open cross-sections
- Box girders: For two cable planes and medium spans, box girders are not required.
- Solid cross-sections: The elastic support of the beam from the stay cables provides a good distribution of heavy single traffic loads. For smaller spans, a solid slab may be used.

2.6.2 One central cable plane

The cables can be anchored at the center line of the beam in case of one central cable plane is used, the use of this system is for small and medium spans. a central cable plane also requires, for concrete beams, a box girder to carry the torsional moments from eccentric live loads. [1]

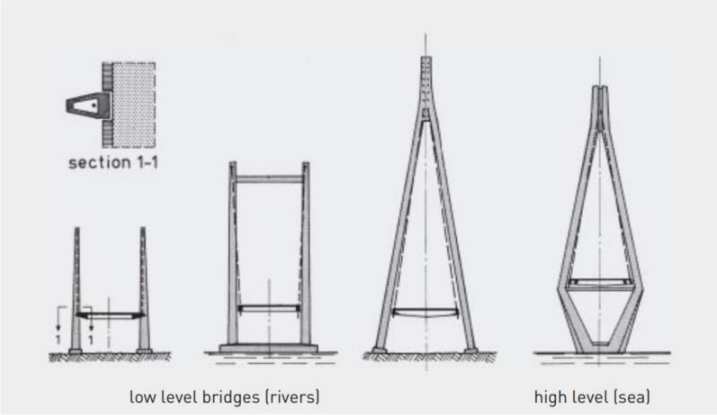

Figure 12 Towers for two cable planes [1]

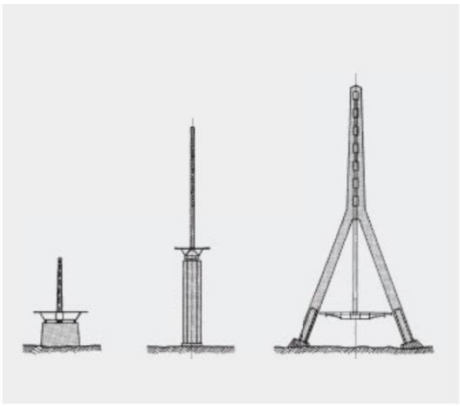

Figure 11 Towers for one cable plane [1]

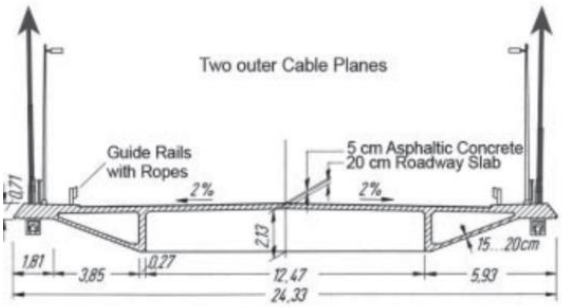

Figure 9 Open concrete cross-section with two cables [1]

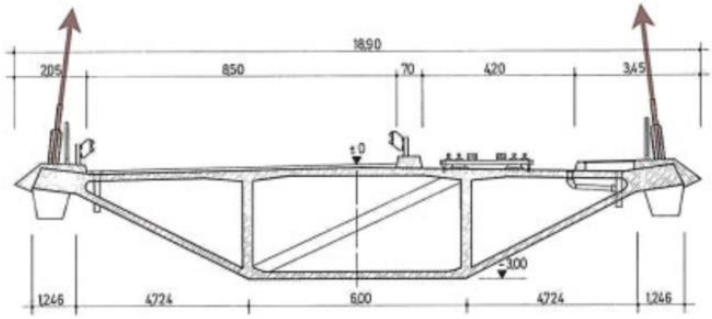

Figure 10 Concrete box girder with two cables [1]

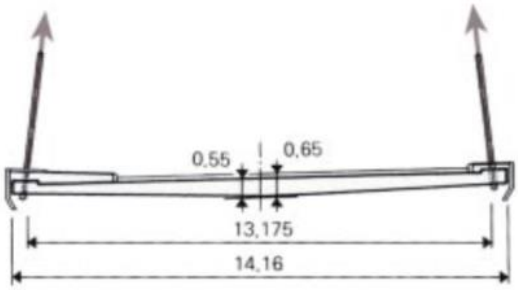

Figure 7 Concrete box girder with central cable [1]

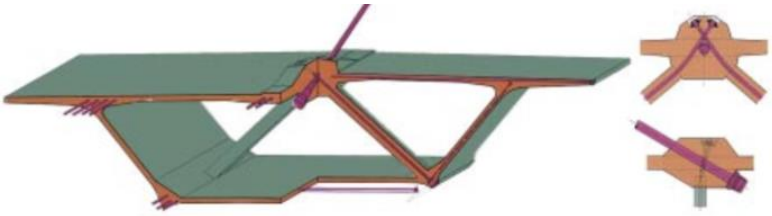

Figure 8 Solid section with two cables [1]

2.7 Stay cables

Stay cables are the characteristic structural components of cable-stayed bridges. Their performance governs the behavior of the complete bridge, not only in the final stage but also during construction. The durability of the stay cables determines the robustness of a cable-stayed bridge [1].

2.7.1 Systems

The currently used stay cable systems are locked coil ropes, parallel wire cables, and parallel strand cables as outlined in Table 1 [1].

For economic reasons, parallel strand cables are mostly used worldwide today. The corrosion protection for every single strand comprises the following: [1]

– galvanizing of every single wire in the strand

– filling the interstices between the single wires with grease

– surrounding each strand with a directly extruded PE-sheath.

Table 1 Current stay cable systems [1]

Characteristics		Modern locked coil rope	Parallel wire cable	Parallel strand cable
		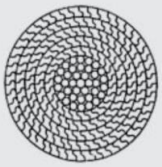		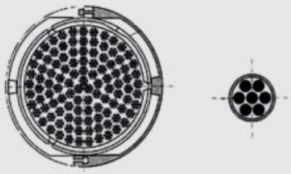
$E \cdot 10^{-6}$	[N/mm²]	0.170	0.205	0.195
f_u	[N/mm²]	1470	1670	1870
$\Delta\sigma$	[N/mm²]	150	200	200

2.7.2 Cable anchorages

The stay cables typically run through a steel pipe to their anchor points. These split shims prevent the sliding of the anchor heads. The lengths of the cables and thus their forces can be adjusted by changes in the thickness of the shims. [1]

2.7.2.1 At beam

In concrete: A typical cable anchorage at a concrete beam is shown in Fig. 15 The cable forces are directly introduced into the main girder. The anchor head is supported by shims on pressure plates welded to the end of the steel pipe which transfers the cable forces either directly or via the steel pipe and shear rings into the concrete, where the tensile forces are covered by reinforcement. [1]

2.7.2.2 At the tower

In concrete: The simplest way to anchor individual cables at the tip of a concrete tower is to overlap them and thus to anchor them by compression, Fig. 13. Usually, the stay cables are anchored inside a tower box section, similar to that shown for a concrete beam. The tensile forces between forestays and backstays can be covered by short tendons, Fig. 15. [1]

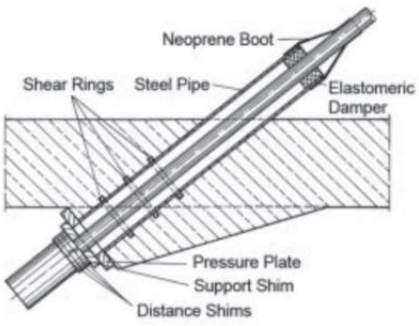

Figure 15 cable anchorage in concrete [1]

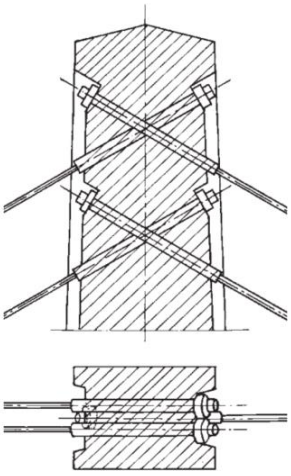

Figure 13 Cable anchorage by overlapping [1]

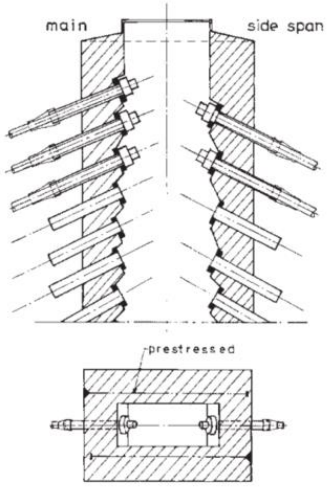

Figure 14 Cable anchorage inside box [1]

2.8 The behavior of the cable-stayed bridge

The basic load-bearing behavior of cable-stayed bridges is outlined in Fig. 16. Loads in the main span are carried by the forestays to the tower heads and from there anchored by tension via the concentrated backstays in the anchor piers. The inner stay cables of the side spans receive no forces at all from this loading. The horizontal cable components act in compression in the beam and equal one. [1]

Loads in a side span are transmitted by the side span cables to the tower head and from there via compression (meaning reduction of tensile forces from permanent loads) in the backstays to the anchor piers where they cause compression. The horizontal components of the side spans are balanced by those of the backstays by tension in the side spans. [1]

The backstays are thus governing the stiffness of a cable-stayed bridge and receive important load changes. [1]
The ratio between side spans and main spans strongly influences the stress changes in the backstay cables. [1]

Live loads in the main span increase the stresses from permanent loads, while live loads in the side spans decrease them. These stress changes must not exceed the permissible fatigue range of the actual stay cable system. These fatigue stresses increase with increasing span ratios. [1]

The span range also influences the size of the vertical uplift forces in the outer anchor piers. These anchorage forces decrease with increasing span ratios. The compression created in the backstays by live loads in the side spans decreases their tensile force from permanent loads increasingly with increasing span ratios. In this way, the effective cable stiffness decreases [1]

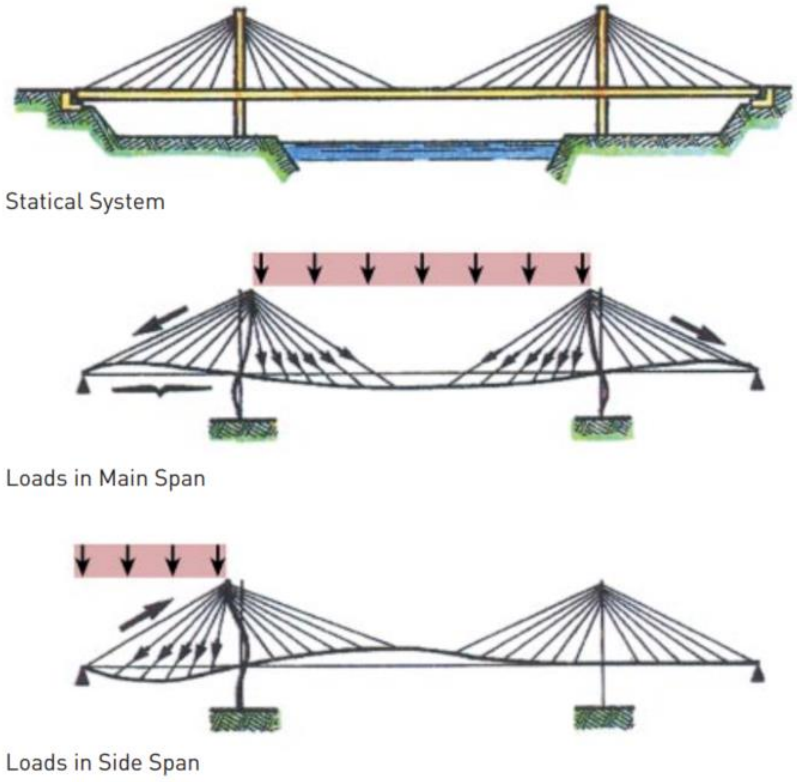

Figure 16 Load transfer in cable-stayed bridges [1]

2.8.1 Ideal state

What would be the best jacking stress of each cable in terms of increasing the girder span capacity? [2]

This is a unique question to cable-stayed bridges during structural analyses and design. From the girder capacities' perspective, the answer is found when the maximum bending moments due to dead loads on the girder are the same as those of a continuous girder [2]

if the dead load distribution reaches the desired state, the span capacity can be increased. This simple idea is since both the girder and the pylons are more efficient under axial compression than under tension and compression due to large bending moments. [2]

2.9 Design parameter and FEM model

2.9.1 Design parameters

In this work the following parameters have been chosen:

1- Using a modified fan system since it has benefited from both harp and fan system.
2- Using one central cable plane, as a result, the cross-section will be a concrete box girder to account for the torsional effect.
3- The used main span is 180 m and the side span will be 90 m so the ratio between the main span to side span will be 0.5 (the reason for this ratio is to prevent the tension reaction in the abutments)
4- The height of the pylon will be 45m so the ratio between the height of the pylon to the main span will be 0.25.
5- Using of Pylon beam system where the pylon and the beam are connected (fixed connection) and placed on the substructure.
6- The spacing of cables in the main span will be 7.25 m as will the side span.
7- The use of diagonal members at the place of cable anchorage to improve the distribution of the load from the cable to the entire section.
8- The use of cast in place segmental bridge and free cantilever method in construction

To eliminate the tensile forces in the abutment under the worst case, a different girder section has been used in the main span and the side span. The side span has a thicker upper slab.

The following figures are for the side span, main span, abutment, and pier sections.

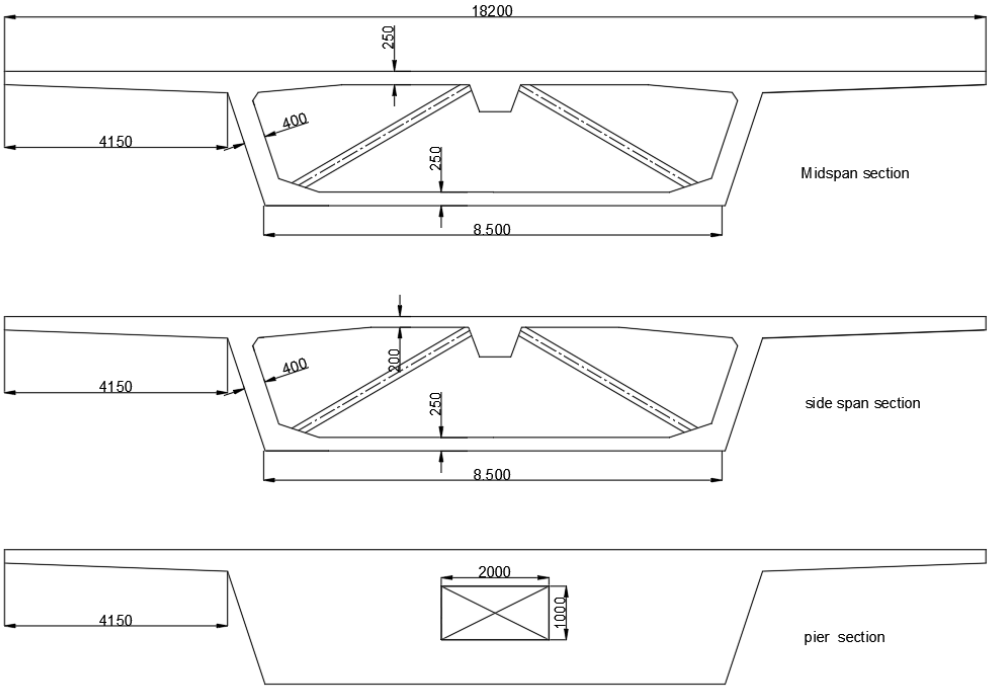

Figure 17 sections

The following picture describes the arrangement of the bridge.

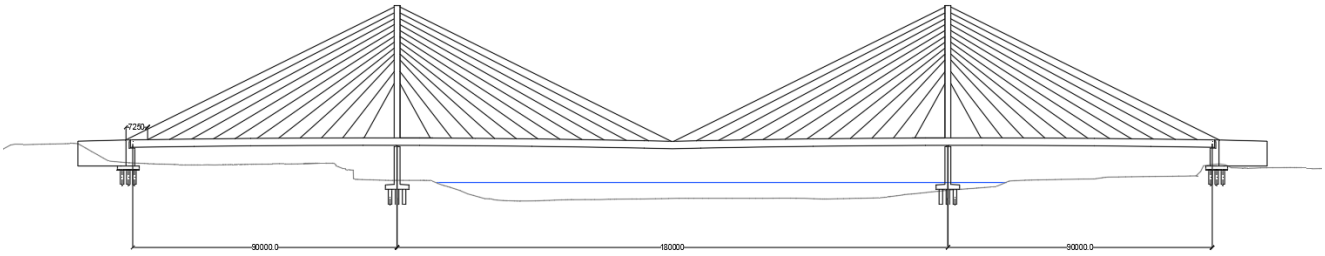

Figure 18 Bridge arrangement

For allowing the bridge to move freely under the effect of the temperature, one fixed point has been considered under the pier, the following figure shows the articulation of the bridge.

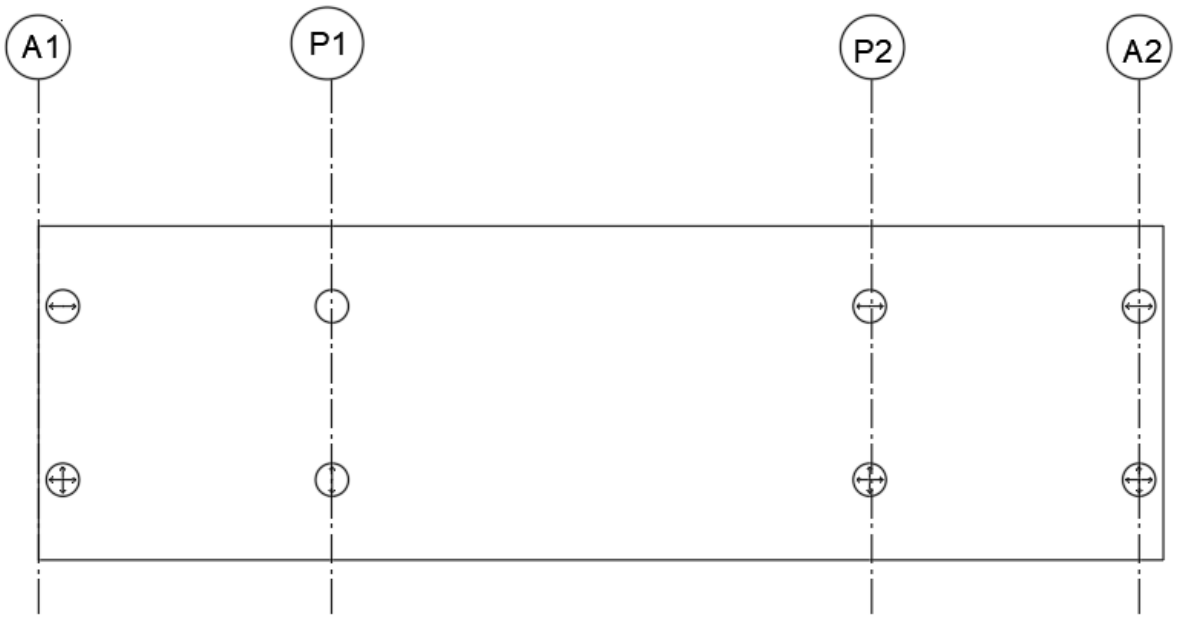

Figure 19 Bridge bearing

2.9.2 FEM modeling.

2.9.2.1 Beam model

The bridge has been modeled using beam model in the Midas Civil, the beam model has been used for construction stage analysis, SLS &ULS check for both deck and cables. The cables have been modeled as truss elements that carry tension force only. All the loads have been applied to the model as described in chapter 3.

The following figure shows the model which has been used in the analysis and the support restriction.

.

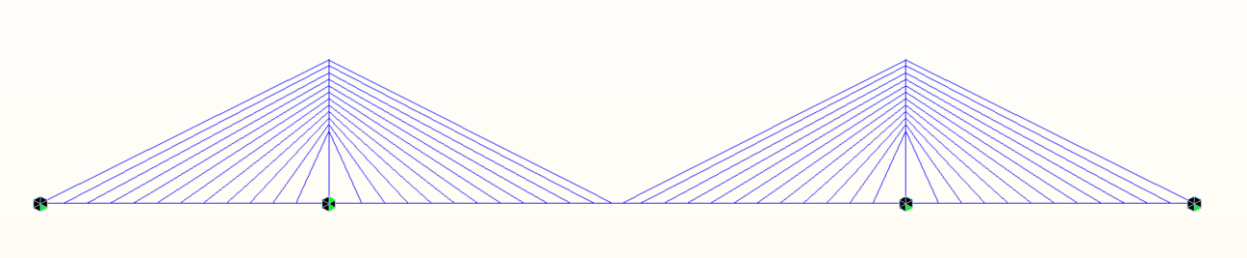

Figure 20 Midas Civil beam model

2.9.2.2 Plate model

Bridge also has been modeled using plate model in Midas Civil. This model has been used to check the shear lag effect and also to perform transverse analysis.

The Midas Civil does not offer a tapered plate, approximation thickness has been considered for parts of the section. The figure below shows the section which has been considered in the model where parts of the model have different thickness, the first figure considers the section far from the anchorage cable and the second consider the section which contains the anchorage of the cables. The second section also has high thickness for the upper and lower flange which have been used as anchorage for temporary prestressed which have been used in the construction and have two diagonal concrete members which are acted to transfer the cable force to the entire box section.

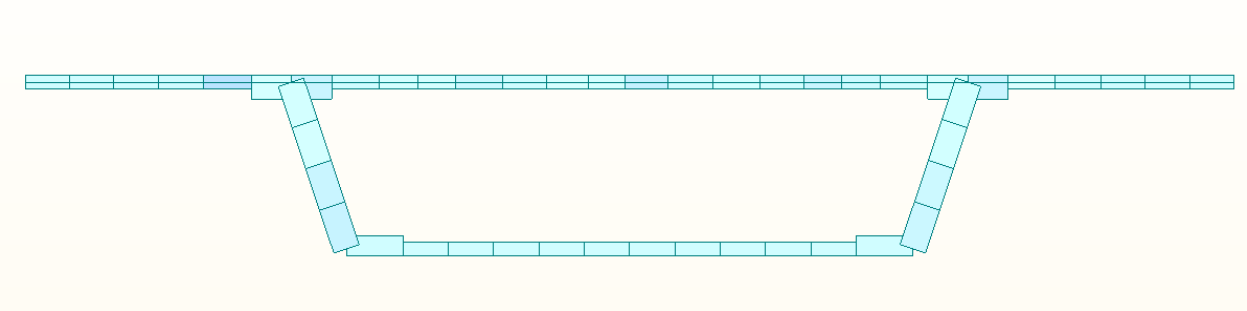

Figure 21 Section between anchorage points

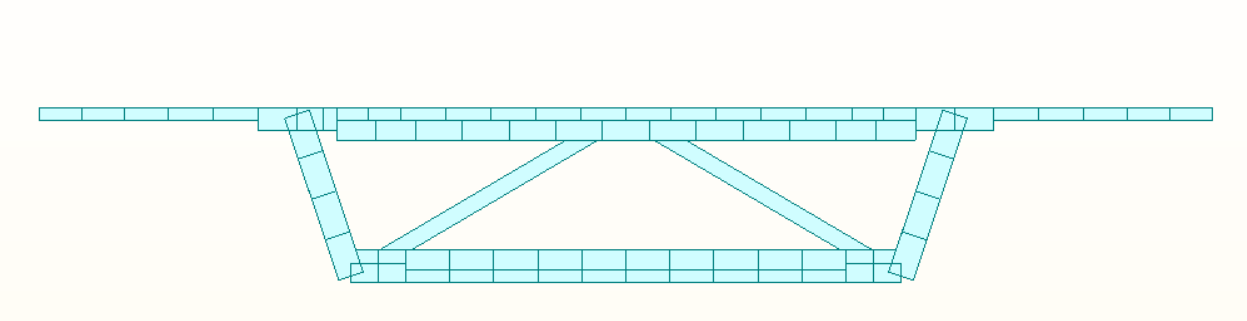

Figure 22 Section at anchorage points

The figure below shows the model (after hiding the upper flange) which includes the concrete ties and spring support and edge support.

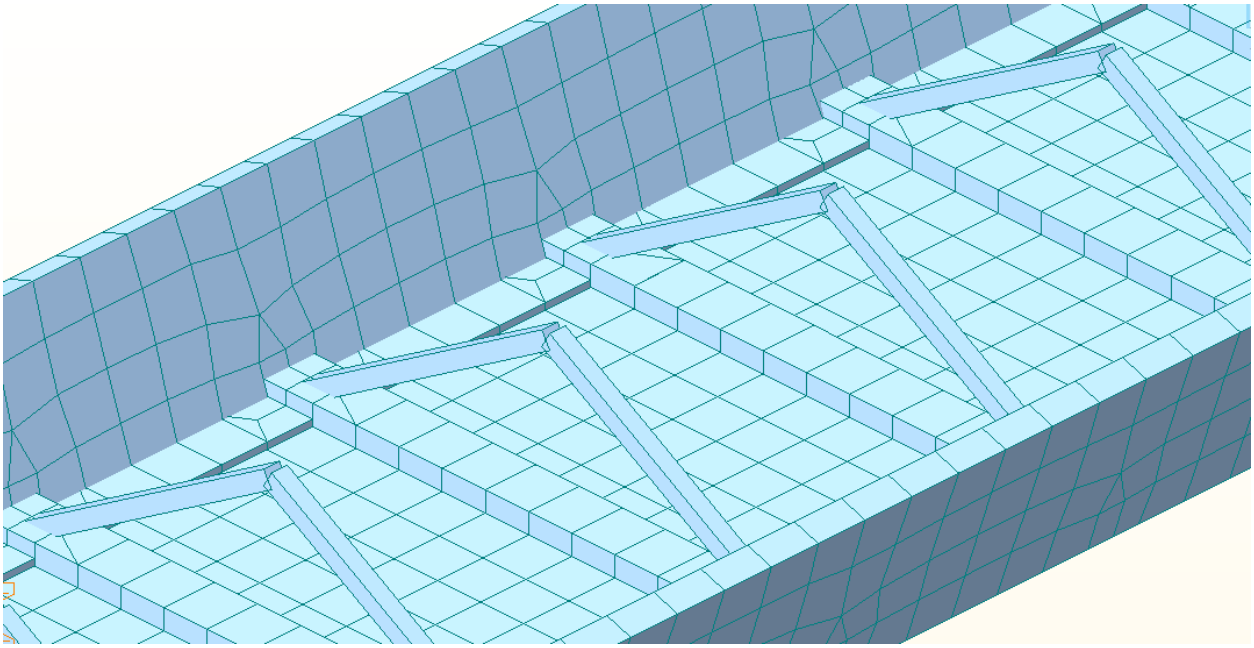

Figure 23 Plate model which shows the main parts of section (the top slab is hidden)

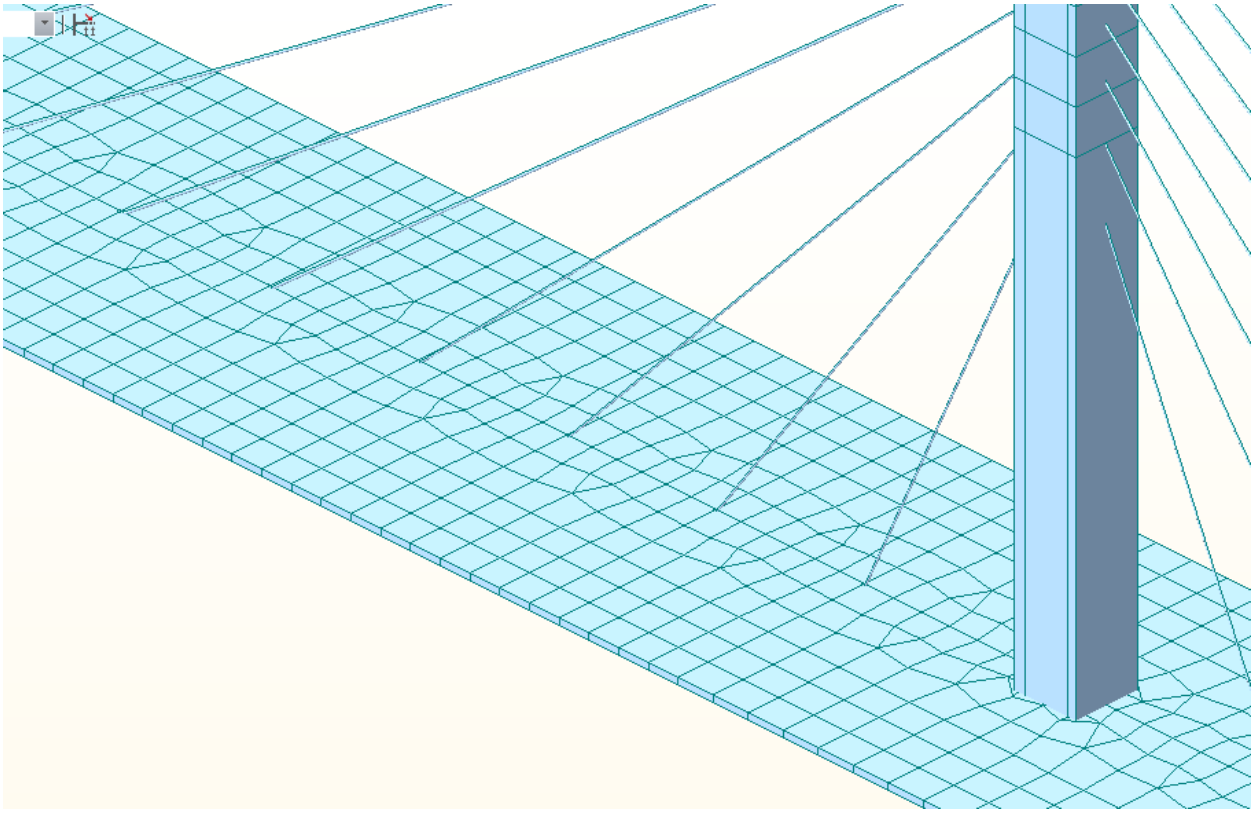

Figure 24 Part of the model shows the pylon and cables

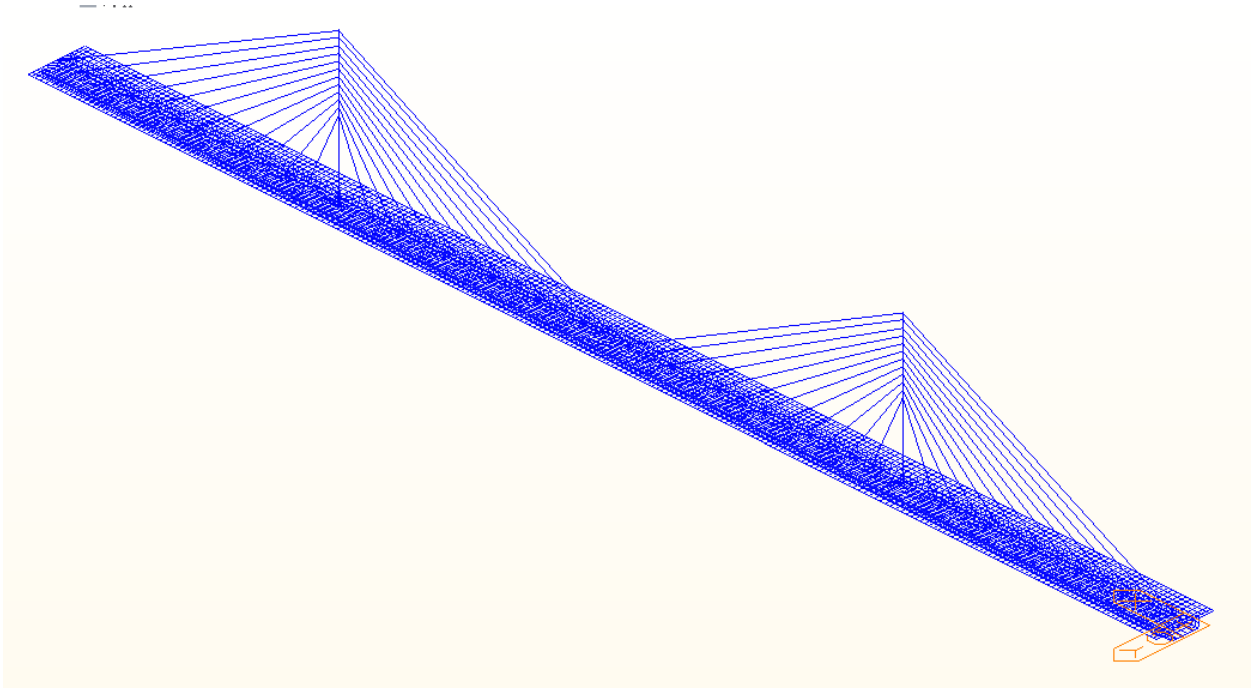

Figure 25 full plate model in Midas Civil

2.10 Material

The construction of the box girder, pylon, and substructure is made of concrete class C50 / 60, The material of prestressing reinforcement and stay cables are considered as Y1860 steel.

2.10.1 Concrete

Table 2 Concrete properties

Concrete C50/60			
Symbol	**Description**	**Value**	**Unit**
fck	Characteristic cylinder compressive strength	50	MPa
fck, cube	Characteristic cube compressive strength	60	MPa
fcm	Mean compressive strength	58	MPa
fctm	Mean tensile strength	4.1	MPa
Ecm	Elastic modulus	37278	MPa
fcd	Design compressive strength (for αcc=1.00)	33.33	MPa
fcd	Design compressive strength (for αcc=0.85)	28.33	MPa
fctd	Design tensile strength (for αct=1.00	1.9	MPa

2.10.2 Reinforced steel

1.1.1. Reinforced steel type B500B. Parameters

Table 3 Reinforcement steel properties

Steel reinforcement			
Parameter	**Symbol**	**Value**	**Unit**
yielding stress, char.	fyk	500	MPa
yielding stress, des.	fyd	435	MPa
Strength in tension	ft	550	MPa
modulus of elasticity	Es	200	GPa

2.10.3 Cable stays and prestressed cables

Steel type Y1860 S7 15.7

Table 4 Prestressed reinforcement

Prestressed reinforcement			
Parameter	**Symbol**	**Value**	**Unit**
Diameter	Ø	15,7	mm
Area	Ap1	150	mm2
Strength in tension	fpk	1860	MPa
proof-stress	fp0,1k	1636,8	MPa

3 Actions on the bridge:

3.1 4.1 Permanent Action

3.1.1 Self-weight

The self-weight was calculated as the product of the area of the cross-section and unit weight of the concrete

3.1.2 Superimposed permanent loads

Other dead load consists of the weight of the asphalt layer (roadway), railing, track, overhead line, and curb.

Table 5 Superimposed load

Member	Size	Longitudinal Load	Unit	Transverse load	
cornice	(0.2*4+0.25*0.5) *24*2	44.4	KN/m	6	[KN/m2]
Railing	2x0.5	1	KN/m	0.5	[kN/m]
Track	0.3x10x25	75	KN/m	7.5	[KN/m2]
Overhead line		1	KN/m	1	[KN/m]
Roadway	0.1x10x25	16.1	KN/m	1	[KN/m2]
Total		137.5	KN/m		

The longitudinal loads have been applied to beam model for longitudinal analysis.

The transverse loads have been applied to the plate model, the self-weight has been applied by the software, the superimposed load has been applied manually as shown in the below figure.

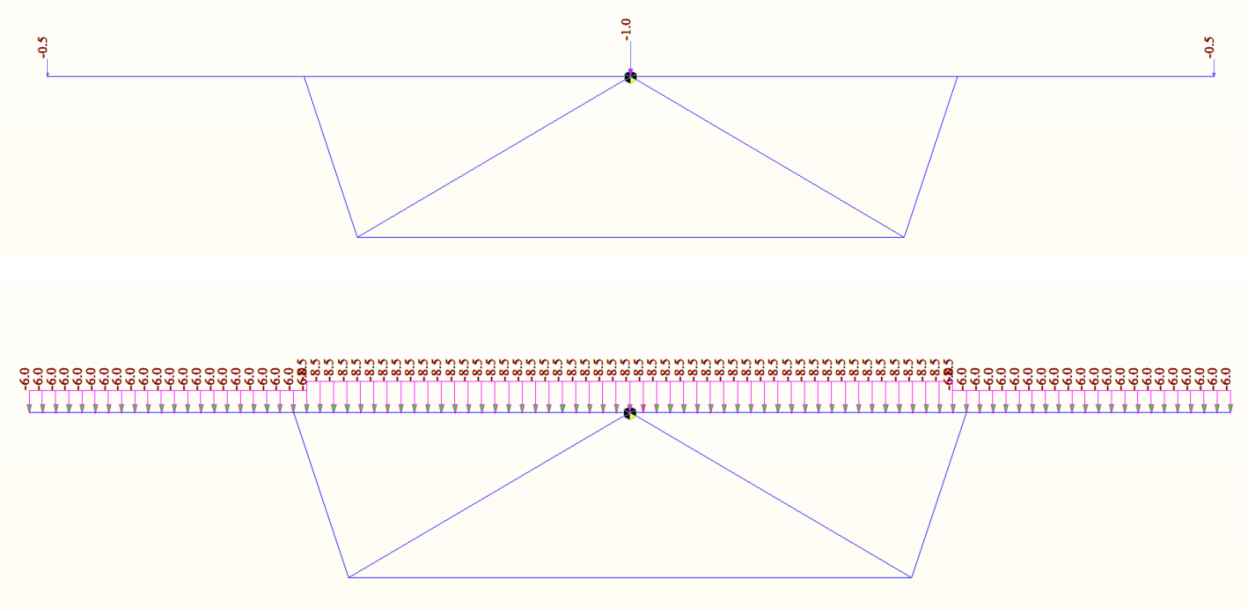

Figure 26 superimposed load to plate model

3.2 Variable actions

3.2.1 Loading during construction

1- The first set Qca corresponds to working personnel, staff, and visitors, with [4]hand tools or other small site equipment. [5]
EN 1991-1-6 recommends that this loading be modeled as a uniformly distributed load qca 1 kN/m2 (characteristic value) to be applied to obtain the most unfavorable effects.

2- The second set Qcb corresponds to the storage of movable items. In general, these loads are unknown in detail and may have a random magnitude. [5]
These actions are modeled as free actions and represented as appropriate by:
- a uniformly distributed load qcb with a recommended characteristic value equal to 0.2 kN/m2 [4]
- a concentrated load Fcb, to be applied to obtain the most unfavorable effect. The recommended characteristic value of its magnitude is equal to 100 kN [5]

3- The third set Qcc corresponds to non-permanent equipment in position for use during execution.
Qcc describes loads that are known only when the construction process commences. At the preliminary design stage, such loads may be difficult to estimate; however, for the most common bridge types, some ratios are well known. For example, in the case of cast-in-place segmental bridges built by the cantilever method, the weight of the traveling form is about 50% of the weight of the heaviest segment. [5]

the center of gravity of the moving scaffolding to be 1/3 of the length of the concrete segment and so in the calculation, the actual weight of the trolley was replaced by an axial force and moment acting on the pervious segment.

the heaviest segment weight is 2258.69KN so 50% of this weight is about 1130 KN

The following tables show the fresh segment equivalent load during construction which is replacing the weight of the fresh segment by axial force and moment (M=F.L/2) on the previous already constructed segment, also the table shows the moving scaffolding equivalent load and moment.

The following tables show the fresh segment equivalent load during construction which is replacing the weight of the fresh segment by axial force and moment (M=F.L/2) on the previous already constructed segment, also the table shows the moving scaffolding equivalent load and moment.

The arrangement of the section is shown in the longitudinal section in the drawing.

The abutment & pier segment has been assumed to be supported on temporary support. The kay segment has been assumed to be supported by the adjacent segment

Table 6 Segments and moving scaffolding load during construction

Seg. Properties					Fresh Seg. Load		Moving Scaffolding Load	
Seg. No	length	Seg. type	Area	Unit weight [KN/m3]	Force[KN]	Moment [KN.m]	Force[KN]2	Moment [KN.m]3
S0	2.00	Pier section	26.10	27.00	-	-	-	-
S1	9.00	Side span	10.14	27.00	2464.02	11088.09	1130.00	3390.00
S2	7.25	Side span	10.14	27.00	1984.91	7195.28	1130.00	2730.83
S3	7.25	Side span	10.14	27.00	1984.91	7195.28	1130.00	2730.83
S4	7.25	Side span	10.14	27.00	1984.91	7195.28	1130.00	2730.83
S5	7.25	Side span	10.14	27.00	1984.91	7195.28	1130.00	2730.83
S6	7.25	Side span	10.14	27.00	1984.91	7195.28	1130.00	2730.83
S7	7.25	Side span	10.14	27.00	1984.91	7195.28	1130.00	2730.83
S8	7.25	Side span	10.14	27.00	1984.91	7195.28	1130.00	2730.83
S9	7.25	Side span	10.14	27.00	1984.91	7195.28	1130.00	2730.83
S10	7.25	Side span	10.14	27.00	1984.91	7195.28	1130.00	2730.83
S11	7.25	Side span	10.14	27.00	1984.91	7195.28	1130.00	2730.83
S12	5.50	Side span	10.14	27.00	1505.79	4140.92	1130.00	2071.67
S-A	2.00	Abutment section	26.10	27.00	-	-	-	-
S0	2.00	Pier section	259.27	27.00	-	-	-	-
S1_2	9.00	Main span	8.55	27.00	2464.02	11088.09	1130.00	3390.00
S2_2	7.25	Main span	8.55	27.00	1673.66	6067.03	1130.00	2730.83
S3_2	7.25	Main span	8.55	27.00	1673.66	6067.03	1130.00	2730.83
S4_2	7.25	Main span	8.55	27.00	1673.66	6067.03	1130.00	2730.83
S5_2	7.25	Main span	8.55	27.00	1673.66	6067.03	1130.00	2730.83
S6_2	7.25	Main span	8.55	27.00	1673.66	6067.03	1130.00	2730.83
S7_2	7.25	Main span	8.55	27.00	1673.66	6067.03	1130.00	2730.83
S8_2	7.25	Main span	8.55	27.00	1673.66	6067.03	1130.00	2730.83
S9_2	7.25	Main span	8.55	27.00	1673.66	6067.03	1130.00	2730.83
S10_2	7.25	Main span	8.55	27.00	1673.66	6067.03	1130.00	2730.83
S11_2	7.25	Main span	8.55	27.00	1673.66	6067.03	1130.00	2730.83
S12_2	5.50	Main span	8.55	27.00	1269.68	3491.61	1130.00	2071.67
S-K	0.50	Key segment	8.55	27.00	115.43	28.86	-	-

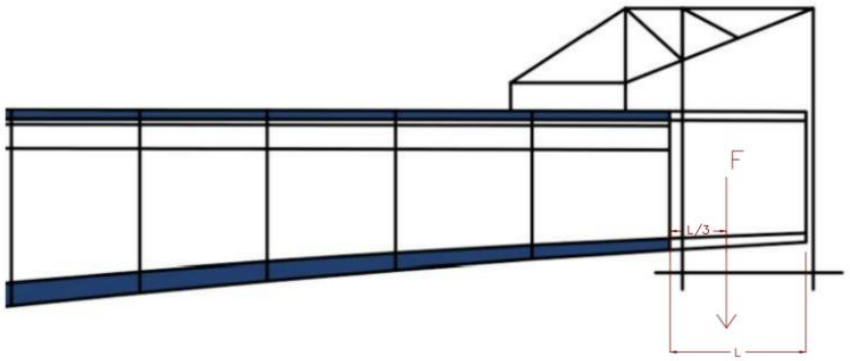

Figure 27 Moving scaffolding load "the center of the moving scaffolding = L/3"

The following figure shows the moving scaffolding load on mid span at end of segment L9.

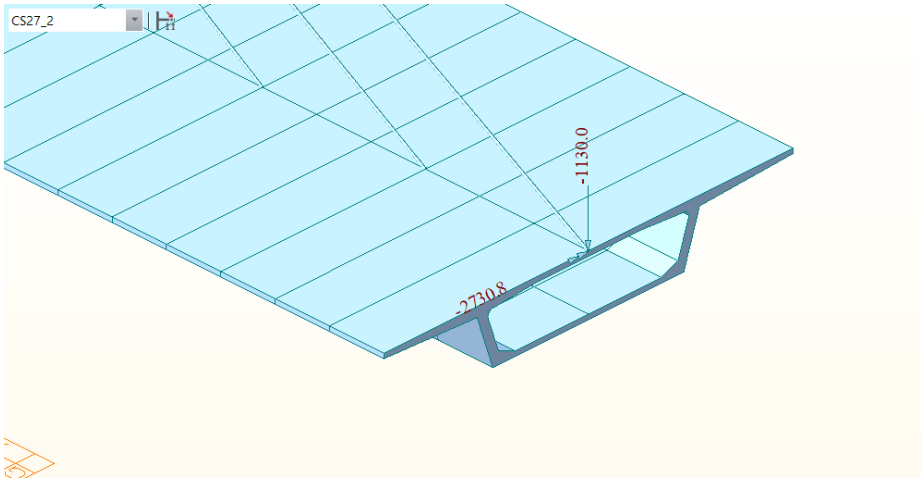

Figure 28 Moving scaffolding load at CS27_2 (see Table no.6) in beam model

The following figure shows the load at end of segment L9 on midspan (fresh concrete weight and

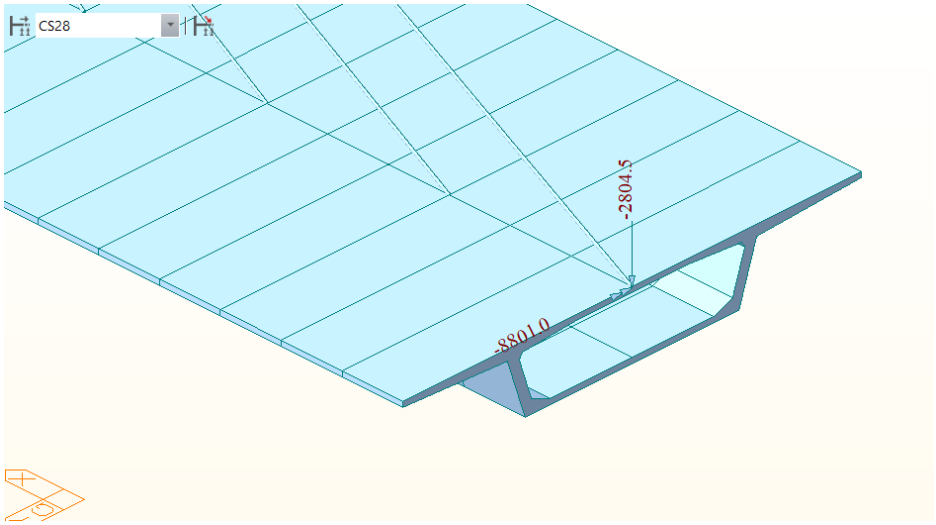

Figure 29 moving scaffolding and fresh segment load acting on mid-span at CS28 (see Tableno.6) in beam model

3.2.2 Therma Action

3.2.2.1 Uniform temperature component

This component induces a variation in the length of the bridge.
The uniform temperature component (ΔTN) depends on the minimum (T, min) and maximum (T, max) temperature which a bridge will achieve. Minimum shade air temperature (T, min) and maximum shade air temperature (T, max) for the site and on the initial bridge temperature to the maximum expansion and contraction ranges of uniform bridge temperatures are defined as: [5]

$$\Delta T_{U,exp} = T_{e,max} - T_0 \quad \Delta T_{U,cont} = T_0 - T_{e,min}$$

Where the values of Te, max and Te, min are the uniform bridge temperature components that are dependent on T, max and T, min, as well as on the type of structural material. [5]
The following figure show the relation between the T, max, T, min, and Te, max, Te, min. [5]

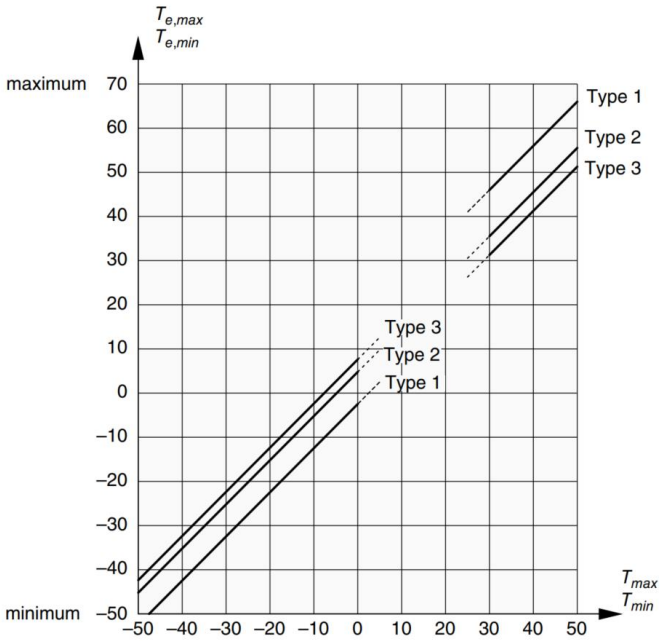

Figure 30 Correlation between and T, min site temperatures and bridge deck uniform temperatures on steel (type 1), composite (type 2), and concrete (type 3) bridge decks. [5]

To =+10° (assumed initial temperature)

T, max = +40° & T, min. =-32°

Te, Max. =41.5° & Te, min. =-24° (Values are from table)

The characteristic value of the maximum expansion range of the uniform bridge temperature component, ΔTN, exp should be taken as: ΔTN, exp = Te .max – To.

$\Delta TN, exp$=41,5−10=31,5°

The characteristic value of the maximum contraction range of the uniform bridge temperature component, ΔTN, con should be taken as: ΔTN, con = T0 – Te, min

$\Delta TN, con$=−24−10=−34°C

3.2.2.2 temperature difference component

The part of a temperature profile in a structural element represents the temperature difference between the outer face of the element and any in-depth point.

Recommended values for TM, heat, and TM, cool are given in following Table.

Table 7 Recommended values of linear temperature difference component for several types of bridge decks for road, foot, and railway bridges, in ECI -1-5 [5]

Type of deck	Top warmer than bottom $\Delta T_{M,heat}$ (°C)	Bottom warmer than top $\Delta T_{M,cool}$ (°C)
Type 1: Steel deck	18	13
Type 2: Composite deck	15	18
Type 3: Concrete deck:		
Concrete box girder	10	5
Concrete beam	15	8
Concrete slab	15	8

ΔTtop, $heat$d=10°C
ΔTbot., $heatd$=0°C
ΔTtop, $cool$d=−5°C
ΔTbot, $coold$=0°C

- The simultaneity of the uniform and temperature difference components
  The uniform temperature component gives rise to action effects in framed bridges such as portal bridges or arch bridges when they are statically undetermined. Physically, the two components (uniform and temperature difference) exist, and they have to be considered simultaneously. Of course, they cannot be both represented by their characteristic value. For that reason, EN 1991-1-5 recommends two expressions that can be termed 'sub-combinations': [5]

$$\Delta T_{\mathrm{M,heat}}(\text{or } \Delta T_{\mathrm{M,cool}}) + 0.35\Delta T_{\mathrm{N,exp}}(\text{or } \Delta T_{\mathrm{N,con}})$$

or

$$0.75\Delta T_{\mathrm{M,heat}}(\text{or } \Delta T_{\mathrm{M,cool}}) + \Delta T_{\mathrm{N,exp}}(\text{or } \Delta T_{\mathrm{N,con}})$$

3.2.3 Footways or Cycle Tracks

For footways, cycle tracks, and footbridges. It consists of a uniform distributed load of 5 kN m−2 specified to cover the static effects of a continuous dense crowd, which should be applied in the relevant parts of the bridge to induce the maximum load effects for the element under study. A Uniformly distributed load of 3.0 kN/m2 is recommended as a combined value. [5]

3.2.4 Traffic load

The bridge is intended for public transportation, for the design tram and buses load has been considered. The bus load has been considered as below, with Qk=90KN. Where 2 buses have been one each direction (total 4 vehicles). [6]

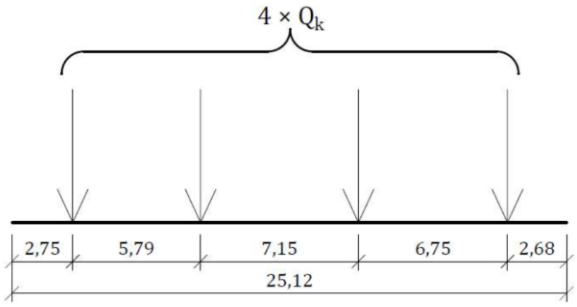

Figure 31 Bus load on the bridge. [7]

tram load is replaced by an ideal load set of two vehicles. These kits shall be placed no more than three on each track, anywhere along the length of the bridge structure in the most efficient position. [8]

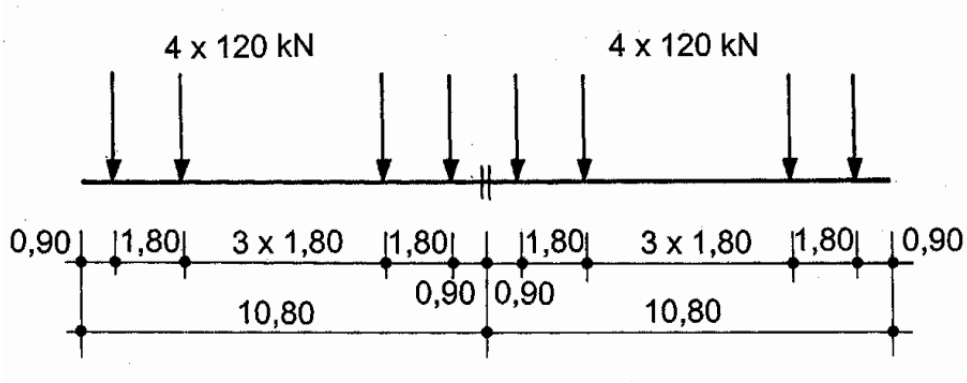

Figure 32 Load set of tram vehicle [8]

Dynamic coefficient

$$\Phi t = 1 + 0{,}85 * (\theta 3 - 1)$$

$$\Phi 3 = \frac{2{,}16}{\sqrt[2]{L\Phi - 0{,}2}} + 0{,}73$$

1< $\Phi 3$ < 2; where LΦ is the 'determinant' length as in table 4:

Table 8 Determinant length [5]

Case	Structural element	Determinant length L_Φ
Main girders		
5.1	Simply supported girders and slabs (including steel beams embedded in concrete)	Span in main girder direction
5.2	Girders and slabs continuous over n spans with $L_m = 1/n(L_1 + L_2 + \ldots + L_n)$	$L_\Phi = k \times L_m$, but not less than max L_i $(i = 1, \ldots, n)$ $n = 2 \quad 3 \quad 4 \quad 5$ $k = 1.2 \quad 1.3 \quad 1.4 \quad 1.5$

$$Lm = \frac{360}{3} = 120m$$

$$L\Phi = 1.3 \times 120 = 156$$

$$\Phi 3 = \frac{2{,}16}{\sqrt[2]{156 - 0{,}2}} + 0{,}73 = 0.9$$

$$\Phi t = 1 + 0{,}85 * (0.9 - 1) = 0.915 \quad use \ 1.13$$

$$Qdyn = Qk * 1{,}13 = 120 * 1{,}13 = 135{,}6\ kN$$

For the tram load, this load has been defined in the software because Midas doesn't have it the following figure shows the definition of this load by editing the LM71 in the software.

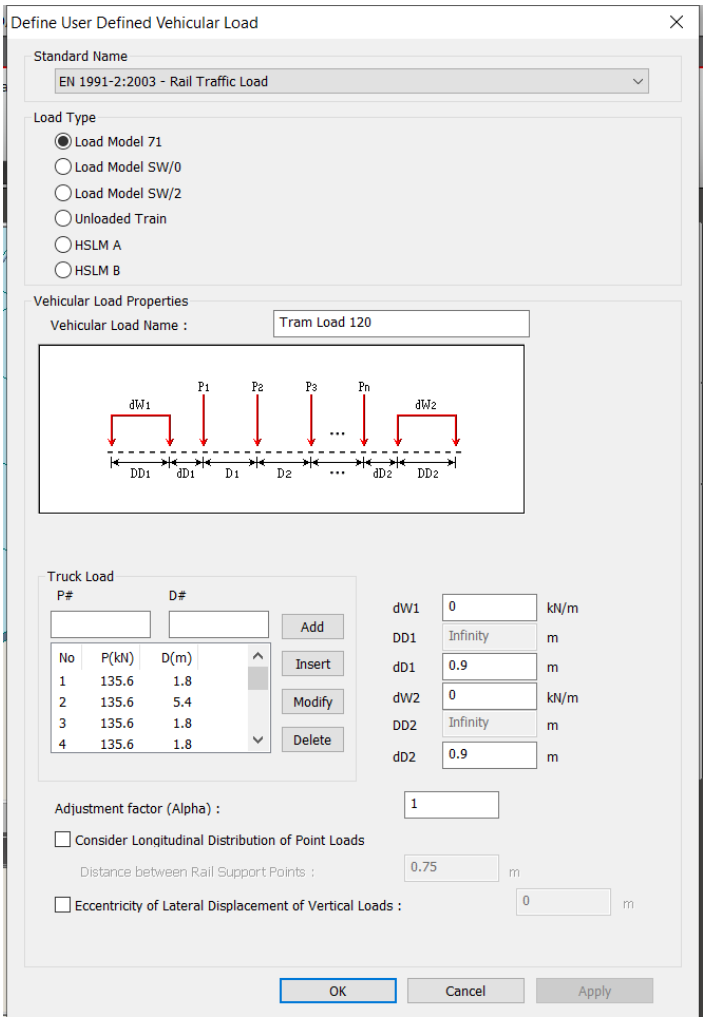

*Figure 33 Tram load 8*135.6 axial load definition*

The traffic load has been assigned to line lane and placed on the structure as moving load. The figure below shows the tram load to give the max. moment at the middle of the bridge.

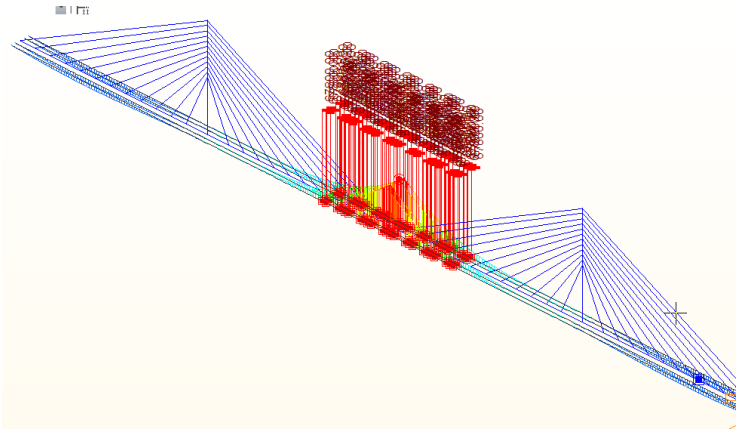

Figure 34 3 Tram vehicles on the mid span to give the max. bending moment in the middle of bridge

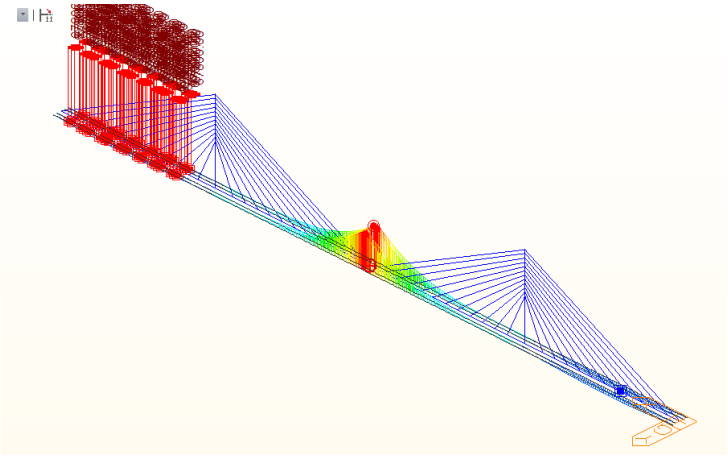

Figure 35 3 Tram vehicles on the side span to give the min. bending moment in the middle of bridge

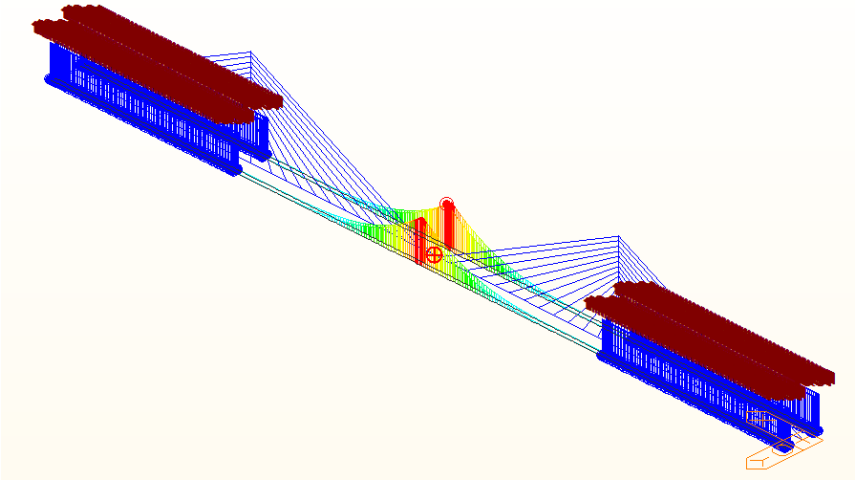

Figure 36 Pedestrian load on the side span to give the min. bending moment in the middle of bridge

3.3 Combinations of actions

1.1.2. Combination of actions for ultimate limit states

according to EN 1990 is possible to use EQ 6.10 for ultimate load combination. [9]

Table 9 General expressions of combinations of actions for ULS [8]

Combination	Reference: EN 1990	General expression
Fundamental (for persistent and transient design situations)	(6.10)	$\sum_{j\geq 1}\gamma_{Gj}G_{kj}\,''+''\,\gamma_P P\,''+''\,\gamma_{Q,1}Q_{k,1}\,''+''\,\sum_{i>1}\gamma_{Q,i}\psi_{0,i}Q_{k,i}$

1.1.3. Combinations of actions and criteria for serviceability

Table 10 General expressions of combinations of actions for SLS [10]

Combination	Reference: EN 1990	General expression
Characteristic	(6.14)	$\sum_{j\geq 1}G_{k,j}\,''+''\,P\,''+''\,Q_{k,1}\,''+''\,\sum_{i>1}\psi_{0,i}Q_{k,i}$
Frequent	(6.15)	$\sum_{j\geq 1}G_{k,j}\,''+''\,P\,''+''\,\psi_{1,1}Q_{k,1}\,''+''\,\sum_{i>1}\psi_{2,i}Q_{k,i}$
Quasi-permanent	(6.16)	$\sum_{j\geq 1}G_{k,j}\,''+''\,P\,''+''\,\sum_{i\geq 1}\psi_{2,i}Q_{k,i}$

The following safety factor have been used:

γQ = 1.45 (for rail load)

γp=1.00 (for prestressing)

γG, sup = 1.35 (unfavorable Permanente load)

γG, inf = 1.00 ((unfavorable Permanente load)

γQ = 1.50 for other traffic actions and other variable actions

γQ =1.35 when Q represents unfavorable actions due to road or pedestrian traffic (0 when favorable)

$\psi 0$=0.8, $\psi 1$=0.7, $\psi 2$=0 for rail load (2 tracks are simultaneously loaded) (the tram load has considered like the LM71 load)

ψ0=0.4, ψ1=0.4, ψ2=0.0 for pedestrian

ψ0=0.6, ψ1=0.6, ψ2=0.5 for thermal action

4 Initial load of cables and cable sizing

The cables have been designed according to the assumption that they will behave under permanent load as supports for a continuous bridge deck. In the bar model of the structure, the cables are replaced by supports at the points of their connection to the bridge deck (see fig.19). The reactions Rz are then taken from this model, which is converted to the force in the hinges Nz according to the formula below.

$$Nz = \frac{Rz}{\sin(\alpha)}$$

Where α is the inclination angle and Rz is the reaction at the support.

The design of the cables itself is made from the condition of limiting the tension in the cable to 0.45 fpk. The required hinge area is calculated according to the formula below.

$$Az, req = \frac{Nz}{0{,}45 fpk}$$

From this required area, the number of strands in the cable n, req is finally calculated, with an area of one strand of 150 mm2.

The cables' areas have been adjected later to satisfy the stresses limits and to ensure linear behavior of the cables as shown in the last column in the table.

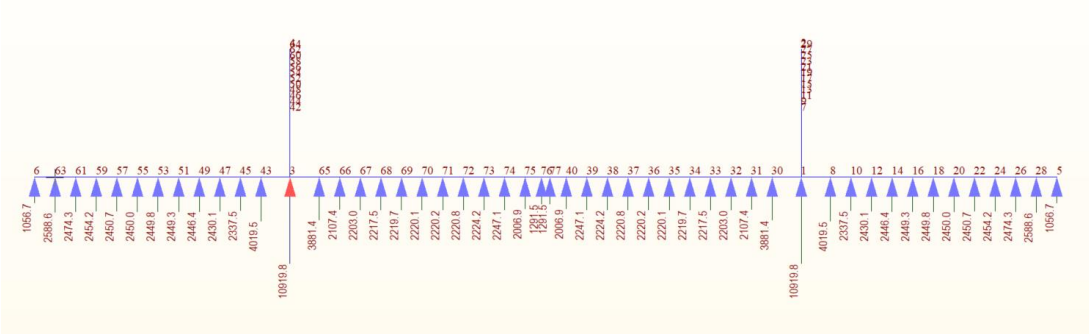

Figure 37 cable as rigid support model

Table 11 Beam on rigid supports results

Cable	Rz [KN]	degree	alpha rad	Sin alpha	Nz	Az, req mm2	n, req	n, prov.	As prov.mm2	N adjusted	As adjusted[mm2]
L1	1056.7	26.31	0.46	0.44	2384.12	2848.41	18.99	35	5250	25	3750
L2	2588.59	27.18	0.47	0.46	5666.02	6769.44	45.13	35	5250	60	9000
L3	2474.31	28.21	0.49	0.47	5234.35	6253.7	41.69	60	9000	75	11250
L4	2454.22	29.43	0.51	0.49	4995.14	5967.9	39.79	60	9000	70	10500

L5	2450.68	30.89	0.54	0.51	4772.86	5702.34	38.02	60	9000	70	10500
L6	2450.04	32.69	0.57	0.54	4535.74	5419.04	36.13	60	9000	75	11250
L7	2449.84	34.95	0.61	0.57	4276.43	5109.24	34.06	60	9000	70	10500
L8	2449.32	37.85	0.66	0.61	3991.77	4769.14	31.79	60	9000	70	10500
L9	2446.45	41.69	0.73	0.67	3678.39	4394.73	29.3	60	9000	55	8250
L10	2430.15	46.96	0.82	0.73	3325.21	3972.77	26.49	60	9000	50	7500
L11	2337.47	54.46	0.95	0.81	2872.52	3431.93	22.88	35	5250	35	5250
L12	4019.5	65.51	1.14	0.91	4416.94	5277.11	35.18	35	5250	35	5250
L13	3881.38	65.51	1.14	0.91	4265.16	5095.77	33.97	35	5250	35	5250
L14	2107.38	54.46	0.95	0.81	2589.76	3094.1	20.63	35	5250	35	5250
L15	2202.99	46.96	0.82	0.73	3014.38	3601.41	24.01	35	5250	35	5250
L16	2217.53	41.69	0.73	0.67	3334.19	3983.5	26.56	60	9000	35	5250
L17	2219.74	37.85	0.66	0.61	3617.61	4322.12	28.81	60	9000	75	11250
L18	2220.09	34.95	0.61	0.57	3875.37	4630.07	30.87	60	9000	75	11250
L19	2220.22	32.69	0.57	0.54	4110.27	4910.71	32.74	60	9000	65	9750
L20	2220.76	30.89	0.54	0.51	4325.07	5167.35	34.45	60	9000	70	10500
L21	2224.24	29.43	0.51	0.49	4527.05	5408.67	36.06	60	9000	70	10500
L22	2247.14	28.21	0.49	0.47	4753.76	5679.52	37.86	60	9000	60	9000
L23	2006.87	27.18	0.47	0.46	4392.73	5248.18	34.99	60	9000	65	9750
L24	1291.48	26.31	0.46	0.44	2913.83	3481.28	23.21	60	9000	60	9000

L1-to L24 are connected to the first pier P1 and cable L25-L48 are connected to pier P2 and they are symmetric to cables from L1to L24.

Internal pretension forces in the cables have been introduced to reach almost zero displacements at the place of the cable anchored with the girder [11], also another criterion is to get no tensile reaction at the abutment support under any combinations of ULS and SLS. To get the pretension in the cables an optimization method has been used provided my Midas Civil, the procedure for the optimization was done as follows:

1) Calculation of the area of the cables as in table 7
2) Provide the value Nz in table 7 as the initial guess for cable pretention.
3) put the constraints on the optimization method in Midas Civil (Unknown Load Factor)
4) the constraints are the lower and upper limits of the deflection in the girder, the abutment reaction to being compression, and the minimum cable pretension to be zero (this is to eliminate the compression forces in the optimization process once the cables have been modeled as truss elements.
5) New values of pretension have been calculated.
6) The area of the cables has been adjusted to fit the stress limits in the ULS.

This process produces cables' forces which when applied to the structure (Without considering construction stages, it applies on the undeformed shape of the structure) produce the same construction constraints in point 4 (which have entered in the Unknown load factor method).

However, during construction, the cable forces are applied to the deformed shape of the segment (due to self-weight and construction load), there is a "Lack of fit forces" which the software calculates from the value of the deflection and add it the cable forces applied on the undeformed structure (Without

considering Construction stages analysis). The figure below shows the “Lack of fit forces” and how the software calculate it. [11]

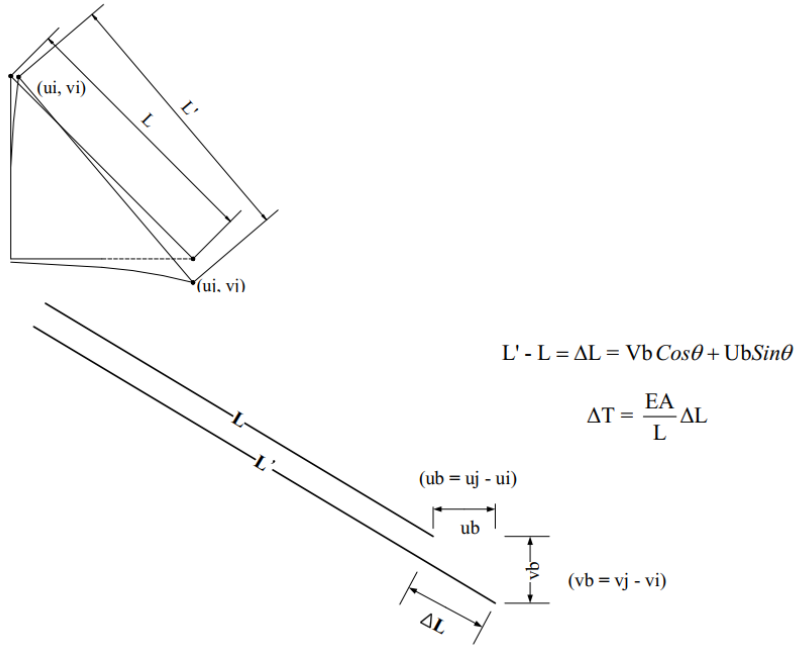

Figure 38 Lack of fit forces in Midas software [11]

The results of forces including lack of fit forces are presented in the following tables.

Table 12 Cable pretension

Cable forces (prestressing of cables)		
span	**Cable**	**F= KN**
Side Span	L1	2144.35
Side Span	L2	4415.11
Side Span	L3	4943.71
Side Span	L4	4893.33
Side Span	L5	4441.52
Side Span	L6	4440.44
Side Span	L7	4440.18
Side Span	L8	4439.48
Side Span	L9	3104.54
Side Span	L10	3084.19
Side Span	L11	2950.33
Side Span	L12	3881.38
Main Span	L13	3881.38
Main Span	L14	2950.33
Main Span	L15	3084.19
Main Span	L16	3104.54
Main Span	L17	4439.48
Main Span	L18	4440.18
Main Span	L19	4440.44
Main Span	L20	4441.52

Main Span	L21	4893.33
Main Span	L22	4943.71
Main Span	L23	4415.11
Main Span	L24	3185.76

The value of the pretensions of cables from L25 toL48 is symmetric to the value from L1to L24.

4.1 Results from the model

In this section, the results of the model in the final stage have been shown from the load cases and load combination with the cable pretension forces, the moment My are in KN.m, Normal forces N are in KN and the shear forces Vz are in the in KN.

The results of the construction stages are discussed later.

4.1.1 Internal forces from the single load cases:

4.1.1.1 Internal forces from self-weight.

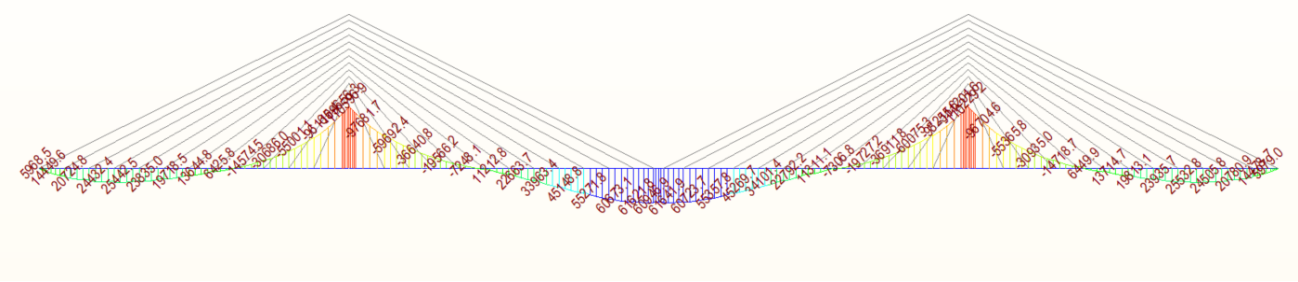

Figure 39 My-Self-weight

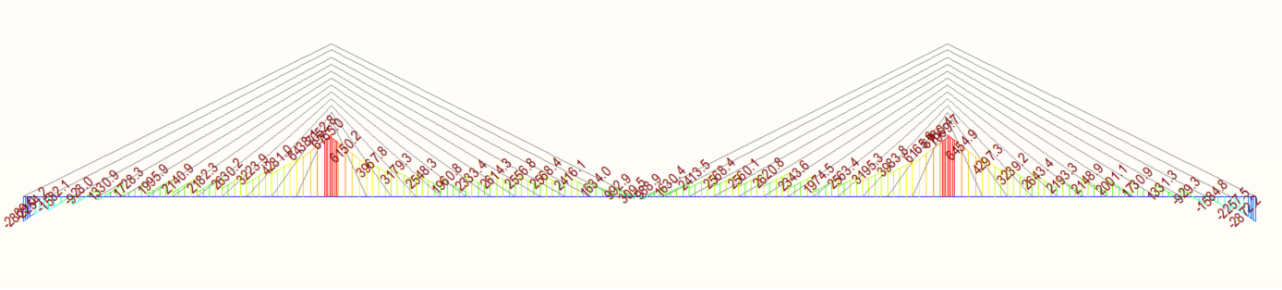

Figure 40 Fz-Self-weight

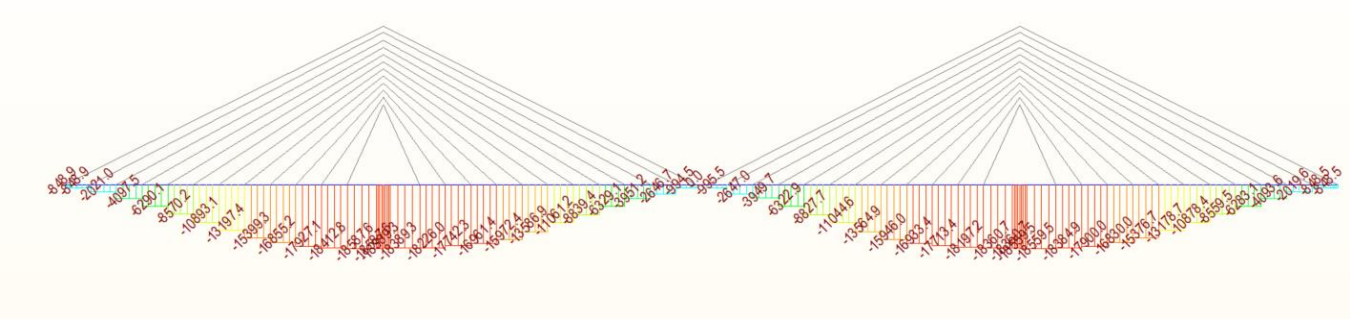

Figure 41 Fx-Self-weight

4.1.1.2 Internal forces from other permanent loads.

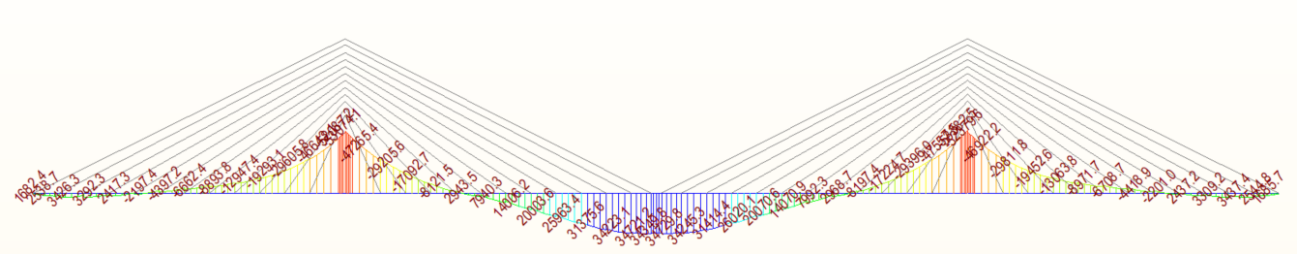

Figure 42 My-Permanent loads

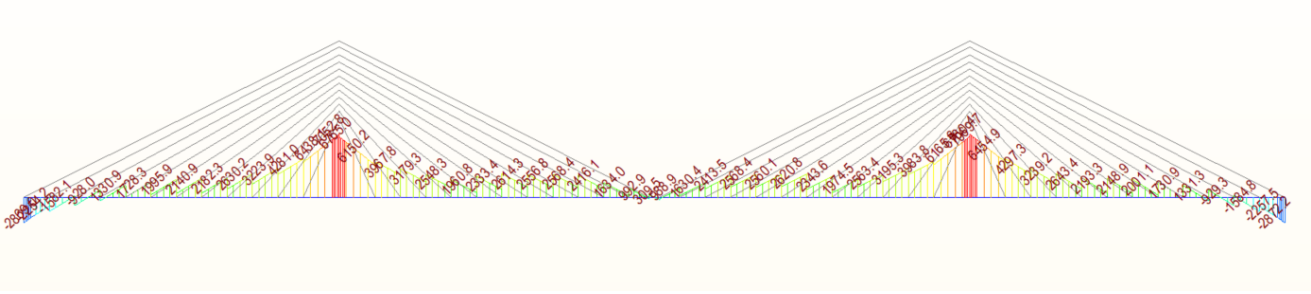

Figure 43 Fz-Permanent loads

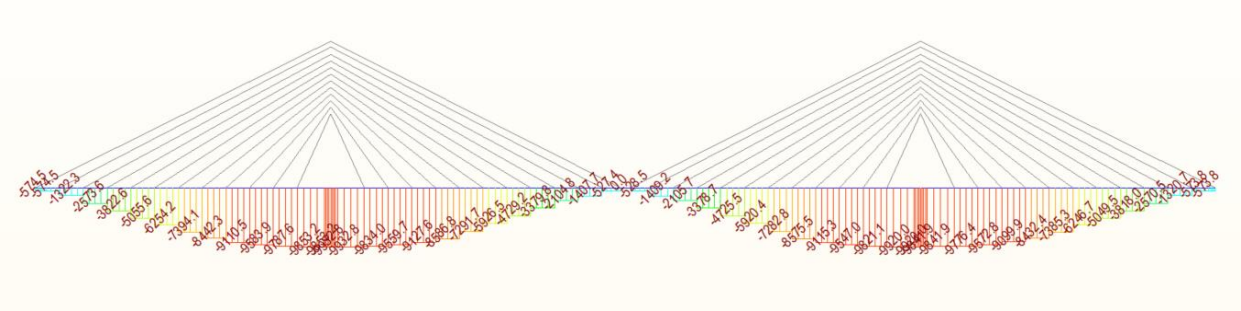

Figure 44 Fx-Permanent loads

4.1.1.3 Internal forces from cables pretension.

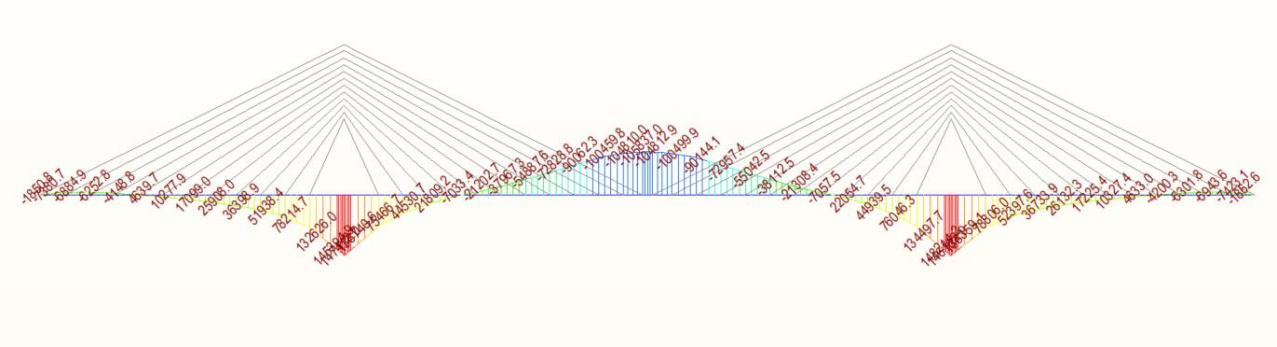

Figure 45 My-Cables pretension

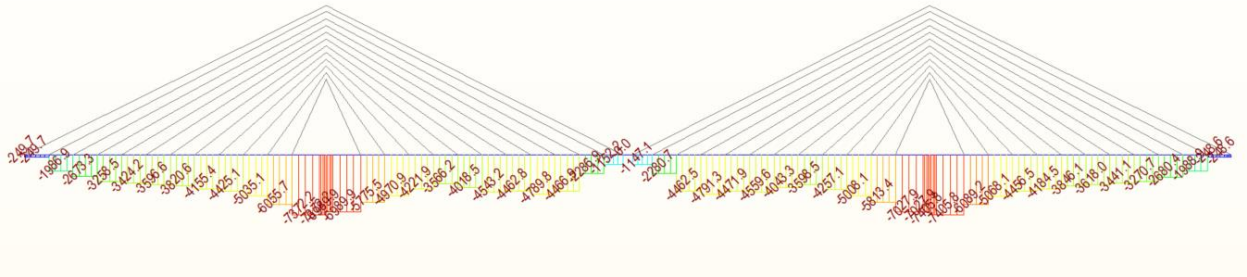

Figure 46 Fx-cables pretension

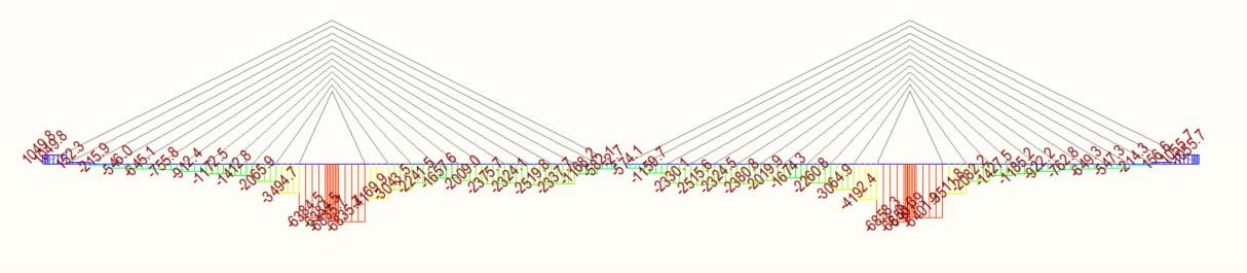

Figure 47 Fz-Cables pretension

4.1.2 Internal forces from load combinations:

4.1.2.1 Internal forces from permanent load + cables pretension.

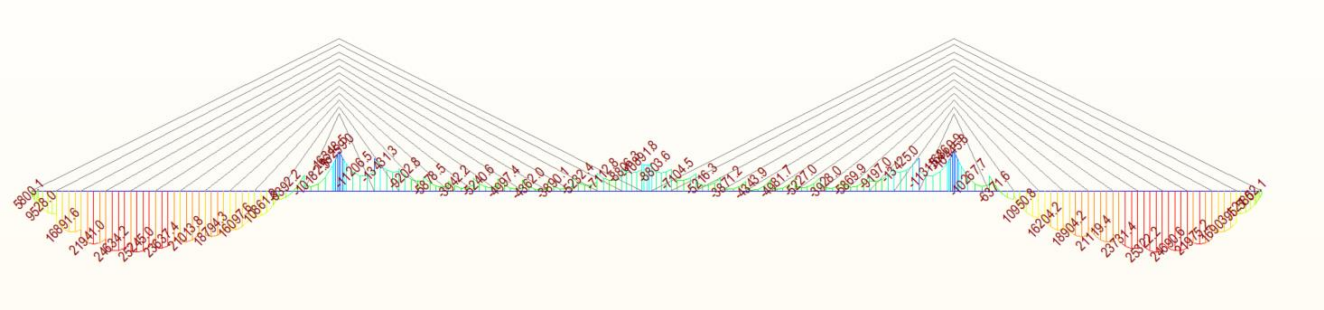

Figure 48 My-permanent load + cables pretension

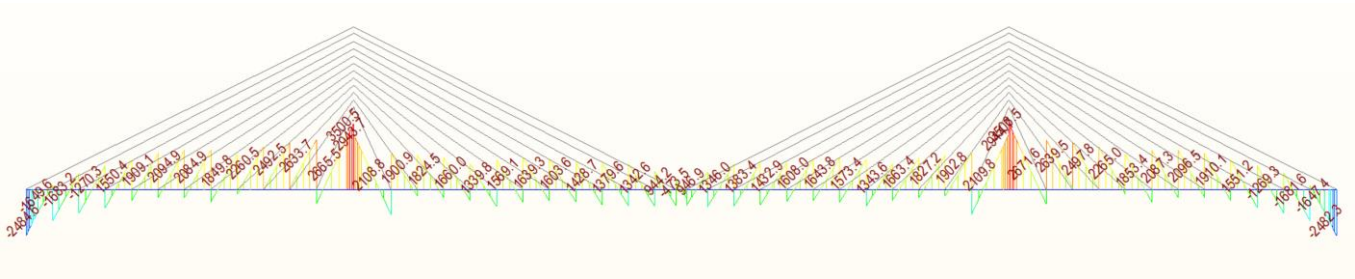

Figure 49 Fz-permanent load + cables pretension

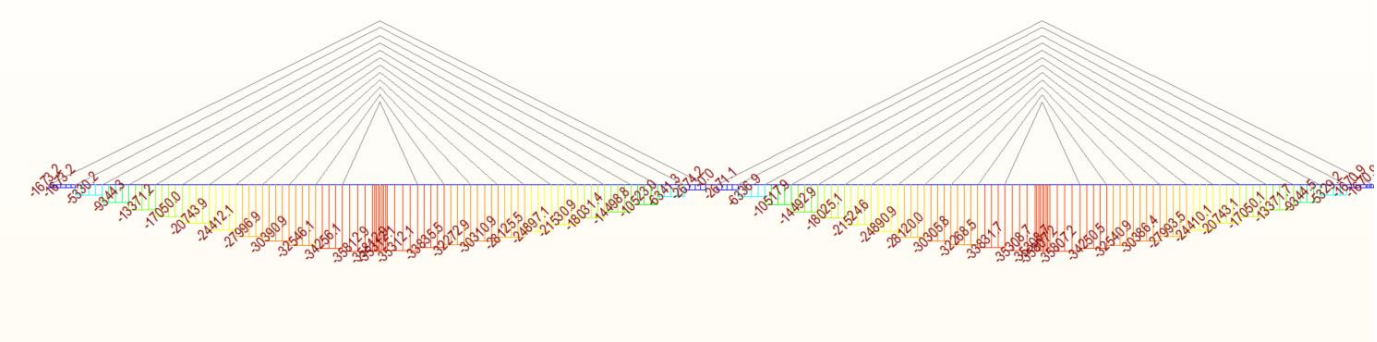

Figure 50 Fx - permanent load + self-wight + cables pretension

4.2 Support reaction

By using the influence line it's possible to calculate the maximum and minimum support reaction using the FEM model in Midas Civil.
In the table below it is shown the vertical reaction for the left abutment(A1) (Near Fixed point), the right abutment(A2), left pier (Near Fixed point) (P1) and right pier(P2) from the Ultimate limit state combination and all the service limit state combinations are summarized in the following table.

Table 13 Reactions from load combinations

		Max.		Min.	
Support	**Combination type**	**Fz [kN]**	**My [KN.m]**	**Fz [kN]2**	**My [KN.m]3**
P1	Ultimate limit state	96706.4	0	87448.6	0
P2	Ultimate limit state	96881.6	0	87232.3	0
A1	Ultimate limit state	7482.8	0	1249.7	0
A2	Ultimate limit state	7511.6	0	1107.7	0
P1	Quasi-permanent combinations-SLS	65390.4	0	65246.5	0
P2	Quasi-permanent combinations-SLS	65502.7	0	65227.4	0
A1	Quasi-permanent combinations-SLS	2201.4	0	2067.7	0
A2	Quasi-permanent combinations-SLS	2211	0	1982.8	0
P1	Characteristic combinations-SLS	70040.1	0	64823.6	0
P2	Characteristic combinations-SLS	69781.3	0	64659.4	0
A1	Characteristic combinations-SLS	6370.4	0	960.6	0
A2	Characteristic combinations-SLS	6651.3	0	863.8	0
P1	Frequent combinations-SLS	67305.6	0	65150.4	0
P2	Frequent combinations-SLS	67187	0	65042.9	0
A1	Frequent combinations-SLS	4066.2	0	1703.6	0
A2	Frequent combinations-SLS	4235	0	1619.2	0

4.3 The stiffness of the cables

Now the stiffness of the cable must be checked, the cable can undergo a geometrical non-linear behavior under low stresses and high length.

In the following figures, it is shown the effect of cable length and stress on the effective stiffness modules E, eff of the cable which has been calculated by Ernst formula form following formula.

$$E_{eff} = \frac{E_0}{1 + \frac{\gamma^2 * l_h^2 * E_0}{12 * \sigma^3}}$$

For high length we need more stress to reach the initial stiffness modules E0

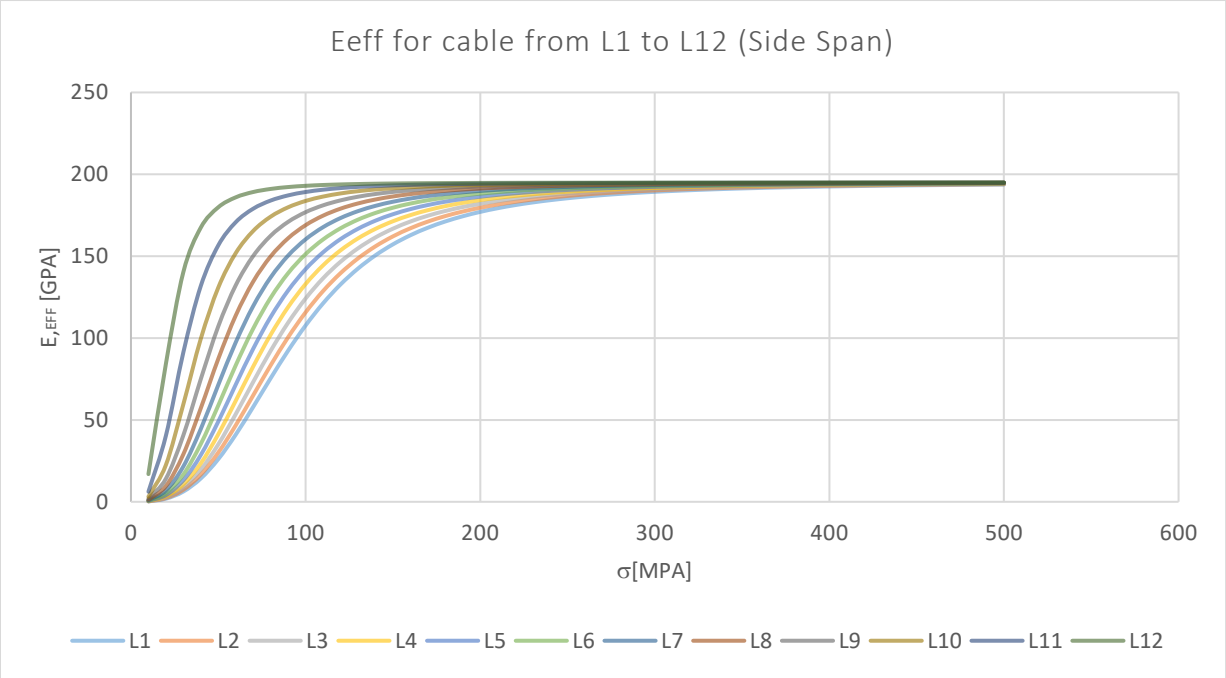

Figure 51 Side span cables nonlinear behavior

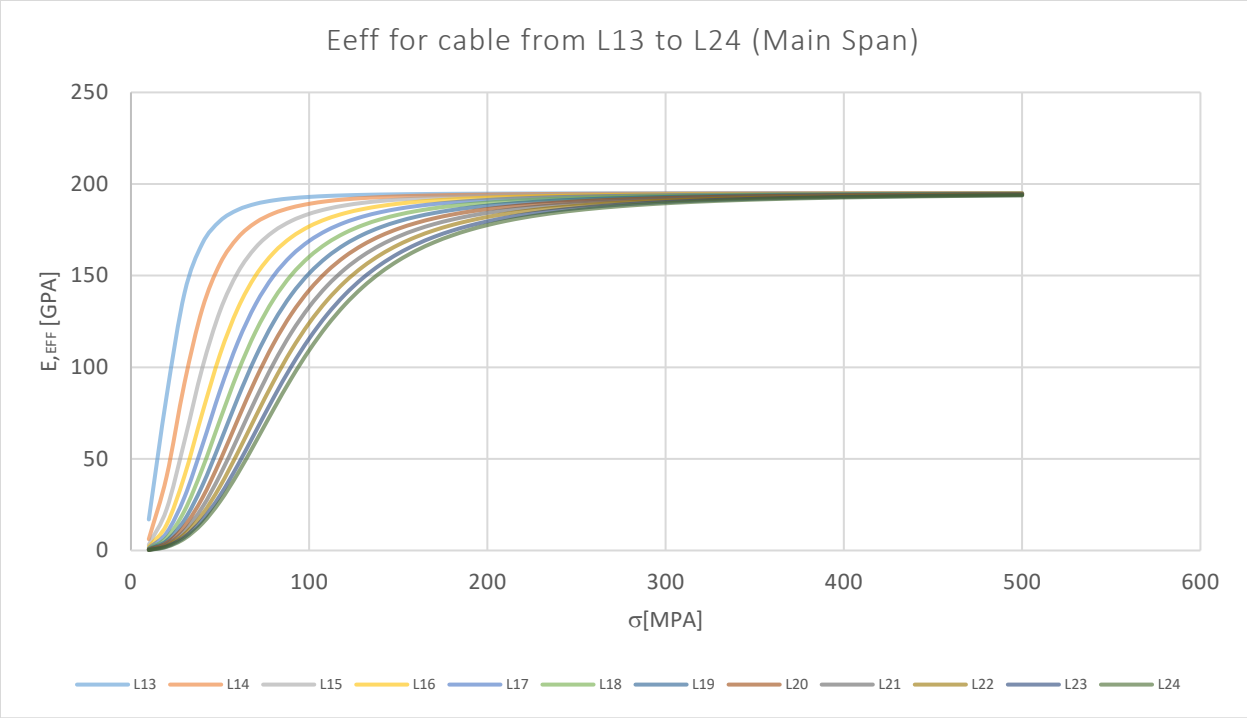

Figure 52 Main span cables nonlinear behavior

In the next table the stresses from permanent load combination and SLS-characteristic combination for each cable and the E, eff and the E, eff/E0 ratio have been calculated.

Table 14 E, eff for Cables of tower Near Fixed Point

Lh[m]	Permenant load[KN]	SLS-Ch-Max[KN]	SLS-Ch-Min[KN]	E.eff Permanent Load[GPa]	E.eff SLS-Ch-Max [GPa]	E.eff SLS-Ch-Min [GPa]	E,eff/E0 Permenant load [GPa]	E,eff/E0 SLS-Ch-Max [GPa]	E,eff/E0 SLS-Ch-Min [GPa]
99.5	472.40	568.3	405.3	193.18	193.95	192.14	0.99	0.99	0.99
93.0	560.40	643	506.9	194.04	194.37	193.71	1.00	1.00	0.99
85.7	362.90	432.1	322.3	192.05	193.24	190.81	0.98	0.99	0.98
78.4	376.00	431.8	348.1	192.77	193.52	192.20	0.99	0.99	0.99
71.1	359.50	404.1	340.6	192.90	193.52	192.53	0.99	0.99	0.99
63.9	374.90	410.6	361.6	193.50	193.86	193.33	0.99	0.99	0.99
56.7	380.00	415.4	366.6	193.86	194.13	193.73	0.99	1.00	0.99
49.7	373.20	409.6	360.4	194.08	194.30	193.97	1.00	1.00	0.99
42.9	380.00	417.4	367.2	194.35	194.51	194.28	1.00	1.00	1.00
35.5	418.80	457.4	404.7	194.66	194.74	194.63	1.00	1.00	1.00
27.7	551.70	588.6	536.1	194.91	194.93	194.90	1.00	1.00	1.00
20.3	689.60	716.5	673.5	194.98	194.98	194.97	1.00	1.00	1.00
20.3	636.30	669.1	624.3	194.97	194.97	194.97	1.00	1.00	1.00
27.7	485.40	532.4	473.7	194.87	194.90	194.86	1.00	1.00	1.00
35.5	527.80	579.8	519.4	194.83	194.87	194.82	1.00	1.00	1.00
42.9	539.80	591.9	534.3	194.77	194.83	194.77	1.00	1.00	1.00
49.7	323.70	373.5	319.5	193.59	194.08	193.53	0.99	1.00	0.99
56.7	348.50	396.1	342.1	193.53	193.99	193.44	0.99	0.99	0.99
63.9	416.70	464.5	406.8	193.91	194.21	193.82	0.99	1.00	0.99
71.1	351.00	399.7	335	192.74	193.47	192.41	0.99	0.99	0.99

78.4	378.90	429.3	355.3	192.82	193.50	192.36	0.99	0.99	0.99
85.7	668.30	721.2	635.6	194.52	194.62	194.44	1.00	1.00	1.00
93.0	381.10	440.5	338.7	191.99	193.04	190.75	0.98	0.99	0.98
99.1	483.40	549.8	432.4	193.32	193.85	192.66	0.99	0.99	0.99
99.1	483.40	543.70	441.80	193.32	193.82	192.80	0.99	0.99	0.99
93.0	380.90	437.10	347.10	191.99	193.00	191.04	0.98	0.99	0.98
85.7	667.40	720.20	642.40	194.52	194.62	194.46	1.00	1.00	1.00
78.4	377.80	427.70	360.70	192.80	193.48	192.48	0.99	0.99	0.99
71.1	349.70	397.70	339.20	192.72	193.44	192.50	0.99	0.99	0.99
63.9	415.30	461.90	409.50	193.89	194.20	193.85	0.99	1.00	0.99
56.7	347.10	394.70	343.20	193.51	193.98	193.46	0.99	0.99	0.99
49.7	322.40	371.40	318.50	193.57	194.06	193.52	0.99	1.00	0.99
42.9	538.80	589.00	532.90	194.77	194.82	194.76	1.00	1.00	1.00
35.5	527.10	576.40	518.70	194.83	194.87	194.82	1.00	1.00	1.00
27.7	485.30	528.80	474.00	194.87	194.90	194.86	1.00	1.00	1.00
20.3	636.50	665.70	622.70	194.97	194.97	194.97	1.00	1.00	1.00
20.3	689.20	733.30	663.00	194.98	194.98	194.97	1.00	1.00	1.00
27.7	550.80	600.80	534.20	194.91	194.93	194.90	1.00	1.00	1.00
35.5	417.60	468.00	405.10	194.66	194.76	194.63	1.00	1.00	1.00
42.9	378.70	428.60	365.60	194.34	194.55	194.27	1.00	1.00	1.00
49.7	372.40	419.40	357.50	194.07	194.35	193.95	1.00	1.00	0.99
56.7	379.40	421.20	363.00	193.86	194.16	193.69	0.99	1.00	0.99
63.9	374.20	411.90	358.50	193.49	193.87	193.29	0.99	0.99	0.99
71.1	358.80	403.60	345.10	192.89	193.51	192.63	0.99	0.99	0.99
78.4	375.30	428.20	354.30	192.76	193.48	192.34	0.99	0.99	0.99
85.7	362.10	427.00	327.00	192.03	193.18	190.99	0.98	0.99	0.98
93.0	559.60	637.90	506.20	194.04	194.35	193.71	1.00	1.00	0.99
99.5	471.30	562.90	398.10	193.17	193.92	191.98	0.99	0.99	0.98

The following figures summarize the results.

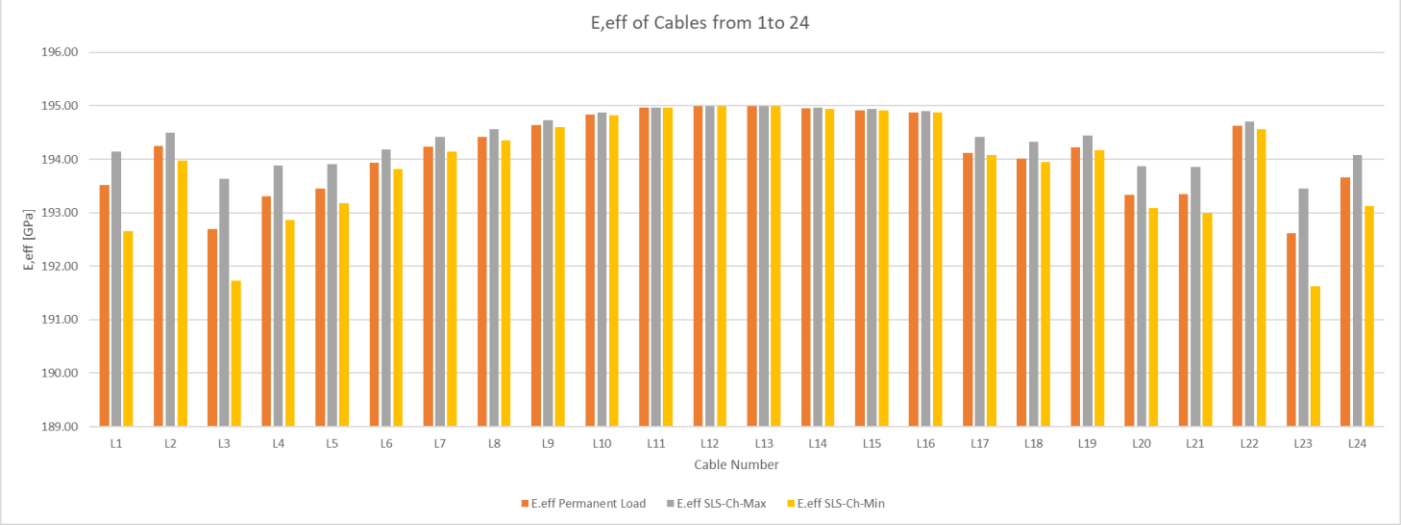

Figure 53 Cables of tower 1to 24

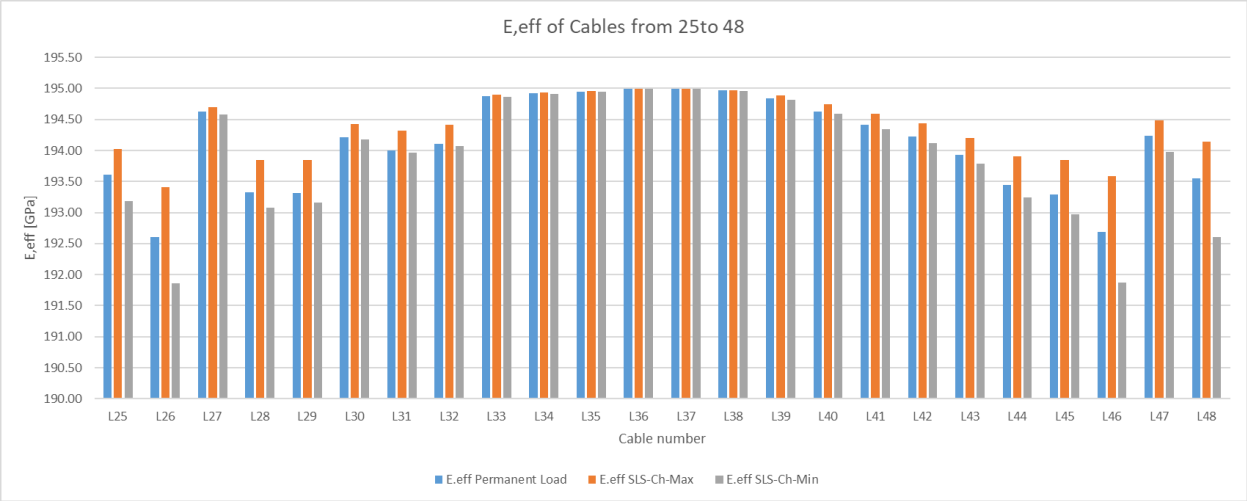

Figure 54 Cables of tower 25 to48

As it is shown that the most cables have developed the E0, the critical cables develop 98% of E0, the following figure shows cable L23 and the developed E, eff = 191.62 GPa.

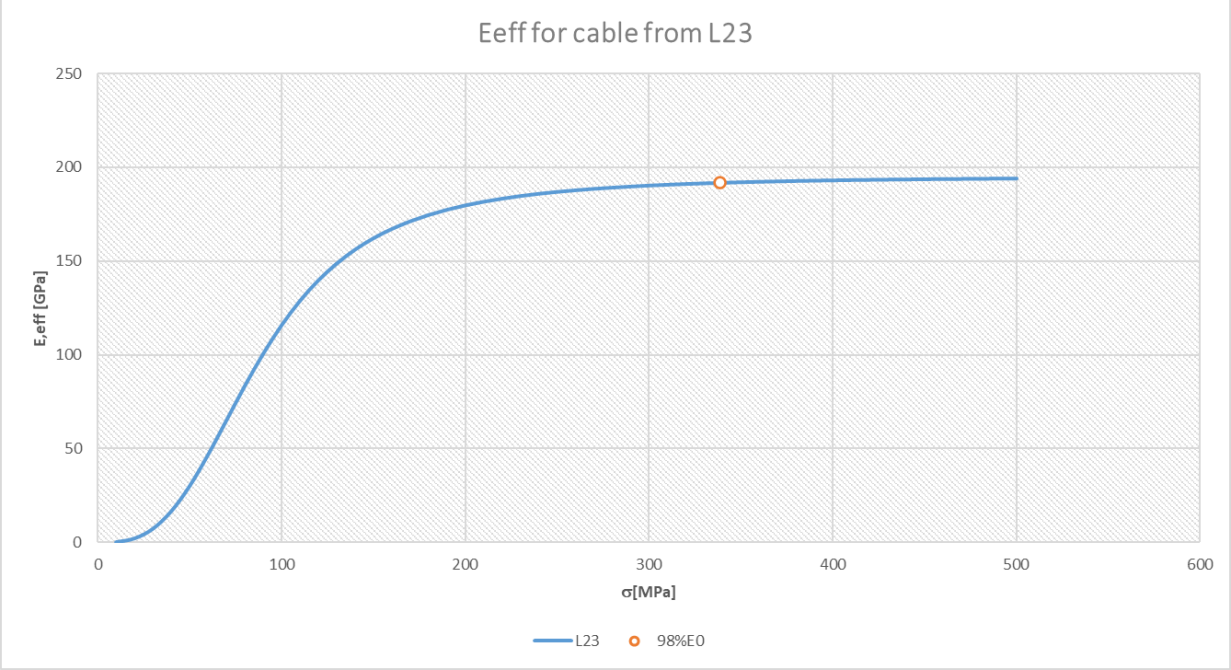

Figure 55 the behavior of the L23 cable

Once almost all cables more than 99% of E0, the nonlinear behavior of the cables can be neglect and linear analysis is enough.

5 Prestressing

5.1 Effective flange width and the shear lag effect

In wide flanges, in-plane shear flexibility leads to a non-uniform distribution of bending stress across the flange width. This effect is known as shear lag. The stress in the flange adjacent to the web is consequently found to be greater than expected from section analysis with gross cross-sections, while the stress in the flange remote from the web is lower than expected. This shear lag also leads to an apparent loss of stiffness of a section in bending. [4]

The determination of the actual distribution of stress is a complex problem that can, in theory, be determined by 3D finite element analysis (with appropriate choice of elements) if realistic behavior of reinforcement and concrete can be modelled. [4]

In this work, the effect of shear lag has been assessed using the plate model, the assessment has been done using different section in the longitudinal direction (in the midspan, near the tower, mid of the side span, near the abutment) for different load cases (Tram load, Pedestrian load, self-weight).

Scale factor has been obtained from this assessment where the scale factor is equal to the highest value of normal force in the section divided by the average value of the normal forces in the section.

This scale factor has been multiplied by the corresponding load case when checking the stresses in the longitudinal direction which obtained from the beam model. So, the effect of shear lag can be included in the beam model. The following figures show the axial force for different sections for different load cases.

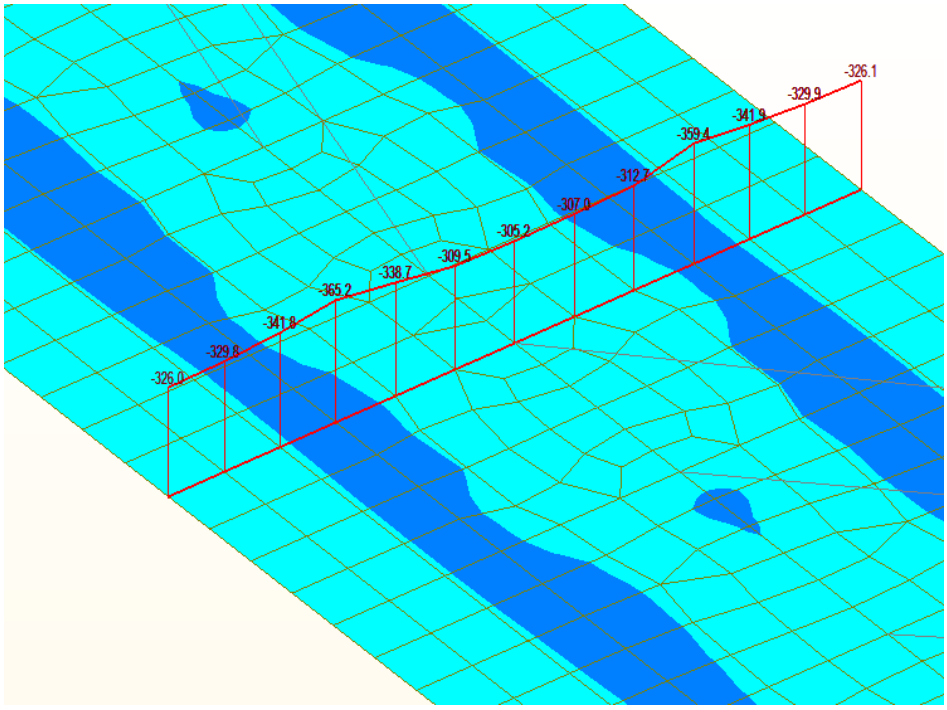

Figure 56 normal force in the top slap @Mid span due to tram loading case

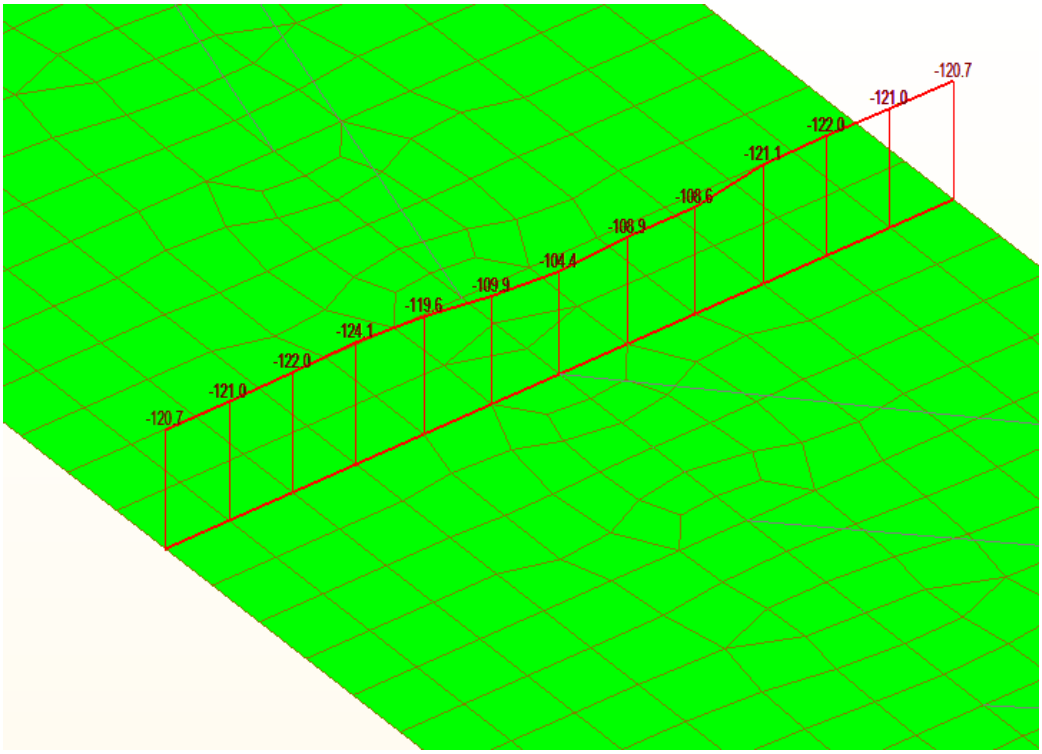

Figure 57 normal force in the top slap @Mid span due to pedestrian loading case

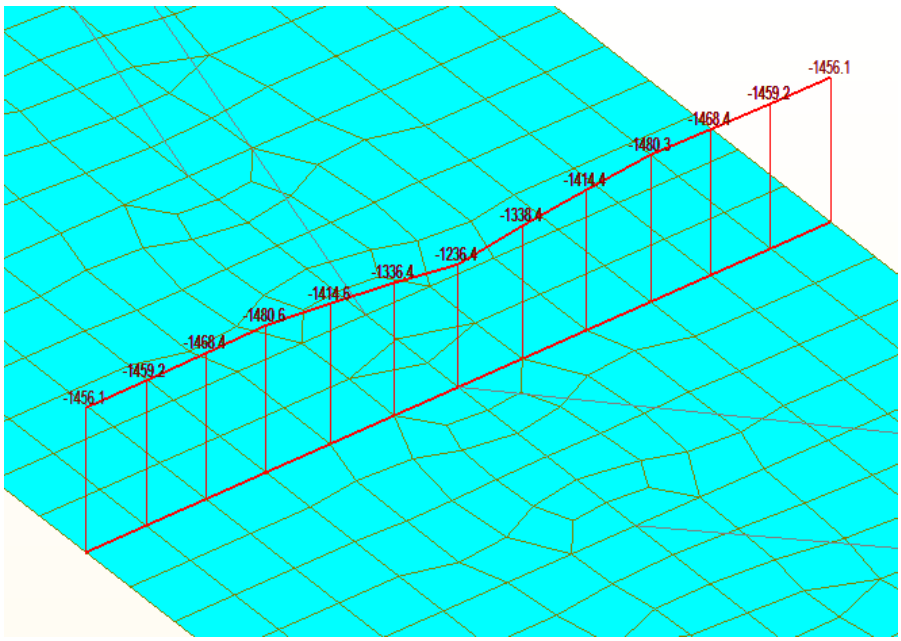

Figure 58 normal force in the top slap @Mid span due to self-weight

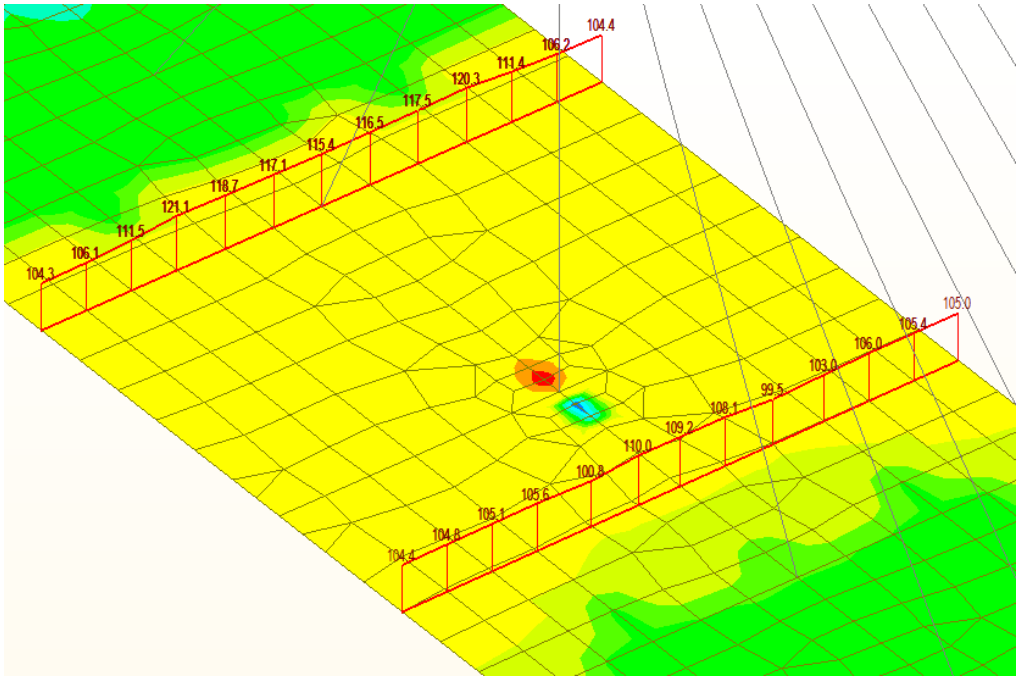

Figure 59 normal force in the top slap near the pier due to tram loading case

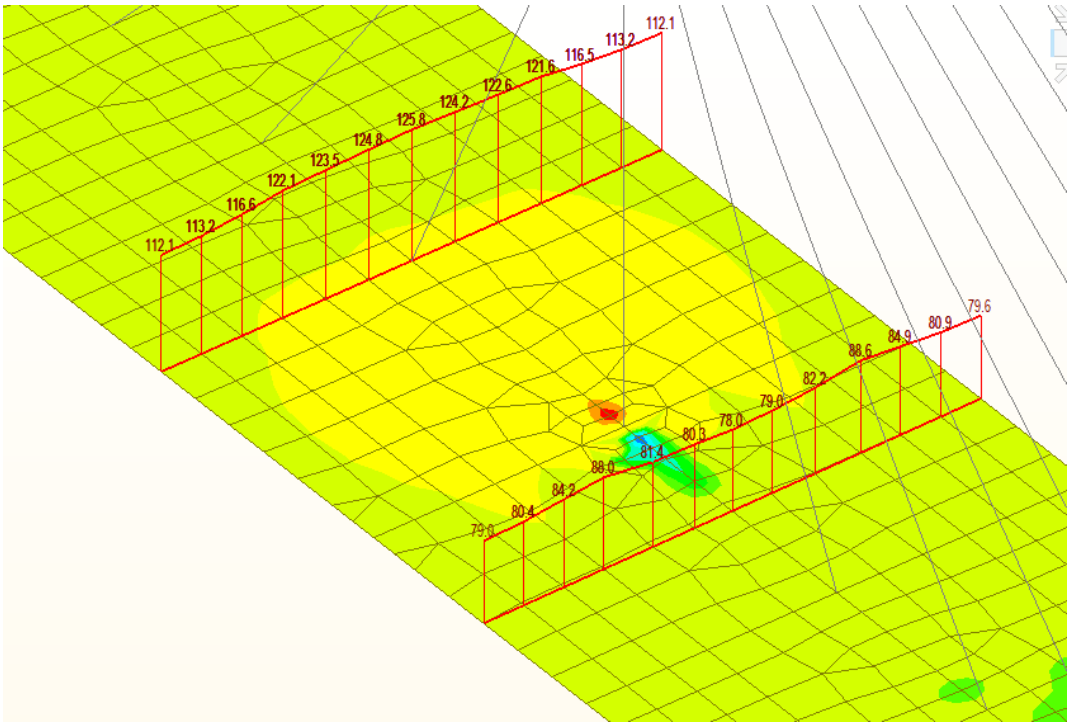

Figure 60normal force in the top slap near the pier due to pedestrian loading case

The following table summarized the result, and the scale factor has been calculated.

Load case	Self-weight			Tram-load			Pedestrian load		
Location of the section	**Avg. Value**	**Max**	**Scale factor**	**Avg. Value**	**Max**	**Scale factor**	**Avg. Value**	**Max**	**Scale factor**
Near the pier (Mid span	1410.86	1503.84	1.07	113.84	121.11	1.06	119.67	125.78	1.05
Near the abutment	-325.07	-350.10	1.08	-179.31	-198.23	1.11	-70.69	-76.85	1.09
Near the pier (Side span)	497.61	593.59	1.19	105.18	109.95	1.05	82.27	88.63	1.08
Middle of the mid span	-1417.71	-1480.63	1.04	-330.58	-365.18	1.10	-116.95	-124.08	1.06
Middle of the side span	-615.55	-623.63	1.01	-388.49	-414.73	1.07	-156.88	-160.59	1.02
Max Scale factor			1.26			1.11			1.09

As it is shown in the table, the tram and pedestrian loading cases have almost uniform scaling factors with low values, the effect of shear lag due to those load cases can be considered by multiplying the tram and pedestrian load with the corresponding scale factor when checking the stresses.

For the self-weight loading, the in the middle of the mid-span and side span can be neglected, for the pier and abutment, in SLS combination, this region is not a critical region for tensile stress because there are good compression stresses also the increase of the compression stresses in this place does not violate any limits.

During the construction temporary post-tension bar have been used Y1230 (40 mm diameter Plain rounded bar), after construction cables have been stressed and all the temporary post-tension have been released.

All the cables are 7-wire strands (150 mm2), the number of strands in the tendons is 12. the cables have been anchored between the abutment and pier segment for side span post-tension cables and between the two piers segment for mid-span cables appears in the appendixes.

The maximum stresses are calculated according to the following equation:

$$\sigma_{p,max} = \min(0{,}8 * f_{pk}; 0{,}9 * f_{p0,1k})$$

$$\sigma_{p,max} = \min(0{,}8 * 1860; 0{,}9 * 1637) = 1473{,}12 \text{ MPa}$$

The cover of the ordinary reinforced concrete is calculated based on the equation below, the class of the concrete (C50/60 - XF2, XD1, XC4), 100-year design life, the class of the construction S5.

$$c_{nom} = c_{mim} + \Delta c_{dev}$$

$$c_{nom} = 40 + 10 = 50 \text{ mm}$$

The cover for post-tension is considered as in the ČSN EN 1992-1-1 as the max of 80mm and the diameter of the used duct.

In this project is has been assumed to use Corrugated plastic duct provided by the VSL company.

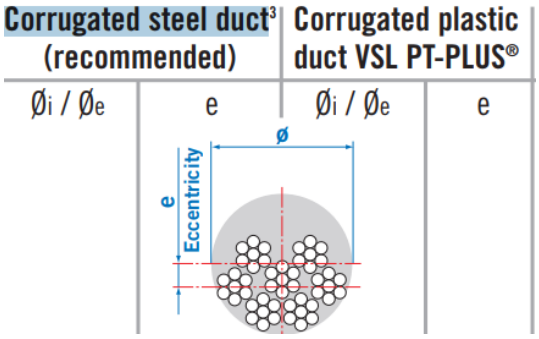

Figure 61 VSL duct for tendon 15mm (0.6'') [12]

The value of the ϕi/ϕe= 65/72 so the cover is equal 80mm. [12]

ANCHORAGES TYPE E @ 43/53 MPa unit 6-12 has been used with the following dimension:

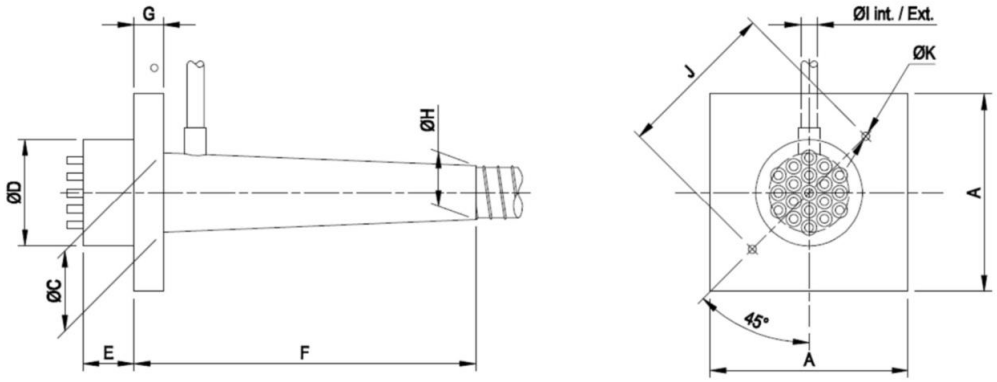

Figure 62 Anchorage's type E @ 43/53 MPa dimensions [13]

Table 15 Anchorage's type E @ 43/53 MPa dimensions [13]

Unit	□A	ØC	Anchor heads E/EP		Anchor heads E(QT)/EP(QT)		F	G	ØH	ØI	J (1)	K
			ØD	E	ØD	E						
6-1	65	18	53	50	53	50	150	10	25	21/25	78	Ø5
6-2	95	50	90	50	86	50	200	10	50	21/25	115	Ø5
6-3	120	56	95	50	95	50	205	15	55	21/25	135	M12
6-4	130	65	110	55	106	50	210	20	60	21/25	150	M12
6-7	160	84	135	60	135	55	315	25	72	28/32	190	M12
6-12	210	118	170	75	166	62	495	35	92	28/32	240	M16
6-15	240	143	190	85	186	68	580	40	97	28/32	275	M16
6-19	270	150	200	95	196	73	635	45	107	28/32	280	M16
6-22	290	172	220	100	216	78	740	50	122	28/32	310	M16
6-27	320	185	240	110	236	85	685	55	132	28/32	330	M16
6-31	340	192	260	120	256	90	750	60	142	28/32	360	M16
6-37	375	215	280	135	276	98	895	65	155	28/32	370	M16
6-43	410	248	320	145	316	105	1020	70	165	28/32	420	M20
6-55	450	255	340	160	340	118	1030	80	185	28/32	452	M20

The force in the cables is calculated from the maximum stress from the following equation:

$$N_p = A_p * \sigma_{p.max}$$

The first design of the cables is done by assuming 25% stresses losses, the statical indeterminant moment is ignored, the stresses are calculated in the upper and lower fibers from the following equations:

$$\sigma_{c,h} = \frac{N_E}{A_c} + \frac{M_E}{W_{el,y,h}} + \frac{N_p}{A_c} + \frac{M_p}{W_{el,y,h}}$$

$$\sigma_{c,d} = \frac{N_E}{A_c} + \frac{M_E}{W_{el,y}} + \frac{N_p}{A_c} + \frac{M_p}{W_{el,y,d}}$$

The initial calculation is done by excel and the stress limit have been checked, the excel table is in the following table:

The following table shows the properties of the cross-sections for the main and side span.

Table 16 Section properties

Prop.	Box girder side span	Box girder main span	Box Girder Pier section
Area (m^2)	10.144	8.554	23.77
Iyy (m^4)	9.528	7.888	14.41
Zh(m)	0.917	0.870	1.12
Zd (m)	1.583	1.630	1.38
Wel, h (mm^3)	10.390	9.062	12.86
Wel, d (mm^3)	6.019	4.840	10.44

																	Ch SLS Env.(max)		Ch SLS Env.(min)		Quasi SLS(max)		Quasi SLS(min)								
Position	Elem	σ,p,ma	ϕ	Ap,1[mm	n,lan	n,h	Ap,h[m]	e,p,h[m	N,ph[MN]	M,ph[MN.m	n,d	Ap,d[mm2]	e,p,d[m	N,pd[MN]	M,pd[MN.m]	σ,d5	σ,h6	σ,d	σ,h	σ,d2	σ,h3	σ,d3	σ,d8	0.45*fc	0.6*fc	fctm	CH SLS	Quasi SLS	CH SLS	Quasi SLS2
0.00	1.00	1104.48	15.70	150.00	12.00	12.00	21600.00	-0.97	-23.86	23.14	12.00	21600.00	1.23	-23.86	-29.34	-4.14	-4.07	-4.28	-4.19	-4.19	-4.12	-4.22	-4.14	-22.50	-30.00	4.10	OK	OK	OK	OK
2.00	2.00	1104.48	15.70	150.00	12.00	12.00	21600.00	-0.77	-23.86	18.30	12.00	21600.00	1.43	-23.86	-34.19	-5.08	-4.99	-6.78	-6.01	-6.39	-5.76	-6.48	-5.82	-22.50	-30.00	4.10	OK	OK	OK	OK
7.25	3.00	1104.48	15.70	150.00	12.00	12.00	21600.00	-0.77	-23.86	18.30	12.00	21600.00	1.43	-23.86	-34.19	-0.84	-2.55	-6.80	-6.05	-5.42	-5.22	-5.70	-5.39	-22.50	-30.00	4.10	OK	OK	OK	OK
14.50	4.00	1104.48	15.70	150.00	12.00	12.00	21600.00	-0.77	-23.86	18.30	12.00	21600.00	1.43	-23.86	-34.19	-0.67	-2.64	-8.77	-7.43	-6.09	-5.80	-6.66	-6.16	-22.50	-30.00	4.10	OK	OK	OK	OK
21.75	5.00	1104.48	15.70	150.00	12.00	12.00	21600.00	-0.77	-23.86	18.30	12.00	21600.00	1.43	-23.86	-34.19	-0.94	-2.99	-10.40	-8.59	-6.71	-6.36	-7.63	-6.92	-22.50	-30.00	4.10	OK	OK	OK	OK
29.00	6.00	1104.48	15.70	150.00	12.00	12.00	21600.00	-0.77	-23.86	18.30	12.00	21600.00	1.43	-23.86	-34.19	-1.45	-3.48	-11.57	-9.48	-7.13	-6.80	-8.44	-7.59	-22.50	-30.00	4.10	OK	OK	OK	OK
36.25	7.00	1104.48	15.70	150.00	12.00	12.00	21600.00	-0.77	-23.86	18.30	12.00	21600.00	1.43	-23.86	-34.19	-2.01	-3.96	-12.25	-10.04	-7.28	-7.04	-9.02	-8.08	-22.50	-30.00	4.10	OK	OK	OK	OK
43.50	8.00	1104.48	15.70	150.00	12.00	12.00	21600.00	-0.77	-23.86	18.30	12.00	21600.00	1.43	-23.86	-34.19	-2.90	-4.64	-12.85	-10.57	-7.57	-7.38	-9.71	-8.64	-22.50	-30.00	4.10	OK	OK	OK	OK
50.75	9.00	1104.48	15.70	150.00	12.00	12.00	21600.00	-0.77	-23.86	18.30	12.00	21600.00	1.43	-23.86	-34.19	-3.62	-5.17	-13.21	-10.89	-7.81	-7.62	-10.28	-9.08	-22.50	-30.00	4.10	OK	OK	OK	OK
58.00	10.00	1104.48	15.70	150.00	12.00	12.00	21600.00	-0.77	-23.86	18.30	12.00	21600.00	1.43	-23.86	-34.19	-4.57	-5.88	-13.92	-11.46	-8.42	-8.14	-11.15	-9.74	-22.50	-30.00	4.10	OK	OK	OK	OK
65.25	11.00	1104.48	15.70	150.00	12.00	12.00	21600.00	-0.77	-23.86	18.30	12.00	21600.00	1.43	-23.86	-34.19	-4.64	-6.00	-13.84	-11.49	-8.17	-8.07	-11.16	-9.82	-22.50	-30.00	4.10	OK	OK	OK	OK
72.50	12.00	1104.48	15.70	150.00	12.00	12.00	21600.00	-0.77	-23.86	18.30	12.00	21600.00	1.43	-23.86	-34.19	-5.94	-6.79	-14.58	-11.96	-8.77	-8.46	-11.96	-10.33	-22.50	-30.00	4.10	OK	OK	OK	OK
79.75	13.00	1104.48	15.70	150.00	12.00	12.00	21600.00	-0.77	-23.86	18.30	12.00	21600.00	1.43	-23.86	-34.19	-7.95	-8.04	-16.73	-13.29	-10.59	-9.59	-14.03	-11.60	-22.50	-30.00	4.10	OK	OK	OK	OK
88.00	14.00	1104.48	15.70	150.00	12.00	12.00	21600.00	-0.97	-23.86	23.14	12.00	21600.00	1.23	-23.86	-29.34	-5.50	-5.65	-10.84	-10.05	-6.84	-6.75	-9.04	-8.55	-22.50	-30.00	4.10	OK	OK	OK	OK
92.00	15.00	1104.48	15.70	150.00	12.00	12.00	21600.00	-0.97	-23.86	23.14	12.00	21600.00	1.23	-23.86	-29.34	-9.32	-8.72	-15.11	-13.48	-10.78	-9.91	-13.18	-11.87	-22.50	-30.00	4.10	OK	OK	OK	OK
100.25	16.00	1104.48	15.70	150.00	12.00	12.00	21600.00	-0.72	-23.86	17.19	12.00	21600.00	1.48	-23.86	-35.30	-13.75	-11.71	-25.10	-18.00	-17.11	-13.54	-21.80	-16.07	-22.50	-30.00	4.10	OK	OK	OK	OK
107.50	17.00	1104.48	15.70	150.00	12.00	12.00	21600.00	-0.72	-23.86	17.19	12.00	21600.00	1.48	-23.86	-35.30	-12.07	-10.81	-23.05	-16.90	-15.82	-12.84	-20.06	-15.14	-22.50	-30.00	4.10	OK	OK	OK	OK
114.75	18.00	1104.48	15.70	150.00	12.00	12.00	21600.00	-0.72	-23.86	17.19	12.00	21600.00	1.48	-23.86	-35.30	-13.20	-11.40	-23.94	-17.36	-17.32	-13.63	-21.22	-15.75	-22.50	-30.00	4.10	OK	OK	OK	OK
122.00	19.00	1104.48	15.70	150.00	12.00	12.00	21600.00	-0.72	-23.86	17.19	12.00	21600.00	1.48	-23.86	-35.30	-11.40	-10.20	-21.80	-15.97	-15.76	-12.56	-19.33	-14.50	-22.50	-30.00	4.10	OK	OK	OK	OK
129.25	20.00	1104.48	15.70	150.00	12.00	12.00	21600.00	-0.72	-23.86	17.19	12.00	21600.00	1.48	-23.86	-35.30	-8.19	-8.28	-18.06	-13.77	-12.63	-10.69	-15.85	-12.44	-22.50	-30.00	4.10	OK	OK	OK	OK
136.50	21.00	1104.48	15.70	150.00	12.00	12.00	21600.00	-0.72	-23.86	17.19	12.00	21600.00	1.48	-23.86	-35.30	-5.16	-6.55	-15.02	-12.01	-9.88	-9.10	-12.91	-10.76	-22.50	-30.00	4.10	OK	OK	OK	OK
143.75	22.00	1104.48	15.70	150.00	12.00	12.00	21600.00	-0.72	-23.86	17.19	12.00	21600.00	1.48	-23.86	-35.30	-2.43	-4.92	-12.33	-10.39	-7.48	-7.65	-10.34	-9.22	-22.50	-30.00	4.10	OK	OK	OK	OK
151.00	23.00	1104.48	15.70	150.00	12.00	12.00	21600.00	-0.72	-23.86	17.19	12.00	21600.00	1.48	-23.86	-35.30	-1.27	-4.21	-11.12	-9.63	-6.62	-7.10	-9.31	-8.57	-22.50	-30.00	4.10	OK	OK	OK	OK
158.25	24.00	1104.48	15.70	150.00	12.00	12.00	21600.00	-0.72	-23.86	17.19	12.00	21600.00	1.48	-23.86	-35.30	-0.06	-3.33	-9.75	-8.64	-5.68	-6.36	-8.19	-7.73	-22.50	-30.00	4.10	OK	OK	OK	OK
165.50	25.00	1104.48	15.70	150.00	12.00	12.00	21600.00	-0.72	-23.86	17.19	12.00	21600.00	1.48	-23.86	-35.30	-0.32	-3.36	-10.20	-8.74	-6.13	-6.49	-8.90	-8.00	-22.50	-30.00	4.10	OK	OK	OK	OK
172.75	26.00	1104.48	15.70	150.00	12.00	12.00	21600.00	-0.72	-23.86	17.19	12.00	21600.00	1.48	-23.86	-35.30	-0.21	-3.03	-10.30	-8.49	-6.13	-6.20	-9.20	-7.87	-22.50	-30.00	4.10	OK	OK	OK	OK
178.50	27.00	1104.48	15.70	150.00	12.00	12.00	21600.00	-0.72	-23.86	17.19	12.00	21600.00	1.48	-23.86	-35.30	-1.20	-3.46	-11.23	-8.85	-7.13	-6.64	-10.35	-8.37	-22.50	-30.00	4.10	OK	OK	OK	OK
178.50	28.00	1104.48	15.70	150.00	12.00	12.00	21600.00	-0.72	-23.86	17.19	12.00	21600.00	1.48	-23.86	-35.30	-1.50	-3.40	-11.49	-8.74	-7.40	-6.55	-10.63	-8.27	-22.50	-30.00	4.10	OK	OK	OK	OK
181.50	29.00	1104.48	15.70	150.00	12.00	12.00	21600.00	-0.72	-23.86	17.19	12.00	21600.00	1.48	-23.86	-35.30	-1.18	-3.45	-11.21	-8.84	-7.12	-6.63	-10.37	-8.38	-22.50	-30.00	4.10	OK	OK	OK	OK
187.25	30.00	1104.48	15.70	150.00	12.00	12.00	21600.00	-0.72	-23.86	17.19	12.00	21600.00	1.48	-23.86	-35.30	-0.13	-2.98	-10.21	-8.44	-6.10	-6.19	-9.29	-7.92	-22.50	-30.00	4.10	OK	OK	OK	OK
194.50	31.00	1104.48	15.70	150.00	12.00	12.00	21600.00	-0.72	-23.86	17.19	12.00	21600.00	1.48	-23.86	-35.30	-0.19	-3.29	-10.04	-8.66	-6.08	-6.46	-9.04	-8.08	-22.50	-30.00	4.10	OK	OK	OK	OK
201.75	32.00	1104.48	15.70	150.00	12.00	12.00	21600.00	-0.72	-23.86	17.19	12.00	21600.00	1.48	-23.86	-35.30	0.13	-3.21	-9.43	-8.47	-5.61	-6.32	-8.25	-7.78	-22.50	-30.00	4.10	OK	OK	OK	OK
209.00	33.00	1104.48	15.70	150.00	12.00	12.00	21600.00	-0.72	-23.86	17.19	12.00	21600.00	1.48	-23.86	-35.30	-1.03	-4.07	-10.61	-9.36	-6.54	-7.05	-9.22	-8.54	-22.50	-30.00	4.10	OK	OK	OK	OK
216.25	34.00	1104.48	15.70	150.00	12.00	12.00	21600.00	-0.72	-23.86	17.19	12.00	21600.00	1.48	-23.86	-35.30	-2.15	-4.76	-11.83	-10.13	-7.39	-7.60	-10.27	-9.19	-22.50	-30.00	4.10	OK	OK	OK	OK
223.50	35.00	1104.48	15.70	150.00	12.00	12.00	21600.00	-0.72	-23.86	17.19	12.00	21600.00	1.48	-23.86	-35.30	-4.85	-6.37	-14.57	-11.78	-9.77	-9.04	-12.86	-10.74	-22.50	-30.00	4.10	OK	OK	OK	OK
230.75	36.00	1104.48	15.70	150.00	12.00	12.00	21600.00	-0.72	-23.86	17.19	12.00	21600.00	1.48	-23.86	-35.30	-7.91	-8.11	-17.83	-13.65	-12.53	-10.63	-15.83	-12.44	-22.50	-30.00	4.10	OK	OK	OK	OK
238.00	37.00	1104.48	15.70	150.00	12.00	12.00	21600.00	-0.72	-23.86	17.19	12.00	21600.00	1.48	-23.86	-35.30	-11.13	-10.03	-21.67	-15.91	-15.65	-12.49	-19.35	-14.52	-22.50	-30.00	4.10	OK	OK	OK	OK
245.25	38.00	1104.48	15.70	150.00	12.00	12.00	21600.00	-0.72	-23.86	17.19	12.00	21600.00	1.48	-23.86	-35.30	-12.83	-11.18	-23.95	-17.37	-17.16	-13.54	-21.30	-15.80	-22.50	-30.00	4.10	OK	OK	OK	OK
252.50	39.00	1104.48	15.70	150.00	12.00	12.00	21600.00	-0.72	-23.86	17.19	12.00	21600.00	1.48	-23.86	-35.30	-11.61	-10.54	-23.20	-16.98	-15.60	-12.72	-20.20	-15.23	-22.50	-30.00	4.10	OK	OK	OK	OK
259.75	40.00	1104.48	15.70	150.00	12.00	12.00	21600.00	-0.72	-23.86	17.19	12.00	21600.00	1.48	-23.86	-35.30	-13.06	-11.33	-25.42	-18.18	-16.77	-13.35	-22.02	-16.20	-22.50	-30.00	4.10	OK	OK	OK	OK
268.00	41.00	1104.48	15.70	150.00	12.00	12.00	21600.00	-0.97	-23.86	23.14	12.00	21600.00	1.23	-23.86	-29.34	-8.85	-8.34	-15.36	-13.69	-10.54	-9.72	-13.34	-12.00	-22.50	-30.00	4.10	OK	OK	OK	OK
272.00	42.00	1104.48	15.70	150.00	12.00	12.00	21600.00	-0.97	-23.86	23.14	12.00	21600.00	1.23	-23.86	-29.34	-4.63	-4.94	-11.39	-10.50	-6.41	-6.40	-9.35	-8.80	-22.50	-30.00	4.10	OK	OK	OK	OK
280.25	43.00	1104.48	15.70	150.00	12.00	12.00	21600.00	-0.77	-23.86	18.30	12.00	21600.00	1.43	-23.86	-34.19	-6.64	-7.26	-17.53	-13.76	-9.93	-9.20	-14.47	-11.87	-22.50	-30.00	4.10	OK	OK	OK	OK
287.50	44.00	1104.48	15.70	150.00	12.00	12.00	21600.00	-0.77	-23.86	18.30	12.00	21600.00	1.43	-23.86	-34.19	-4.61	-6.00	-15.18	-12.32	-8.24	-8.14	-12.29	-10.53	-22.50	-30.00	4.10	OK	OK	OK	OK
294.75	45.00	1104.48	15.70	150.00	12.00	12.00	21600.00	-0.77	-23.86	18.30	12.00	21600.00	1.43	-23.86	-34.19	-3.87	-5.53	-14.17	-11.69	-7.77	-7.83	-11.35	-9.94	-22.50	-30.00	4.10	OK	OK	OK	OK
302.00	46.00	1104.48	15.70	150.00	12.00	12.00	21600.00	-0.77	-23.86	18.30	12.00	21600.00	1.43	-23.86	-34.19	-3.94	-5.50	-14.03	-11.54	-8.08	-7.94	-11.24	-9.80	-22.50	-30.00	4.10	OK	OK	OK	OK
309.25	47.00	1104.48	15.70	150.00	12.00	12.00	21600.00	-0.77	-23.86	18.30	12.00	21600.00	1.43	-23.86	-34.19	-3.29	-4.96	-13.18	-10.88	-7.59	-7.49	-10.28	-9.09	-22.50	-30.00	4.10	OK	OK	OK	OK
316.50	48.00	1104.48	15.70	150.00	12.00	12.00	21600.00	-0.77	-23.86	18.30	12.00	21600.00	1.43	-23.86	-34.19	-3.08	-4.73	-12.77	-10.53	-7.45	-7.30	-9.64	-8.61	-22.50	-30.00	4.10	OK	OK	OK	OK
323.75	49.00	1104.48	15.70	150.00	12.00	12.00	21600.00	-0.77	-23.86	18.30	12.00	21600.00	1.43	-23.86	-34.19	-2.80	-4.40	-12.13	-9.98	-7.19	-6.98	-8.92	-8.03	-22.50	-30.00	4.10	OK	OK	OK	OK
331.00	50.00	1104.48	15.70	150.00	12.00	12.00	21600.00	-0.77	-23.86	18.30	12.00	21600.00	1.43	-23.86	-34.19	-2.62	-4.15	-11.43	-9.41	-7.01	-6.73	-8.33	-7.53	-22.50	-30.00	4.10	OK	OK	OK	OK
338.25	51.00	1104.48	15.70	150.00	12.00	12.00	21600.00	-0.77	-23.86	18.30	12.00	21600.00	1.43	-23.86	-34.19	-2.60	-3.94	-10.27	-8.52	-6.61	-6.30	-7.53	-6.86	-22.50	-30.00	4.10	OK	OK	OK	OK
345.50	52.00	1104.48	15.70	150.00	12.00	12.00	21600.00	-0.77	-23.86	18.30	12.00	21600.00	1.43	-23.86	-34.19	-2.86	-3.91	-8.67	-7.37	-6.03	-5.77	-6.58	-6.11	-22.50	-30.00	4.10	OK	OK	OK	OK
352.75	53.00	1104.48	15.70	150.00	12.00	12.00	21600.00	-0.77	-23.86	18.30	12.00	21600.00	1.43	-23.86	-34.19	-3.57	-4.13	-6.75	-6.02	-5.39	-5.20	-5.65	-5.36	-22.50	-30.00	4.10	OK	OK	OK	OK
358.00	54.00	1104.48	15.70	150.00	12.00	12.00	21600.00	-0.77	-23.86	18.30	12.00	21600.00	1.43	-23.86	-34.19	-5.83	-5.42	-6.77	-6.00	-6.38	-5.75	-6.47	-5.82	-22.50	-30.00	4.10	OK	OK	OK	OK
360.00	55.00	1104.48	15.70	150.00			0.00	-0.97	0.00	0.00		0.00	1.23	0.00	0.00	0.11	0.07	-0.03	-0.06	0.06	0.02	0.02	-0.01	-22.50	-30.00	4.10	OK	OK	OK	OK

the value of stresses in the upper and lower fiber have been plotted against position as in the following figures:

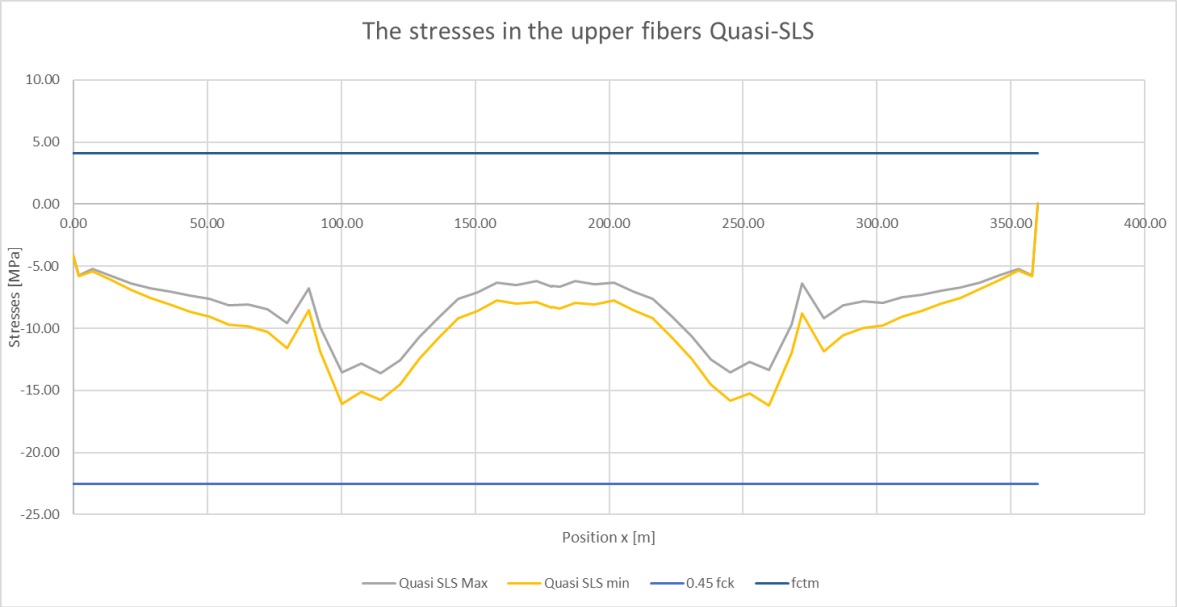

Figure 63 The stresses in the upper fibers Quasi-permeant SLS

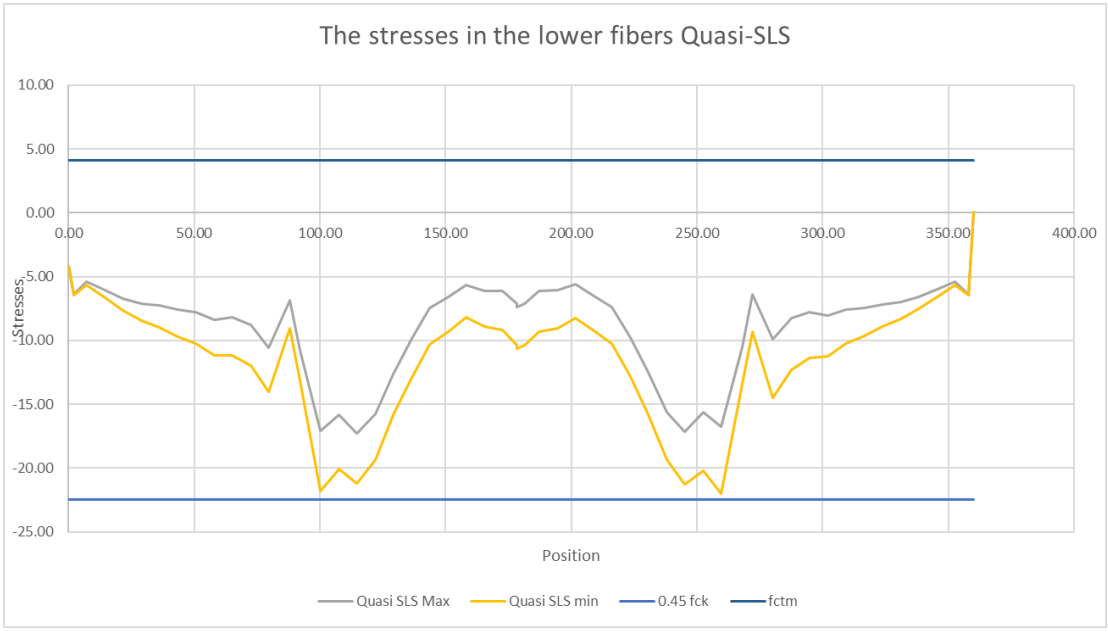

Figure 64 The stresses in the lower fibers Quasi-permeant SLS

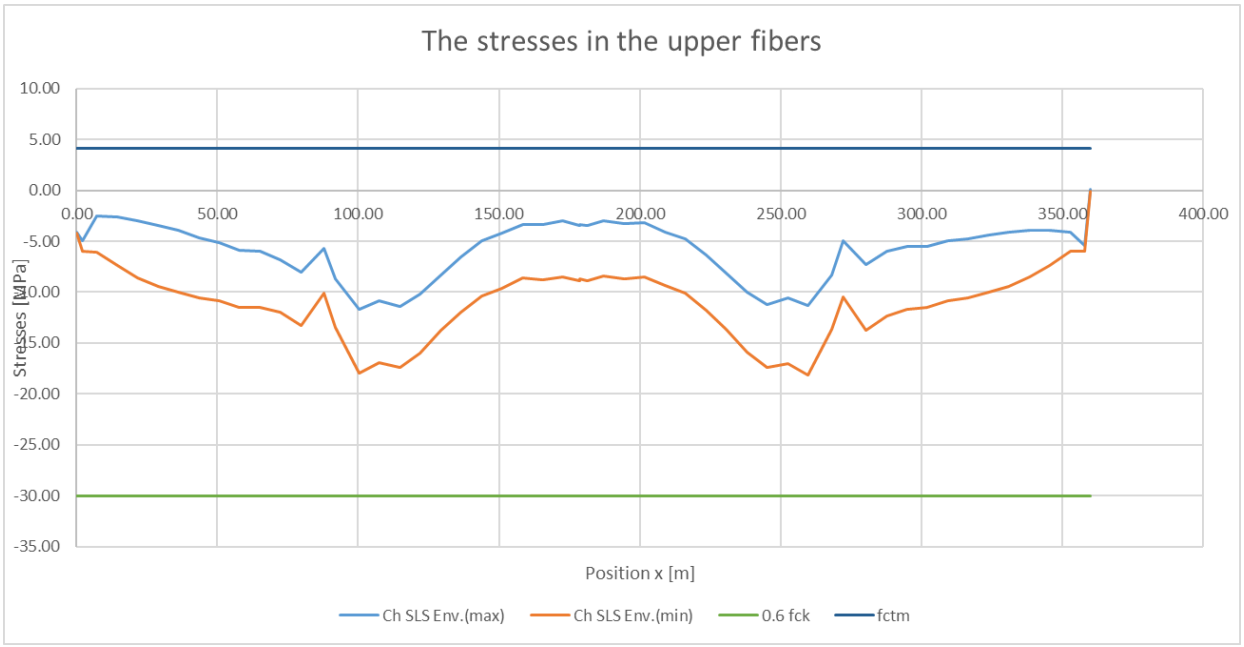

Figure 65 The stresses in the upper fibers Ch-SLS

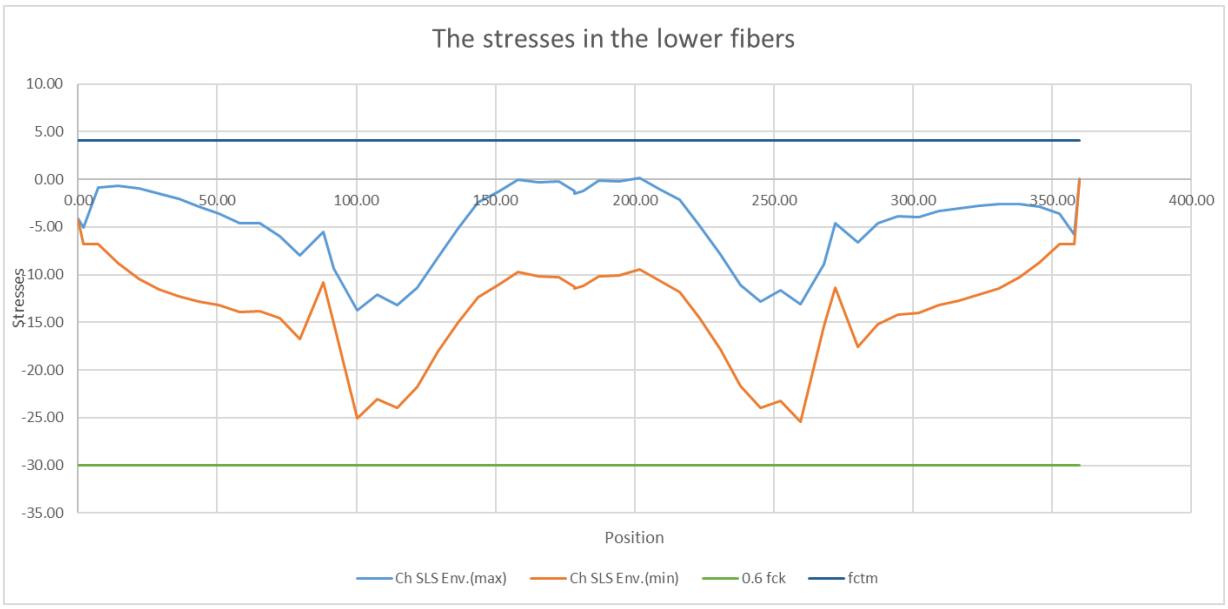

Figure 66 The stresses in the lower fibers Ch-SLS

The below fig. shows the used of eccentricity along the bridge.

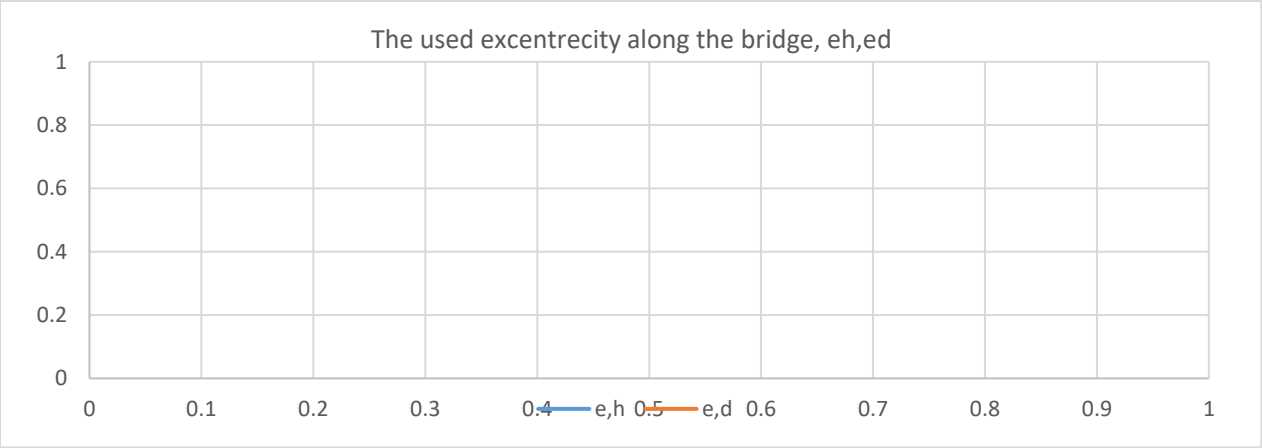

Figure 67 eh, ed vs x

12 cables have been used for the upper & lower slab; each cable have 12*7-wire strands (150mm2 area).

The following figure shows the distribution of the cables in the cross section for the main span section, side span section and pier section (also abutment section).

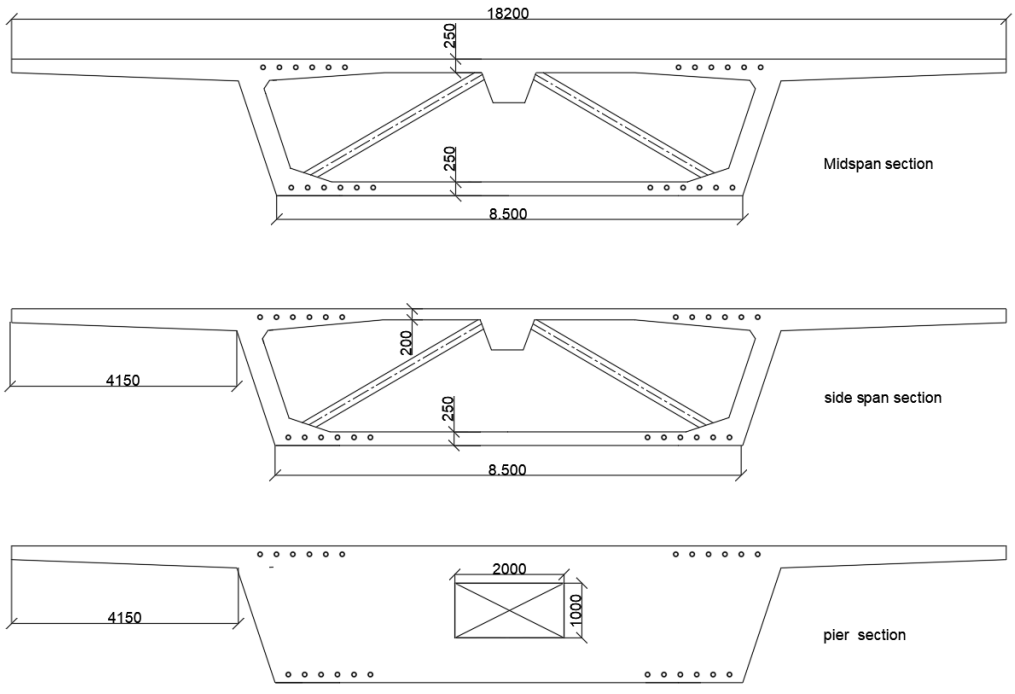

Figure 68 Distribution of post-tension cables in the sections

For the construction stages, temporary prestressed bars have been used with an anchorage at rib (Temporary bar anchorage blister) constructed at the location of the cable anchorage at the upper and lower slab.

22 bars 40mm (Y1230H-40.0-P) have been used for each slab, the following figure shows the temporary prestressed bars. Fpk=1230 Mpa and fp0.1k=1080 Mpa, the stressing force is the min (0.8*1230,0.9*1080)=970 Mpa. [14]

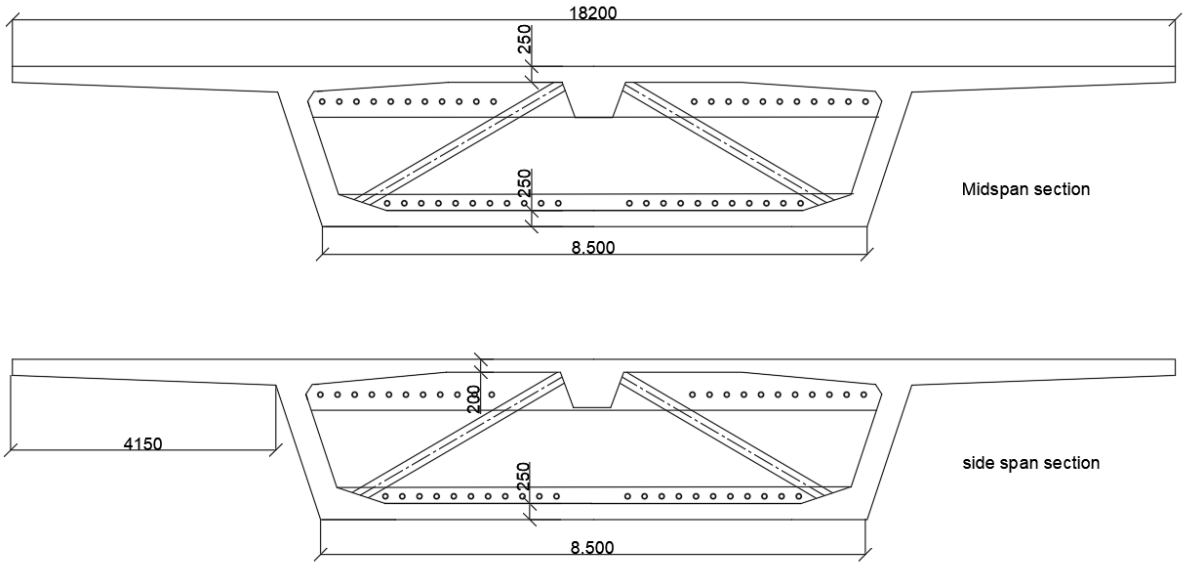

Figure 69Temporary prestressing bars during construction

All the cables have been modeled in the program Midas civil and all the losses, time-dependent effect, and secondary moment due to indeterminate structure have been included.

The following losses have been included:

- Immediate losses: friction losses, slip losses (6mm).
- time-dependent losses: creep and shrinkage losses, long-term relaxation.

The time-dependent effect (creep and shrinkage have been considered based on Eurocode with cement class R and relative humidity 70%).

Figure 70 Definition od the prestress in the section in Midas Civil

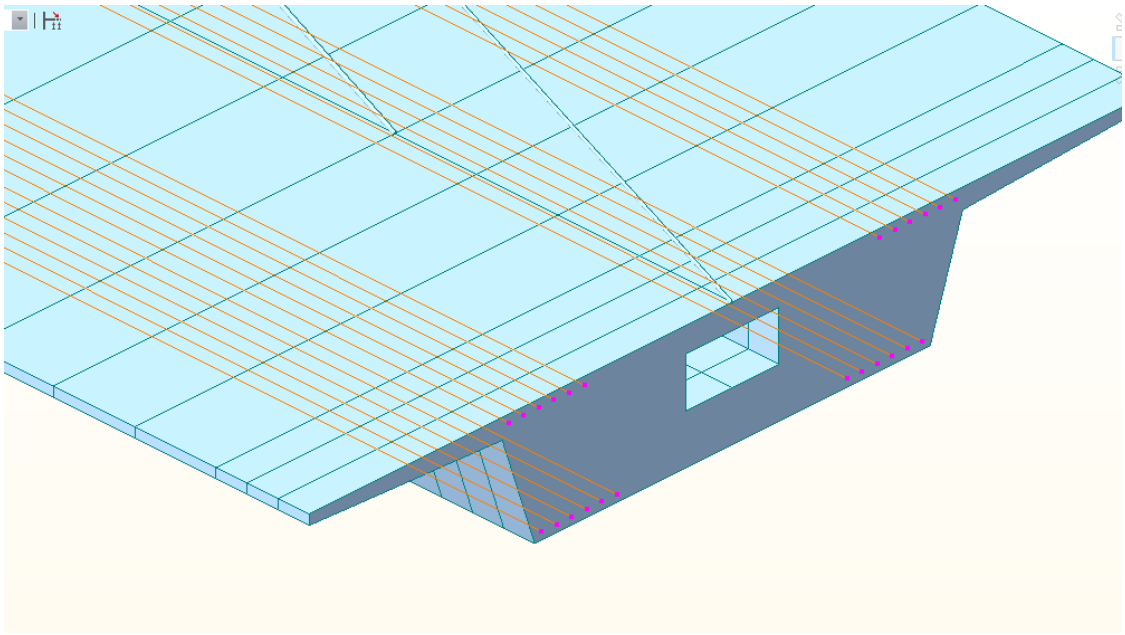

Figure 71 post-tension cables at the abutment section

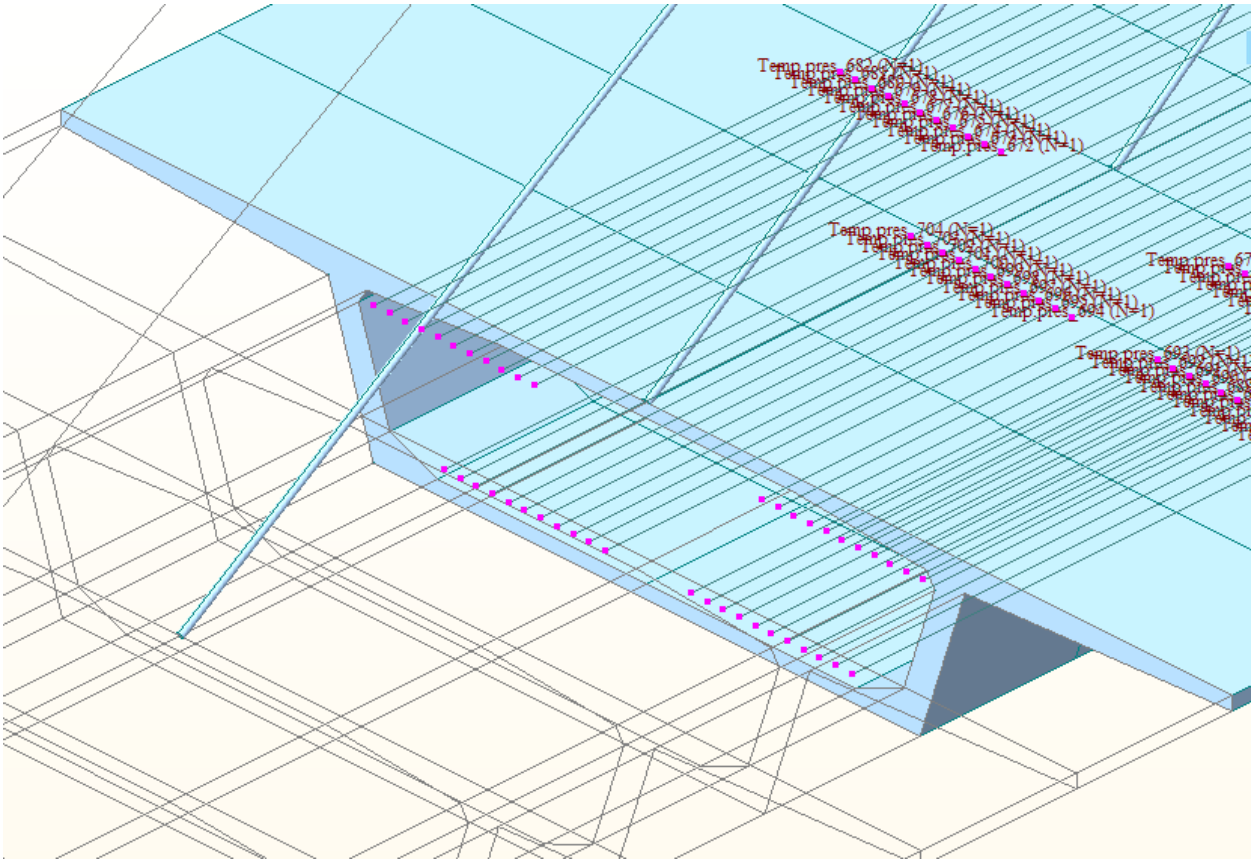

Figure 72 the temporary post tension which used for construction

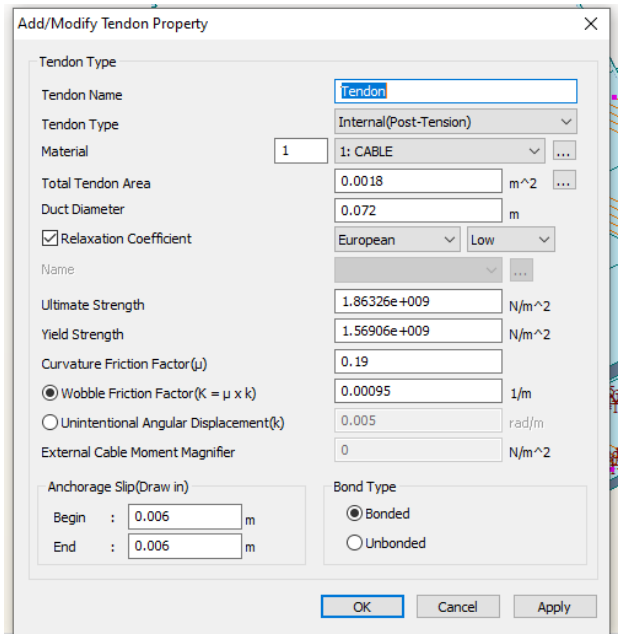

Figure 73 Prestress prop.

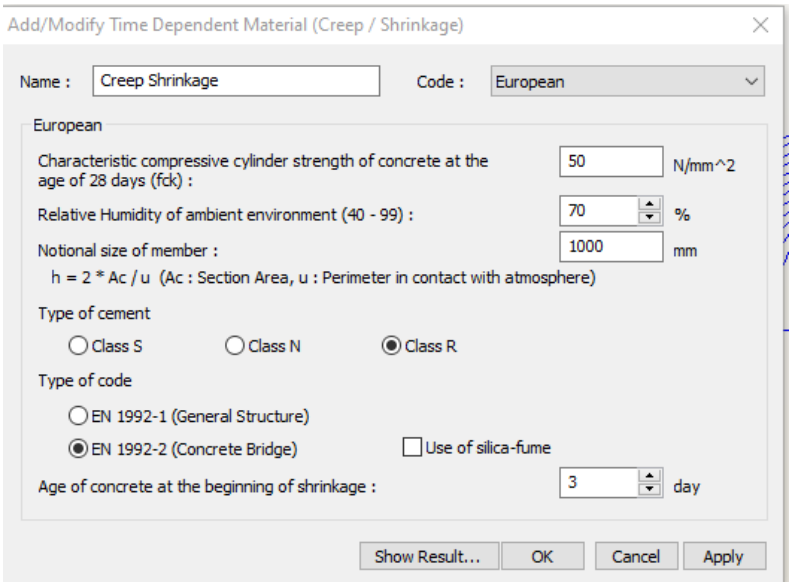

Figure 74 Time dependent material in Midas Civil

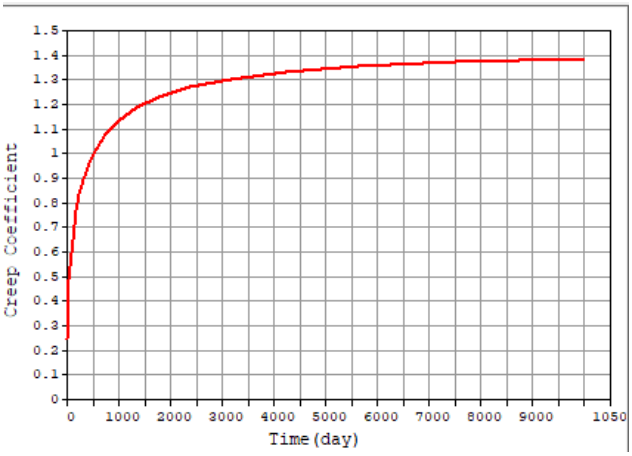

Figure 76 creep coff. vs time

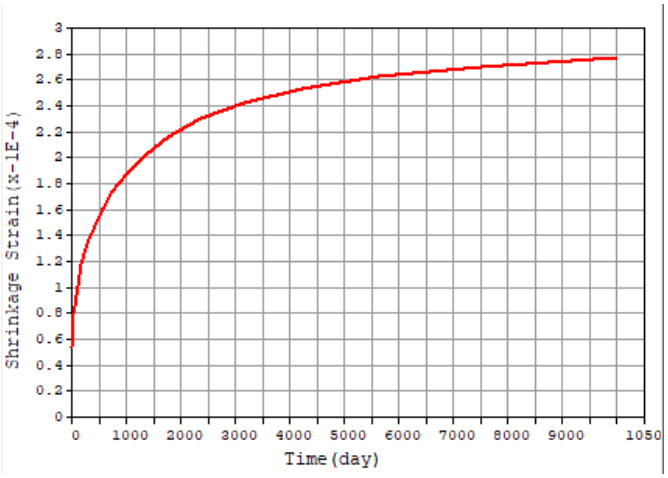

Figure 75 shrinkage strain vs time

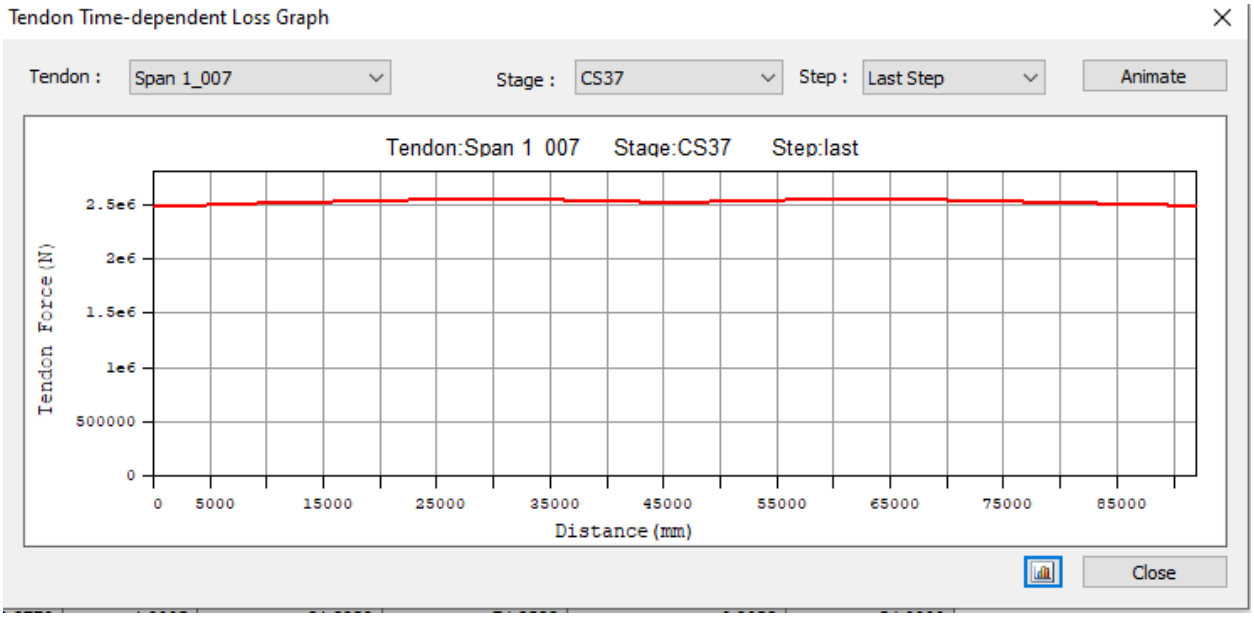

Figure 77 Side Span Post-tension immediate losses

6 Construction stage analysis

One of the main advantages of a cable-stayed bridge is the ease of construction by using the free cantilever method, the main advantage of using this method in a cable-stayed bridge is the existence of the cables which can be used as support for the cantilever which reduces the cantilever moment during construction.

in this project, all the time-dependent effect has been considered by the software.
The construction schedule was considered as follows, first, the pier and pylon have been constructed, then the pier segment has been constructed, after that the following segments have been constructed using a traveling form. After that, the cables on both sides have been installed and tuned to the full load.
The tuning of the cables has been done just in one step which is at the time of installation.
The following table shows the description and timing for each stage.

Table 17 Construction stage description

Stage	Description	Duration	Time
CS0	construction of the substructure of the bridge, pylon construction and temporary fixed support	14	14
CS1	construction of the pier segment(S0), apply travelling form for the next segment, apply load of the next segment at the end	14	28
CS2	activation segment 1 & temp. prestressing,, remove the current segment load, move the travelling form to construct the next segment	7	35
CS3_1	cable install and tuning the right side	0	35
CS3_2	cable install and tuning in the left side	0	35
CS4	apply the load of the next segment	7	42
CS5	activation segment 2 & temp. prestressing,, remove the current segment load, move the travelling form to construct the next segment	7	49
CS6_1	cable install and tuning the right side	0	49
CS6_2	cable install and tuning in the left side	0	49
CS7	apply the load of the next segment	7	56
CS8	activation segment 3 & temp. prestressing, remove the current segment load, move the travelling form to construct the next segment	7	63
CS9_1	cable install and tuning the right side	0	63
CS9_2	cable install and tuning in the left side	0	63
CS10	apply the load of the next segment	7	70
CS11	activation segment 4 & temp. prestressing, remove the current segment load, move the travelling form to construct the next segment	7	77
CS12_1	cable install and tuning the right side	0	77
CS12_2	cable install and tuning in the left side	0	77
CS13	apply the load of the next segment	7	84
CS14	activation segment 5 & temp. prestressing, remove the current segment load, move the travelling form to construct the next segment	7	91
CS15_1	cable install in the right side	0	91
CS15_2	cable install and tuning the right side	0	91
CS16	cable install and tuning in the left side	7	98
CS17	activation segment 6 & temp. prestressing,, remove the current segment load, move the travelling form to	7	105

	construct the next segment		
CS18_1	cable install and tuning the right side	0	105
CS18_2	cable install and tuning in the left side	0	105
CS19	apply the load of the next segment	7	112
CS20	activation segment 7 & temp. prestressing,, remove the current segment load, move the travelling form to construct the next segment	7	119
CS21_1	cable install and tuning the right side	0	119
CS21_2	cable install and tuning in the left side	0	119
CS22	apply the load of the next segment	7	126
CS23	activation segment 8 & temp. prestressing,, remove the current segment load, move the travelling form to construct the next segment	7	133
CS24_1	cable install and tuning the right side	0	133
CS24_2	cable install and tuning in the left side	0	133
CS25	apply the load of the next segment	7	140
CS26	activation segment 9 & temp. prestressing,, remove the current segment load, move the travelling form to construct the next segment	7	147
CS27_1	cable install and tuning the right side	0	147
CS27_2	cable install and tuning in the left side	0	147
CS28	apply the load of the next segment	7	154
CS29	activation segment 10 & temp. prestressing,, remove the current segment load, move the travelling form to construct the next segment	7	161
CS30_1	cable install and tuning the right side	0	161
CS30_2	cable install and tuning in the left side	0	161
CS31	apply the load of the next segment	7	168
CS32	activation segment 11 & temp. prestressing,, remove the current segment load, move the travelling form to construct the next segment	7	175
CS33_1	cable install and tuning the right side	0	175
CS33_2	cable install and tuning in the left side	0	175
CS34	apply the load of the next segment (Segment 12)	7	182
CS35	activation segment 12, remove the current segment load, move the travelling form to construct the key segment	7	189
CS36	activate the key segment and abutment segment, remove the temp. support, and apply the real support	7	196
CS37	remove the temporary prestressing and applying post tension tendons	1	197
CS38_1	cable install and tuning the right side	0	197
CS38_2	cable install and tuning in the left side	0	197
CS39	remove the construction load and apply the sup. Imposed load and the prestress	30	227
CS40	apply the moving load	20	247
CS41	end of the use	36253	36500

During the construction, a temporary prestressed bar has been used prestress, and after the construction, the bars have been released, and post-tension cables have been stressed for the whole structure (straight cables).

During construction, cambers have been used by elevation of the traveling form, the reason to apply the camper is to reach a situation of zero deflection at the end of the construction.

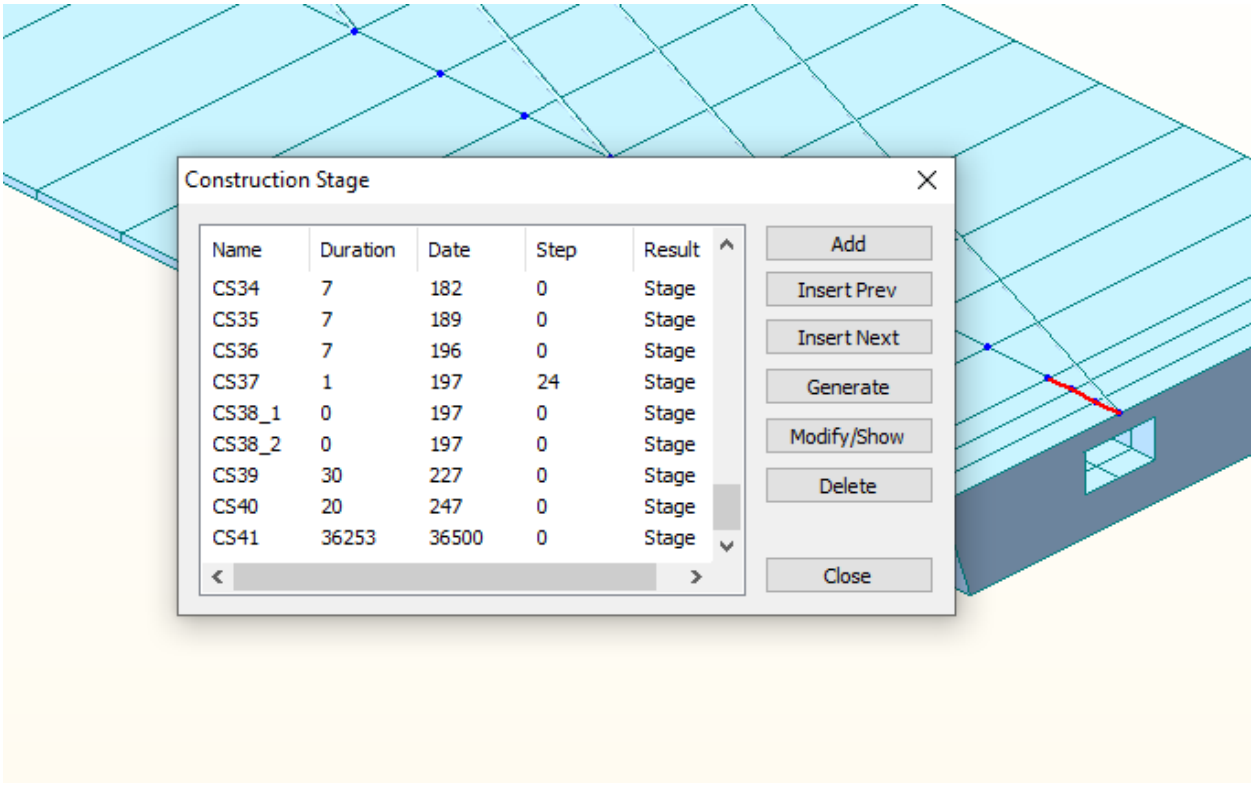

Figure 78 Definition of construction stages in Midas civil

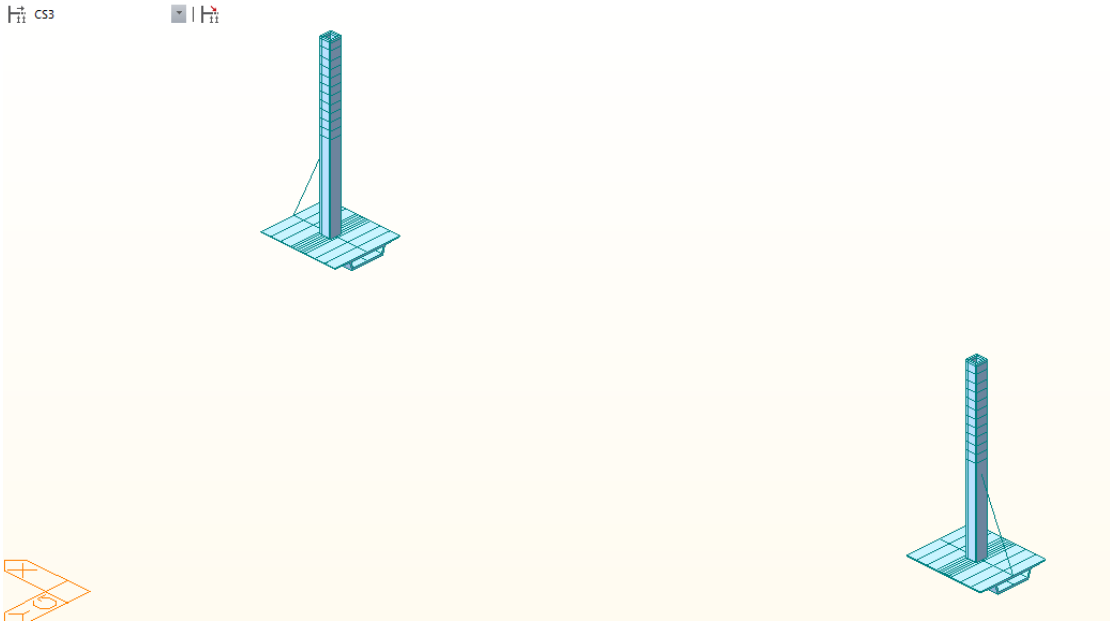

Figure 79 CS3_1 (see Table no.17)

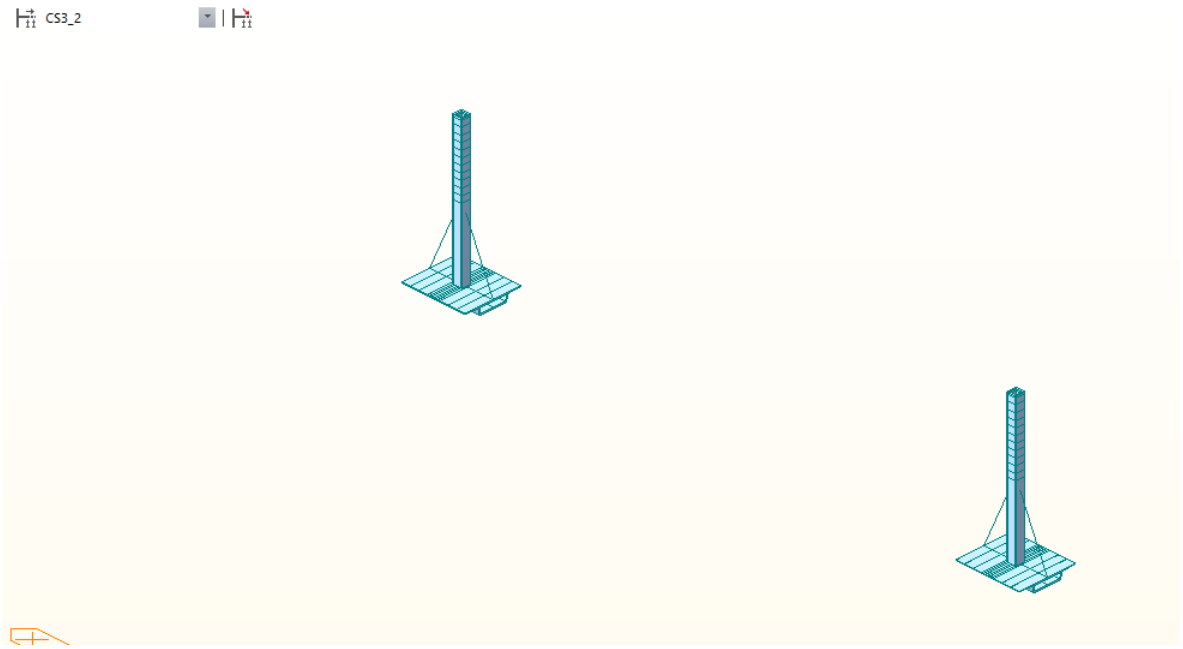

Figure 80 CS3_2 (see Table no.17)

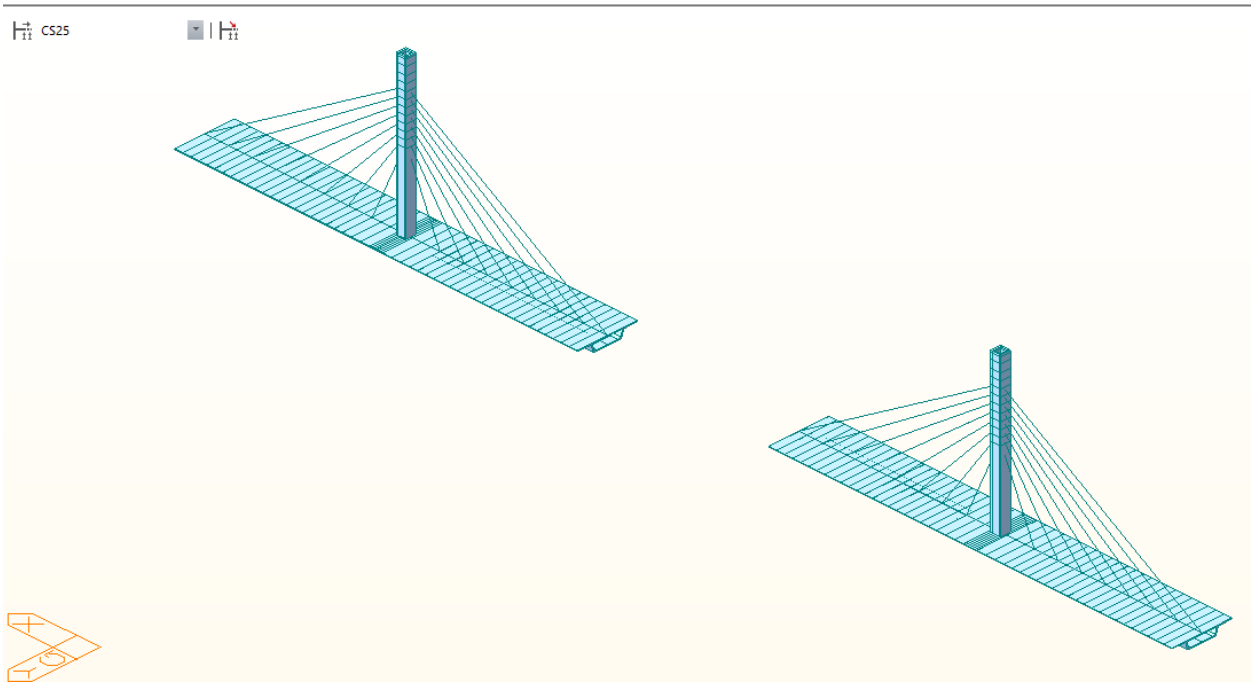

Figure 81 CS25_1 (see Table no.17)

To consider the sequential jacking of the post-tension cables, the construction stage CS37 has been divided into 24 steps, at each step a separate tension has been jacked and activated. The figure below shows the additional steps in the CS37 and the activated cable at each step.

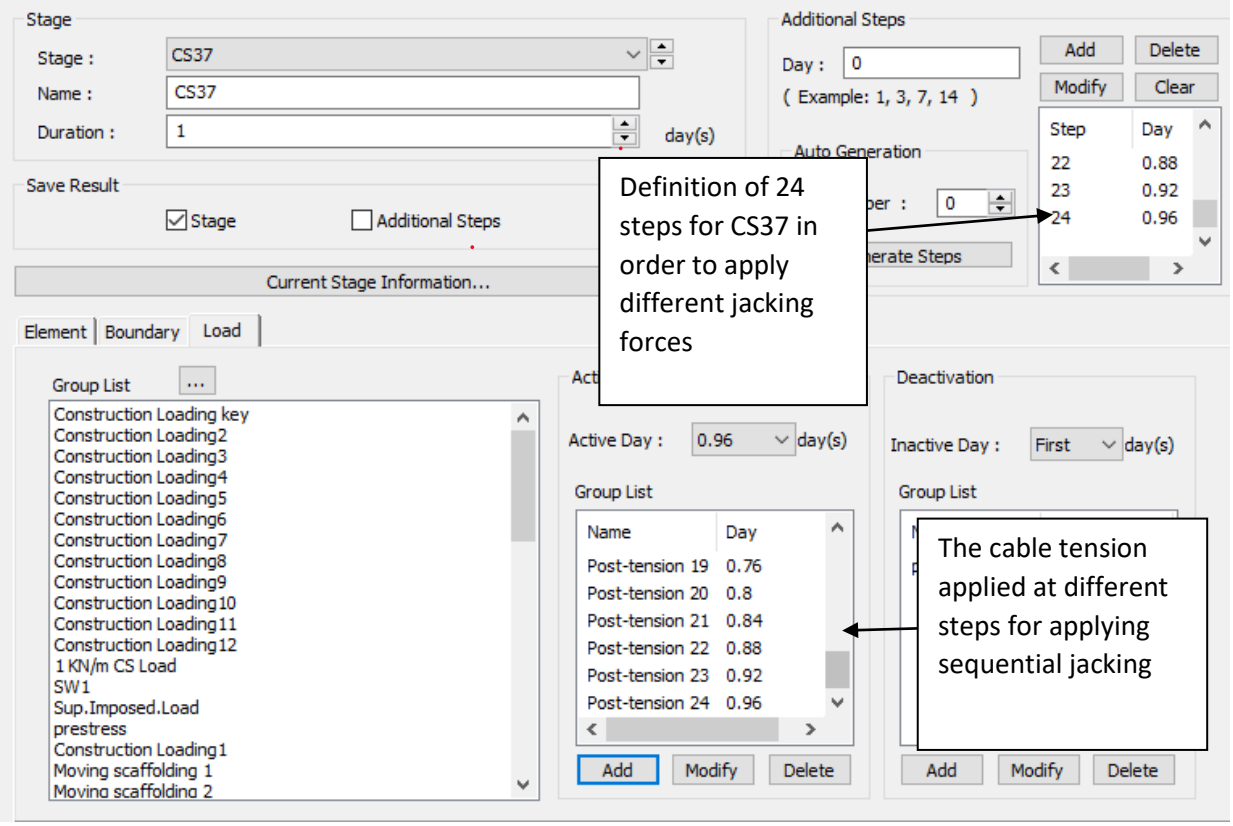

Figure 82 definition of sequence of prestressing in Midas Civil

The following figure shows the cables numbered from 1-24 which represent the sequence of prestressing.

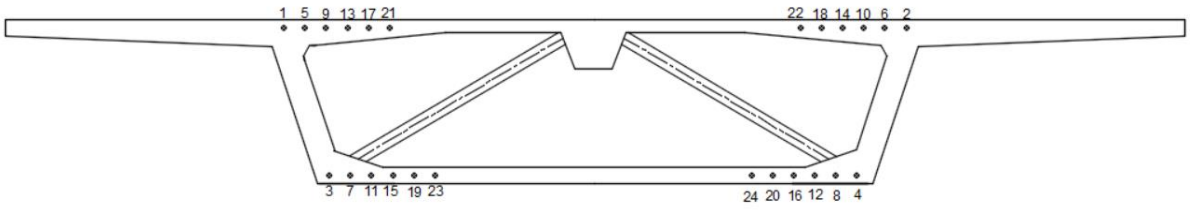

Figure 83 sequential jacking of post-tension cables

The following figure shows the jacking sequence for the temporary prestress bras which used during construction.

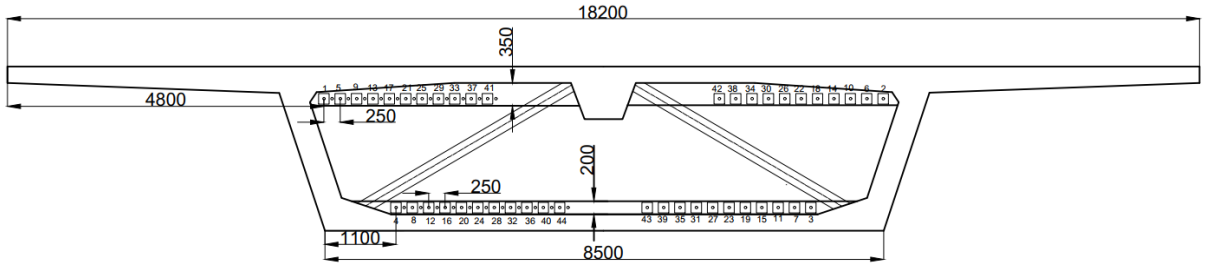

Figure 84 sequential jacking of prestress bars

6.1 Internal forces from the combination for the ultimate limit state

The following figures show the moment, axial and shear force for the ULS

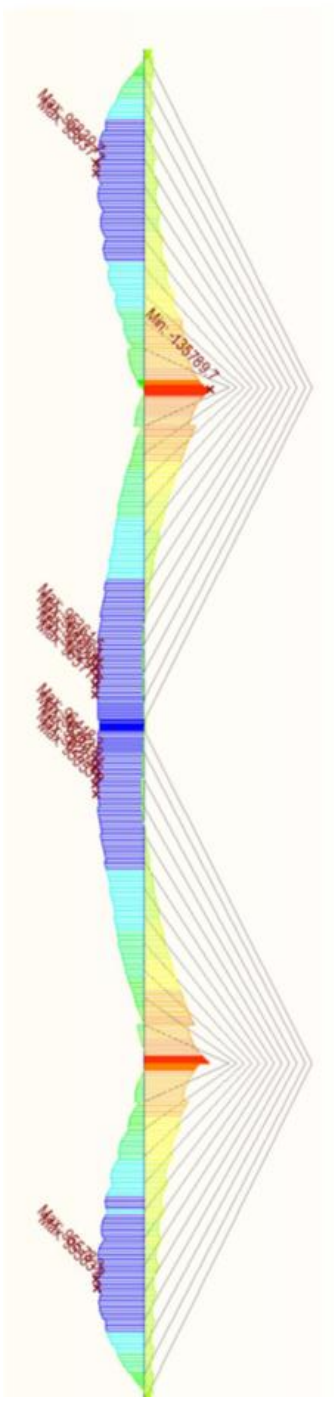

Figure 85 Moment ULS

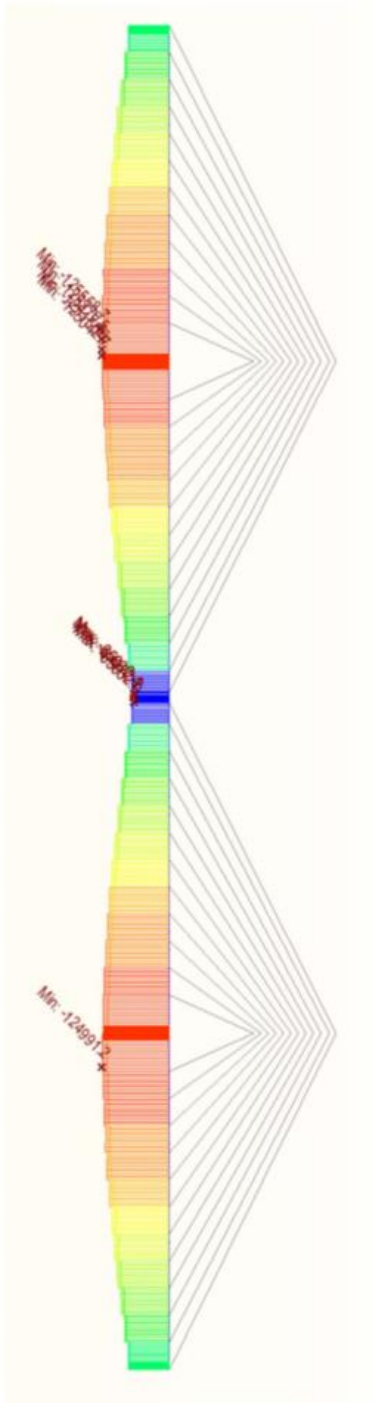

Figure 87 Axial Load ULS

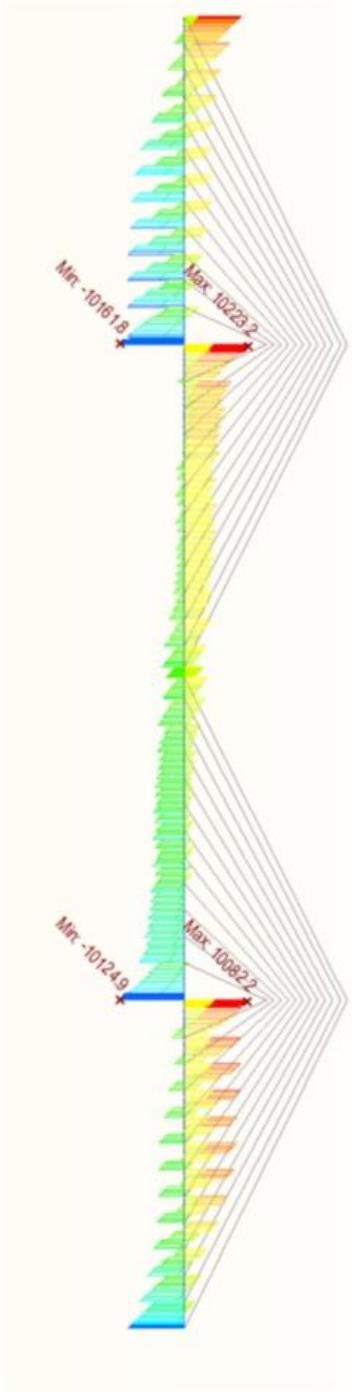

Figure 86 Shear Force ULS

6.2 Internal forces from the combination for the service limit state.

6.2.1 Characteristic load combination

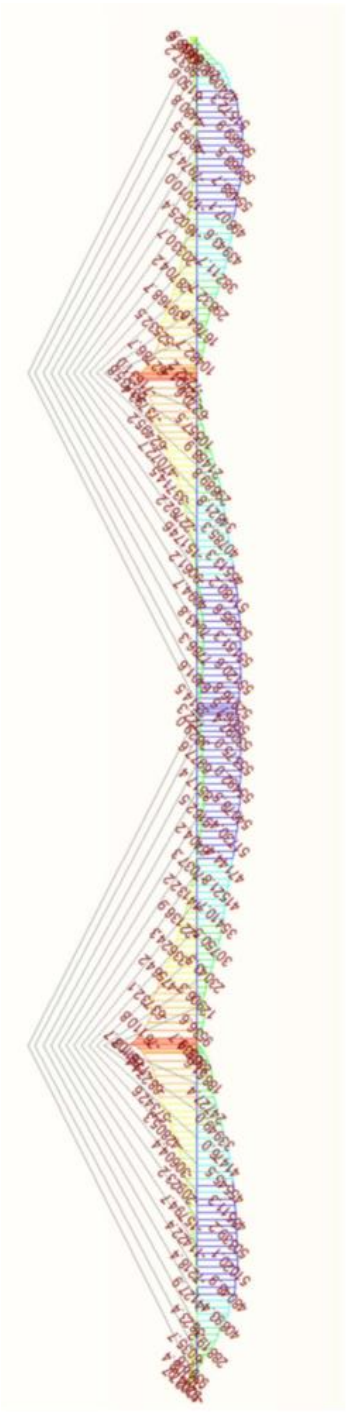

Figure 88 Moment Diagram Ch Combination

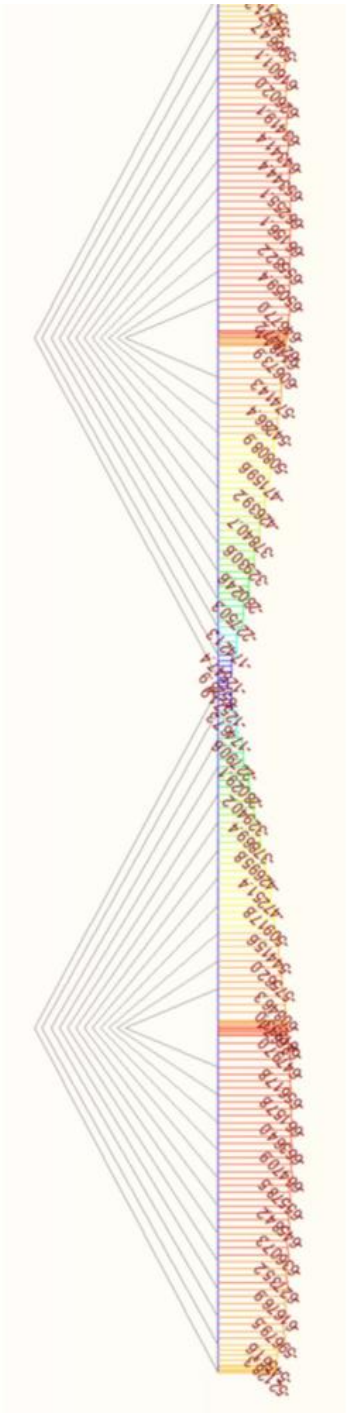

Figure 89 Axial Load Diagram Ch. Combination

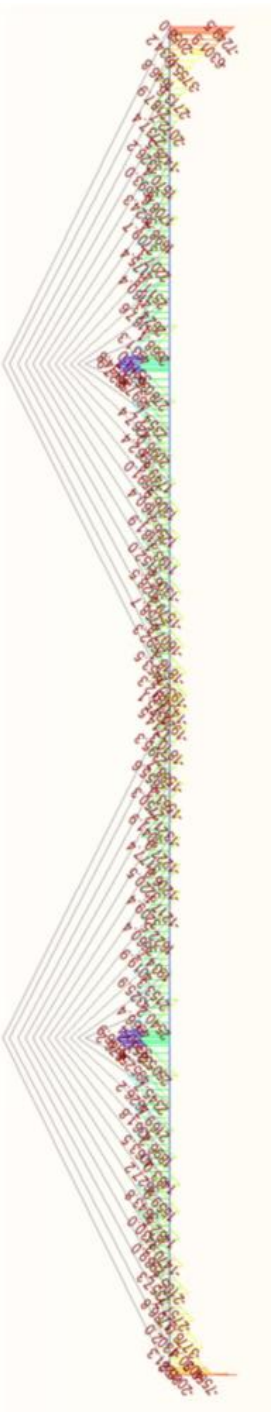

Figure 90 Shear Force Diagram Ch. Combination

6.2.2 Frequent load combination

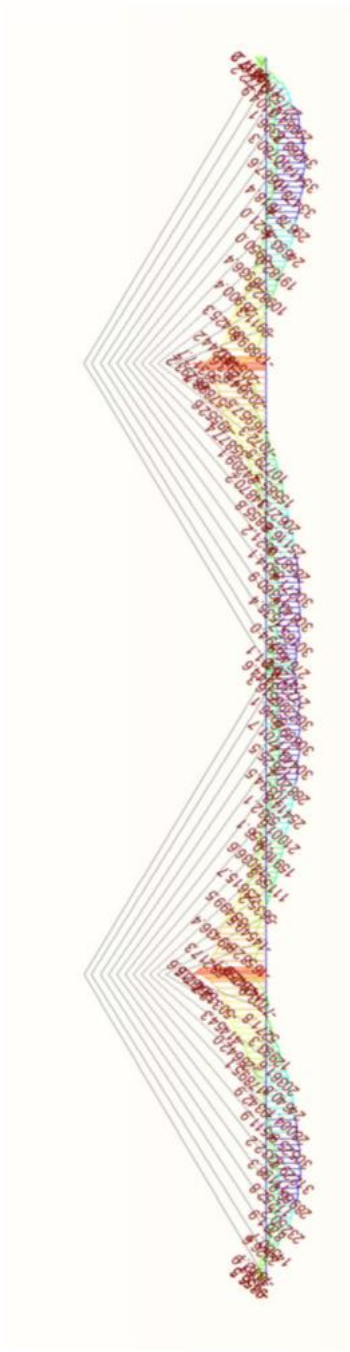

Figure 93 Moment diagram Freq. combination

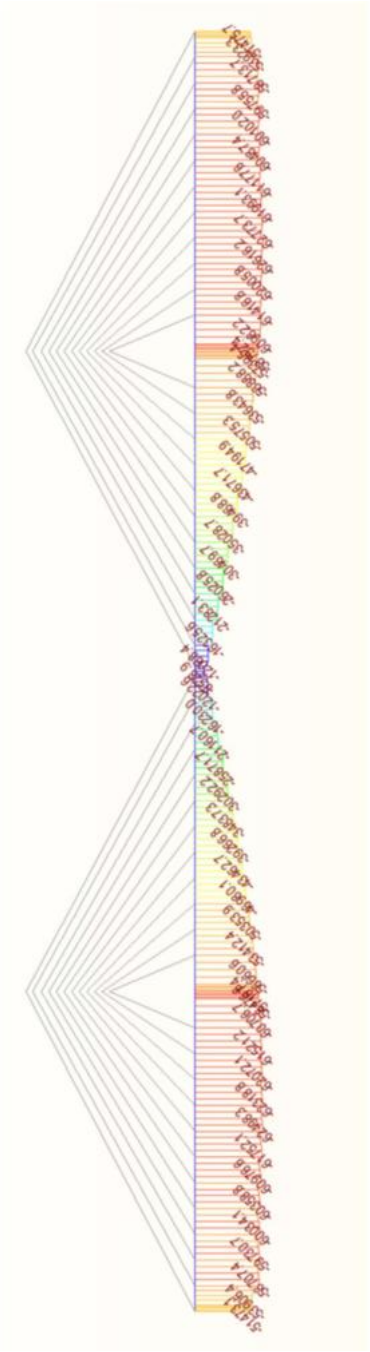

Figure 91 Axial Load diagram Freq. combination

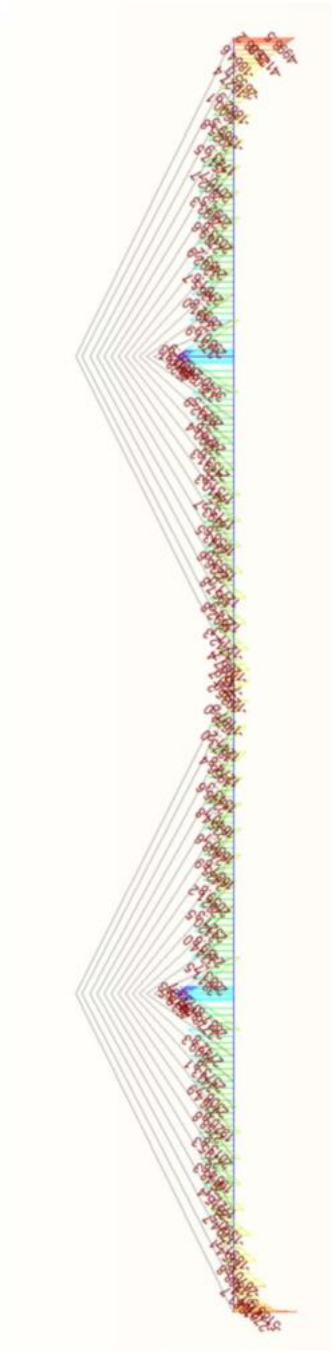

Figure 92 Shear force diagram Freq. combination

6.2.3 Quasi-static load combination

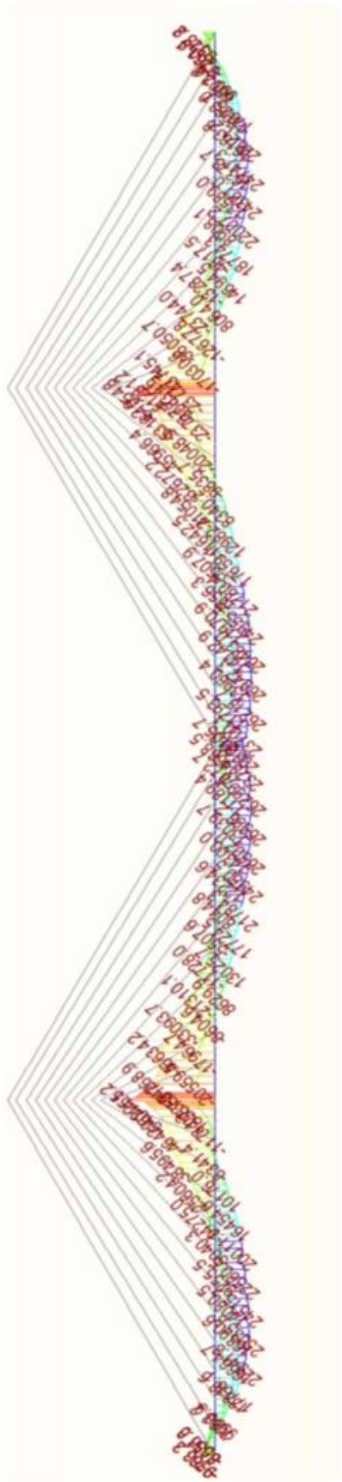

Figure 94 Moment Diagram Quasi-Static Combination

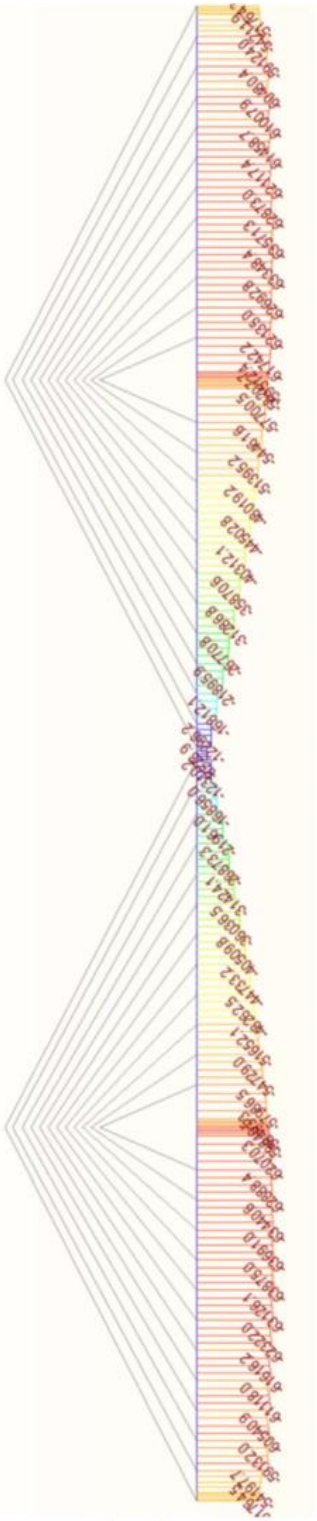

Figure 96 Axial Load Diagram Quasi-Static Combination

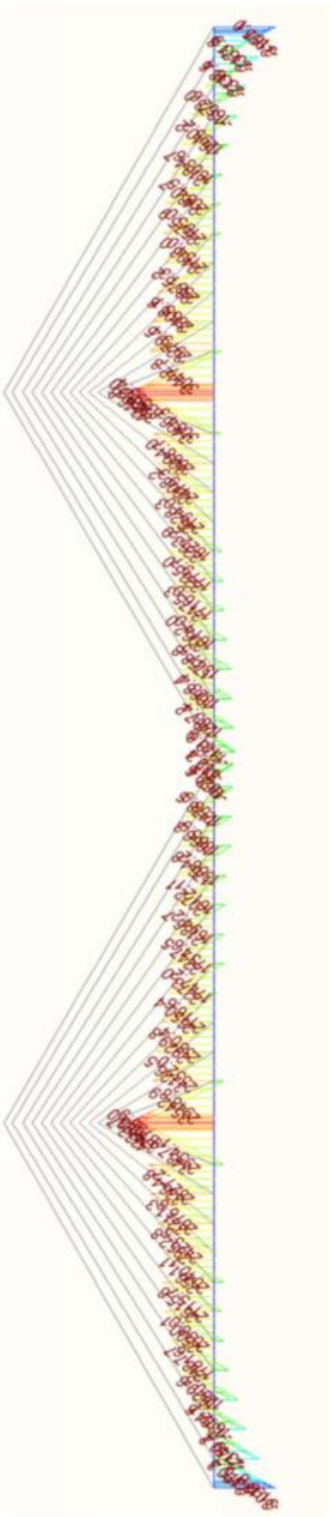

Figure 95 Shear Force Diagram Quasi-Static Combination

7 Service limit state

In the service limit state, the stresses in the box girder and the cables must be checked in all stages of the construction and at the service stage, also the deformation has to be checked.

7.1 Stress limits in concrete

7.1.1 During construction

The stresses in the structure have been checked in all the construction stages described in table 12 Construction stage description.

The value of the strength of concrete has been calculated based on function βcc and with s=0.2 for cement strength class R based on the following formula: [15]

$$f_{cm}(t) = \beta_{cc}(t) f_{cm}$$

Where:

$$\beta_{cc}(t) = \exp\left\{ s\left[1 - \left(\frac{28}{t} \right)^{0.5} \right] \right\}$$

Fcm(t) is the mean compressive strength of concrete at age t (in days) and fcm is the mean compressive strength at age of 28 days, the fck(t) can be taken from the following formulas:

$$f_{ck}(t) = f_{cm}(t) - 8\ (\text{MPa}) \quad \text{for } 3 < t < 28 \text{ days}$$

$$f_{ck}(t) = f_{ck} \quad \text{for } t \geq 28 \text{ days}$$

For concrete C50/60, fcm = 58 Mpa.

The mean tensile strength at any time t may be taken as:

$$f_{ctm}(t) = [\beta_{cc}(t)]^{\alpha} f_{ctm}$$

Where α = 1 for t < 28

The mean tensile strength for concrete at age 28 days equal C50/60= 4.1 Mpa, the check of the stresses during construction has been done using characteristic load combination.

The age of the segments in individual construction stages are in table 18, the value of the 0.6*fck(t) for each segment at each construction stage are in table 19, the value of the fctm(t) for each segment at each construction stage are in table 20.

Table 18 local age of segments

Stage	S1	S2	S3	S4	S5	S6	S7	S8	S9	S10	S11	S12	S-Key
CS0	-	-	-	-	-	-	-	-	-	-	-	-	-
CS1	-	-	-	-	-	-	-	-	-	-	-	-	-
CS2	7	-	-	-	-	-	-	-	-	-	-	-	-
CS3_1	7	-	-	-	-	-	-	-	-	-	-	-	-
CS3_2	7	-	-	-	-	-	-	-	-	-	-	-	-
CS4	14	-	-	-	-	-	-	-	-	-	-	-	-
CS5	21	7	-	-	-	-	-	-	-	-	-	-	-
CS6_1	21	7	-	-	-	-	-	-	-	-	-	-	-
CS6_2	21	7	-	-	-	-	-	-	-	-	-	-	-
CS7	28	14	-	-	-	-	-	-	-	-	-	-	-
CS8	35	21	7	-	-	-	-	-	-	-	-	-	-
CS9_1	35	21	7	-	-	-	-	-	-	-	-	-	-
CS9_2	35	21	7	-	-	-	-	-	-	-	-	-	-
CS10	42	28	14	-	-	-	-	-	-	-	-	-	-
CS11	49	35	21	7	-	-	-	-	-	-	-	-	-
CS12_1	49	35	21	7	-	-	-	-	-	-	-	-	-
CS12_2	49	35	21	7	-	-	-	-	-	-	-	-	-
CS13	56	42	28	14	-	-	-	-	-	-	-	-	-
CS14	63	49	35	21	7	-	-	-	-	-	-	-	-
CS15_1	63	49	35	21	7	-	-	-	-	-	-	-	-
CS15_2	63	49	35	21	7	-	-	-	-	-	-	-	-
CS16	70	56	42	28	14	-	-	-	-	-	-	-	-
CS17	77	63	49	35	21	7	-	-	-	-	-	-	-
CS18_1	77	63	49	35	21	7	-	-	-	-	-	-	-
CS18_2	77	63	49	35	21	7	-	-	-	-	-	-	-
CS19	84	70	56	42	28	14	-	-	-	-	-	-	-
CS20	91	77	63	49	35	21	7	-	-	-	-	-	-
CS21_1	91	77	63	49	35	21	7	-	-	-	-	-	-
CS21_2	91	77	63	49	35	21	7	-	-	-	-	-	-
CS22	98	84	70	56	42	28	14	-	-	-	-	-	-
CS23	105	91	77	63	49	35	21	7	-	-	-	-	-
CS24_1	105	91	77	63	49	35	21	7	-	-	-	-	-
CS24_2	105	91	77	63	49	35	21	8	-	-	-	-	-
CS25	112	98	84	70	56	42	28	15	-	-	-	-	-
CS26	119	105	91	77	63	49	35	9	7	-	-	-	-
CS27_1	119	105	91	77	63	49	35	9	7	-	-	-	-
CS27_2	119	105	91	77	63	49	35	10	8	-	-	-	-
CS28	126	112	98	84	70	56	42	17	15	-	-	-	-
CS29	133	119	105	91	77	63	49	11	9	7	-	-	-
CS30_1	133	119	105	91	77	63	49	11	9	7	-	-	-
CS30_2	133	119	105	91	77	63	49	12	10	8	-	-	-
CS31	140	126	112	98	84	70	56	19	17	15	-	-	-
CS32	147	133	119	105	91	77	63	13	11	9	7	-	-
CS33_1	147	133	119	105	91	77	63	13	11	9	7	-	-
CS33_2	147	133	119	105	91	77	63	14	12	10	8	-	-
CS34	154	140	126	112	98	84	70	21	19	17	15	-	-
CS35	161	147	133	119	105	91	77	15	13	11	9	7	
CS36	168	154	140	126	112	98	84	22	20	18	16	14	7
CS37	169	155	141	127	113	99	85	16	14	12	10	15	8
CS38_1	170	156	142	128	114	100	86	17	15	13	11	16	8
CS38_2	170	156	142	128	114	100	86	17	15	13	11	16	8
CS39	200	186	172	158	144	130	116	47	45	43	41	46	38
CS40	220	206	192	178	164	150	136	67	65	63	61	66	58
CS41	36474	36460	36446	36432	36418	36404	36390	36321	36319	36317	36315	36320	36312

Table 19 0.6 fck(t) for local age of segments

Stage	S1	S2	S3	S4	S5	S6	S7	S8	S9	S10	S11	S12	S-Key
CS0	-	-	-	-	-	-	-	-	-	-	-	-	-
CS1	-	-	-	-	-	-	-	-	-	-	-	-	-
CS2	23.69	-	-	-	-	-	-	-	-	-	-	-	-
CS3_1	23.69	-	-	-	-	-	-	-	-	-	-	-	-
CS3_2	23.69	-	-	-	-	-	-	-	-	-	-	-	-
CS4	27.23	-	-	-	-	-	-	-	-	-	-	-	-
CS5	28.94	23.69	-	-	-	-	-	-	-	-	-	-	-
CS6_1	28.94	23.69	-	-	-	-	-	-	-	-	-	-	-
CS6_2	28.94	23.69	-	-	-	-	-	-	-	-	-	-	-
CS7	30.00	27.23	-	-	-	-	-	-	-	-	-	-	-
CS8	30.00	28.94	23.69	-	-	-	-	-	-	-	-	-	-
CS9_1	30.00	28.94	23.69	-	-	-	-	-	-	-	-	-	-
CS9_2	30.00	28.94	23.69	-	-	-	-	-	-	-	-	-	-
CS10	30.00	30.00	27.23	-	-	-	-	-	-	-	-	-	-
CS11	30.00	30.00	28.94	23.69	-	-	-	-	-	-	-	-	-
CS12_1	30.00	30.00	28.94	23.69	-	-	-	-	-	-	-	-	-
CS12_2	30.00	30.00	28.94	23.69	-	-	-	-	-	-	-	-	-
CS13	30.00	30.00	30.00	27.23	-	-	-	-	-	-	-	-	-
CS14	30.00	30.00	30.00	28.94	23.69	-	-	-	-	-	-	-	-
CS15_1	30.00	30.00	30.00	28.94	23.69	-	-	-	-	-	-	-	-
CS15_2	30.00	30.00	30.00	28.94	23.69	-	-	-	-	-	-	-	-
CS16	30.00	30.00	30.00	30.00	27.23	-	-	-	-	-	-	-	-
CS17	30.00	30.00	30.00	30.00	28.94	23.69	-	-	-	-	-	-	-
CS18_1	30.00	30.00	30.00	30.00	28.94	23.69	-	-	-	-	-	-	-
CS18_2	30.00	30.00	30.00	30.00	28.94	23.69	-	-	-	-	-	-	-
CS19	30.00	30.00	30.00	30.00	30.00	27.23	-	-	-	-	-	-	-
CS20	30.00	30.00	30.00	30.00	30.00	28.94	23.69	-	-	-	-	-	-
CS21_1	30.00	30.00	30.00	30.00	30.00	28.94	23.69	-	-	-	-	-	-
CS21_2	30.00	30.00	30.00	30.00	30.00	28.94	23.69	-	-	-	-	-	-
CS22	30.00	30.00	30.00	30.00	30.00	30.00	27.23	-	-	-	-	-	-
CS23	30.00	30.00	30.00	30.00	30.00	30.00	28.94	23.69	-	-	-	-	-
CS24_1	30.00	30.00	30.00	30.00	30.00	30.00	28.94	23.69	-	-	-	-	-
CS24_2	30.00	30.00	30.00	30.00	30.00	30.00	28.94	24.44	-	-	-	-	-
CS25	30.00	30.00	30.00	30.00	30.00	30.00	30.00	27.54	-	-	-	-	-
CS26	30.00	30.00	30.00	30.00	30.00	30.00	30.00	25.07	23.69	-	-	-	-
CS27_1	30.00	30.00	30.00	30.00	30.00	30.00	30.00	25.07	23.69	-	-	-	-
CS27_2	30.00	30.00	30.00	30.00	30.00	30.00	30.00	25.62	24.44	-	-	-	-
CS28	30.00	30.00	30.00	30.00	30.00	30.00	30.00	28.08	27.54	-	-	-	-
CS29	30.00	30.00	30.00	30.00	30.00	30.00	30.00	26.09	25.07	23.69	-	-	-
CS30_1	30.00	30.00	30.00	30.00	30.00	30.00	30.00	26.09	25.07	23.69	-	-	-
CS30_2	30.00	30.00	30.00	30.00	30.00	30.00	30.00	26.52	25.62	24.44	-	-	-
CS31	30.00	30.00	30.00	30.00	30.00	30.00	30.00	28.54	28.08	27.54	-	-	-
CS32	30.00	30.00	30.00	30.00	30.00	30.00	30.00	26.89	26.09	25.07	23.69	-	-
CS33_1	30.00	30.00	30.00	30.00	30.00	30.00	30.00	26.89	26.09	25.07	23.69	-	-
CS33_2	30.00	30.00	30.00	30.00	30.00	30.00	30.00	27.23	26.52	25.62	24.44	-	-
CS34	30.00	30.00	30.00	30.00	30.00	30.00	30.00	28.94	28.54	28.08	27.54	-	-
CS35	30.00	30.00	30.00	30.00	30.00	30.00	30.00	27.54	26.89	26.09	25.07	23.69	-
CS36	30.00	30.00	30.00	30.00	30.00	30.00	30.00	29.12	28.75	28.32	27.82	27.23	23.69
CS37	30.00	30.00	30.00	30.00	30.00	30.00	30.00	27.82	27.23	26.52	25.62	27.54	24.44
CS38_1	30.00	30.00	30.00	30.00	30.00	30.00	30.00	28.08	27.54	26.89	26.09	27.82	24.44
CS38_2	30.00	30.00	30.00	30.00	30.00	30.00	30.00	28.08	27.54	26.89	26.09	27.82	24.44
CS39	30.00	30.00	30.00	30.00	30.00	30.00	30.00	30.00	30.00	30.00	30.00	30.00	30.00
CS40	30.00	30.00	30.00	30.00	30.00	30.00	30.00	30.00	30.00	30.00	30.00	30.00	30.00
CS41	30.00	30.00	30.00	30.00	30.00	30.00	30.00	30.00	30.00	30.00	30.00	30.00	30.00

Table 20 fctm(t) for local age of segments

Stage	S1	S2	S3	S4	S5	S6	S7	S8	S9	S10	S11	S12	S-Key
CS0	-	-	-	-	-	-	-	-	-	-	-	-	-
CS1	-	-	-	-	-	-	-	-	-	-	-	-	-
CS2	3.36	-	-	-	-	-	-	-	-	-	-	-	-
CS3_1	3.36	-	-	-	-	-	-	-	-	-	-	-	-
CS3_2	3.36	-	-	-	-	-	-	-	-	-	-	-	-
CS4	3.77	-	-	-	-	-	-	-	-	-	-	-	-
CS5	3.98	3.36	-	-	-	-	-	-	-	-	-	-	-
CS6_1	3.98	3.36	-	-	-	-	-	-	-	-	-	-	-
CS6_2	3.98	3.36	-	-	-	-	-	-	-	-	-	-	-
CS7	4.10	3.77	-	-	-	-	-	-	-	-	-	-	-
CS8	4.10	3.98	3.36	-	-	-	-	-	-	-	-	-	-
CS9_1	4.10	3.98	3.36	-	-	-	-	-	-	-	-	-	-
CS9_2	4.10	3.98	3.36	-	-	-	-	-	-	-	-	-	-
CS10	4.10	4.10	3.77	-	-	-	-	-	-	-	-	-	-
CS11	4.10	4.10	3.98	3.36	-	-	-	-	-	-	-	-	-
CS12_1	4.10	4.10	3.98	3.36	-	-	-	-	-	-	-	-	-
CS12_2	4.10	4.10	3.98	3.36	-	-	-	-	-	-	-	-	-
CS13	4.10	4.10	4.10	3.77	-	-	-	-	-	-	-	-	-
CS14	4.10	4.10	4.10	3.98	3.36	-	-	-	-	-	-	-	-
CS15_1	4.10	4.10	4.10	3.98	3.36	-	-	-	-	-	-	-	-
CS15_2	4.10	4.10	4.10	3.98	3.36	-	-	-	-	-	-	-	-
CS16	4.10	4.10	4.10	4.10	3.77	-	-	-	-	-	-	-	-
CS17	4.10	4.10	4.10	4.10	3.98	3.36	-	-	-	-	-	-	-
CS18_1	4.10	4.10	4.10	4.10	3.98	3.36	-	-	-	-	-	-	-
CS18_2	4.10	4.10	4.10	4.10	3.98	3.36	-	-	-	-	-	-	-
CS19	4.10	4.10	4.10	4.10	4.10	3.77	-	-	-	-	-	-	-
CS20	4.10	4.10	4.10	4.10	4.10	3.98	3.36	-	-	-	-	-	-
CS21_1	4.10	4.10	4.10	4.10	4.10	3.98	3.36	-	-	-	-	-	-
CS21_2	4.10	4.10	4.10	4.10	4.10	3.98	3.36	-	-	-	-	-	-
CS22	4.10	4.10	4.10	4.10	4.10	4.10	3.77	-	-	-	-	-	-
CS23	4.10	4.10	4.10	4.10	4.10	4.10	3.98	3.36	-	-	-	-	-
CS24_1	4.10	4.10	4.10	4.10	4.10	4.10	3.98	3.36	-	-	-	-	-
CS24_2	4.10	4.10	4.10	4.10	4.10	4.10	3.98	3.44	-	-	-	-	-
CS25	4.10	4.10	4.10	4.10	4.10	4.10	4.10	3.81	-	-	-	-	-
CS26	4.10	4.10	4.10	4.10	4.10	4.10	4.10	3.52	3.36	-	-	-	-
CS27_1	4.10	4.10	4.10	4.10	4.10	4.10	4.10	3.52	3.36	-	-	-	-
CS27_2	4.10	4.10	4.10	4.10	4.10	4.10	4.10	3.58	3.44	-	-	-	-
CS28	4.10	4.10	4.10	4.10	4.10	4.10	4.10	3.87	3.81	-	-	-	-
CS29	4.10	4.10	4.10	4.10	4.10	4.10	4.10	3.64	3.52	3.36	-	-	-
CS30_1	4.10	4.10	4.10	4.10	4.10	4.10	4.10	3.64	3.52	3.36	-	-	-
CS30_2	4.10	4.10	4.10	4.10	4.10	4.10	4.10	3.69	3.58	3.44	-	-	-
CS31	4.10	4.10	4.10	4.10	4.10	4.10	4.10	3.93	3.87	3.81	-	-	-
CS32	4.10	4.10	4.10	4.10	4.10	4.10	4.10	3.73	3.64	3.52	3.36	-	-
CS33_1	4.10	4.10	4.10	4.10	4.10	4.10	4.10	3.73	3.64	3.52	3.36	-	-
CS33_2	4.10	4.10	4.10	4.10	4.10	4.10	4.10	3.77	3.69	3.58	3.44	-	-
CS34	4.10	4.10	4.10	4.10	4.10	4.10	4.10	3.98	3.93	3.87	3.81	-	-
CS35	4.10	4.10	4.10	4.10	4.10	4.10	4.10	3.81	3.73	3.64	3.52	3.36	-
CS36	4.10	4.10	4.10	4.10	4.10	4.10	4.10	4.00	3.95	3.90	3.84	3.77	3.36
CS37	4.10	4.10	4.10	4.10	4.10	4.10	4.10	3.84	3.77	3.69	3.58	3.81	3.44
CS38_1	4.10	4.10	4.10	4.10	4.10	4.10	4.10	3.87	3.81	3.73	3.64	3.84	3.44
CS38_2	4.10	4.10	4.10	4.10	4.10	4.10	4.10	3.87	3.81	3.73	3.64	3.84	3.44
CS39	4.10	4.10	4.10	4.10	4.10	4.10	4.10	4.10	4.10	4.10	4.10	4.10	4.10
CS40	4.10	4.10	4.10	4.10	4.10	4.10	4.10	4.10	4.10	4.10	4.10	4.10	4.10
CS41	4.10	4.10	4.10	4.10	4.10	4.10	4.10	4.10	4.10	4.10	4.10	4.10	4.10

The figures below show the top and bottom stress in all construction stages shown in table 17

Figure 97 CS3_1 Top Stress [MPa]

Figure 98 CS3_1 Bottom Stress [MPa]

Figure 99 CS3_2Top Stress [MPa]

Figure 100 CS3_2 Bottom Stress [MPa]

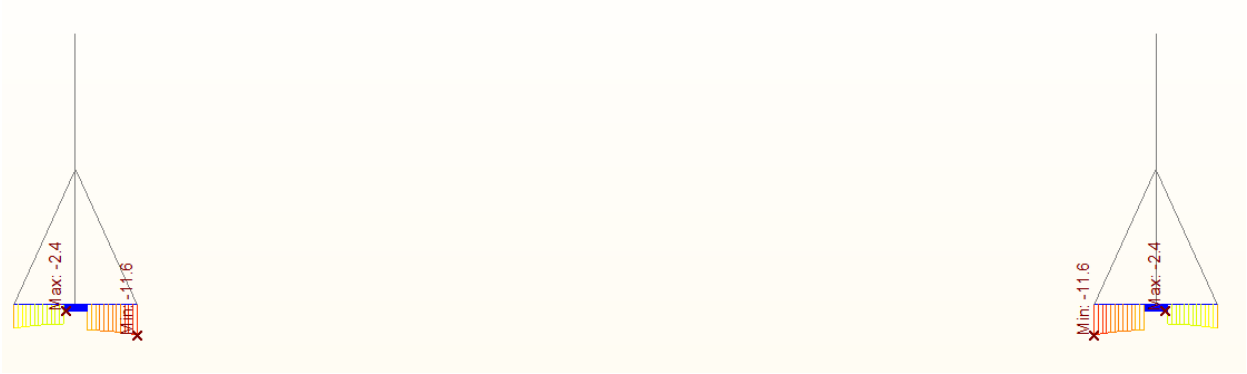

Figure 101 CS4 Top Stress [MPa]

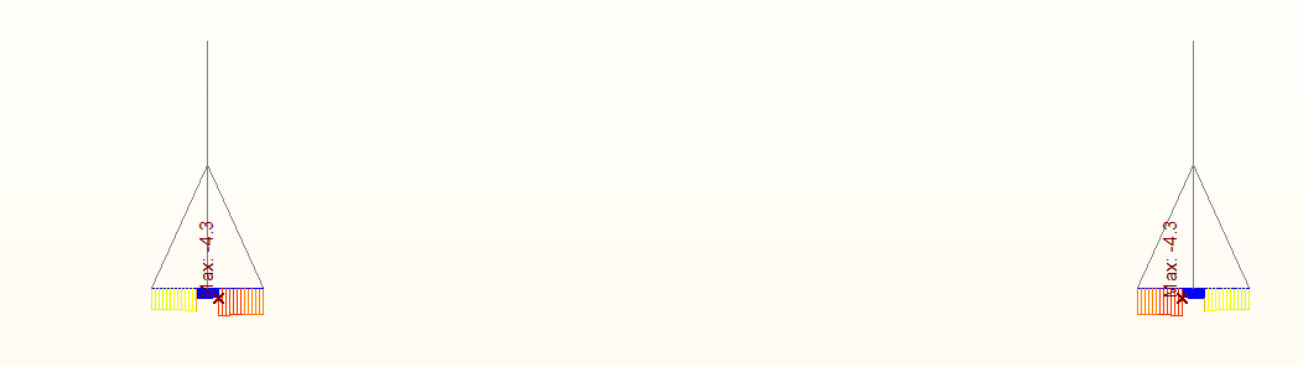

Figure 102 CS4 Bottom Stress [MPa]

Figure 103 CS5 Top Stress [MPa]

Figure 104 CS5 Bottom Stress [MPa]

Figure 105 CS6_1 Top Stress [MPa]

Figure 106 CS6_1 Bottom Stress [MPa]

Figure 107 CS6_2 Top Stress [MPa]

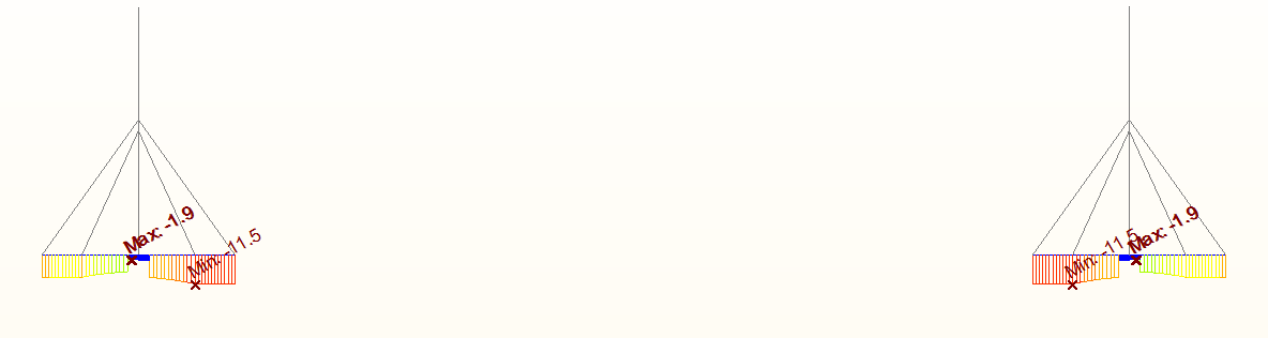

Figure 108 CS6_2 Bottom Stress [MPa]

Figure 109 CS7 Top Stress [MPa]

Figure 110 CS7 Bottom Stress [MPa]

Figure 111 CS8 Top Stress [MPa]

Figure 112 CS8 Bottom Stress [MPa]

Figure 113 CS9_1 Top Stress [MPa]

Figure 114 CS9_1 Bottom Stress [MPa]

Figure 115 CS9_2 Top Stress [MPa]

Figure 116 CS9_2 Bottom Stress [MPa]

Figure 117 CS10 Top Stress [MPa]

Figure 118 CS10 Bottom Stress [MPa]

Figure 119 CS11 Top Stress [MPa]

Figure 120 CS11 Bottom Stress [MPa]

Figure 121 CS12_1 Top Stress [MPa]

Figure 122 CS12_1 Top Stress [MPa]

Figure 123 CS12_2 Top Stress [MPa]

Figure 124 CS12_2 Bottom Stress [MPa]

Figure 125 CS13 Top Stress [MPa]

Figure 126 CS13 Bottom Stress [MPa]

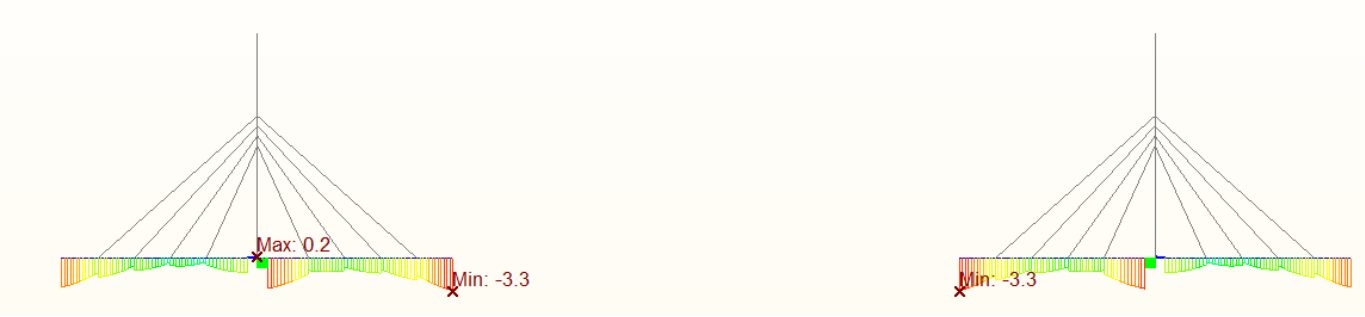

Figure 127 CS14 Top Stress [MPa]

Figure 128 CS14 Bottom Stress [MPa]

Figure 129 CS15_1 Top Stress [MPa]

Figure 130 CS15_1 Bottom Stress [MPa]

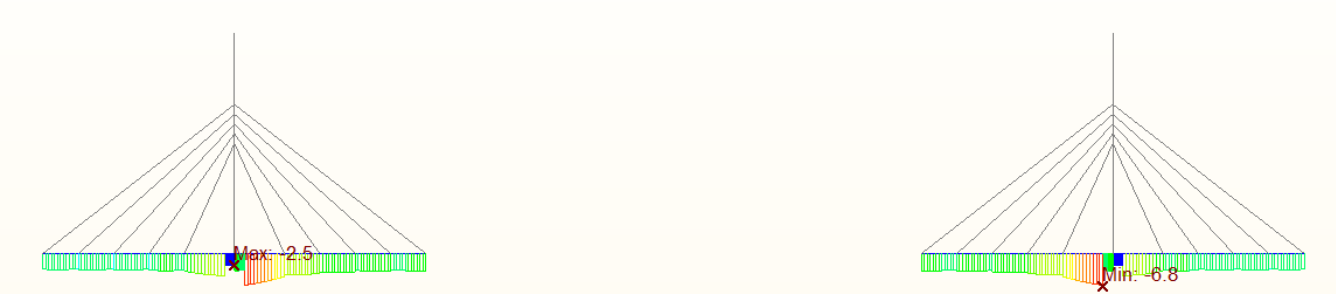

Figure 131 CS15_2 Top Stress [MPa]

Figure 132 CS15_2 Bottom Stress [MPa]

Figure 133 CS16 Top Stress [MPa]

Figure 134 CS16 Bottom Stress [MPa]

Figure 135 CS17 Top Stress [MPa]

Figure 136 CS17 Bottom Stress [MPa]

Figure 137 CS18_1 Top Stress [MPa]

Figure 138 CS18_1 Bottom Stress [MPa]

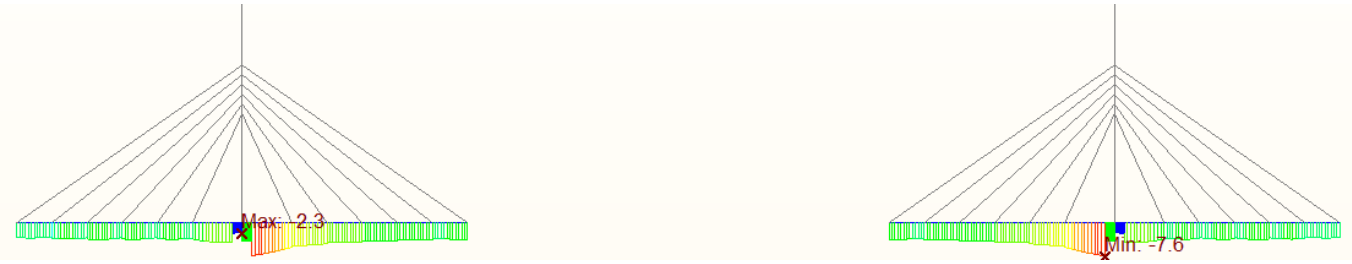

Figure 139 CS18_2 Top Stress [MPa]

Figure 140 CS18_2 Bottom Stress [MPa]

Figure 141 CS19 Top Stress [MPa]

Figure 142 CS19 Top Stress [MPa]

Figure 143 CS20 Top Stress [MPa]

Figure 144 CS20 Bottom Stress [MPa]

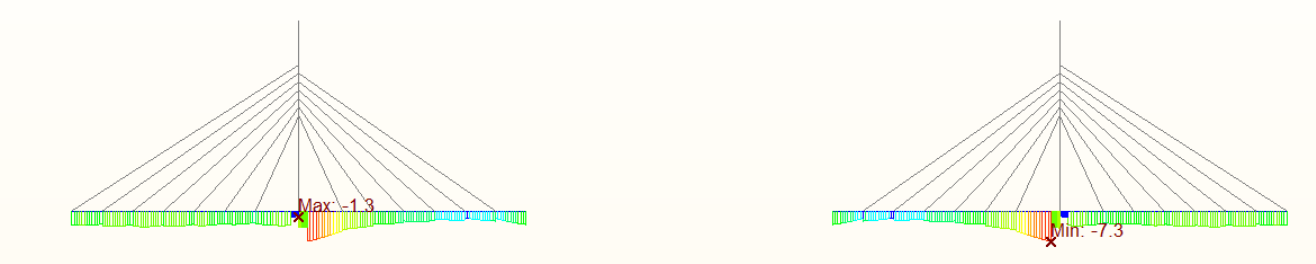

Figure 145 CS21_1 Top Stress [MPa]

Figure 146 CS21_1 Top Stress [MPa]

Figure 147 CS21_2 Bottom Stress [MPa]

Figure 148 CS21_2 Bottom Stress [MPa]

Figure 149 CS22 Top Stress [MPa]

Figure 150 CS22 Bottom Stress [MPa]

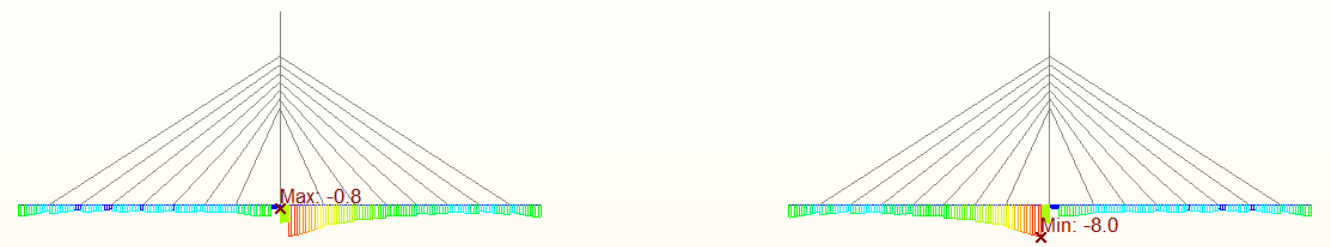

Figure 151 CS23 Top Stress [MPa]

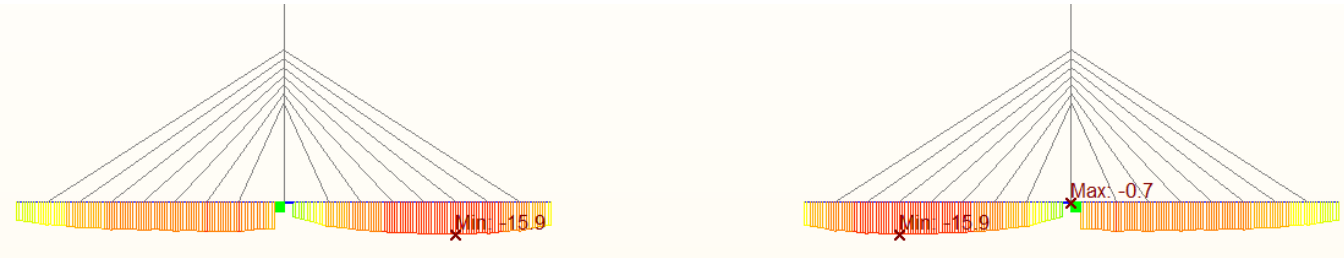

Figure 152 CS23 Bottom Stress [MPa]

Figure 153 CS24_1 Top Stress [MPa]

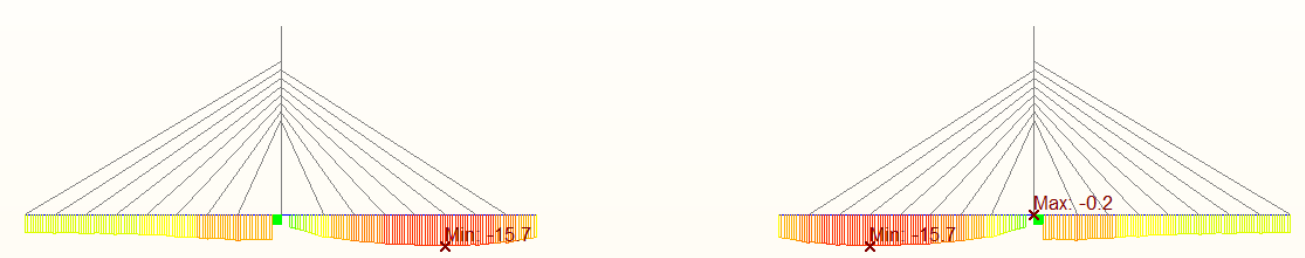

Figure 154 CS24_1 Bottom Stress [MPa]

Figure 155 CS24_2 Top Stress [MPa]

Figure 156 CS24_2 Bottom Stress [MPa]

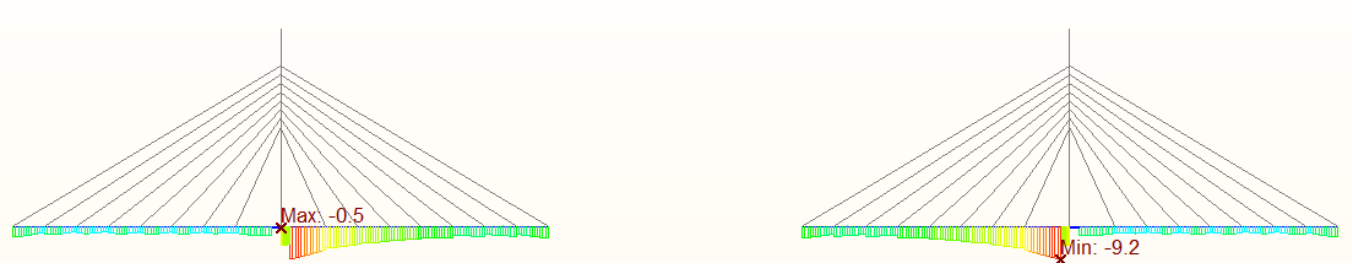

Figure 157 CS25 Top Stress [MPa]

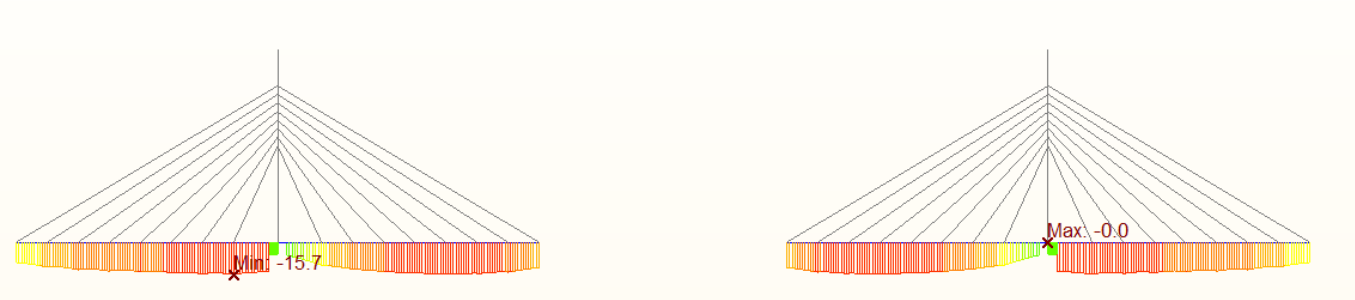

Figure 158 CS25 Bottom Stress [MPa]

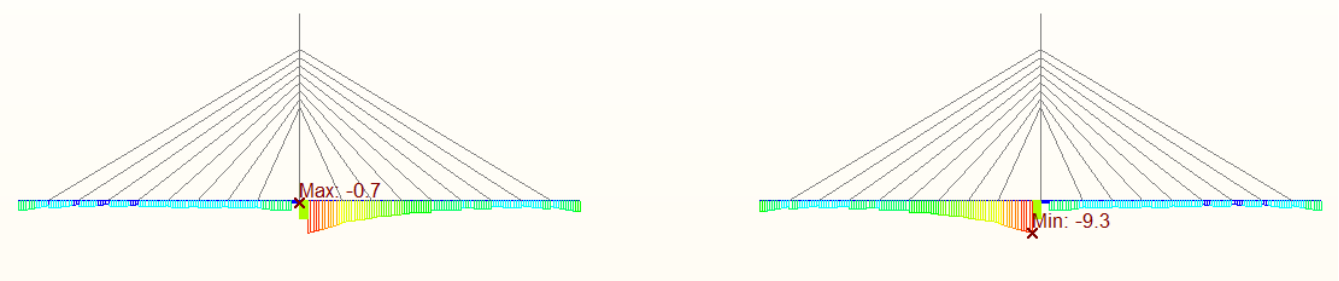

Figure 159 CS26 Top Stress [MPa]

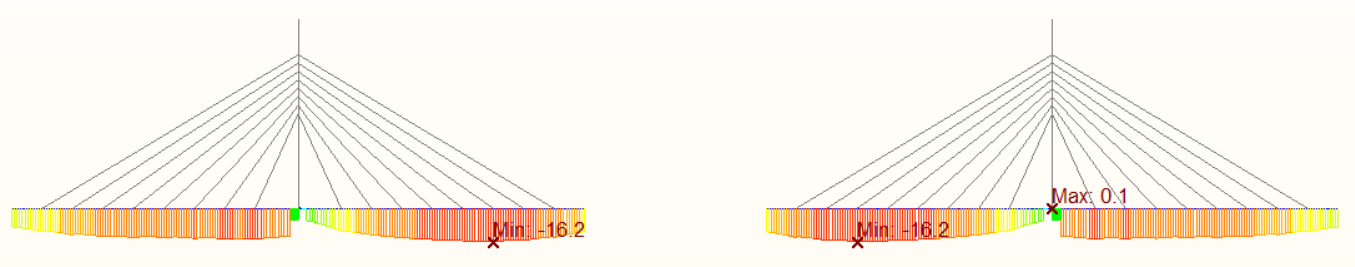

Figure 160 CS26 Bottom Stress [MPa]

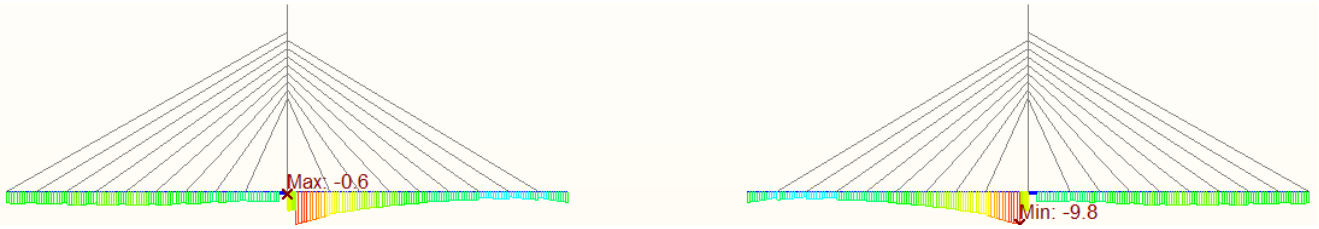

Figure 161 CS27_1 Top Stress [MPa]

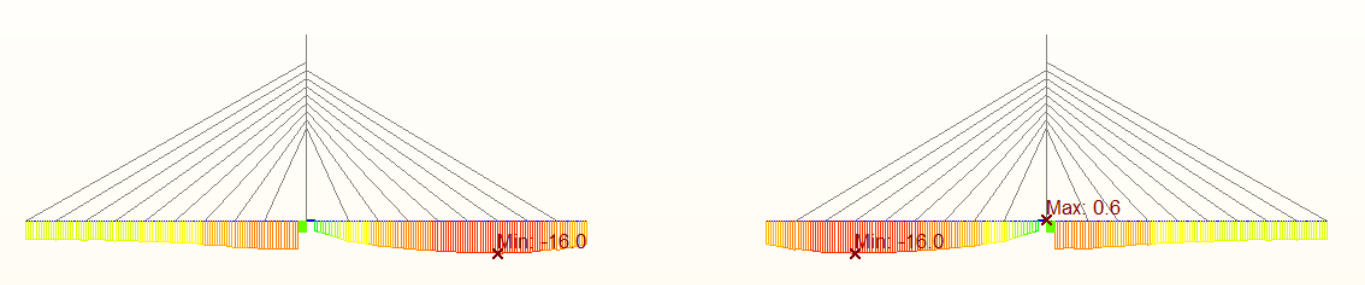

Figure 162 CS27_1 Bottom Stress [MPa]

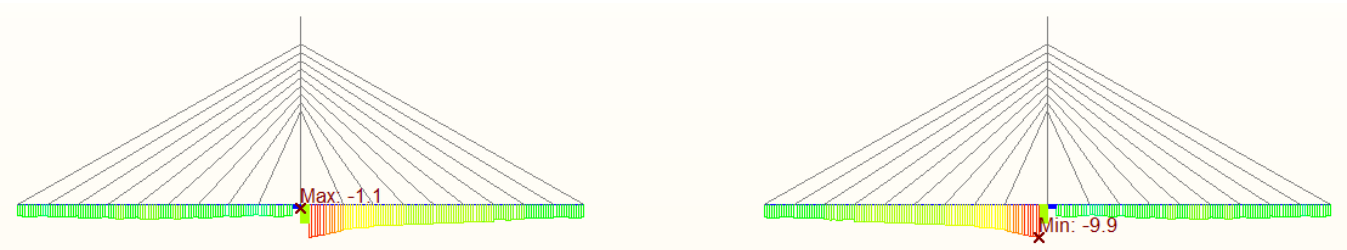

Figure 163 CS27_2 Top Stress [MPa]

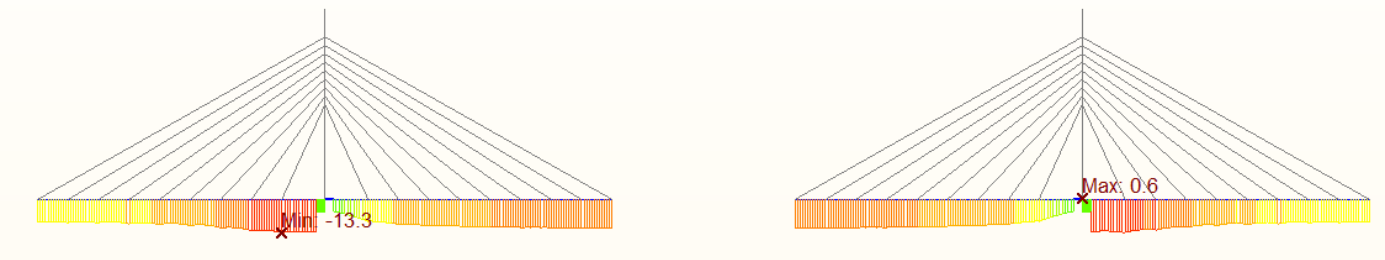

Figure 164 CS27_2 Bottom Stress [MPa]

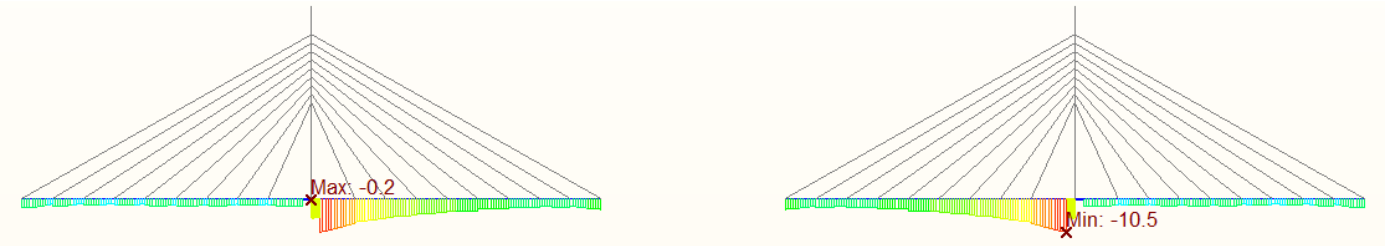

Figure 165 CS28 Top Stress [MPa]

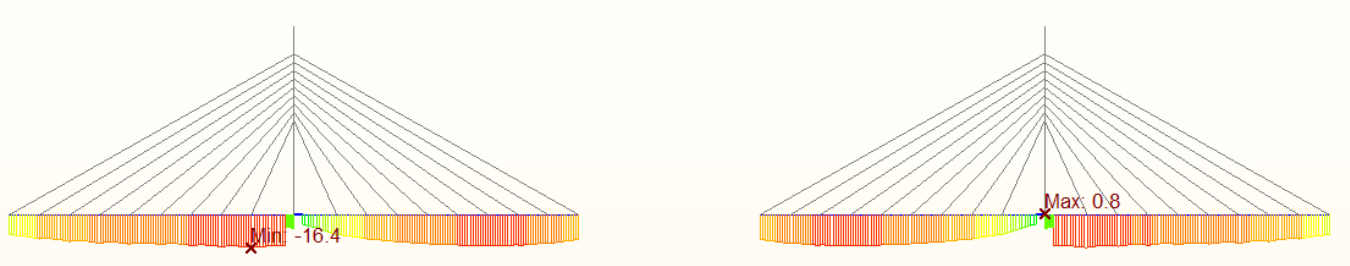

Figure 166 CS28 Bottom Stress [MPa]

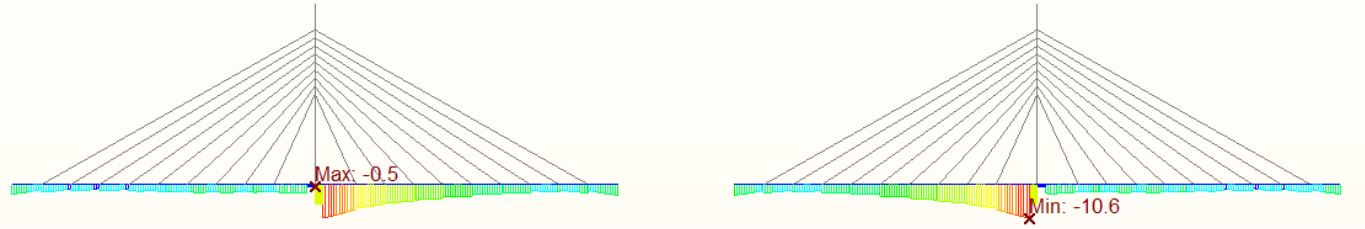

Figure 167 CS29 Top Stress [MPa]

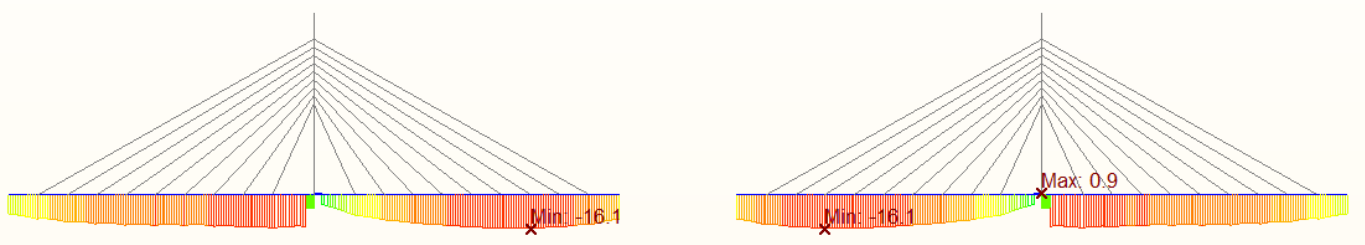

Figure 168 CS29 Bottom Stress [MPa]

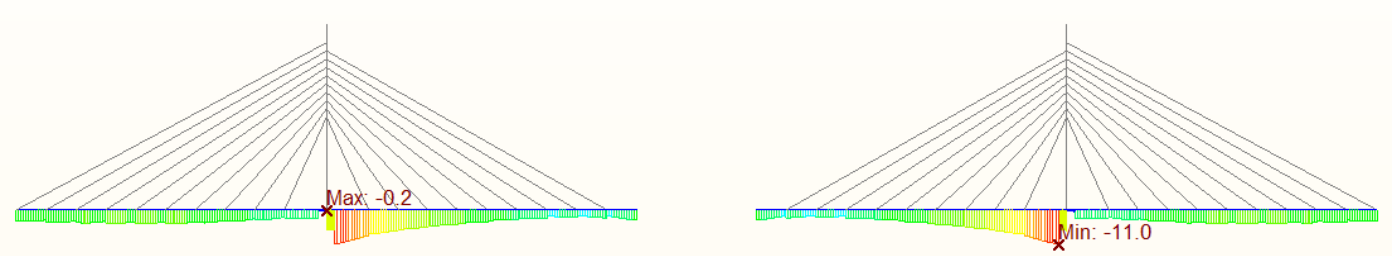

Figure 169 CS30_1 Top Stress [MPa]

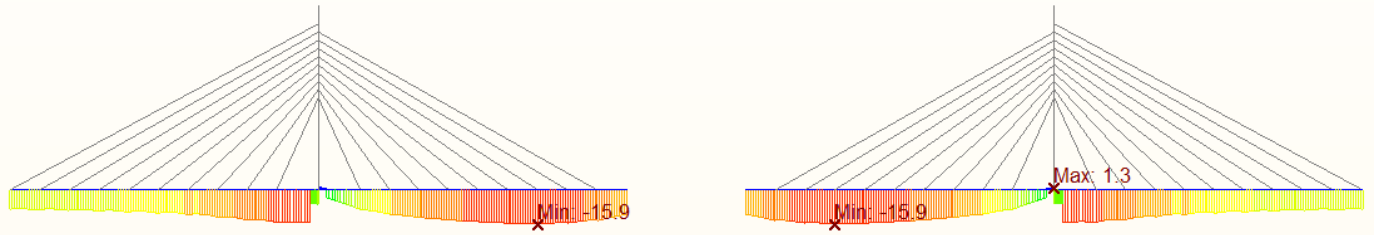

Figure 170 CS30_1 Bottom Stress [MPa]

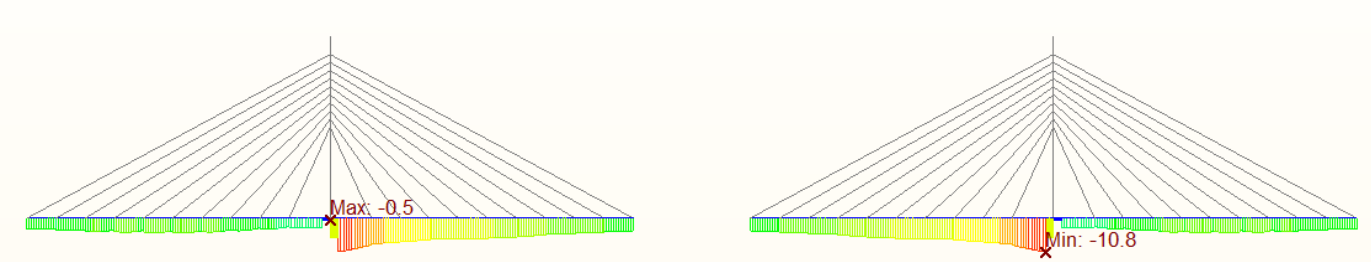

Figure 171 CS30_2 Top Stress [MPa]

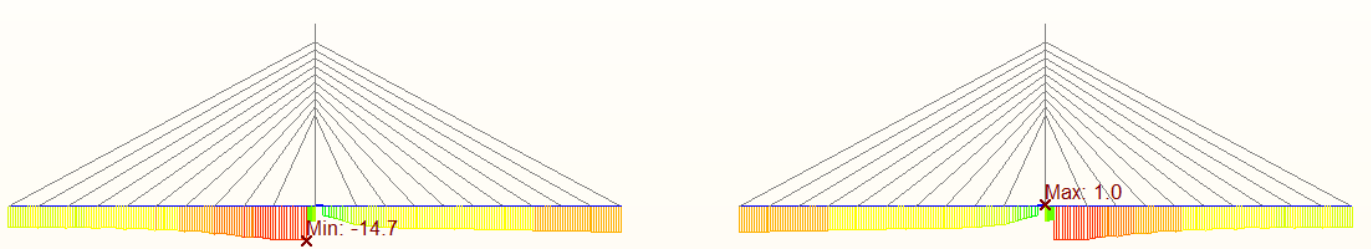

Figure 172 CS30_2 Bottom Stress [MPa]

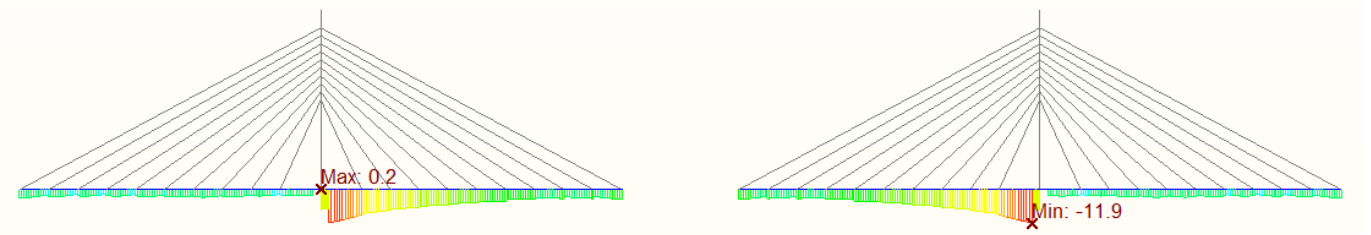

Figure 173 CS31 Top Stress [MPa]

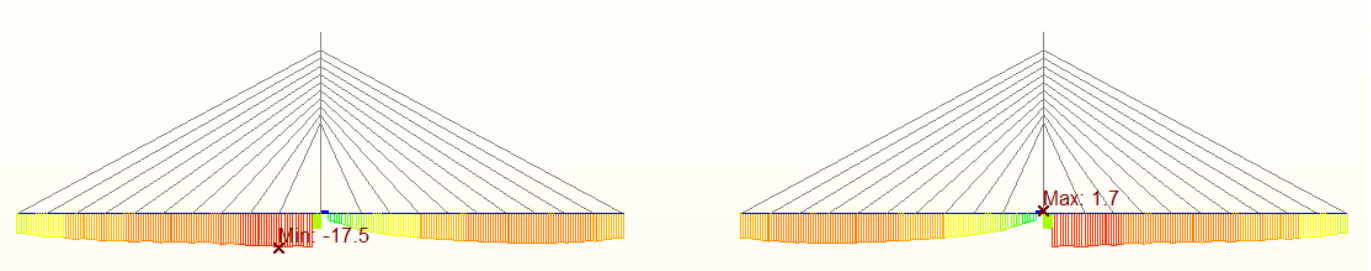

Figure 174 CS31 Bottom Stress [MPa]

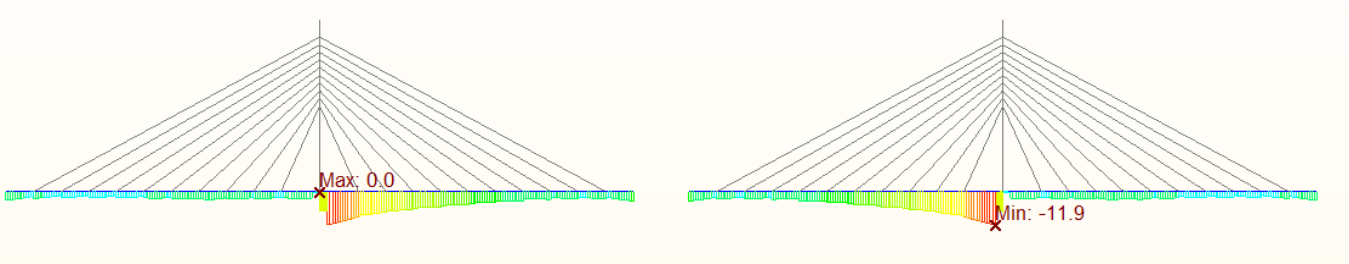

Figure 175 CS32 Top Stress [MPa]

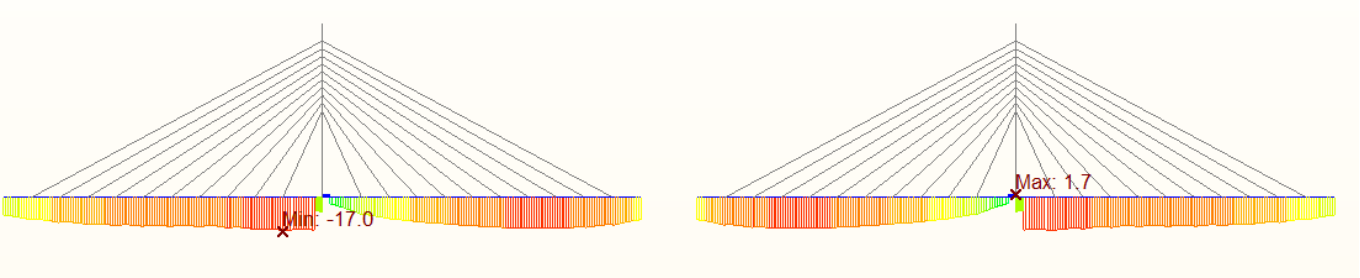

Figure 176 CS32 Bottom Stress [MPa]

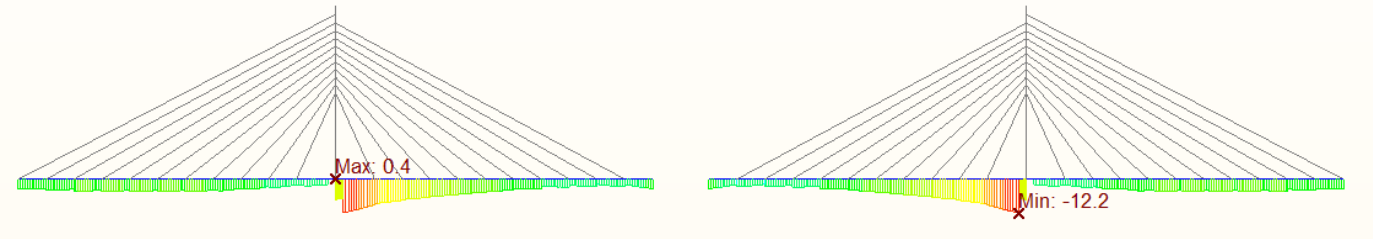

Figure 177 CS33_1 Top Stress [MPa]

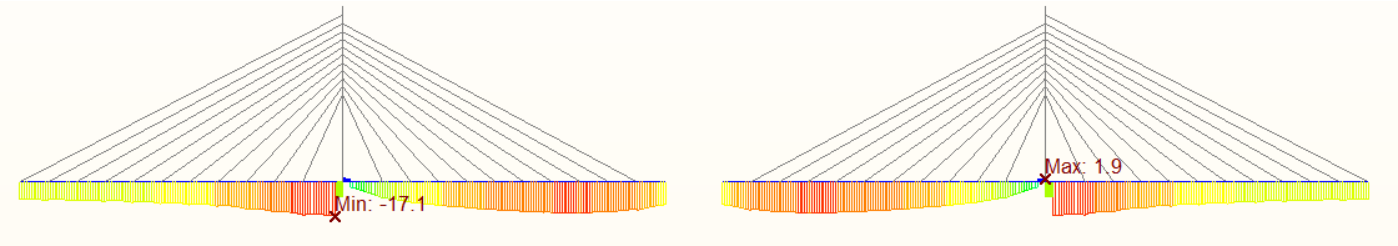

Figure 178 CS33_1 Bottom Stress [MPa]

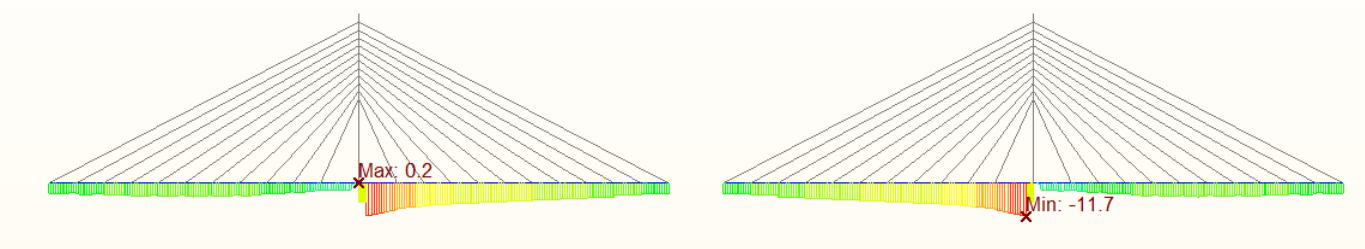

Figure 179 CS33_2 Top Stress [MPa]

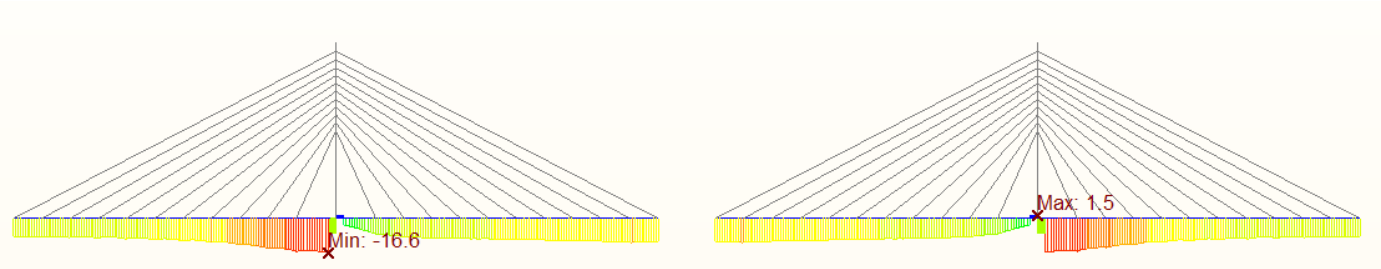

Figure 180 CS33_2 Bottom Stress [MPa]

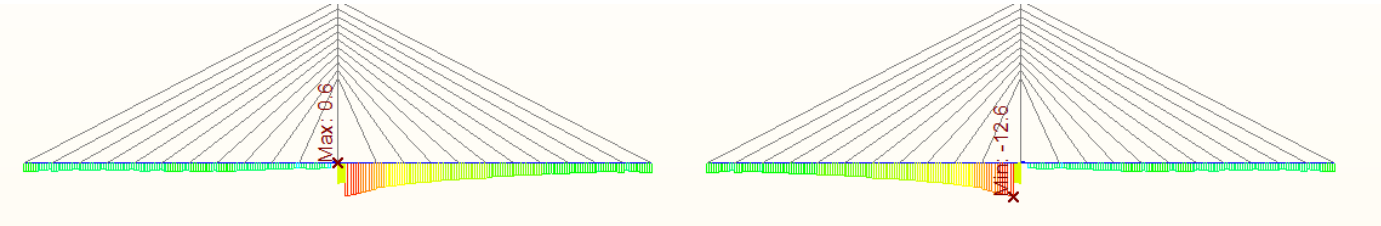

Figure 181 CS34 Top Stress [MPa]

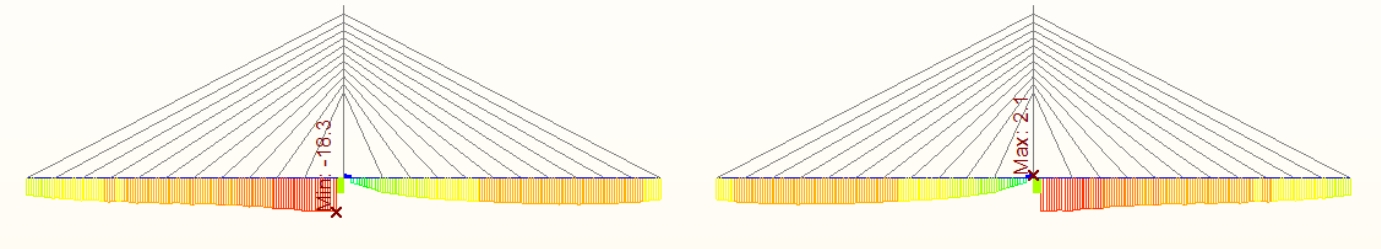

Figure 182 CS34 Bottom Stress [MPa]

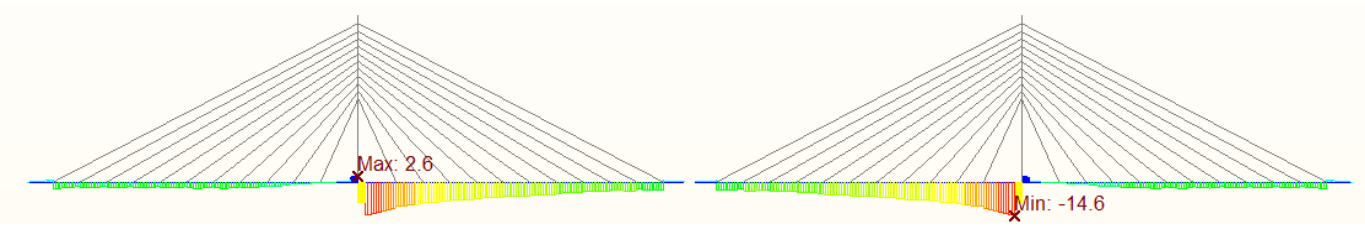

Figure 183 CS35 Top Stress [MPa]

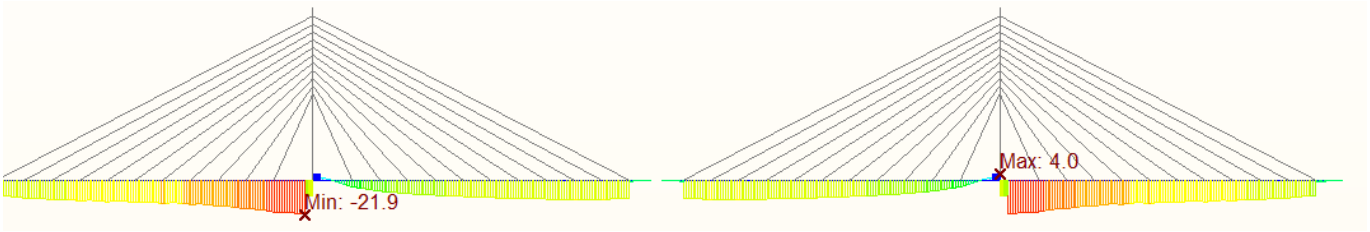

Figure 184 CS35 Bottom Stress [MPa]

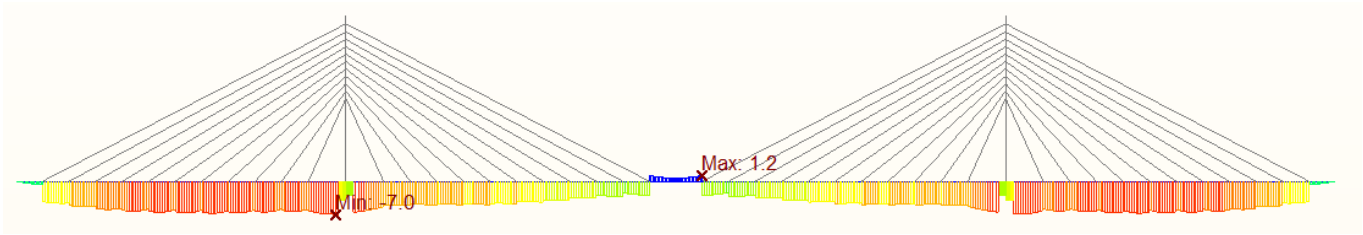

Figure 185 CS36 Top Stress [MPa]

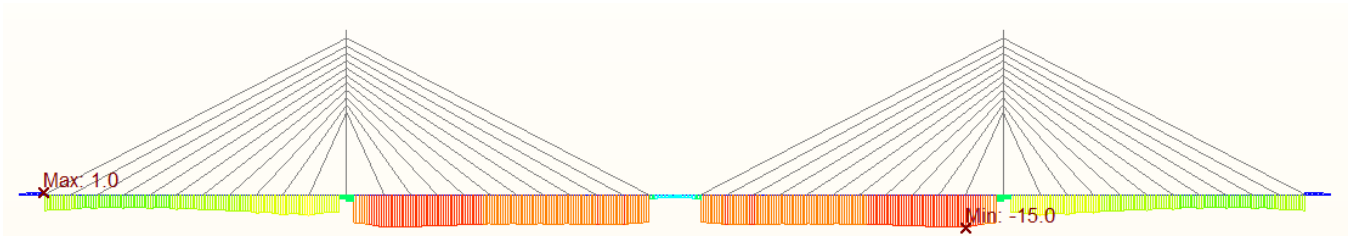

Figure 186 CS36 Bottom Stress [MPa]

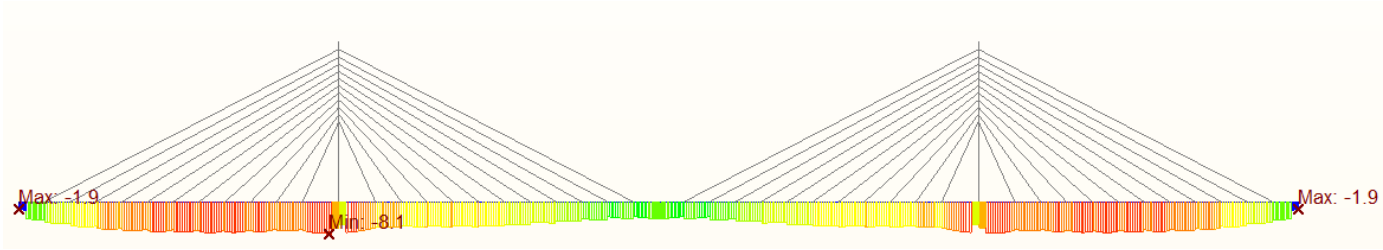

Figure 187 CS37 Top Stress [MPa]

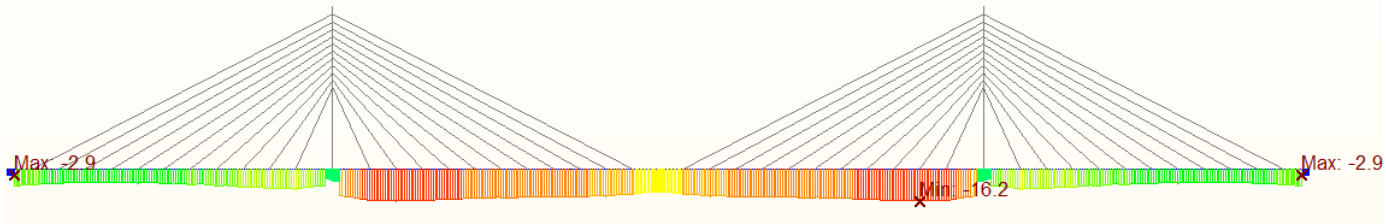

Figure 188 CS37 Bottom Stress [MPa]

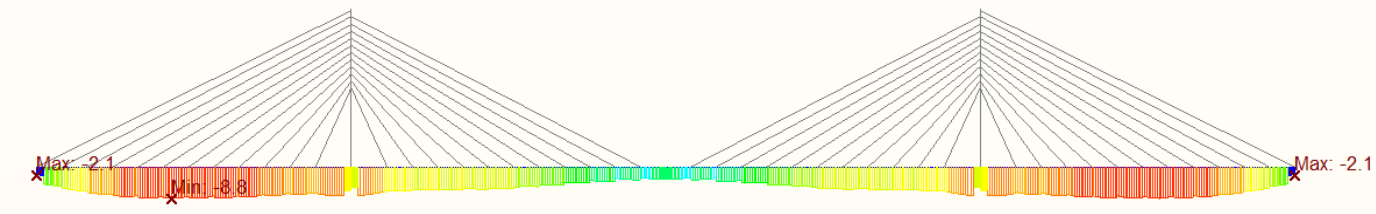

Figure 189 CS38_1 Top Stress [MPa]

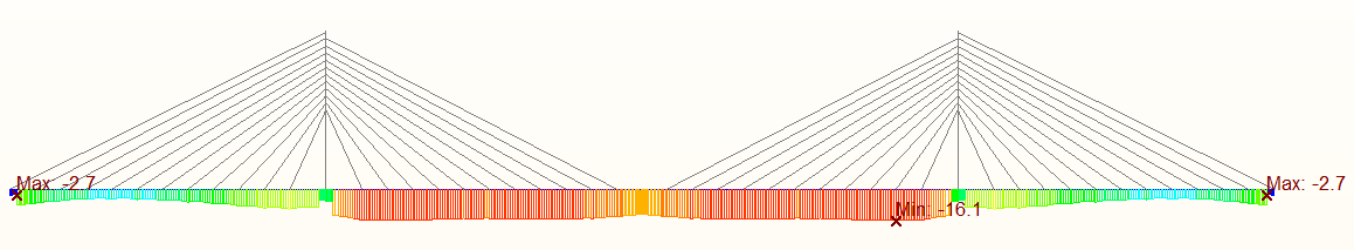

Figure 190 CS38_1 Bottom Stress [MPa]

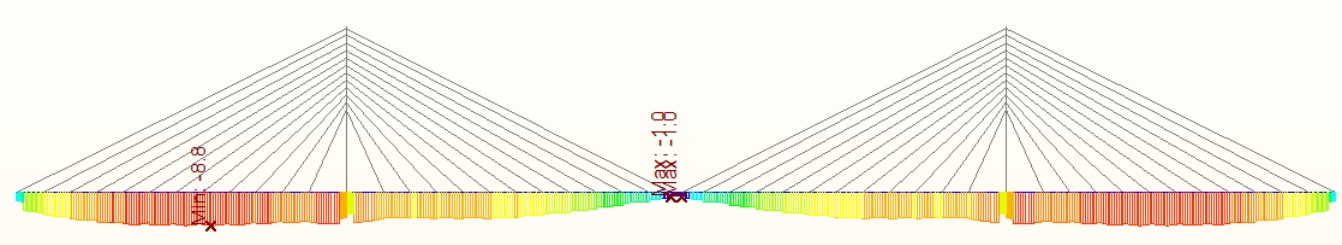

Figure 191 CS38_2 Top Stress [MPa]

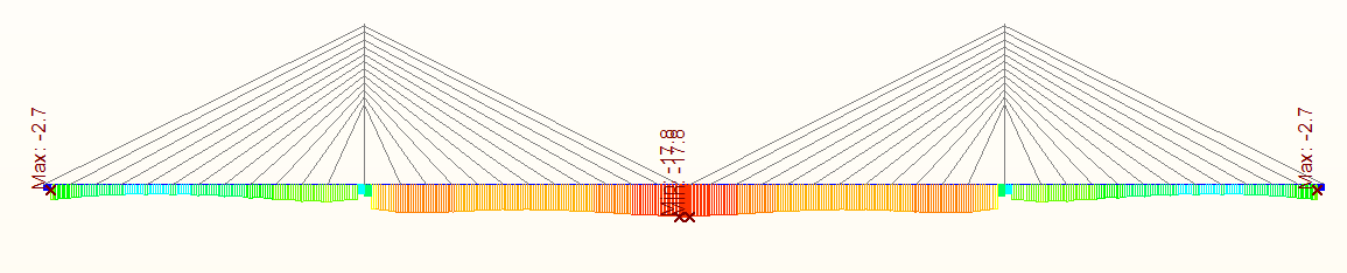

Figure 192 CS38 Bottom Stress [MPa]

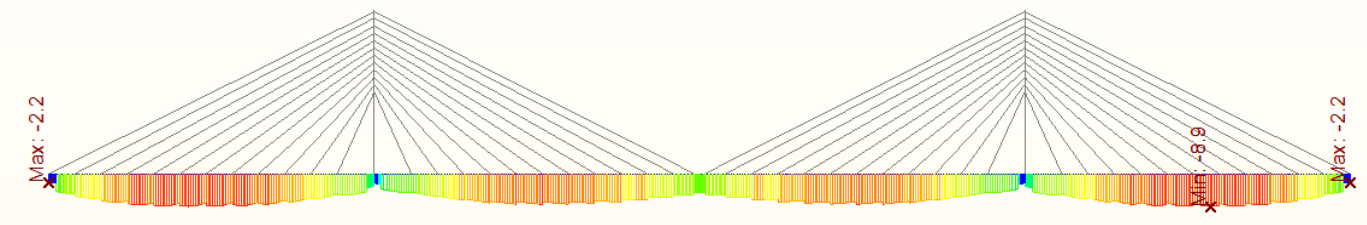

Figure 193 CS39 Top Stress [MPa]

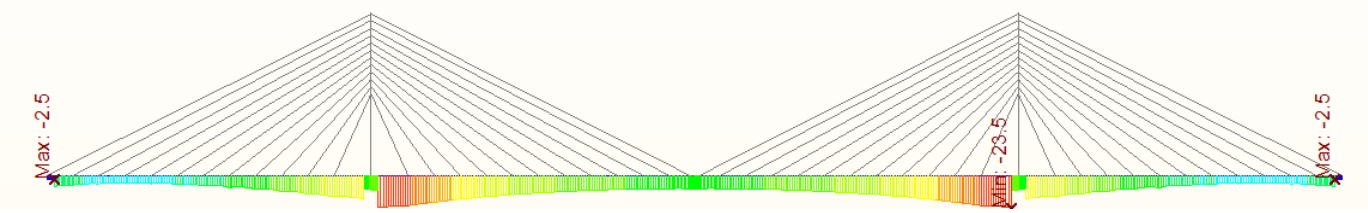

Figure 194 CS39 Bottom Stress [MPa]

Also, the stresses have been exported to excel and all construction stages have been checked for the top and bottom stresses and have been compared with the 0.6fck(t) and fctm(t), the excel sheet has more than 3000 rows, a sample of the sheet for CS10 is presented below.

Table 21 CS10 Top and bottom stresses check for left part of the structure for characteristic combination during construction

Stage	Seg.	Bottom Stresses	Top Stresses	fctm(t)	0.6*fck(t)	Check stresses (fctm(t)>stress>0.6fck(t)
CS10	S3	-10.10	-2.61	0.00	-27.23	ok
CS10	S3	-10.60	-2.35	3.77	-27.23	ok
CS10	S3	-11.30	-1.93	3.77	-27.23	ok
CS10	S2	-12.10	-1.66	4.10	-30.00	ok
CS10	S2	-12.30	-1.55	4.10	-30.00	ok
CS10	S2	-12.80	-1.26	4.10	-30.00	ok
CS10	S1	-13.40	-1.11	4.10	-30.00	ok
CS10	S1	-12.90	-1.38	4.10	-30.00	ok
CS10	S1	-12.80	-1.46	4.10	-30.00	ok
CS10	S0	-5.49	0.14	4.10	-30.00	ok
CS10	S0	-5.54	0.18	4.10	-30.00	ok
CS10	S0	-5.62	0.25	4.10	-30.00	ok
CS10	S0	-4.76	-0.42	4.10	-30.00	ok
CS10	S0	-4.70	-0.47	4.10	-30.00	ok
CS10	S0	-4.66	-0.51	4.10	-30.00	ok
CS10	S0	-14.50	-2.40	4.10	-30.00	ok
CS10	S1_2	-14.70	-2.33	4.10	-30.00	ok
CS10	S1_2	-15.10	-2.09	4.10	-30.00	ok
CS10	S1_2	-15.80	-1.36	4.10	-30.00	ok
CS10	S2_2	-15.20	-1.71	4.10	-30.00	ok
CS10	S2_2	-14.70	-1.94	4.10	-30.00	ok
CS10	S2_2	-14.80	-1.74	4.10	-30.00	ok
CS10	S3_2	-13.80	-2.28	3.77	-27.23	ok
CS10	S3_2	-13.00	-2.69	3.77	-27.23	ok
CS10	S3_2	-12.50	-2.98	3.77	-27.23	ok

7.1.2 Stresses at the time of service

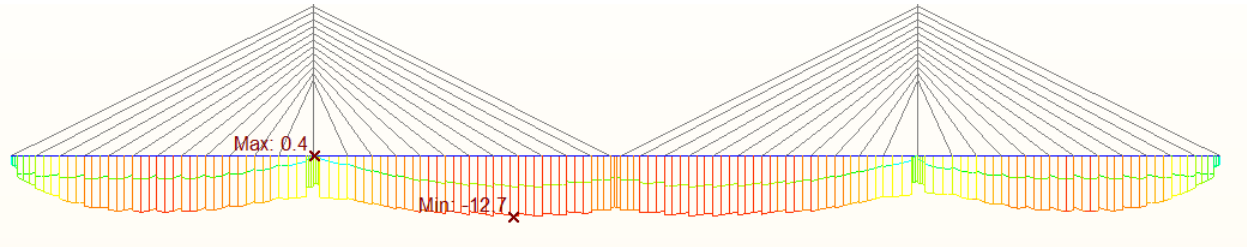

Figure 198 Top fiber stress envelop Ch SLS combination [MPa]

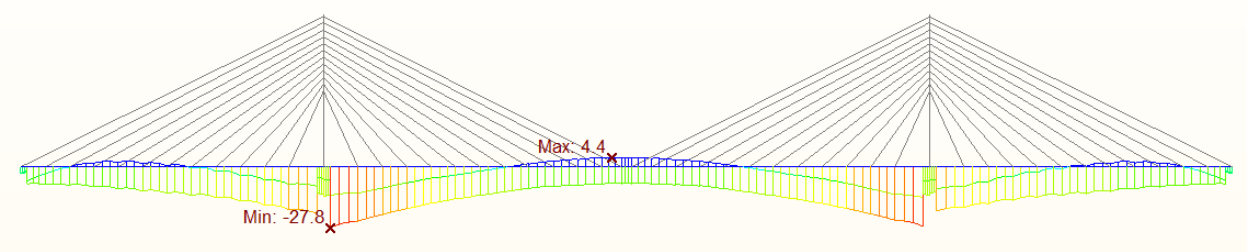

Figure 199 Bottom fiber stress envelop Ch SLS combination [MPa]

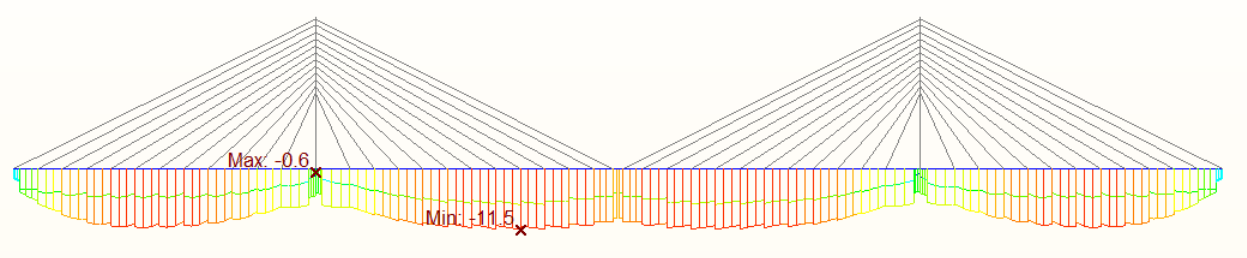

Figure 200 Top fiber stress envelop Ch Freq.SLS combination [MPa]

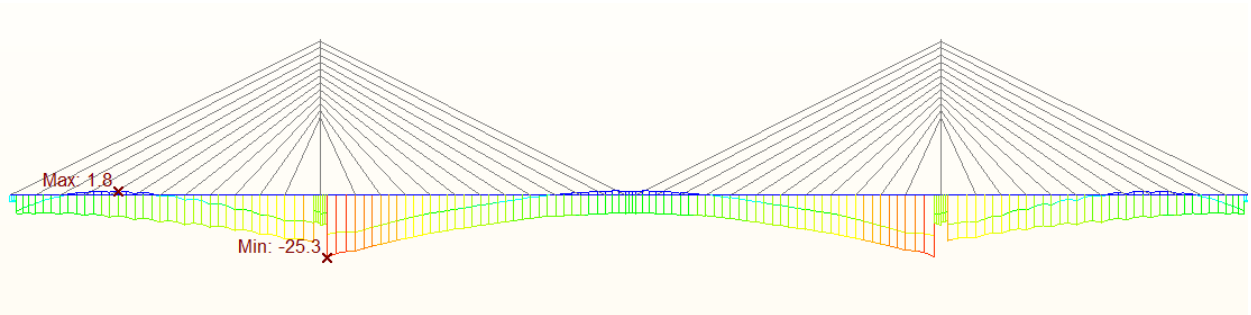

Figure 201 Bottom fiber stress envelop Ch Freq.SLS combination [MPa]

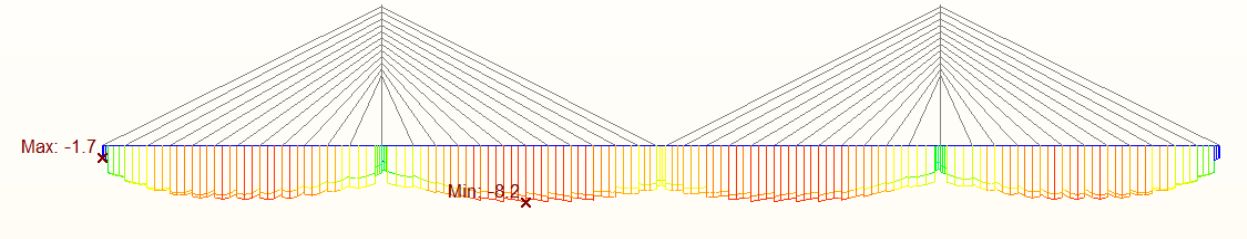

Figure 202Top fiber stress envelop Quasi Static SLS combination [MPa]

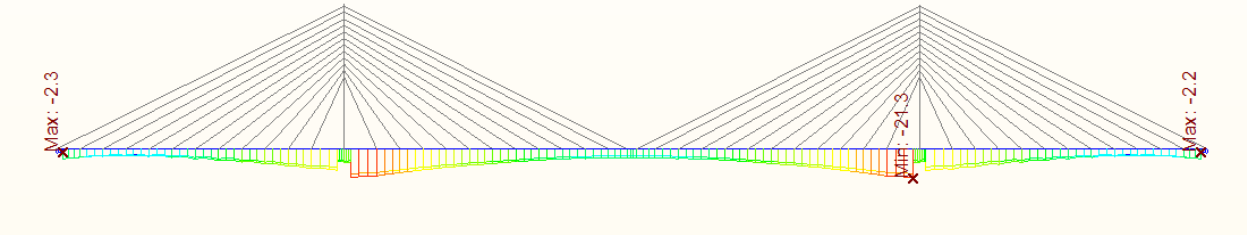

Figure 203 Bottom fiber stress envelop Quasi Static SLS combination [MPa]

7.1.3 Stresses at the end service [100 years]

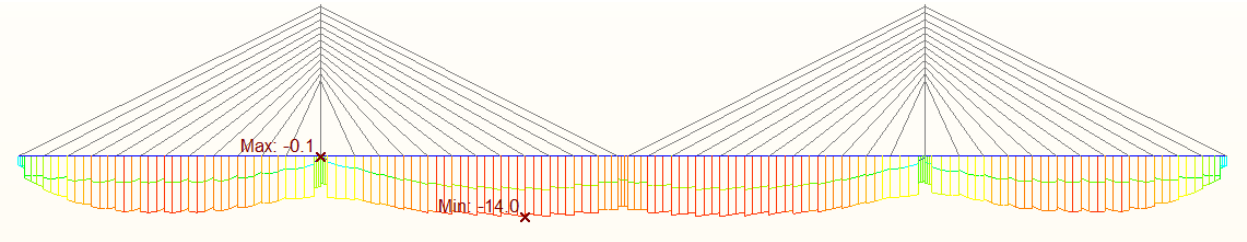

Figure 204 Top fiber stress envelop Ch SLS combination [MPa]

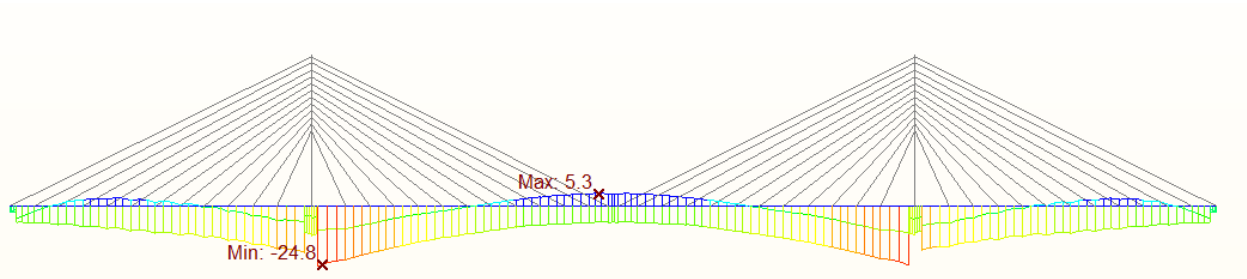

Figure 205 Bottom fiber stress envelop Ch SLS combination [MPa]

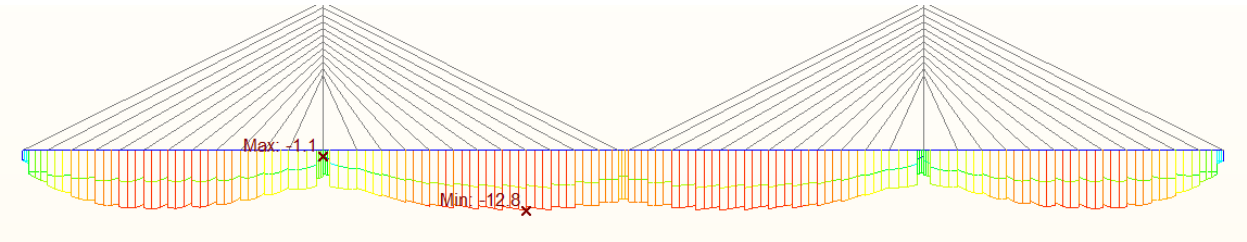

Figure 206Top fiber stress envelop Ch Freq.SLS combination [MPa]

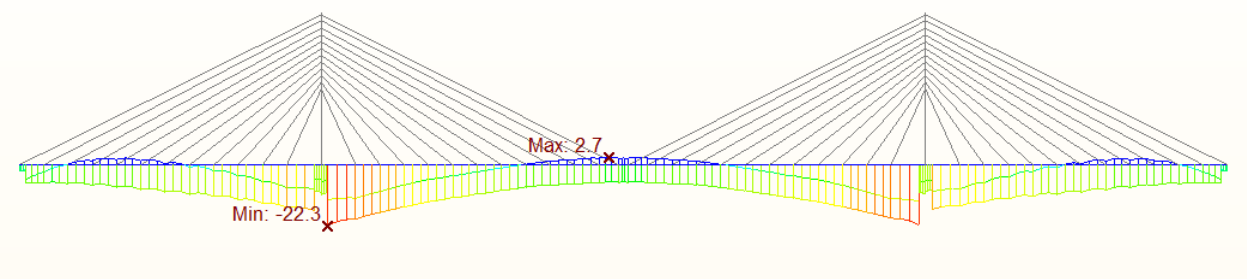

Figure 207 Bottom fiber stress envelop Ch Freq.SLS combination [MPa]

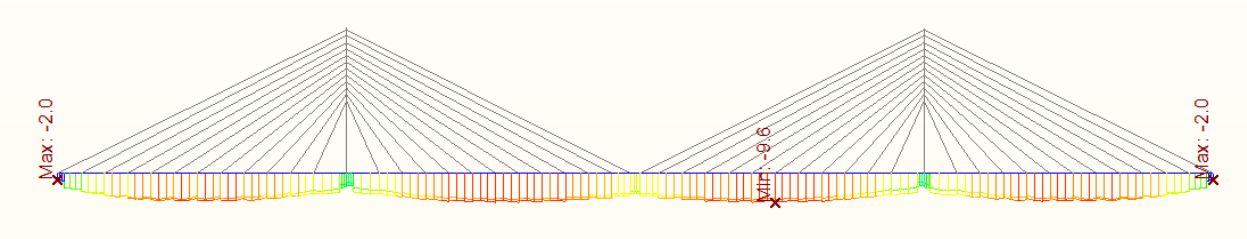

Figure 208 Top fiber stress envelop Quasi Static SLS combination [MPa]

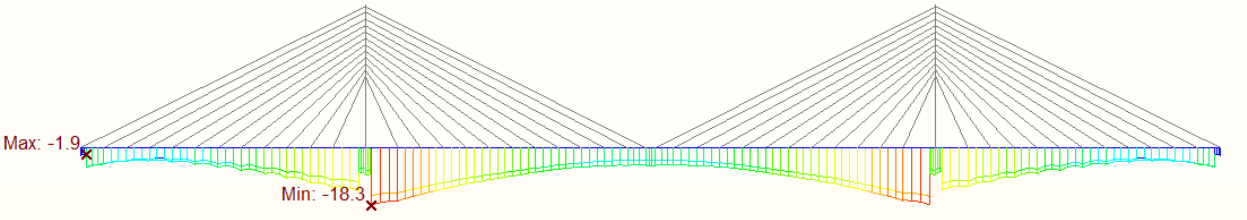

Figure 209 Bottom fiber stress envelop Quasi Static SLS combination [MPa]

7.2 Crack Control and stress limit

The concrete tensile strength fctm=4.1 Mpa has not been exceeded at the characteristic combination of all the construction stages, time of service, and time of the end of serve have. So, the cracking calculation is not necessary,. [14]

Table 22 Recommended values of w,max and relevant combination rules (ČSN EN 1992-2 NA ed. A)

ČSN EN 1992-2 NA ed. A

Table NA.1 – Recommended values of w_{max} and relevant combination rules[d), f), g)]

Exposure class	Reinforced members and prestressed members without bonded tendons (quasi-permanent load combination)	Prestressed members with bonded tendons (frequent load combination)		
		Pretensioned concrete	Posttensioned concrete	
		Protection level of prestressing reinforcement PL1 to PL3[c)]	Protection level of prestressing reinforcement PL1[c)]	Protection level of prestressing reinforcement PL2 and PL3[c)]
X0, XC1	0,4[a)]	0,2	0,2	0,3
XC2, XC3, XC4	0,3	0,1[b)]	0,2[b)]	0,3
XD, XS, XF	0,2	Decompression[e)]	0,1[b)]	0,2

For quasi-permanent limit state, its required to check the state of decompression, as it shown om figure of stresses, the stresses in this limit state are all in compression, so the state of decompression is guaranteed.

7.3 Limit stresses in the stay cables

The stresses in the stay cables have been restricted to the value of 0.45fpk =0.45*1860 = 837 MPa, this check is in the following table, due to symmetry on part of the structure has been considered during construction.

According to check the cable stresses are satisfied this limit in all construction stages, in-service condition, and at the end life of the structure.

Also, the E, eff have been calculated and compared with the E0 which is 195 Gpa, the ratio between the E, eff and E0 have been computed to check the validation of linear analysis assumption, the cable with the lowest E, eff was L3 where E, eff =183.21 Gpa with a ratio of 94% in construction stage so the assumption of linear analysis is realistic.

7.3.1 During construction

Table 23 Stresses during construction (characteristic combination)

Stage	Stress [Mpa]	Cable	E, eff	Eeff/E0*100%	check σ/0.45*fpk	Stage	Stress [Mpa]	Cable	E, eff	Eeff/E0*100%	check σ/0.45*fpk
CS3	617.60	L12	194.99	100.00	0.74	CS28	258.60	L17	193.28	99.12	0.31
CS3_2	629.50	L13	194.99	100.00	0.75	CS28	295.70	L18	193.38	99.17	0.35
CS3_2	691.90	L12	194.99	100.00	0.83	CS28	400.80	L21	193.60	99.28	0.48
CS4	648.50	L13	194.99	100.00	0.77	CS28	372.90	L5	193.61	99.29	0.45
CS4	716.60	L12	194.99	100.00	0.86	CS28	356.00	L6	193.76	99.36	0.43

CS5	653.60	L13	194.99	100.00	0.78	CS28	421.00	L4	193.79	99.38	0.50
CS5	721.60	L12	194.99	100.00	0.86	CS28	294.40	L8	193.83	99.40	0.35
CS6	419.80	L11	194.92	99.96	0.50	CS28	329.90	L7	193.83	99.40	0.39
CS6_2	437.60	L14	194.93	99.96	0.52	CS28	384.60	L19	194.01	99.49	0.46
CS6_2	491.30	L11	194.95	99.97	0.59	CS28	277.60	L9	194.07	99.52	0.33
CS6	621.60	L12	194.99	100.00	0.74	CS28	301.70	L10	194.57	99.78	0.36
CS6_2	633.50	L13	194.99	100.00	0.76	CS28	474.70	L16	194.81	99.90	0.57
CS6_2	676.30	L12	194.99	100.00	0.81	CS28	479.70	L15	194.89	99.94	0.57
CS6	721.40	L13	194.99	100.00	0.86	CS28	435.10	L11	194.93	99.96	0.52
CS7	485.60	L14	194.95	99.97	0.58	CS28	472.60	L14	194.94	99.97	0.56
CS7	547.60	L11	194.96	99.98	0.65	CS28	599.80	L12	194.99	100.00	0.72
CS7	659.70	L13	194.99	100.00	0.79	CS28	661.70	L13	194.99	100.00	0.79
CS7	706.10	L12	194.99	100.00	0.84	CS29	251.70	L17	193.13	99.04	0.30
CS8	495.50	L14	194.95	99.97	0.59	CS29	342.80	L20	193.21	99.08	0.41
CS8	556.70	L11	194.97	99.98	0.67	CS29	289.70	L18	193.28	99.12	0.35
CS8	662.40	L13	194.99	100.00	0.79	CS29	370.60	L5	193.58	99.27	0.44
CS8	708.80	L12	194.99	100.00	0.85	CS29	402.40	L21	193.61	99.29	0.48
CS9	268.20	L10	194.38	99.68	0.32	CS29	351.70	L6	193.71	99.34	0.42
CS9_2	323.60	L10	194.65	99.82	0.39	CS29	288.50	L8	193.76	99.36	0.34
CS9_2	445.00	L15	194.86	99.93	0.53	CS29	324.40	L7	193.77	99.37	0.39
CS9	437.70	L11	194.93	99.96	0.52	CS29	421.50	L4	193.79	99.38	0.50
CS9_2	440.00	L14	194.93	99.96	0.53	CS29	380.20	L19	193.98	99.48	0.45
CS9_2	489.30	L11	194.95	99.97	0.58	CS29	272.10	L9	194.01	99.49	0.33
CS9	558.00	L14	194.97	99.98	0.67	CS29	297.20	L10	194.55	99.77	0.36
CS9	630.30	L12	194.99	100.00	0.75	CS29	467.80	L16	194.80	99.90	0.56
CS9_2	632.20	L13	194.99	100.00	0.76	CS29	473.50	L15	194.89	99.94	0.57
CS9_2	671.60	L12	194.99	100.00	0.80	CS29	432.30	L11	194.93	99.96	0.52
CS9	709.90	L13	194.99	100.00	0.85	CS29	467.90	L14	194.94	99.97	0.56
CS10	403.00	L10	194.82	99.91	0.48	CS29	599.00	L12	194.99	100.00	0.72
CS10	530.20	L15	194.92	99.96	0.63	CS29	659.10	L13	194.99	100.00	0.79
CS10	501.20	L14	194.95	99.98	0.60	CS30_2	241.90	L20	190.00	97.44	0.29
CS10	544.90	L11	194.96	99.98	0.65	CS30_2	284.10	L21	191.11	98.01	0.34
CS10	663.90	L13	194.99	100.00	0.79	CS30_2	225.80	L18	191.40	98.15	0.27
CS10	697.20	L12	194.99	100.00	0.83	CS30	315.10	L3	191.51	98.21	0.38
CS11	413.50	L10	194.83	99.91	0.49	CS30_2	205.70	L17	191.60	98.26	0.25
CS11	540.40	L15	194.92	99.96	0.65	CS30	279.70	L5	191.74	98.33	0.33
CS11	505.40	L14	194.95	99.98	0.60	CS30_2	323.50	L3	191.77	98.34	0.39
CS11	548.60	L11	194.96	99.98	0.66	CS30_2	282.60	L5	191.83	98.38	0.34
CS11	664.70	L13	194.99	100.00	0.79	CS30	312.00	L4	192.05	98.49	0.37
CS11	696.90	L12	194.99	100.00	0.83	CS30_2	317.70	L4	192.20	98.57	0.38
CS12	246.60	L9	193.68	99.32	0.29	CS30	279.90	L6	192.46	98.70	0.33
CS12_2	282.40	L9	194.12	99.55	0.34	CS30_2	280.40	L6	192.47	98.70	0.34
CS12	299.90	L10	194.56	99.77	0.36	CS30_2	269.80	L7	192.87	98.91	0.32
CS12_2	335.30	L10	194.68	99.84	0.40	CS30_2	297.60	L19	192.88	98.91	0.36
CS12_2	444.10	L16	194.77	99.88	0.53	CS30	271.20	L7	192.91	98.93	0.32
CS12_2	452.50	L15	194.87	99.93	0.54	CS30	249.40	L17	193.08	99.02	0.30
CS12_2	442.20	L14	194.93	99.96	0.53	CS30_2	249.70	L8	193.09	99.02	0.30
CS12	460.00	L11	194.94	99.97	0.55	CS30	252.70	L8	193.15	99.05	0.30
CS12	581.70	L15	194.94	99.97	0.69	CS30	288.70	L18	193.26	99.11	0.34
CS12_2	494.40	L11	194.95	99.97	0.59	CS30	346.50	L20	193.27	99.11	0.41
CS12	542.80	L14	194.96	99.98	0.65	CS30	409.10	L21	193.68	99.32	0.49
CS12_2	631.60	L13	194.99	100.00	0.75	CS30_2	247.50	L9	193.69	99.33	0.30
CS12	641.60	L12	194.99	100.00	0.77	CS30	251.30	L9	193.75	99.36	0.30
CS12_2	670.70	L12	194.99	100.00	0.80	CS30	381.20	L19	193.99	99.48	0.46
CS12	694.30	L13	194.99	100.00	0.83	CS30_2	590.90	L22	194.46	99.72	0.71
CS13	380.20	L9	194.64	99.81	0.45	CS30_2	284.50	L10	194.48	99.73	0.34
CS13	411.20	L10	194.83	99.91	0.49	CS30	288.70	L10	194.50	99.75	0.34
CS13	557.50	L16	194.88	99.94	0.67	CS30_2	438.10	L16	194.76	99.88	0.52
CS13	545.50	L15	194.93	99.96	0.65	CS30	464.80	L16	194.80	99.90	0.56
CS13	507.80	L14	194.95	99.98	0.61	CS30_2	458.10	L15	194.88	99.94	0.55
CS13	541.90	L11	194.96	99.98	0.65	CS30	470.50	L15	194.89	99.94	0.56

CS13	665.60	L13	194.99	100.00	0.80	CS30_2	428.50	L11	194.92	99.96	0.51
CS13	687.80	L12	194.99	100.00	0.82	CS30	432.30	L11	194.93	99.96	0.52
CS14	387.60	L9	194.66	99.82	0.46	CS30_2	463.80	L14	194.94	99.97	0.55
CS14	413.60	L10	194.83	99.91	0.49	CS30	465.60	L14	194.94	99.97	0.56
CS14	568.30	L16	194.89	99.94	0.68	CS30_2	600.10	L12	194.99	100.00	0.72
CS14	549.90	L15	194.93	99.96	0.66	CS30	602.60	L12	194.99	100.00	0.72
CS14	508.00	L14	194.95	99.98	0.61	CS30	658.00	L13	194.99	100.00	0.79
CS14	541.20	L11	194.96	99.98	0.65	CS30_2	661.50	L13	194.99	100.00	0.79
CS14	664.30	L13	194.99	100.00	0.79	CS31	320.20	L20	192.81	98.88	0.38
CS14	686.20	L12	194.99	100.00	0.82	CS31	244.20	L17	192.96	98.95	0.29
CS15_2	231.40	L17	192.60	98.77	0.28	CS31	276.50	L18	193.02	98.99	0.33
CS15	240.90	L8	192.87	98.91	0.29	CS31	376.40	L21	193.31	99.13	0.45
CS15_2	263.90	L8	193.38	99.17	0.32	CS31	358.60	L5	193.44	99.20	0.43
CS15	251.10	L9	193.75	99.36	0.30	CS31	340.00	L6	193.58	99.27	0.41
CS15_2	274.10	L9	194.03	99.50	0.33	CS31	276.70	L8	193.59	99.28	0.33
CS15	301.50	L10	194.56	99.78	0.36	CS31	429.00	L3	193.60	99.28	0.51
CS15_2	325.20	L10	194.65	99.82	0.39	CS31	312.80	L7	193.63	99.30	0.37
CS15_2	453.70	L16	194.79	99.89	0.54	CS31	409.30	L4	193.68	99.32	0.49
CS15_2	458.00	L15	194.88	99.94	0.55	CS31	361.90	L19	193.82	99.39	0.43
CS15	600.40	L16	194.91	99.95	0.72	CS31	259.20	L9	193.86	99.41	0.31
CS15_2	445.60	L14	194.93	99.97	0.53	CS31	282.40	L10	194.47	99.73	0.34
CS15	458.50	L11	194.94	99.97	0.55	CS31	696.00	L22	194.67	99.83	0.83
CS15	580.10	L15	194.94	99.97	0.69	CS31	466.30	L16	194.80	99.90	0.56
CS15_2	483.00	L11	194.95	99.97	0.58	CS31	478.40	L15	194.89	99.94	0.57
CS15	536.20	L14	194.96	99.98	0.64	CS31	415.10	L11	194.92	99.96	0.50
CS15_2	634.00	L13	194.99	100.00	0.76	CS31	478.30	L14	194.95	99.97	0.57
CS15	637.60	L12	194.99	100.00	0.76	CS31	581.30	L12	194.99	99.99	0.69
CS15_2	659.80	L12	194.99	100.00	0.79	CS31	671.00	L13	194.99	100.00	0.80
CS15	687.80	L13	194.99	100.00	0.82	CS32	315.30	L20	192.71	98.83	0.38
CS16	333.30	L17	194.19	99.59	0.40	CS32	237.70	L17	192.79	98.86	0.28
CS16	364.50	L8	194.38	99.68	0.44	CS32	270.00	L18	192.88	98.91	0.32
CS16	356.80	L9	194.56	99.77	0.43	CS32	373.40	L21	193.27	99.11	0.45
CS16	385.10	L10	194.79	99.89	0.46	CS32	353.60	L5	193.37	99.16	0.42
CS16	541.80	L16	194.87	99.94	0.65	CS32	271.10	L8	193.50	99.23	0.32
CS16	528.30	L15	194.92	99.96	0.63	CS32	334.20	L6	193.50	99.23	0.40
CS16	494.30	L14	194.95	99.97	0.59	CS32	306.90	L7	193.55	99.26	0.37
CS16	516.90	L11	194.96	99.98	0.62	CS32	427.70	L3	193.59	99.28	0.51
CS16	658.90	L13	194.99	100.00	0.79	CS32	405.90	L4	193.65	99.31	0.48
CS16	668.50	L12	194.99	100.00	0.80	CS32	355.90	L19	193.76	99.36	0.43
CS17	339.20	L17	194.23	99.61	0.41	CS32	254.50	L9	193.79	99.38	0.30
CS17	369.10	L8	194.40	99.69	0.44	CS32	279.00	L10	194.45	99.72	0.33
CS17	357.30	L9	194.56	99.78	0.43	CS32	695.70	L22	194.67	99.83	0.83
CS17	383.00	L10	194.79	99.89	0.46	CS32	460.30	L16	194.80	99.89	0.55
CS17	542.50	L16	194.87	99.94	0.65	CS32	473.30	L15	194.89	99.94	0.57
CS17	525.60	L15	194.92	99.96	0.63	CS32	413.30	L11	194.92	99.96	0.49
CS17	490.20	L14	194.95	99.97	0.59	CS32	474.60	L14	194.94	99.97	0.57
CS17	513.80	L11	194.96	99.98	0.61	CS32	581.20	L12	194.99	99.99	0.69
CS17	655.80	L13	194.99	100.00	0.78	CS32	669.10	L13	194.99	100.00	0.80
CS17	666.40	L12	194.99	100.00	0.80	CS33_1	243.50	L20	190.09	97.48	0.29
CS18_2	227.90	L17	192.49	98.71	0.27	CS33_1	319.50	L23	190.98	97.94	0.38
CS18_2	255.10	L18	192.49	98.71	0.30	CS33_1	283.80	L21	191.10	98.00	0.34
CS18	258.60	L7	192.59	98.76	0.31	CS33_1	311.10	L3	191.37	98.14	0.37
CS18_2	271.20	L7	192.91	98.93	0.32	CS33	311.80	L3	191.40	98.15	0.37
CS18	248.60	L8	193.06	99.01	0.30	CS33_1	273.60	L5	191.52	98.21	0.33
CS18_2	260.30	L8	193.31	99.13	0.31	CS33	273.80	L5	191.52	98.22	0.33
CS18	257.00	L9	193.83	99.40	0.31	CS33_1	231.70	L18	191.66	98.29	0.28
CS18_2	268.60	L9	193.97	99.47	0.32	CS33_1	307.00	L4	191.91	98.41	0.37
CS18	353.20	L17	194.32	99.65	0.42	CS33	307.50	L4	191.92	98.42	0.37
CS18	305.40	L10	194.58	99.79	0.36	CS33_1	213.90	L17	191.97	98.45	0.26
CS18_2	317.60	L10	194.63	99.81	0.38	CS33	272.60	L6	192.25	98.59	0.33
CS18_2	448.80	L16	194.78	99.89	0.54	CS33_1	273.00	L6	192.27	98.60	0.33

CS18_2	453.90	L15	194.87	99.93	0.54	CS33	234.00	L17	192.68	98.81	0.28
CS18	555.10	L16	194.88	99.94	0.66	CS33	262.60	L7	192.70	98.82	0.31
CS18	538.00	L15	194.92	99.96	0.64	CS33_1	263.30	L7	192.71	98.83	0.31
CS18_2	444.00	L14	194.93	99.96	0.53	CS33	318.50	L20	192.78	98.86	0.38
CS18	460.50	L11	194.94	99.97	0.55	CS33	268.10	L18	192.83	98.89	0.32
CS18_2	473.70	L11	194.94	99.97	0.57	CS33	242.80	L8	192.92	98.93	0.29
CS18	503.10	L14	194.95	99.98	0.60	CS33_1	243.70	L8	192.94	98.95	0.29
CS18_2	634.90	L13	194.99	100.00	0.76	CS33_1	301.40	L19	192.96	98.95	0.36
CS18	637.50	L12	194.99	100.00	0.76	CS33	379.80	L21	193.35	99.16	0.45
CS18_2	650.20	L12	194.99	100.00	0.78	CS33	240.00	L9	193.56	99.26	0.29
CS18	667.90	L13	194.99	100.00	0.80	CS33_1	240.80	L9	193.58	99.27	0.29
CS19	313.30	L17	194.03	99.50	0.37	CS33	356.30	L19	193.76	99.36	0.43
CS19	352.50	L18	194.04	99.51	0.42	CS33	537.10	L2	194.14	99.56	0.64
CS19	373.80	L7	194.19	99.59	0.45	CS33_1	537.70	L2	194.14	99.56	0.64
CS19	346.60	L8	194.28	99.63	0.41	CS33	275.70	L10	194.43	99.71	0.33
CS19	335.20	L9	194.47	99.73	0.40	CS33_1	276.00	L10	194.43	99.71	0.33
CS19	362.10	L10	194.75	99.87	0.43	CS33_1	589.50	L22	194.46	99.72	0.70
CS19	520.20	L16	194.86	99.93	0.62	CS33	705.50	L22	194.68	99.84	0.84
CS19	509.40	L15	194.91	99.95	0.61	CS33_1	448.40	L16	194.78	99.89	0.54
CS19	481.70	L14	194.95	99.97	0.58	CS33	455.40	L16	194.79	99.89	0.54
CS19	494.90	L11	194.95	99.97	0.59	CS33	467.80	L15	194.88	99.94	0.56
CS19	651.20	L12	194.99	100.00	0.78	CS33_1	470.40	L15	194.89	99.94	0.56
CS19	654.10	L13	194.99	100.00	0.78	CS33_1	417.10	L11	194.92	99.96	0.50
CS20	312.50	L17	194.02	99.50	0.37	CS33	417.70	L11	194.92	99.96	0.50
CS20	356.50	L18	194.07	99.52	0.43	CS33	469.30	L14	194.94	99.97	0.56
CS20	376.70	L7	194.21	99.60	0.45	CS33_1	477.10	L14	194.94	99.97	0.57
CS20	345.80	L8	194.28	99.63	0.41	CS33_1	586.90	L12	194.99	99.99	0.70
CS20	332.00	L9	194.46	99.72	0.40	CS33	588.30	L12	194.99	99.99	0.70
CS20	357.70	L10	194.74	99.87	0.43	CS33	665.00	L13	194.99	100.00	0.79
CS20	516.30	L16	194.85	99.93	0.62	CS33_1	672.80	L13	194.99	100.00	0.80
CS20	503.80	L15	194.91	99.95	0.60	CS34	290.50	L20	192.08	98.50	0.35
CS20	476.30	L14	194.94	99.97	0.57	CS34	258.20	L18	192.58	98.76	0.31
CS20	491.00	L11	194.95	99.97	0.59	CS34	232.20	L17	192.63	98.78	0.28
CS20	649.10	L12	194.99	100.00	0.78	CS34	342.10	L21	192.75	98.85	0.41
CS20	650.60	L13	194.99	100.00	0.78	CS34	398.90	L23	192.92	98.93	0.48
CS21	268.80	L6	192.14	98.53	0.32	CS34	329.90	L5	193.00	98.97	0.39
CS21_2	219.00	L17	192.18	98.55	0.26	CS34	394.60	L3	193.21	99.08	0.47
CS21_2	246.60	L18	192.22	98.58	0.29	CS34	315.10	L6	193.21	99.08	0.38
CS21_2	277.80	L6	192.40	98.67	0.33	CS34	259.30	L8	193.29	99.12	0.31
CS21	265.70	L7	192.77	98.86	0.32	CS34	291.80	L7	193.32	99.14	0.35
CS21_2	273.00	L7	192.95	98.95	0.33	CS34	377.30	L4	193.32	99.14	0.45
CS21	253.60	L8	193.17	99.06	0.30	CS34	337.60	L19	193.54	99.25	0.40
CS21_2	259.70	L8	193.30	99.13	0.31	CS34	244.70	L9	193.64	99.31	0.29
CS21_2	323.00	L19	193.34	99.15	0.39	CS34	269.70	L10	194.39	99.69	0.32
CS21	259.70	L9	193.87	99.42	0.31	CS34	623.20	L2	194.45	99.72	0.74
CS21_2	265.20	L9	193.93	99.45	0.32	CS34	658.70	L22	194.61	99.80	0.79
CS21	318.60	L17	194.07	99.53	0.38	CS34	460.60	L16	194.80	99.90	0.55
CS21	364.60	L18	194.13	99.56	0.44	CS34	478.80	L15	194.89	99.94	0.57
CS21	305.60	L10	194.58	99.79	0.37	CS34	403.20	L11	194.91	99.95	0.48
CS21_2	311.40	L10	194.60	99.80	0.37	CS34	483.90	L14	194.95	99.97	0.58
CS21_2	441.30	L16	194.77	99.88	0.53	CS34	570.50	L12	194.99	99.99	0.68
CS21	521.30	L16	194.86	99.93	0.62	CS34	678.60	L13	194.99	100.00	0.81
CS21_2	449.40	L15	194.87	99.93	0.54	CS35	260.50	L20	190.97	97.94	0.31
CS21	508.80	L15	194.91	99.95	0.61	CS35	305.00	L21	191.85	98.38	0.36
CS21_2	443.50	L14	194.93	99.96	0.53	CS35	350.20	L23	191.94	98.43	0.42
CS21	458.20	L11	194.94	99.97	0.55	CS35	242.80	L18	192.09	98.51	0.29
CS21_2	464.90	L11	194.94	99.97	0.56	CS35	223.70	L17	192.35	98.64	0.27
CS21	482.10	L14	194.95	99.97	0.58	CS35	301.40	L5	192.38	98.66	0.36
CS21	633.30	L12	194.99	100.00	0.76	CS35	355.50	L3	192.55	98.75	0.42
CS21_2	637.20	L13	194.99	100.00	0.76	CS35	292.30	L6	192.77	98.85	0.35
CS21_2	640.20	L12	194.99	100.00	0.76	CS35	343.30	L4	192.78	98.86	0.41

CS21	656.80	L13	194.99	100.00	0.78	CS35	274.40	L7	192.98	98.96	0.33
CS22	292.50	L17	193.81	99.39	0.35	CS35	246.60	L8	193.01	98.98	0.29
CS22	333.50	L18	193.87	99.42	0.40	CS35	314.90	L19	193.21	99.08	0.38
CS22	381.30	L6	193.99	99.48	0.46	CS35	235.80	L9	193.49	99.22	0.28
CS22	361.00	L7	194.11	99.54	0.43	CS35	584.20	L2	194.33	99.66	0.70
CS22	329.70	L8	194.16	99.57	0.39	CS35	263.50	L10	194.35	99.67	0.31
CS22	421.80	L19	194.25	99.62	0.50	CS35	615.30	L22	194.52	99.76	0.74
CS22	315.60	L9	194.37	99.67	0.38	CS35	458.60	L16	194.79	99.89	0.55
CS22	341.20	L10	194.70	99.85	0.41	CS35	482.50	L15	194.89	99.95	0.58
CS22	500.90	L16	194.84	99.92	0.60	CS35	398.30	L11	194.91	99.95	0.48
CS22	494.50	L15	194.90	99.95	0.59	CS35	492.20	L14	194.95	99.97	0.59
CS22	473.90	L14	194.94	99.97	0.57	CS35	566.60	L12	194.99	99.99	0.68
CS22	474.60	L11	194.94	99.97	0.57	CS35	688.40	L13	194.99	100.00	0.82
CS22	634.40	L12	194.99	100.00	0.76	CS36	258.70	L3	188.78	96.81	0.31
CS22	653.10	L13	194.99	100.00	0.78	CS36	243.70	L5	190.11	97.49	0.29
CS23	288.30	L17	193.75	99.36	0.34	CS36	265.20	L4	190.24	97.56	0.32
CS23	332.40	L18	193.86	99.41	0.40	CS36	246.60	L20	190.27	97.58	0.29
CS23	383.20	L6	194.00	99.49	0.46	CS36	188.60	L17	190.62	97.75	0.23
CS23	359.50	L7	194.10	99.54	0.43	CS36	217.50	L18	190.98	97.94	0.26
CS23	325.80	L8	194.13	99.56	0.39	CS36	294.70	L21	191.51	98.21	0.35
CS23	425.10	L19	194.27	99.62	0.51	CS36	255.70	L6	191.68	98.30	0.31
CS23	310.60	L9	194.33	99.66	0.37	CS36	344.40	L23	191.78	98.35	0.41
CS23	336.10	L10	194.69	99.84	0.40	CS36	259.80	L7	192.62	98.78	0.31
CS23	494.90	L16	194.84	99.92	0.59	CS36	296.30	L19	192.86	98.90	0.35
CS23	488.00	L15	194.90	99.95	0.58	CS36	255.20	L8	193.21	99.08	0.30
CS23	468.20	L14	194.94	99.97	0.56	CS36	481.90	L2	193.81	99.39	0.58
CS23	470.70	L11	194.94	99.97	0.56	CS36	269.30	L9	193.98	99.48	0.32
CS23	632.60	L12	194.99	100.00	0.76	CS36	607.70	L22	194.51	99.75	0.73
CS23	649.70	L13	194.99	100.00	0.78	CS36	323.10	L10	194.65	99.82	0.39
CS24_1	263.20	L20	191.09	98.00	0.31	CS36	409.50	L16	194.71	99.85	0.49
CS24_1	280.70	L5	191.77	98.34	0.34	CS36	415.50	L15	194.83	99.91	0.50
CS24	281.50	L5	191.80	98.36	0.34	CS36	407.20	L14	194.91	99.95	0.49
CS24_1	243.80	L18	192.13	98.53	0.29	CS36	481.60	L11	194.95	99.97	0.58
CS24_1	219.00	L17	192.18	98.55	0.26	CS36	602.30	L13	194.99	100.00	0.72
CS24_1	281.70	L6	192.51	98.72	0.34	CS36	655.40	L12	194.99	100.00	0.78
CS24	282.00	L6	192.52	98.73	0.34	CS37	262.80	L3	189.05	96.95	0.31
CS24	274.00	L7	192.97	98.96	0.33	CS37	243.10	L5	190.07	97.47	0.29
CS24_1	274.40	L7	192.98	98.96	0.33	CS37	246.30	L20	190.26	97.57	0.29
CS24	256.90	L8	193.24	99.10	0.31	CS37	266.70	L4	190.32	97.60	0.32
CS24_1	318.30	L19	193.27	99.11	0.38	CS37	189.50	L17	190.68	97.78	0.23
CS24_1	258.30	L8	193.27	99.11	0.31	CS37	218.40	L18	191.03	97.96	0.26
CS24	292.80	L17	193.81	99.39	0.35	CS37	293.20	L21	191.46	98.18	0.35
CS24	258.20	L9	193.85	99.41	0.31	CS37	253.30	L6	191.59	98.25	0.30
CS24_1	260.90	L9	193.88	99.43	0.31	CS37	339.10	L23	191.63	98.27	0.41
CS24	338.50	L18	193.92	99.44	0.40	CS37	256.10	L7	192.52	98.73	0.31
CS24	433.40	L19	194.31	99.65	0.52	CS37	296.90	L19	192.87	98.91	0.35
CS24	299.90	L10	194.56	99.77	0.36	CS37	250.40	L8	193.10	99.03	0.30
CS24_1	303.70	L10	194.57	99.78	0.36	CS37	488.30	L2	193.86	99.41	0.58
CS24_1	444.70	L16	194.77	99.88	0.53	CS37	263.80	L9	193.92	99.44	0.32
CS24	498.20	L16	194.84	99.92	0.60	CS37	604.50	L22	194.50	99.74	0.72
CS24_1	456.30	L15	194.87	99.94	0.55	CS37	317.40	L10	194.63	99.81	0.38
CS24	491.10	L15	194.90	99.95	0.59	CS37	410.10	L16	194.71	99.85	0.49
CS24	449.10	L11	194.93	99.97	0.54	CS37	415.50	L15	194.83	99.91	0.50
CS24_1	453.00	L14	194.94	99.97	0.54	CS37	406.80	L14	194.91	99.95	0.49
CS24_1	453.80	L11	194.94	99.97	0.54	CS37	476.50	L11	194.94	99.97	0.57
CS24	471.70	L14	194.94	99.97	0.56	CS37	602.50	L13	194.99	100.00	0.72
CS24	623.20	L12	194.99	100.00	0.74	CS37	652.40	L12	194.99	100.00	0.78
CS24_1	627.60	L12	194.99	100.00	0.75	CS38_1	210.40	L3	183.74	94.23	0.25
CS24_1	646.40	L13	194.99	100.00	0.77	CS38_2	230.30	L3	186.29	95.54	0.28
CS24	653.30	L13	194.99	100.00	0.78	CS38_1	224.30	L4	187.26	96.03	0.27
CS25	366.50	L20	193.54	99.25	0.44	CS38_2	209.80	L20	187.44	96.12	0.25

CS25	277.00	L17	193.59	99.28	0.33	CS38_1	210.70	L5	187.53	96.17	0.25
CS25	317.30	L18	193.69	99.33	0.38	CS38_2	221.70	L5	188.55	96.69	0.26
CS25	387.40	L5	193.76	99.36	0.46	CS38_2	239.70	L4	188.61	96.72	0.29
CS25	373.20	L6	193.92	99.45	0.45	CS38_2	166.40	L17	188.68	96.76	0.20
CS25	348.70	L7	194.01	99.49	0.42	CS38_2	190.40	L18	189.07	96.96	0.23
CS25	314.10	L8	194.03	99.50	0.38	CS38_2	253.90	L21	189.60	97.23	0.30
CS25	407.40	L19	194.17	99.57	0.49	CS38_2	299.60	L23	190.15	97.51	0.36
CS25	297.80	L9	194.25	99.61	0.36	CS38_1	184.90	L17	190.35	97.62	0.22
CS25	322.00	L10	194.64	99.82	0.38	CS38_1	248.80	L20	190.39	97.64	0.30
CS25	488.10	L16	194.83	99.91	0.58	CS38_1	230.50	L6	190.50	97.69	0.28
CS25	486.50	L15	194.90	99.95	0.58	CS38_1	215.60	L18	190.88	97.89	0.26
CS25	455.10	L11	194.94	99.97	0.54	CS38_2	237.50	L6	190.88	97.89	0.28
CS25	472.00	L14	194.94	99.97	0.56	CS38_1	340.50	L1	191.07	97.99	0.41
CS25	617.30	L12	194.99	100.00	0.74	CS38_1	299.20	L21	191.66	98.29	0.36
CS25	656.10	L13	194.99	100.00	0.78	CS38_2	368.80	L1	191.90	98.41	0.44
CS26	270.40	L17	193.49	99.23	0.32	CS38_2	264.20	L19	191.99	98.46	0.32
CS26	368.60	L20	193.56	99.26	0.44	CS38_1	354.00	L23	192.03	98.48	0.42
CS26	312.50	L18	193.63	99.30	0.37	CS38_1	241.90	L7	192.06	98.49	0.29
CS26	388.30	L5	193.77	99.37	0.46	CS38_2	245.30	L7	192.18	98.55	0.29
CS26	371.00	L6	193.90	99.44	0.44	CS38_1	296.40	L19	192.86	98.90	0.35
CS26	344.30	L7	193.97	99.47	0.41	CS38_2	417.80	L24	192.93	98.94	0.50
CS26	308.50	L8	193.98	99.48	0.37	CS38_1	243.80	L8	192.95	98.95	0.29
CS26	405.40	L19	194.16	99.57	0.48	CS38_2	244.30	L8	192.96	98.95	0.29
CS26	291.90	L9	194.20	99.59	0.35	CS38_1	431.30	L2	193.35	99.15	0.52
CS26	316.70	L10	194.62	99.81	0.38	CS38_2	454.20	L2	193.58	99.27	0.54
CS26	480.80	L16	194.82	99.91	0.57	CS38_2	261.70	L9	193.89	99.43	0.31
CS26	479.60	L15	194.89	99.94	0.57	CS38_1	263.50	L9	193.91	99.44	0.31
CS26	451.40	L11	194.94	99.97	0.54	CS38_2	564.30	L22	194.38	99.68	0.67
CS26	466.60	L14	194.94	99.97	0.56	CS38_1	614.60	L22	194.52	99.75	0.73
CS26	615.90	L12	194.99	100.00	0.74	CS38_2	318.60	L10	194.63	99.81	0.38
CS26	653.10	L13	194.99	100.00	0.78	CS38_1	321.90	L10	194.64	99.82	0.38
CS27_2	262.30	L20	191.06	97.98	0.31	CS38_2	391.90	L16	194.67	99.83	0.47
CS27	276.90	L5	191.64	98.28	0.33	CS38_1	404.10	L16	194.70	99.84	0.48
CS27_2	282.10	L5	191.82	98.37	0.34	CS38_2	401.90	L15	194.82	99.91	0.48
CS27_2	306.90	L21	191.90	98.41	0.37	CS38_1	408.60	L15	194.82	99.91	0.49
CS27_2	238.00	L18	191.92	98.42	0.28	CS38_2	397.60	L14	194.90	99.95	0.48
CS27_2	212.80	L17	191.93	98.42	0.25	CS38_1	399.70	L14	194.91	99.95	0.48
CS27	307.90	L4	191.93	98.43	0.37	CS38_2	479.90	L11	194.95	99.97	0.57
CS27_2	315.50	L4	192.15	98.54	0.38	CS38_1	483.80	L11	194.95	99.97	0.58
CS27	278.60	L6	192.43	98.68	0.33	CS38_1	596.60	L13	194.99	100.00	0.71
CS27_2	281.60	L6	192.51	98.72	0.34	CS38_2	597.30	L13	194.99	100.00	0.71
CS27	271.70	L7	192.92	98.93	0.32	CS38_2	656.30	L12	194.99	100.00	0.78
CS27_2	272.70	L7	192.94	98.94	0.33	CS38_1	659.50	L12	194.99	100.00	0.79
CS27_2	254.80	L8	193.20	99.08	0.30	CS39	641.80	L13	194.99	100.00	0.77
CS27_2	314.40	L19	193.20	99.08	0.38	CS39	684.40	L12	194.99	100.00	0.82
CS27	255.20	L8	193.21	99.08	0.30	CS39	486.10	L14	194.95	99.97	0.58
CS27	269.80	L17	193.48	99.22	0.32	CS39	543.70	L11	194.96	99.98	0.65
CS27	375.40	L20	193.64	99.30	0.45	CS39	522.90	L15	194.92	99.96	0.62
CS27	313.80	L18	193.64	99.30	0.37	CS39	409.40	L10	194.83	99.91	0.49
CS27_2	255.20	L9	193.80	99.39	0.30	CS39	531.40	L16	194.87	99.93	0.63
CS27	256.40	L9	193.82	99.40	0.31	CS39	370.50	L9	194.61	99.80	0.44
CS27	409.30	L19	194.18	99.58	0.49	CS39	314.30	L17	194.04	99.51	0.38
CS27_2	295.40	L10	194.54	99.76	0.35	CS39	365.10	L8	194.38	99.68	0.44
CS27	296.70	L10	194.54	99.77	0.35	CS39	340.00	L18	193.93	99.45	0.41
CS27_2	439.60	L16	194.76	99.88	0.53	CS39	374.40	L7	194.20	99.59	0.45
CS27	479.20	L16	194.82	99.91	0.57	CS39	410.30	L19	194.19	99.58	0.49
CS27_2	453.80	L15	194.87	99.93	0.54	CS39	372.40	L6	193.91	99.44	0.44
CS27	477.90	L15	194.89	99.94	0.57	CS39	347.90	L20	193.29	99.12	0.42
CS27_2	442.70	L11	194.93	99.96	0.53	CS39	360.60	L5	193.46	99.21	0.43
CS27	443.50	L11	194.93	99.96	0.53	CS39	380.10	L21	193.36	99.16	0.45
CS27_2	454.50	L14	194.94	99.97	0.54	CS39	381.20	L4	193.37	99.16	0.46

CS27	465.70	L14	194.94	99.97	0.56	CS39	675.30	L22	194.64	99.81	0.81
CS27	615.30	L12	194.99	100.00	0.74	CS39	373.10	L3	192.88	98.91	0.45
CS27_2	615.50	L12	194.99	100.00	0.74	CS39	394.10	L23	192.84	98.89	0.47
CS27_2	650.70	L13	194.99	100.00	0.78	CS39	575.00	L2	194.30	99.64	0.69
CS27	653.30	L13	194.99	100.00	0.78	CS39	500.90	L24	193.79	99.38	0.60
CS28	344.70	L20	193.24	99.10	0.41	CS39	490.10	L1	193.67	99.32	0.59

The following figures shows the maximum and minimum stresses envelop in the cables in all construction stages.

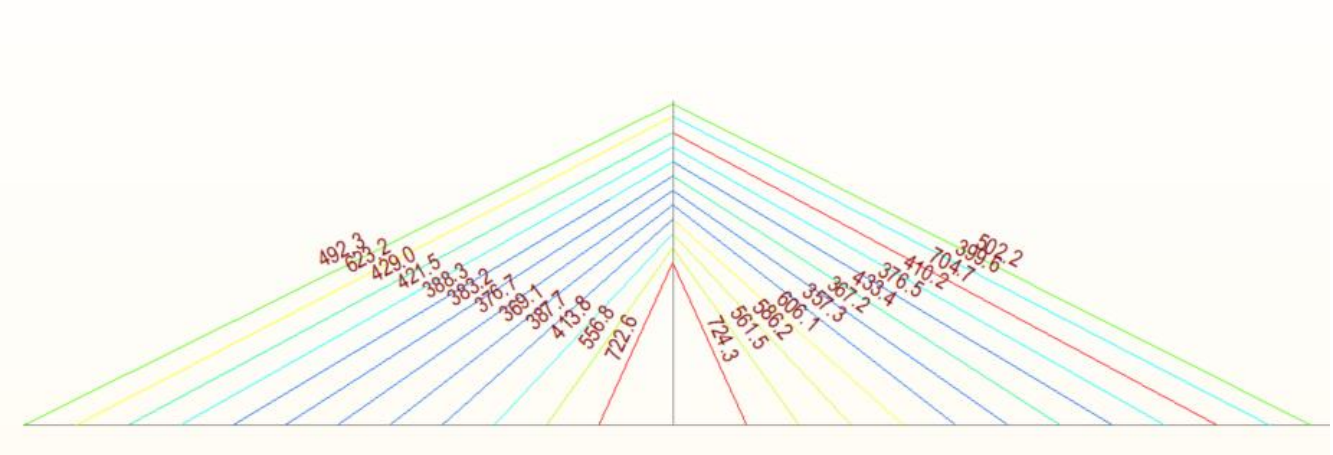

Figure 210 Max stresses envelop on cable during construction [MPa]

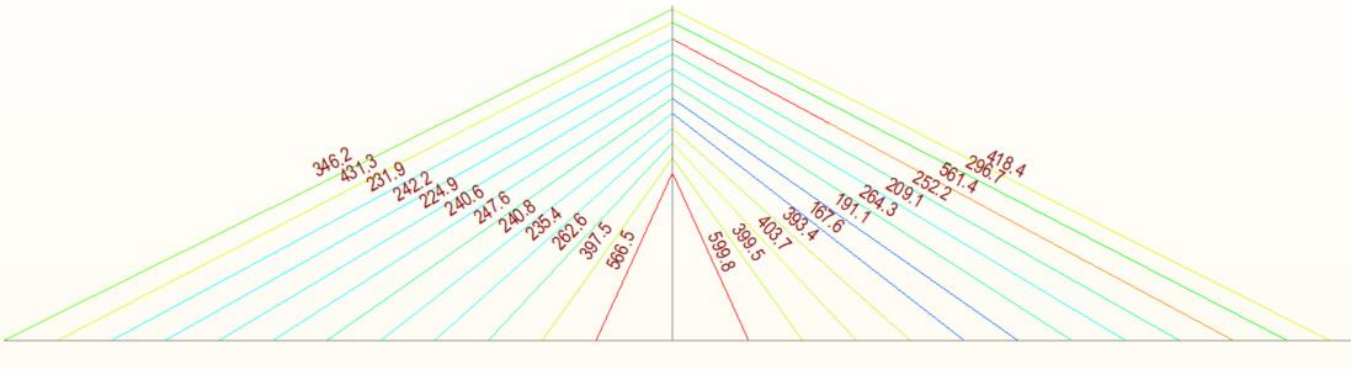

Figure 211 Min stresses envelop on cable during construction [MPa]

7.3.2 During service and end of service.

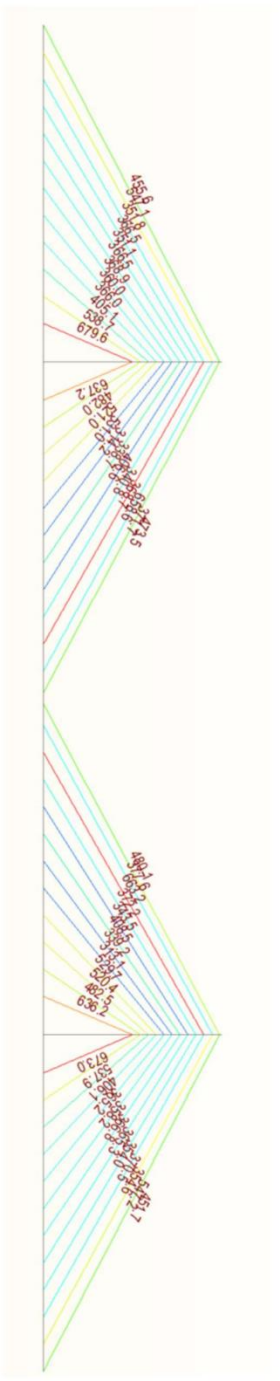

Figure 212 Min stresses value in freq. SLS combination in service life {MPa]

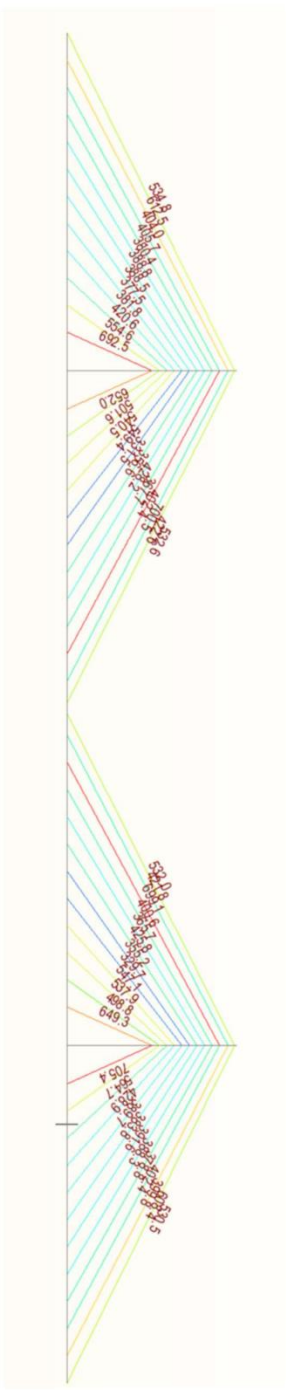

Figure 215 Max stresses value in freq. SLS combination in service life {MPa]

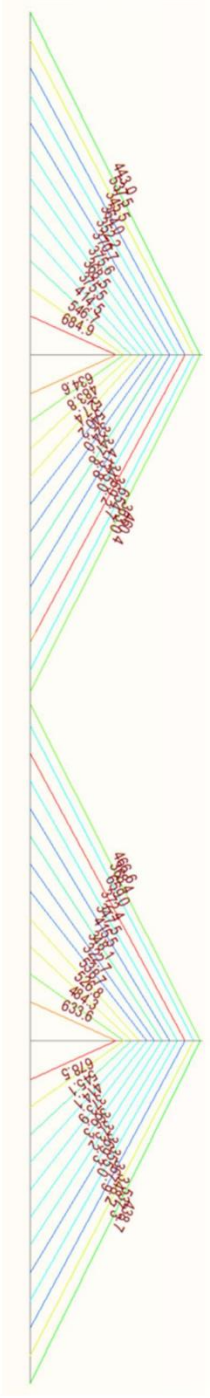

Figure 214 Min stresses value in freq. SLS combination at the end life {MPa]

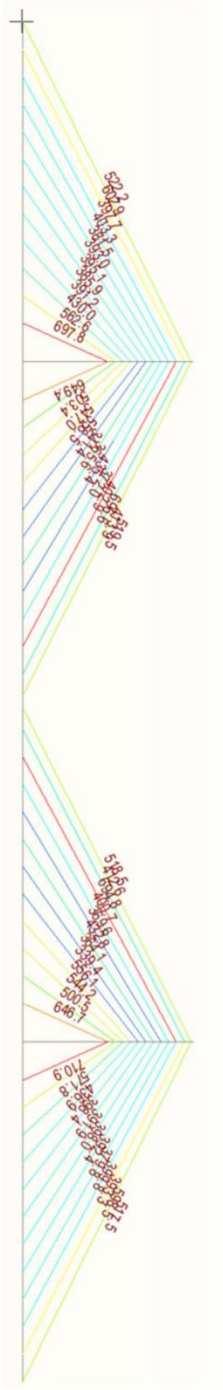

Figure 213 Max stresses value in freq. SLS combination at the end life

The results also have been summarized in the following table.

		End life				Service Life			
Cable	**Load**	**Stress [Mpa]**	**E, eff**	**Eeff/E0**	**check σ/0.45*fpk**	**Stress- [Mpa]**	**E, eff2**	**Eeff/E03**	**check σ/0.45*fpk**
L1	Freq. SLS (min)	443	193.20	99.15	0.54	455.6	193.34	99.15	0.54
L2	Freq. SLS (min)	537.5	194.14	99.58	0.65	547.1	194.19	99.58	0.65
L3	Freq. SLS (min)	345.5	192.34	98.71	0.42	351.8	192.48	98.71	0.42
L4	Freq. SLS (min)	364	193.13	99.06	0.44	366.5	193.17	99.06	0.44
L5	Freq. SLS (min)	352.2	193.35	99.15	0.42	351.1	193.34	99.15	0.42
L6	Freq. SLS (min)	370.7	193.90	99.42	0.44	366.5	193.86	99.42	0.44
L7	Freq. SLS (min)	375.6	194.21	99.57	0.44	368.9	194.16	99.57	0.44
L8	Freq. SLS (min)	368.5	194.40	99.67	0.43	360	194.36	99.67	0.43
L9	Freq. SLS (min)	375.5	194.62	99.79	0.44	366	194.59	99.79	0.44
L10	Freq. SLS (min)	414.5	194.83	99.91	0.48	405.1	194.82	99.91	0.48
L11	Freq. SLS (min)	546.7	194.96	99.98	0.64	538.7	194.96	99.98	0.64
L12	Freq. SLS (min)	684.9	194.99	100.00	0.81	679.6	194.99	100.00	0.81
L13	Freq. SLS (min)	634.6	194.99	100.00	0.76	637.2	194.99	100.00	0.76
L14	Freq. SLS (min)	483.8	194.95	99.97	0.58	482	194.95	99.97	0.58
L15	Freq. SLS (min)	527.4	194.92	99.96	0.62	521	194.92	99.96	0.62
L16	Freq. SLS (min)	540.2	194.87	99.93	0.63	531	194.87	99.93	0.63
L17	Freq. SLS (min)	324	194.12	99.51	0.38	314.2	194.03	99.51	0.38
L18	Freq. SLS (min)	347.8	194.00	99.45	0.40	338.7	193.92	99.45	0.40
L19	Freq. SLS (min)	413.8	194.21	99.57	0.49	406.6	194.16	99.57	0.49
L20	Freq. SLS (min)	345	193.25	99.07	0.41	340.8	193.18	99.07	0.41
L21	Freq. SLS (min)	369.2	193.21	99.08	0.44	368.7	193.20	99.08	0.44
L22	Freq. SLS (min)	654.7	194.60	99.80	0.79	658.6	194.61	99.80	0.79
L23	Freq. SLS (min)	363	192.24	98.68	0.44	371.7	192.43	98.68	0.44
L24	Freq. SLS (min)	460.4	193.45	99.27	0.57	473.5	193.57	99.27	0.57
L25	Freq. SLS (min)	466.6	193.51	99.30	0.57	480.1	193.63	99.30	0.57
L26	Freq. SLS (min)	368.4	192.36	98.74	0.45	377.6	192.55	98.74	0.45
L27	Freq. SLS (min)	659	194.61	99.80	0.79	663.2	194.62	99.80	0.79
L28	Freq. SLS (min)	372.4	193.25	99.10	0.44	372.2	193.25	99.10	0.44
L29	Freq. SLS (min)	347.5	193.28	99.09	0.41	343.5	193.22	99.09	0.41
L30	Freq. SLS (min)	415.5	194.22	99.58	0.49	408.5	194.18	99.58	0.49
L31	Freq. SLS (min)	348.1	194.00	99.45	0.41	339.2	193.92	99.45	0.41
L32	Freq. SLS (min)	322.7	194.11	99.50	0.37	313.1	194.02	99.50	0.37
L33	Freq. SLS (min)	538.7	194.87	99.93	0.63	529.7	194.87	99.93	0.63
L34	Freq. SLS (min)	526.8	194.92	99.96	0.62	520.4	194.92	99.96	0.62
L35	Freq. SLS (min)	484.3	194.95	99.97	0.58	482.5	194.95	99.97	0.58
L36	Freq. SLS (min)	633.6	194.99	100.00	0.76	636.2	194.99	100.00	0.76
L37	Freq. SLS (min)	678.5	194.99	100.00	0.80	673	194.99	100.00	0.80
L38	Freq. SLS (min)	545.1	194.96	99.98	0.64	537.9	194.96	99.98	0.64
L39	Freq. SLS (min)	414.1	194.83	99.91	0.49	406.1	194.82	99.91	0.49
L40	Freq. SLS (min)	373.9	194.62	99.79	0.44	365.2	194.59	99.79	0.44
L41	Freq. SLS (min)	366.3	194.39	99.67	0.43	358.2	194.35	99.67	0.43
L42	Freq. SLS (min)	373.2	194.19	99.56	0.44	366.8	194.15	99.56	0.44
L43	Freq. SLS (min)	369.3	193.89	99.41	0.44	365.3	193.85	99.41	0.44
L44	Freq. SLS (min)	355	193.39	99.17	0.42	354	193.38	99.17	0.42
L45	Freq. SLS (min)	367.9	193.19	99.09	0.44	370.5	193.23	99.09	0.44
L46	Freq. SLS (min)	348.2	192.40	98.74	0.42	354.6	192.54	98.74	0.42
L47	Freq. SLS (min)	537.3	194.14	99.58	0.65	547.2	194.19	99.58	0.65
L48	Freq. SLS (min)	438.7	193.14	99.13	0.54	451.7	193.30	99.13	0.54

The all the cables' stresses satisfy the stress limit and have reached sufficient stresses to develop approximate full modules of elasticity as shown in the above table, so the assumption of linear analysis is realistic and this is done for cables during construction, time of service, and at the end service.

7.4 Deflection

In the construction stage, a specific camper has been considered by rising the end of the moving scaffolding for the newly constructed segment to get zero deflection state at the end of the construction with self and imposed loading. The camber has been applied in the program as displacement.

The camber curve is shown in the following figure and the data are in the following table.

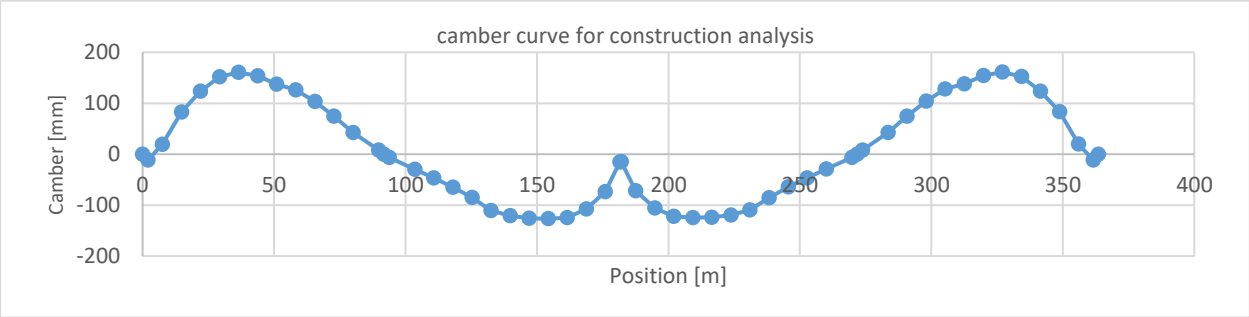

Figure 216 Camber curve

Table 24 Camber values

position[m]	camber [mm]	position[m]2	camber [mm]3
0.00	0.00	182.00	-14.64
2.00	-11.76	187.50	-72.06
7.50	19.31	194.75	-105.42
14.75	82.85	202.00	-122.18
22.00	123.36	209.25	-124.66
29.25	151.91	216.50	-123.98
36.50	160.54	223.75	-119.23
43.75	153.98	231.00	-109.39
51.00	137.17	238.25	-85.67
58.25	125.99	245.50	-64.02
65.50	103.37	252.75	-46.34
72.75	74.32	260.00	-29.27
80.00	42.71	269.75	-6.33
89.75	7.74	271.75	0.00
91.75	0.00	273.75	7.72
93.75	-6.36	283.50	42.58
103.50	-29.41	290.75	74.51
110.75	-46.64	298.00	104.08
118.00	-64.59	305.25	128.10
125.25	-85.16	312.50	137.88
132.50	-110.69	319.75	154.55
139.75	-120.84	327.00	161.02
147.00	-125.85	334.25	152.35
154.25	-126.71	341.50	123.75
161.50	-124.28	348.75	83.34

168.75	-107.33	356.00	19.89
176.00	-73.57	361.50	-11.27
181.50	-15.38	363.50	0.00

The maximum deflection has been restricted to L/600 for the quasi-permanent combination.

$V\_lim = L/600 = 180000/600 = 300\ mm$

The following figure shows the deflection envelop at the end life of the structure after applying the camber during construction, the max deflection in the mid-span is 146mm less than the maximum allowable deflection which is 300 mm.

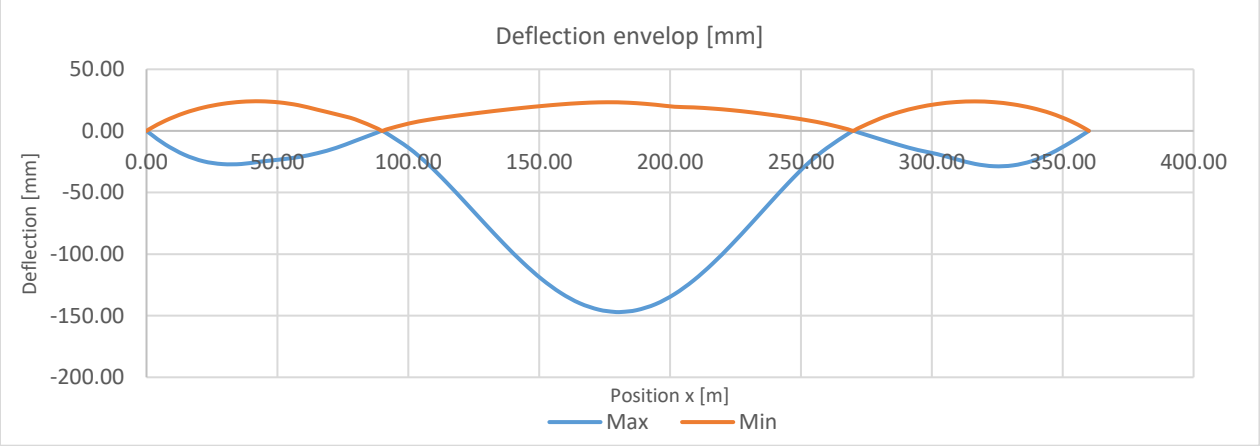

Figure 217 Deflection curve

8 Ultimate limit state

In the ultimate limit state in this work, the box girder section has been checked for moment, shear, torque, and normal forces, the cable has been checked against the normal forces.

8.1 Bending and normal forces.

The section has been checked against the maximum positive moment in the mid-span where the normal force was the smallest and the section near the pier with the max negative moment where the normal forces have been the biggest.

The section has been designed at the end life of the structure (100 years) when all the losses have been occurred and at the construction stage when the temporary bar used.

The accurate design has been carried by program Idea Statica.

8.1.1 at the end of service.

The section has been checked by the interaction diagram. in the creation of the interaction diagram, the prestress equivalent load (axial force and moment) has been included.

So, the moment and axial load have been checked without including the primary effect of prestressing.

The following fig. shows the interaction diagram for the midspan section with the following design forces.

Table 25 Design load for mid span section near the pier and in the middle of mid span

	Load	
Location	**Med [KN.m]**	**Ned [KN]**
In the middle of the bridge	88361.2	-16855.9
Near the pier in the mid span	-98537.2	-68993.6

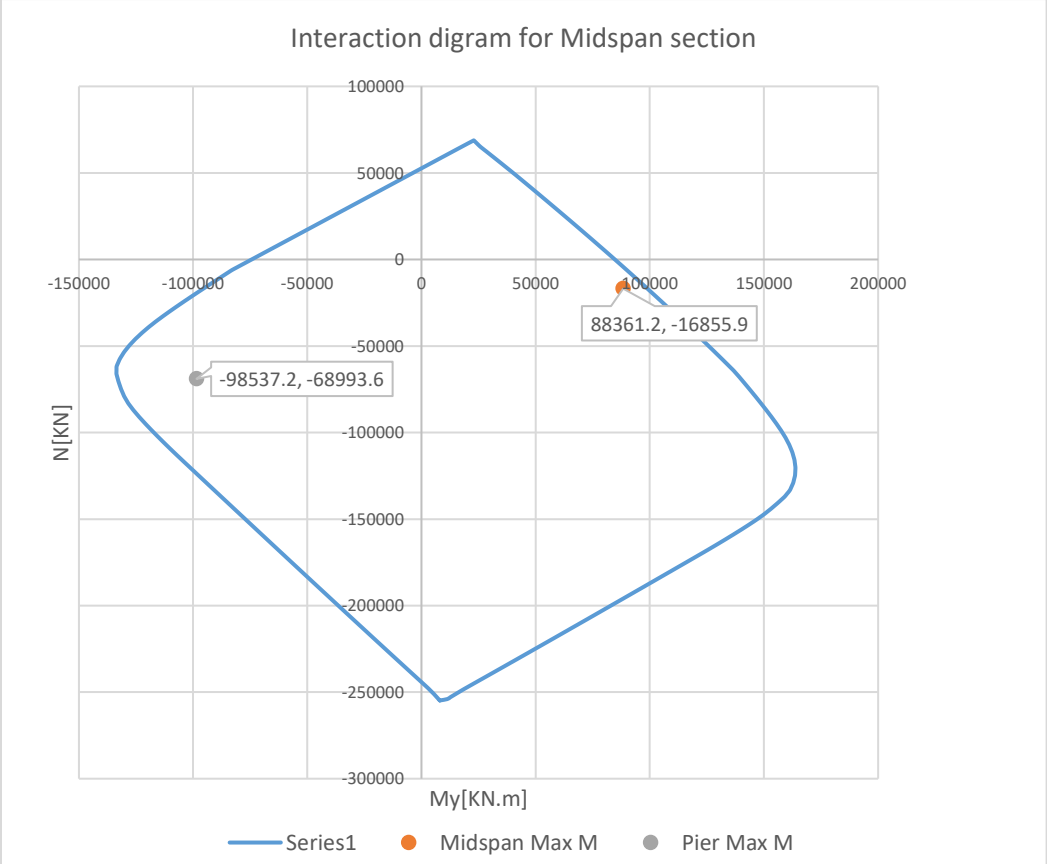

Figure 218 interaction diagram for midspan section

The stresses and strain of the tendon have been also checked and the results are below.

The design values of the steel strength fpd are taken as fp0.1k/γS = 1636.8/1.15=1423.3 and has a strain limit εud = 0.9 εuk =0.035*0.9=3.5% also the fcd =30MPa for concrete C50/60.

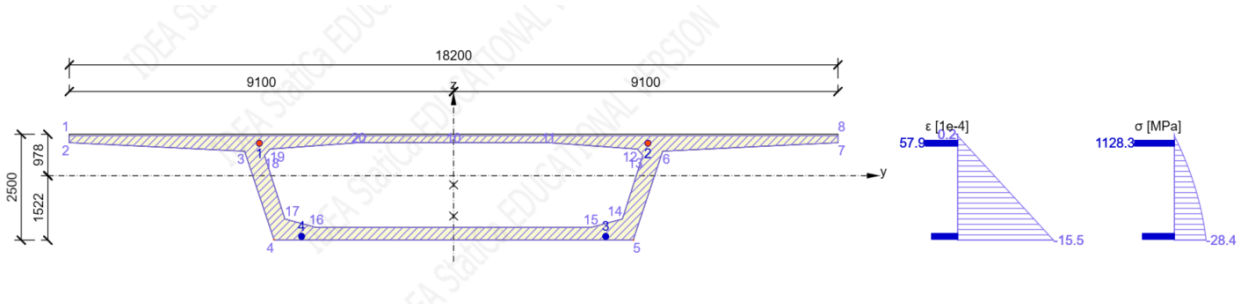

Figure 219 Mid span section near Pier

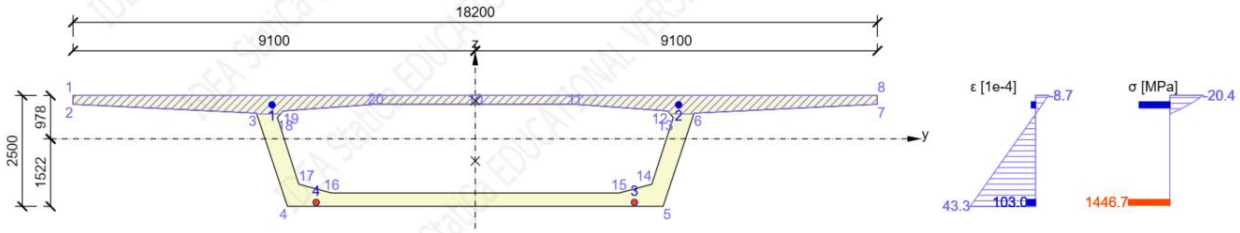

Figure 220 Mid span section mid of the span

The following table summarizes the checking for the concrete and prestress.

Table 26 Strain and stresses check in mid span

		ε [%]	ε lim	σ[Mpa]	σ_{lim} [Mpa]	Value	Check
Pier Moment	**Bottom concrete Fiber**	-0.00155	-0.0035	-28.4	-30	94.8	OK
	Top Tendon	0.00579	0.0315	1128.3	1593.2	70.8	OK
Mid Span moment	**Top concrete Fiber**	-0.00087	-0.0035	-20.4	-30	67.9	OK
	Bottom Tendons	0.0103	0.0315	1446.7	1593.2	90.8	OK

The following fig. show the interaction diagram for Side span section with the following design forces.

Table 27 Design load for Side span section

	Load	
Location	**Med**	**Ned**
In the middle of the side span	84782	-44256.7
Near the pier in the side span	-99750.5	-63179.8

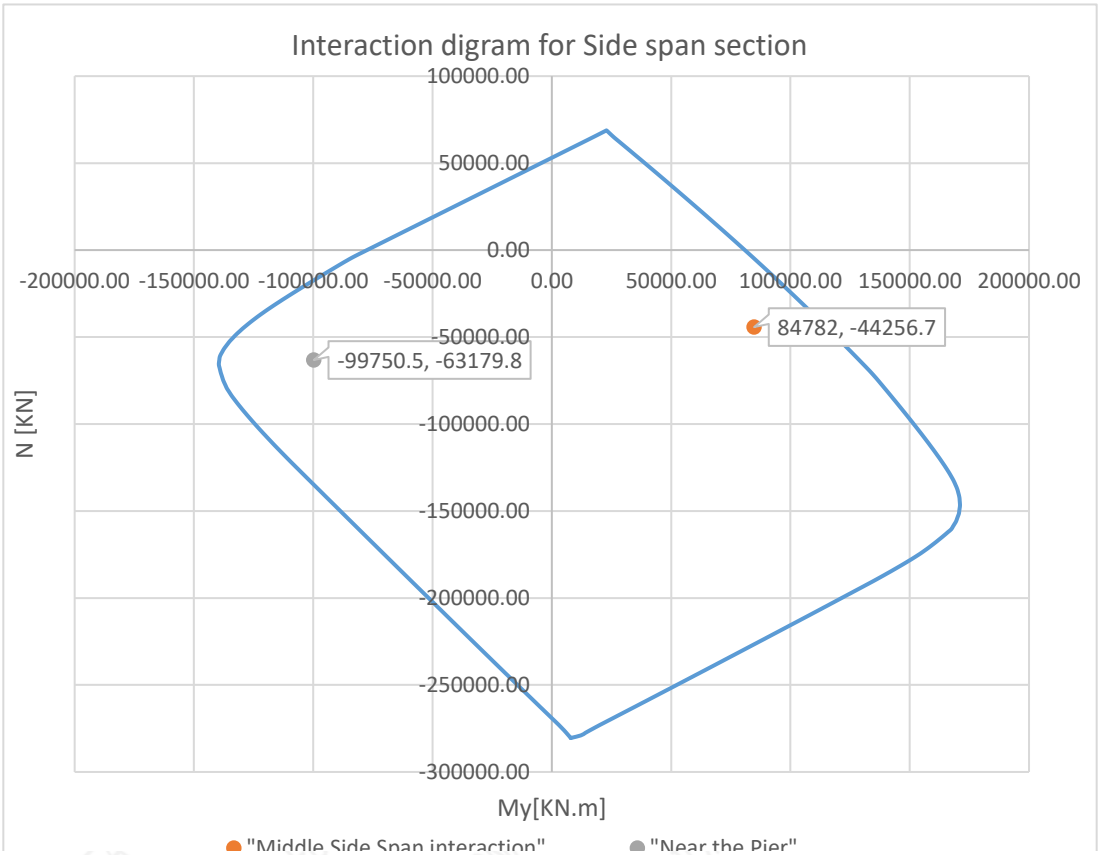

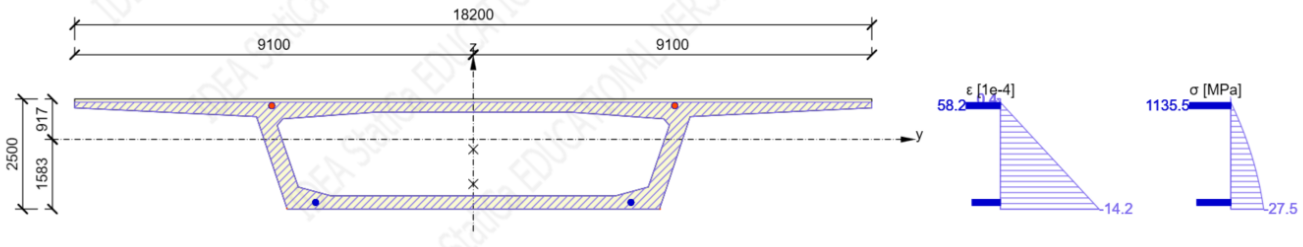

Figure 222 Side span section near pier

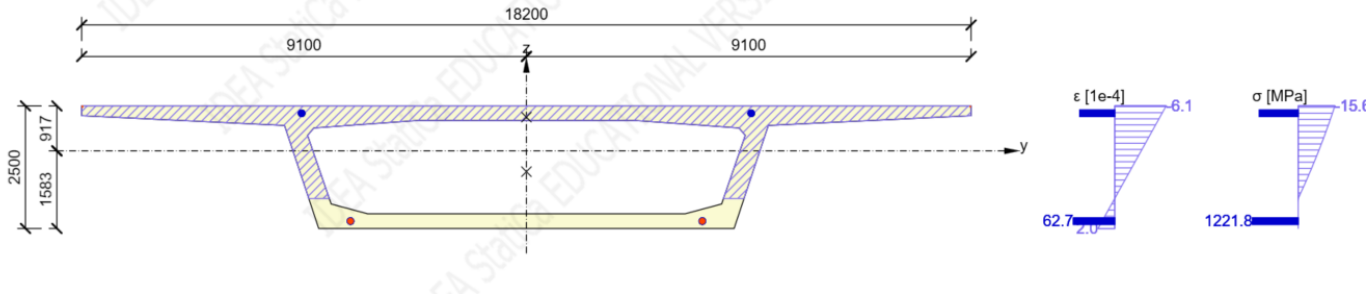

Figure 223 Side span section mid of span

Table 28 Strain and stresses check for side span

		ε	ε lim	σ[Mpa]	σ_{lim} [Mpa]	Value	Check
Pier Moment	**Bottom concrete Fiber**	-0.000142	-0.0035	-27.5	-30	94.8	OK
	Top Tendon	0.00582	0.0315	1135.5	1593.2	70.8	OK
Mid of side Span moment	**Top concrete Fiber**	-0.00061	-0.0035	-15.6	-30	51.8	OK
	Bottom Tendons	0.00627	0.0315	1221.8	1593.2	76.7	OK

8.1.2 During the construction.

The maximum Med and Ned during construction have been obtained from the CS35 (before casting the key segment) for the mid-span near the pier.
Med = 87067.3 KN.m & Ned=-25453.2 KN.

The interaction diagram for this section is below, this section has been stressed during the construction by external bars with diameter 40mm, the prestressing force and moment have been included when constructing the interaction diagram.
The table and figure below show the stresses at ULS for the concrete and prestress bars.

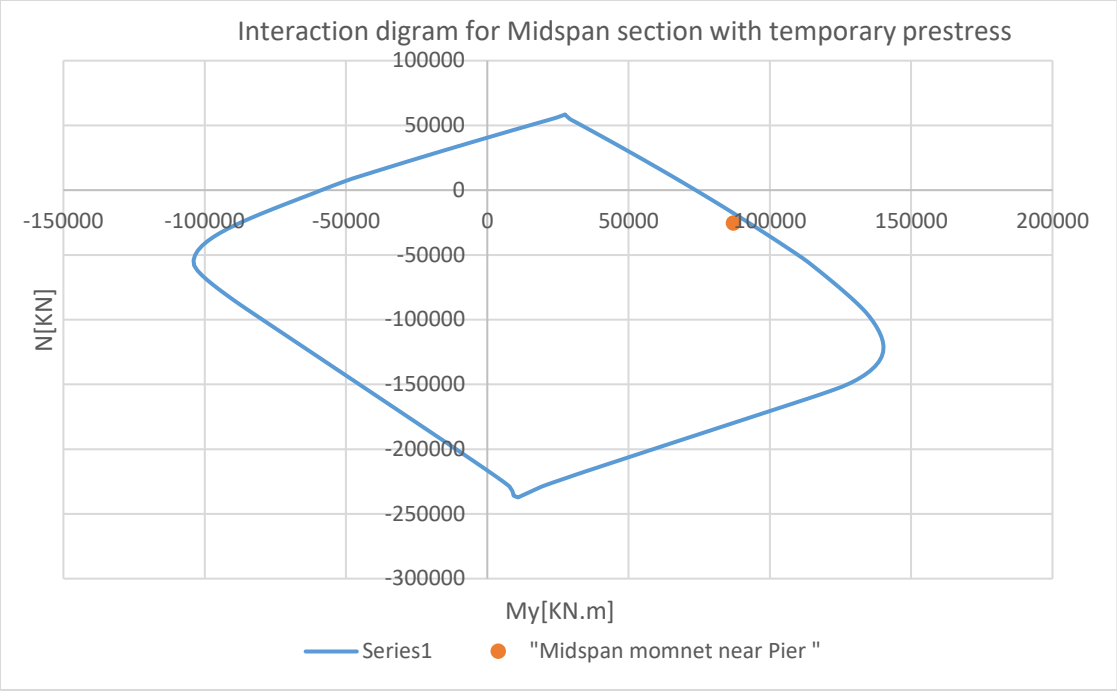

Figure 225 Interaction diagram for Midspan section with temporary prestress

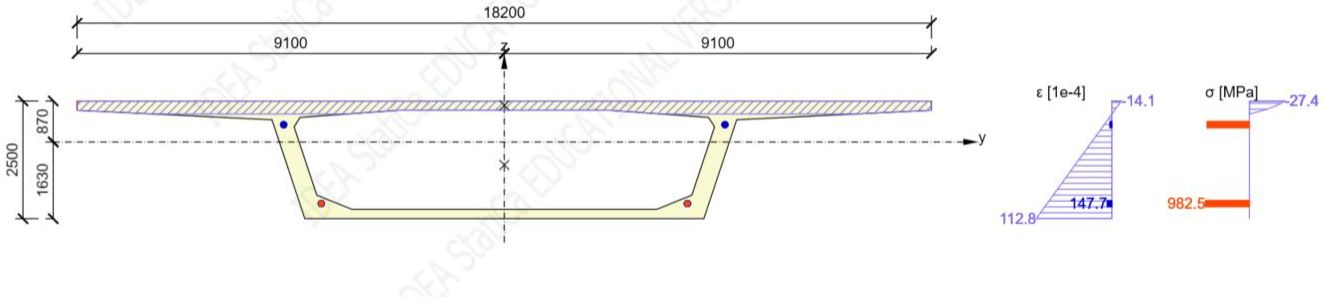

Figure 224 Midspan

Table 29 Strain and stresses check for Critical section in construction analysis

		ε [%]	σ_{lim} [Mpa]	σ[Mpa]	σ_{lim} [Mpa]	Value	Check
Mid Span moment	**Top concrete Fiber**	-0.00141	-0.0035	-27.4	-30	91.2	OK
	Bottom bars	0.01477	0.0315	982.5	1080	90.97	OK

8.1.3 Ductility requirement

2-1-1/clause 5.10.1(5)P requires that prestressed beams should not fail in a brittle manner due to corrosion or failure of individual tendons. It is desirable for a beam to first exhibit cracking, as a warning that there is corrosion occurring [4].

To ensure the ductile behavior of the prestressed box girder, option (a) has been chosen which is described below [4].

a) Ensure that the remaining cables, after corrosion or failures have led to cracking, are adequate to carry the frequent combination design moment.
To do this check, the tendon area is hypothetically reduced so that the calculated cracking moment with the reduced area of tendons is less than or equal to that from the frequent combination of actions, as defined in EN 1990 for serviceability limit states. The cracking moment should be based on the tensile stress, fctm. For each extreme tension fiber of the beam with section modulus Z, the moment at cracking, M, and the prestress force, P, are related by [4]:

$$P/A + Pe/Z - M/Z = -f_{\mathrm{ctm}}$$

where e is the eccentricity of the prestress and A is the section cross-sectional area. The prestressing force required to make the beam crack at moment, M, is thus [4]:

$$P = (M/Z - f_{\mathrm{ctm}})/(1/A + e/Z)$$

The ultimate strength of the beam with the reduced tendon area, but using the material factors for accidental situations, is then again compared against the applied moment from the frequent combination of actions. [4]

the section in the mid-span in the middle of the structure has been considered in this checking.

The results from the frequent load combination and the section property and the calculated reduced prestressing force which ensure that the section will have to crack at the frequent load combination are listed in the table below.

Table 30 Calculation of reduced area of prestressing

Parameter	Value	Unit	Note
Mcr=Mfreq	23.3658	MN.m	Cracking moment
yd	1.630	m	distance from neutral axis to bottom fibers
Z, el, d	4.840	m3	Section Modules
Area (m^2)	8.554	m2	Area of the concrete section
Iyy (m^4)	7.888	m4	Moment of inertia
e	0.380	m	equivalent eccentricity of all the cables
fctm	4.100	Mpa	Meat tensile strength of concrete
P	3.7242432	MN	Prestressing force which will ensure cracking at freq. combination
P	3724.2432	KN	in KN
s, p	1100	MPa	effective prestressing stress
Ap, red	3385.6756	mm	reduced area of prestressing
n	22.571171	-	equivalent number of cables

Unfortunately, the reduced area of prestress is very small and can't hold the cracking moment (frequent moment).

The option (b) in the Eurocode should now be used.

(b) Minimum reinforcement
Brittle fracture may also be avoided by ensuring that there is sufficient longitudinal reinforcement provided to compensate for the loss of resistance when the tensile strength of the concrete is lost. This is achieved by providing a minimum area of reinforcement. This reinforcement is not additional to requirements for other effects and may be used in ultimate bending checks. [4]

The value of min. reinforcement is the value which can resist the cracking bending moment calculated assuming a recommended tensile strength equal to fctm at the extreme tension fiber, ignoring the prestressing. [4]

The calculating of the cracking moment without the effect of prestressing have been done in the following table, the table provide the cracking moment for top fiber (negative moment) and the cracking moment of bottom fiber (positive moment). The reinforcement should be suffocation to resist both moments. [4]

Table 31 Calculation of cracking moment

Parameters	Value	Unite	Note
Wel, h (m^3)	-9.06204	m3	Section Modulus
Wel, d (m^3)	4.840206	m3	Section Modulus
fctm	4.1	Mpa	tensile strength
Mrep, top	-37.1544	MN.m	cracking moment for bottom fibers
Mrep, bot	19.84485	MN.m	cracking moment for top fibers

Longitudinal reinforcement has been provided with ϕ 16mm and S = 200mm to all edge of the section.

The following fig. shows the stress and strain distribution of the section with both cracking moments.

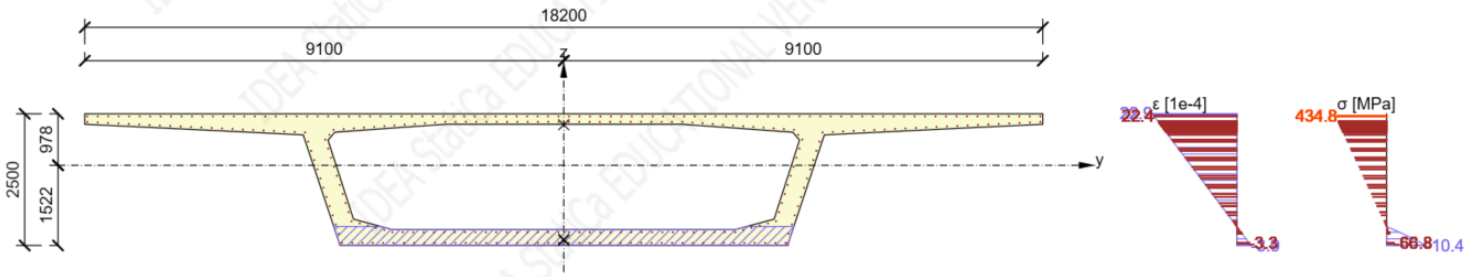

Figure 227 -ve cracking moment

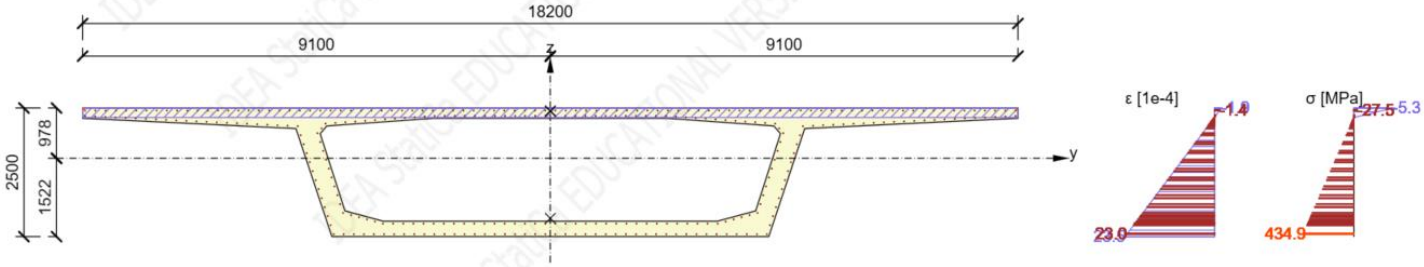

Figure 226 +ve cracking moment

8.2 Shear design.

In Eurocode the shear reinforcement is not required in case that the shear force is less than the concrete resistance force. [14]

The concrete resistance force can be calculated based on whether the section is cracked on flexural or not, if the section is not cracked, the calculation will mainly depend on the principal stresses and the section will hold the shear till the diagonal tension reach the design tensile stresses of concrete.

However, if the section is cracked due to flexure, the shear resistance of the section can be calculated using the empirical formula in Eurocode. In this design of the shear resistance, a cracked section has been considered.

The calculation has been provided for the max. shear forces near the abutment, however, due to the cables which work as internal supports, the shear forces increase and decrease along the span and reach the max at the cable anchorage, pier, and abutment. So, the shear reinforcement has been considered the same along the structure.

The calculation of shear has been done using spread excel sheet and the calculation are below.

Check shear resistance of Concrete, V_Rd, c

- Design Load

N_{Ed} = -76298.400 kN

V_{Ed} = 10233.200 kN

M_{Ed} = -15333.700 kN・m

V_p = 0.000 kN

- Design strength of concrete

$f_{cd} = \alpha_{cc} \cdot f_{ck} / \gamma_c$ = 33.333 MPa

- Design strength of Reinforcement

$f_{yd} = f_{yk} / \gamma_{s\_rebar}$ = 434.783 MPa

- Design value for the shear resistance $V_{Rd, c}$

$V_{Rd, min}$ = $(v_{min} + k_1 \cdot \sigma_{cp}) \cdot b_w \cdot d_p$ = 2563.06 kN

$V_{Rd, c}$ = $[C_{Rd, c} \cdot k \cdot (100 \cdot \rho_1 \cdot f_{ck})^{(1/3)} + k_1 \cdot \sigma_{cp}] \cdot b_w \cdot d_p$ = 3232.606 kN ≥ $V_{Rd, min}$

= 3232.606 kN < V_{Ed} = 10233.2 kN ∴ Shear reinforcement is required

were,

$C_{Rd, c}$ = $0.18 / \gamma_c$ = 0.120

v_{min} = $0.035 \cdot k^{(3/2)} \cdot f_{ck}^{(1/2)}$ = 0.363

k_1 = 0.15

k = $1 + \sqrt{(200 / d_p)} \le 2.0$ = 1.292

ρ_1 = $A_{sl} / (b_w \cdot d_p) \le 0.02$ = 0.020

A_{sl} = 62743.200 mm^2

b_w = 800.0 mm

d_p = 2350.0 mm

σ_{cp} = $N_{Ed} / A_c \le 0.2 \cdot f_{cd}$ = 6.667 MPa

N_{Ed} = 0.000 kN (If compression, $N_{Ed} > 0$)

A_c = 8554390.064 mm^2

fck = 50 Mpa

Check shear resistance of Shear Reinforcement, V_Rd, s

- Design Parameters

cot(α) = 0.000 °

cot(θ) = 2.500 ° (1 ≤ cotθ ≤ 2.5, ∴ 21.8° ≤ θ ≤ 45°)

z = 2115.0 mm

A_{sw} = 1018.000 mm^2 for legs ϕ18 mm (2 for each web)

s = 200.000 mm

$\rho_{w,\,min}$ = $0.08 \cdot \sqrt{f_{ck}} / f_{yk}$ = 0.00113

were, α is the angle between shear reinforcement and the beam axis perpendicular to the shear force.

θ is the angle between the concrete compression strut and the beam axis perpendicular to the shear force.

z is the inner level arm.

A_{sw} is the cross-sectional area of the shear reinforcement

$\rho_{w,\,min}$ is the minimum ratio of shear reinforcement

- Design value for the shear resistance $V_{Rd,\,s}$

$V_{Rd,\,max}$ = $\alpha_{cw} \cdot b_w \cdot z \cdot \nu_1 \cdot f_{cd} \cdot (\cot\theta + \cot\alpha) / (1 + \cot^2\theta)$ = 14586.061 kN

$V_{Rd,\,s}$ = $(A_{sw} / s) \cdot z \cdot f_{ywd} \cdot (\cot\theta + \tan\theta) \cdot \sin\alpha \le V_{Rd,\,max}$ = 13573.714 kN

= 13573.714 kN > V_{Ed} = 10233.2 kN **OK**

were, ν_1 = 0.600

α_{cw} = $1 + \sigma_{cp} / f_{cd}$ = 1.250 0.5fcd>σcp>0.25fcd

σ_{cp} = N_{Ed} / A_c = 8.919 MPa

N_{Ed} = 76298.400 kN (If compression, $N_{Ed} > 0$)

A_c = 8554390.064 mm^2

ν_1 is a strength reduction factor for concrete cracked in shear

α_{cw} is a coefficient taking account of the state of the stress in the compression chord

- Check ratio of shear reinforcement

ρ_w = $A_{sw} / (s \cdot b_w \cdot \sin\alpha)$ = 0.006 > $\rho_{w,\,min}$ = 0.001 **OK**

- Check Spacing of stirrups

$S_{l,\,max}$ = $0.75 \cdot d_p \cdot (1 + \cot\alpha)$ = 1593.8 mm

s = 175.0 mm ≤ $S_{l,\,max}$ = 1593.8 mm **OK**

were, s is the spacing of the stirrups

8.3 Torsion

For the analysis of torsion, a separate simple beam model has been used with eccentric applied moving load and neglected the existence of the cables.
Since the cross-section of the bridge is box girder, it can be assumed that the section can resist the torsion by uniform torsion (circulatory torsion).

It has been assumed that all the support are rigid with respect to torsion. the loading on one span does not influence the torsional moment diagrams in the adjacent spans: there is no continuity. [16]

In the model, the rotation about the x-axis (longitudinal axis of the bridge have been restricted), and the resultant Mx have been considered for the torsion design, the applied traffic load and crowed load has been considered with an eccentricity.

The following figure shows the statical system which have been used in the model.

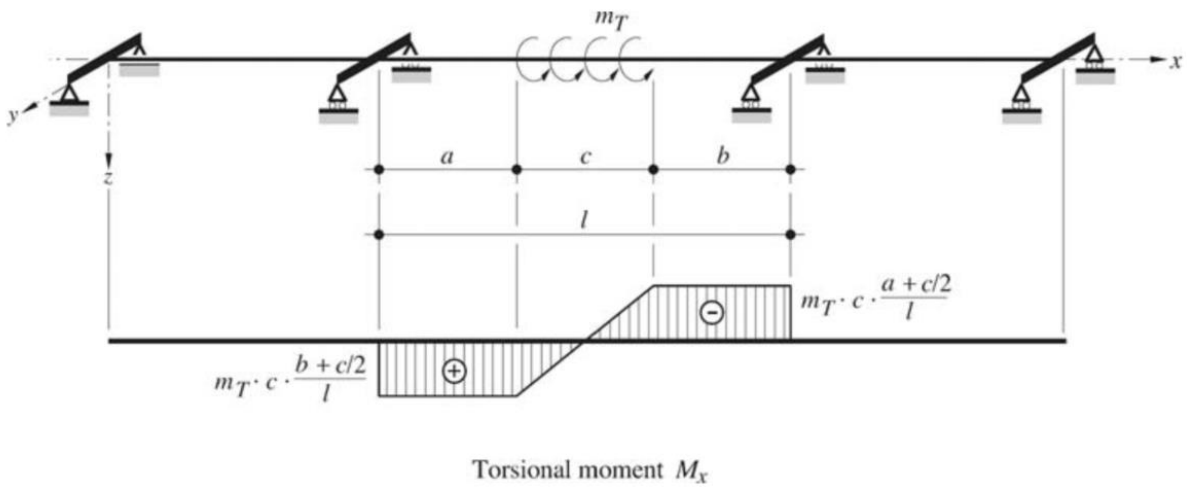

Figure 228 Statical system used in the model [16]

The results of the model Ted (Mx) are below.

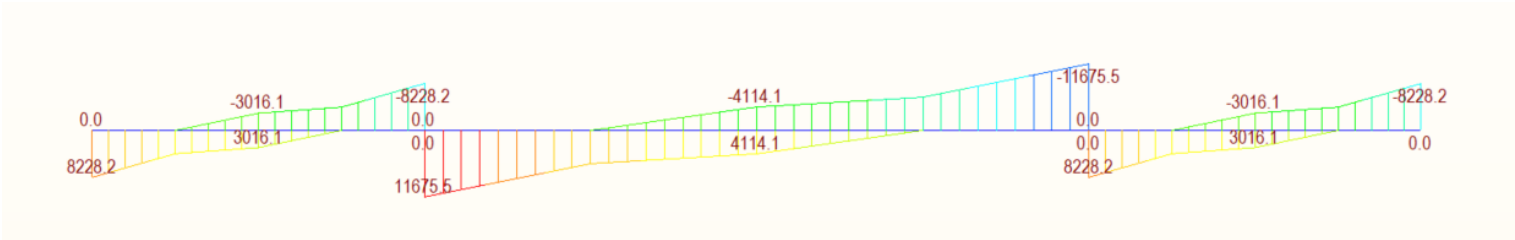

Figure 229 Ted results

The check of the combination of shear and torsion in box girder is done by checking the shear strength of one leg of the box under the shear and torsional sear force as required by Eurocode 2 [14] The calculation is below.

The design check for the torsion has been done in an excel sheet, the results show that the shear reinforcement is enough for also torsion, for longitudinal reinforcement, 16mm/200 for all edges have been provided for the section as min. reinforcement which is also enough.

VEd = 10233.2 KN

Ted = 11675.5 KN.m

- Design strength of concrete

f_{cd} = $\alpha_{cc} \cdot f_{ck} / \gamma_c$ = 33.333 MPa

- Design strength of Reinforcement

f_{yd} = $f_{yk} / \gamma_{s\_rebar}$ = 434.783 MPa

Check Torsional Resistance

- Design Parameters

$t_{ef,\,i}$ = 646.9 mm

A_k = 25770000 mm^2

u_k = 39836.8 mm

t_i = 400.0 mm

d_p = 2125.0 mm

cot(α) = 0.000

cot(θ) = 2.500

where, $t_{ef,\,i}$ is the effective wall thickness

A_k is the area enclosed by the centerlines of the connecting walls, including inner hollow areas

u_k is the perimeter of the area A_k

α is the inclination of the torsional shear reinforcement to the longitudinal axis of the beam.

θ is the angle of compression struts

- Design value for the shear stress per web V^*_{Ed}

$V^*_{Ed} = V_{ed}$/ Number of Webs+ $T_{ed} \cdot z/(2 \cdot A_k)$

= 6004.844 kN

where, Number of Webs = 2

z = 1912.500 mm

A_k = 25770000 mm^2

- Design value for the shear resistance $V_{Rd,\,s}$

VRd, s = $(Asw / s) \cdot z \cdot fywd \cdot (\cot\theta + \tan\theta) \cdot \sin\alpha \le VRd,\,max$ = 13573.714 kN

VRd, s/Web = 6125.89

- Check whether additional designed reinforcement is necessary.

$V_{Rd,\,s}$ = 6786.857 kN

V^*_{Ed} = 6004.844 kN

$V^*_{Ed} \le V_{Rd,\,s}$

∴ additional transverse reinforcement is not required.

- Check longitudinal reinforcement for torsion

Asl/s	=	$(\cot\theta / f_{yd}) \cdot T_{Ed} / (2 \cdot A_k)$			=	1.303	mm^2/m	
Asl/s/edge					=	0.6513	mm^2/m	
A_{sl}	=	1.005 mm^2	>	Asl/s/edge	=	636.161	mm^2	**OK**

∴ Longitudinal reinforcement ϕ16mm /200mm is provided for all edges of the box.

8.4 Normal forces in the cables.

The cables have been checked at the end life of the structure; the allowable stress have been calculated according to the following formula.

$$\frac{f_{p0,1k}}{\gamma s} = \frac{1636.8}{1.35} = 1212.4MPa$$

The following table shows the stresses for every cable at the ultimate limit state.

Table 32 Normal Forces in cable at ULS

Cable	s [Mpa]	s/ lim	Cable	s [Mpa]	s/ lim
L1	828.70	0.68	L25	770.00	0.64
L2	922.40	0.76	L26	622.90	0.51
L3	630.10	0.52	L27	1005.00	0.83
L4	622.00	0.51	L28	613.20	0.51
L5	577.50	0.48	L29	575.40	0.47
L6	579.80	0.48	L30	664.90	0.55
L7	593.20	0.49	L31	577.90	0.48
L8	595.20	0.49	L32	550.90	0.45
L9	615.50	0.51	L33	848.00	0.70
L10	673.70	0.56	L34	831.70	0.69
L11	847.10	0.70	L35	762.60	0.63
L12	1006.00	0.83	L36	933.30	0.77
L13	938.30	0.77	L37	1027.00	0.85
L14	768.10	0.63	L38	857.80	0.71
L15	836.80	0.69	L39	678.10	0.56
L16	852.40	0.70	L40	619.20	0.51
L17	554.60	0.46	L41	596.30	0.49
L18	581.40	0.48	L42	589.40	0.49
L19	671.10	0.55	L43	571.40	0.47
L20	581.80	0.48	L44	569.50	0.47
L21	620.10	0.51	L45	614.20	0.51
L22	1013.00	0.84	L46	622.30	0.51
L23	634.50	0.52	L47	914.70	0.75
L24	782.20	0.65	L48	820.30	0.68

8.5 Fatigue Check in Cables

The fatigue has been checked for the frequent combination, the max. and min. forces have been calculated in the program using the influence line method, the fatigue has been checked by limiting the difference between the maximum and minimum stresses to the value of 200 MPa.

The table below shows the check.

The table below shows the Min. and Max. stresses and the check.

Table 33 Fatigue check in cables

Cable	Stress-Max	Stress-Min	Ds	Check	Cable	Stress-Max	Stress-Min	Ds	Check
L1	580.90	399.50	181.40	0.91	L25	547.30	455.40	91.90	0.46
L2	654.80	503.90	150.90	0.75	L26	442.90	357.10	85.80	0.43
L3	442.70	322.60	120.10	0.60	L27	728.30	649.10	79.20	0.40
L4	441.20	351.70	89.50	0.45	L28	438.50	364.40	74.10	0.37
L5	410.80	345.60	65.20	0.33	L29	411.30	340.70	70.60	0.35
L6	413.50	366.20	47.30	0.24	L30	478.60	409.70	68.90	0.34
L7	426.50	373.70	52.80	0.26	L31	414.30	343.30	71.00	0.36
L8	430.10	369.50	60.60	0.30	L32	393.80	318.80	75.00	0.38
L9	445.30	375.80	69.50	0.35	L33	613.70	531.60	82.10	0.41
L10	488.20	410.20	78.00	0.39	L34	602.00	515.50	86.50	0.43
L11	617.20	538.20	79.00	0.40	L35	552.60	469.40	83.20	0.42
L12	737.40	673.60	63.80	0.32	L36	683.10	618.60	64.50	0.32
L13	685.90	618.50	67.40	0.34	L37	748.40	667.20	81.20	0.41
L14	555.70	467.90	87.80	0.44	L38	622.90	536.60	86.30	0.43
L15	605.10	515.60	89.50	0.45	L39	490.30	409.80	80.50	0.40
L16	616.40	533.10	83.30	0.42	L40	446.90	374.30	72.60	0.36
L17	396.20	320.80	75.40	0.38	L41	430.50	367.50	63.00	0.32
L18	416.60	343.80	72.80	0.36	L42	424.10	371.30	52.80	0.26
L19	482.50	409.30	73.20	0.37	L43	408.70	363.90	44.80	0.22
L20	415.20	339.70	75.50	0.38	L44	406.20	347.00	59.20	0.30
L21	442.60	363.00	79.60	0.40	L45	436.60	354.00	82.60	0.41
L22	732.40	646.80	85.60	0.43	L46	438.20	324.90	113.30	0.57
L23	446.80	353.80	93.00	0.47	L47	650.30	506.30	144.00	0.72
L24	551.30	451.50	99.80	0.50	L48	576.00	401.80	174.20	0.87

9 Transverse analysis.

For transverse analysis, plate model has been used. 30m segment in the med span has been assisted.

The traffic load has been applied throw surface lanes, where the traffic loads (tram load and pedestrian load) have been assigned to each lane exactly. And using influence surface to get the envelopes.

9.1 Prestressing

The transverse tendons (system type VSLab S 6-4 with Flat duct with PT-PLUS® ducting system) [17] provided by VSL Company has been modeled at a spacing of 1m with 4 wire 7-wire (150mm2 area and with fpk=1860) strands per tendon. The following schema [17]and table represent the duct and anchorage.

Table 34 Flat duct with PT-PLUS® ducting system [17]

	A	B	C	D	E	F	G	H	K 1)		L 1)	
									Out	In	Out	In
6-2	175	170	80	75	55	60	315	20	51	37	35	21
6-3	215	210	95	90	55	60	460	20	68	54	35	21
6-4	235	230	115	110	60	60	440	20	86	72	35	21
6-5	265	260	130	125	60	60	440	20	104	90	35	21

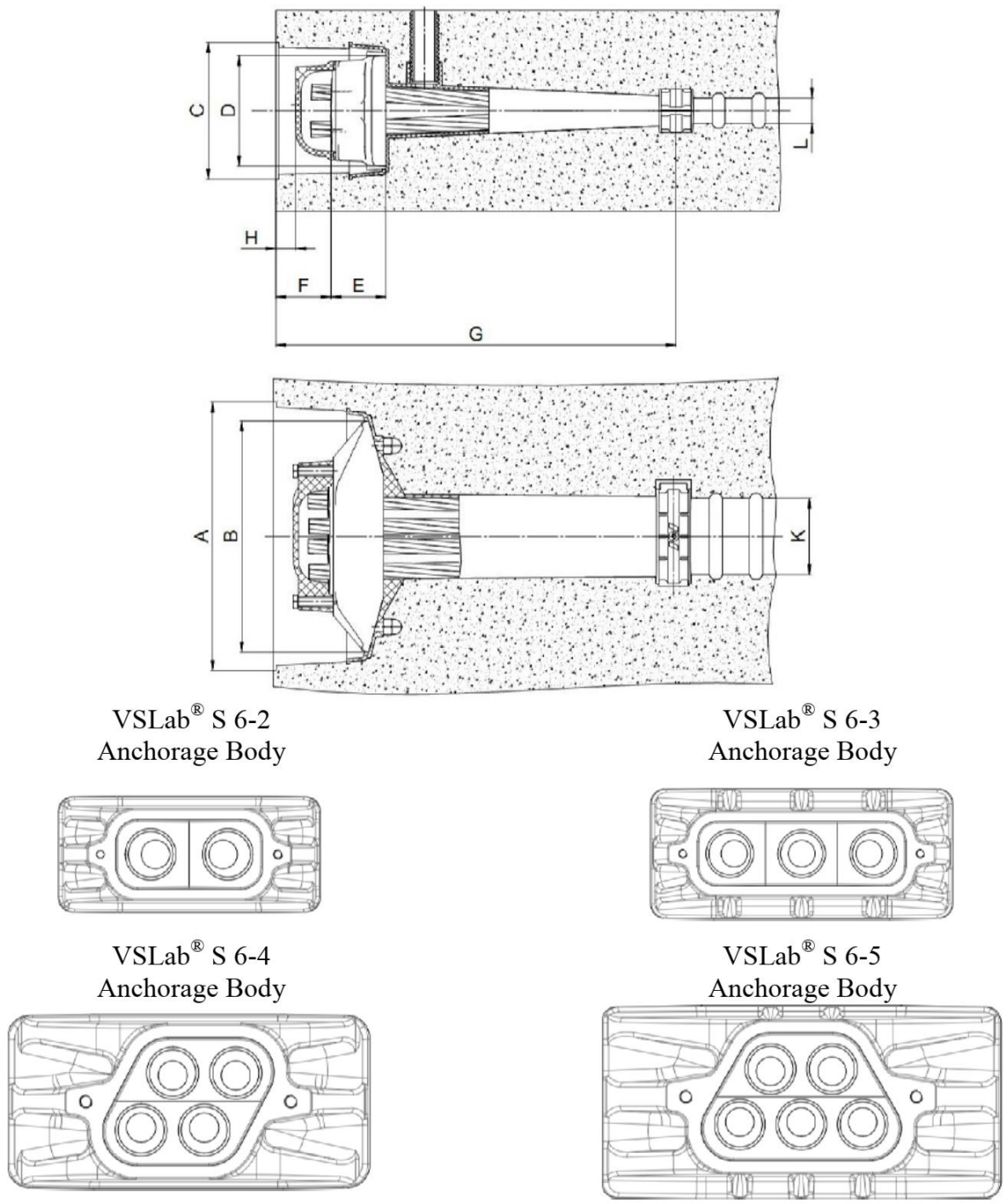

Figure 230 Anchorage body and trumpet [17]

The profile of the cable in the transverse direction has been considered with rising near the web the box and near the place of the cable anchorage in the middle of the structure. The following figure shows the profile of the cable in the transverse analysis.

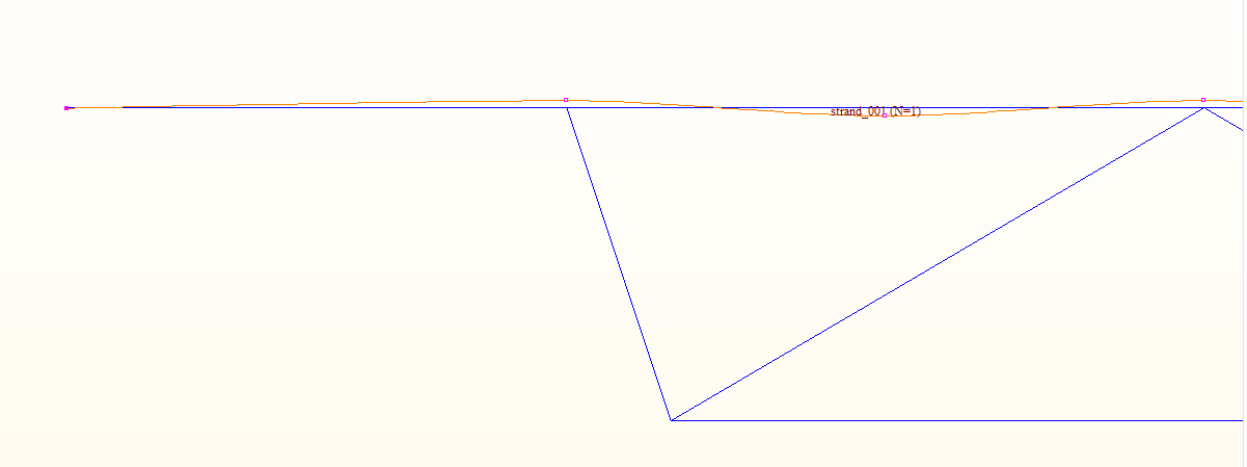

Figure 231 transverse prestressing modeling

For simplicity, the long-term losses of the prestress cable have been considered 25%.

the spacing of the cables has been considered 1m, the prestressing forces (Jacking forces) = 1473 MPa. The following table shows the specification of the transverse prestressing.

Table 35 specification of the transverse prestressing

Parameter	Symbol	Value	Unit
Jacking forces	σp, max	1473	Mpa
Area of the cable	Ap1	600	mm2
spacing of the cable	s	1	m
long term stresses	-	25%	-
Maximum force in the cable	Pmax	0.8838	MN
Design force in the cable	Np	0.66285	MN
Anchorage slipping	s	3	mm
wobble friction Coeff. K	k	0.005	-
coefficient of friction	m	0.19	-

The prestress load has been considered in all type of combinations, the uniform temperature, the pedestrian load, the tam load, the self-wight and other permeant load have been also considered.

9.2 Service limit state.

9.2.1 Limit stresses and cracking

The results of the normal stresses have been introduced below for the top flange of the box girder for both the top and bottom fibers, the results have been checked for two transvers section, one above cable anchorage location and the other is between the two-anchorage cable.

The comparison stresses have been limited in the concrete to the value of 0.6fck = 30MPa in the characteristic combination. For the quasi-permeant combination, the value is 0.45fck=22.5 MPa.

For considering the uncracked section, the cracking stresses have been considered equal to fctm=4.1 MPa in the frequent combination.

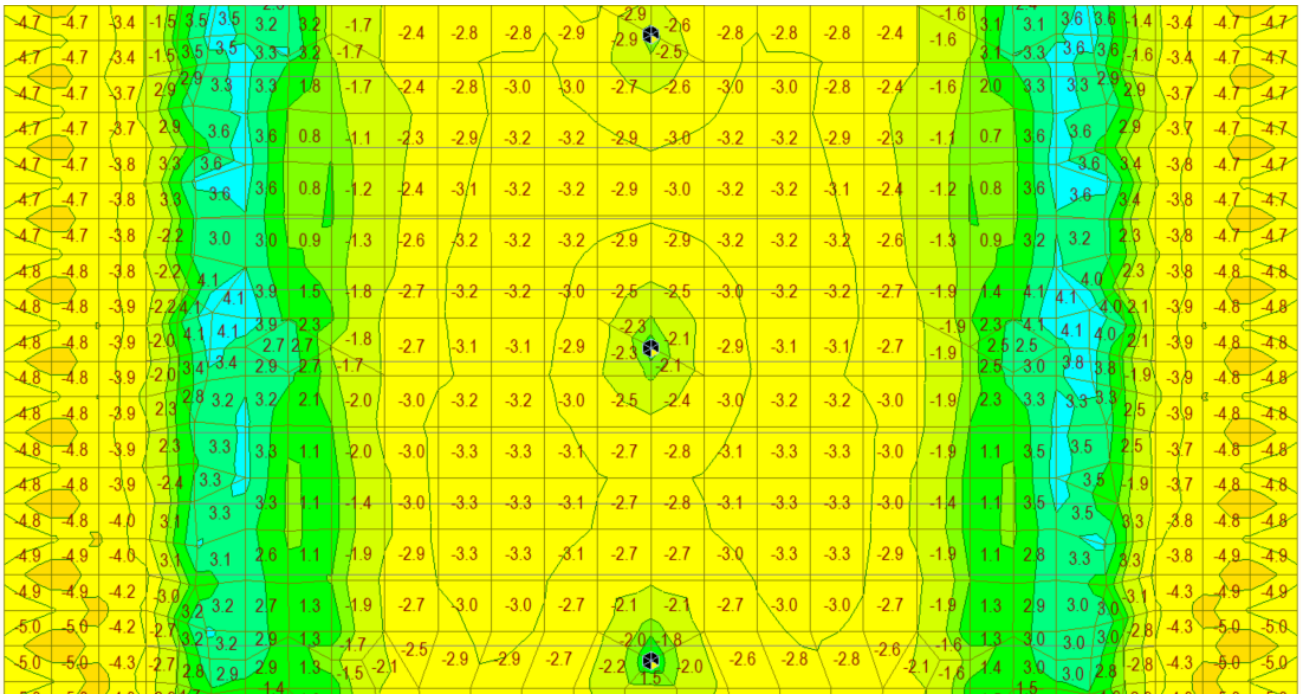

Figure 232 Top fibers stresses Ch. Combination Max [MPa]

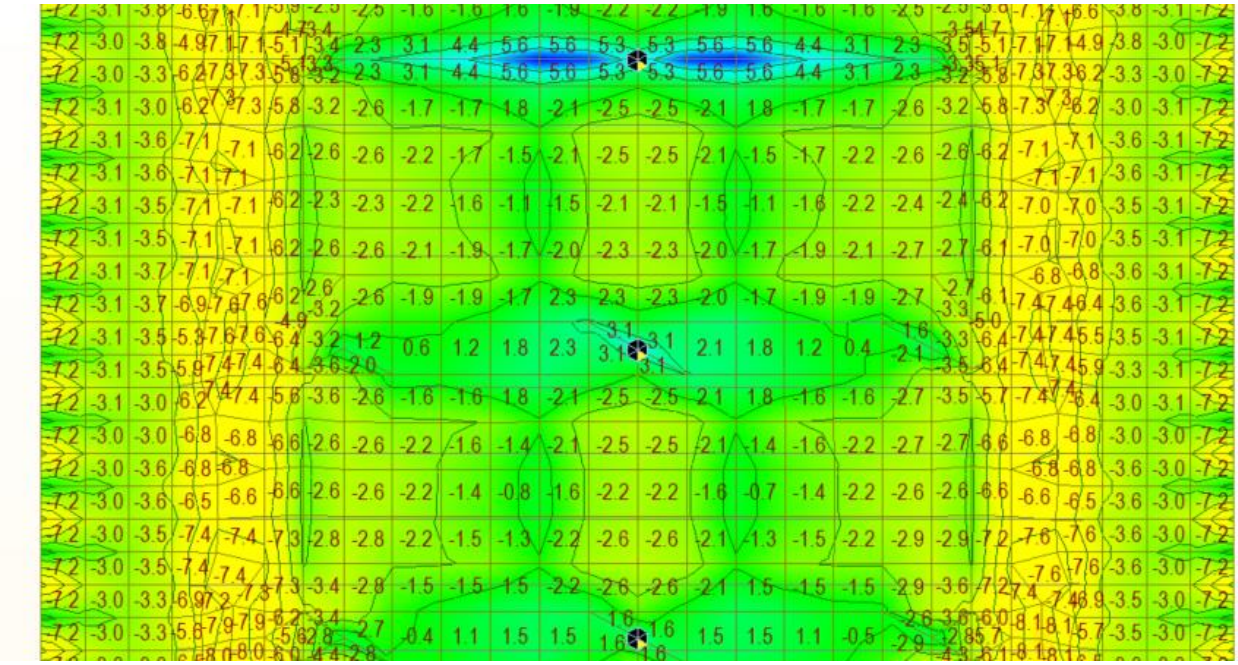

Figure 233 Bottom fiber stresses Ch. Combination Max [MPa]

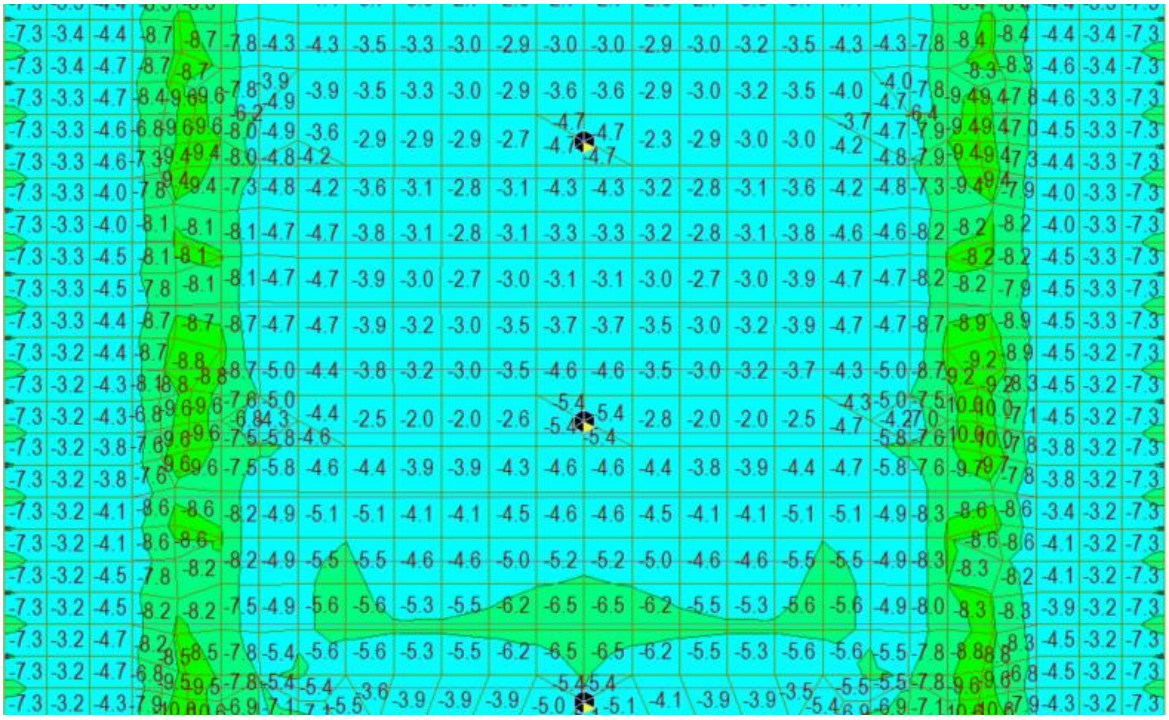

Figure 234 Top fibers stresses Ch. Combination Min [MPa]

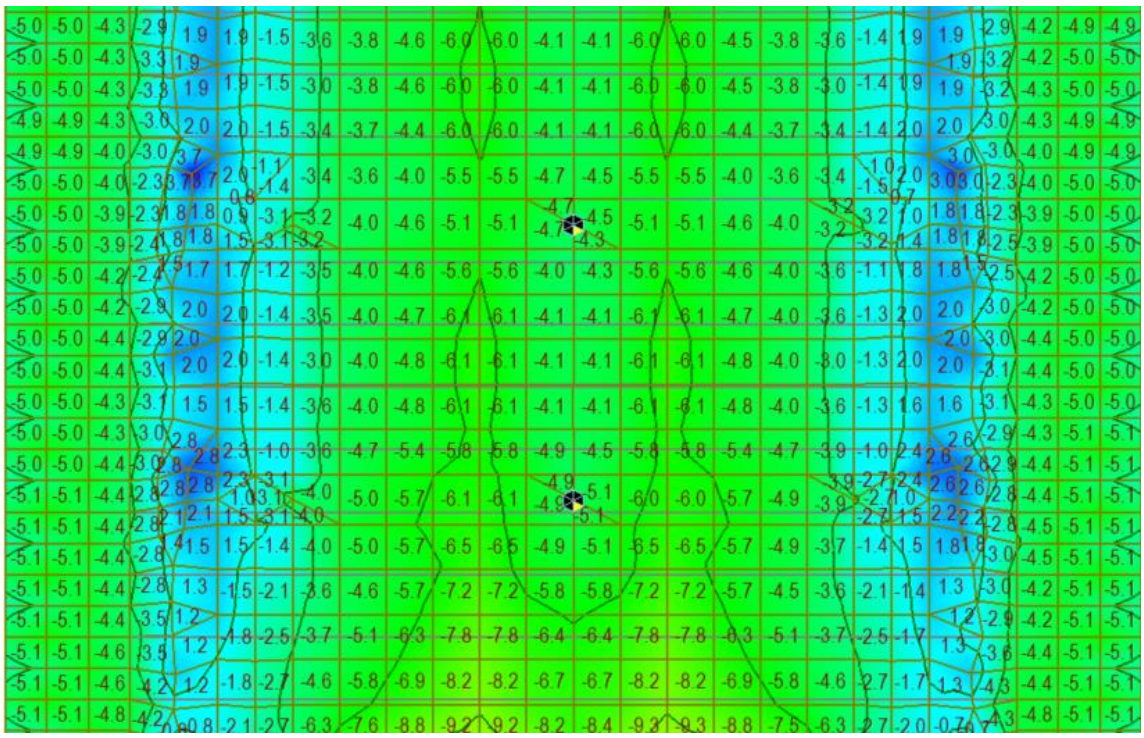

Figure 235 Bottom fiber stresses Ch. Combination Min [MPa]

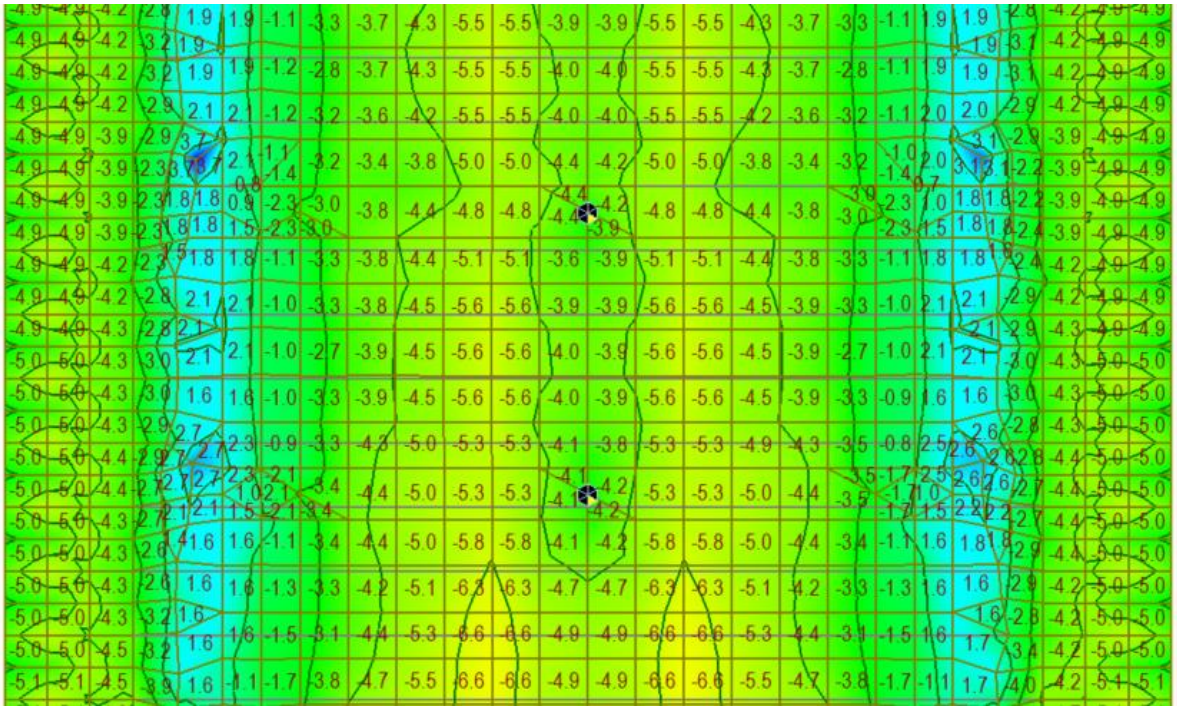

Figure 236 Top fibers stresses frequent combination Max [MPa]

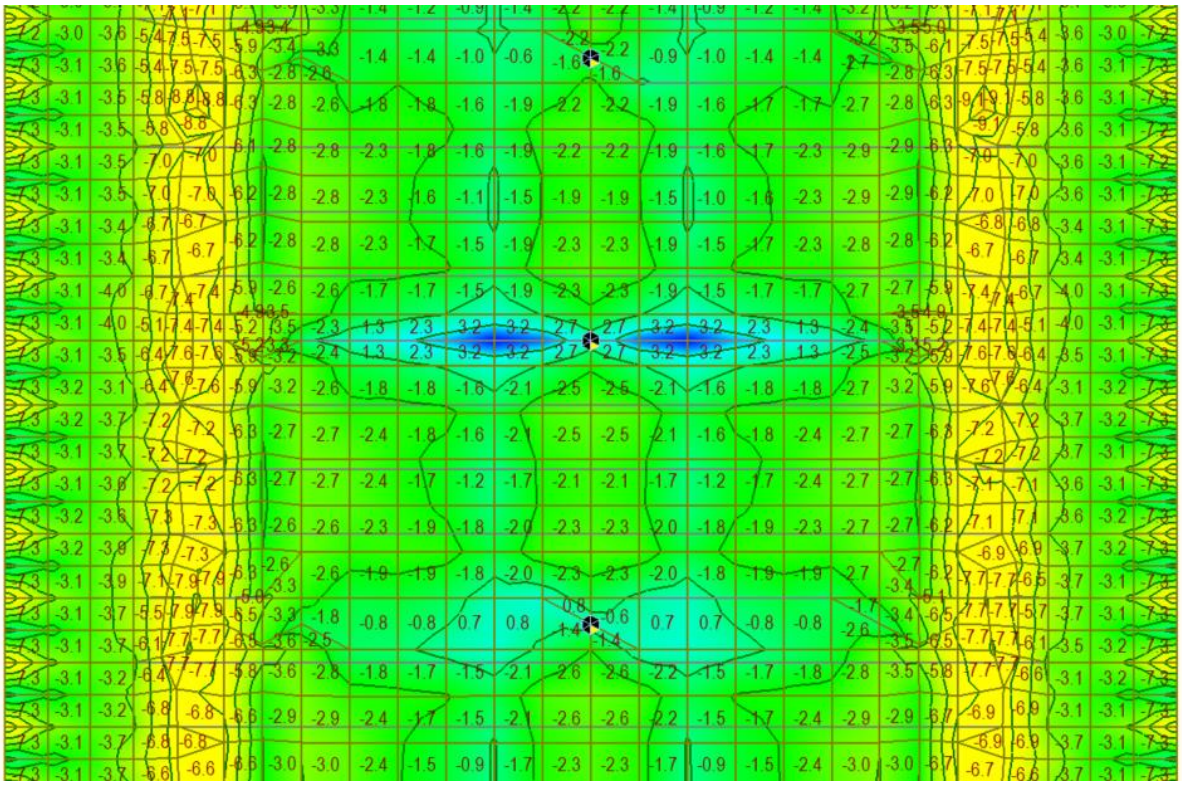

Figure 237 Bottom fiber stresses frequent combination Max [MPa]

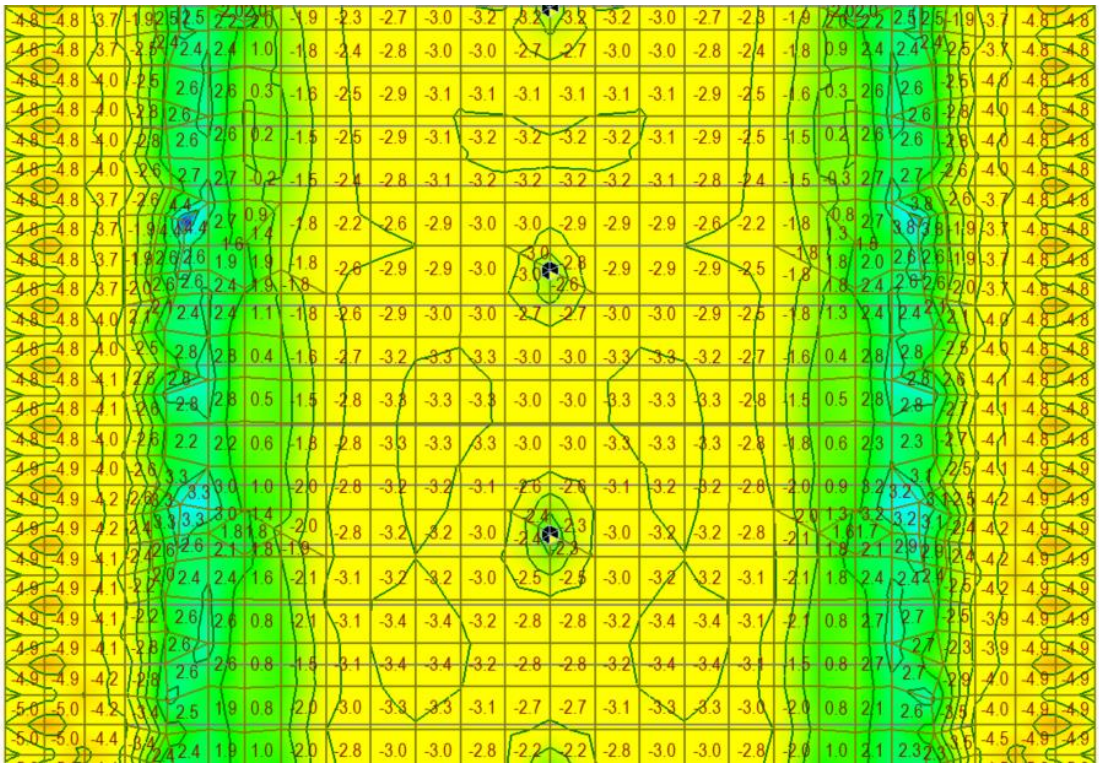

Figure 238 Top fibers stresses frequent combination Min [MPa]

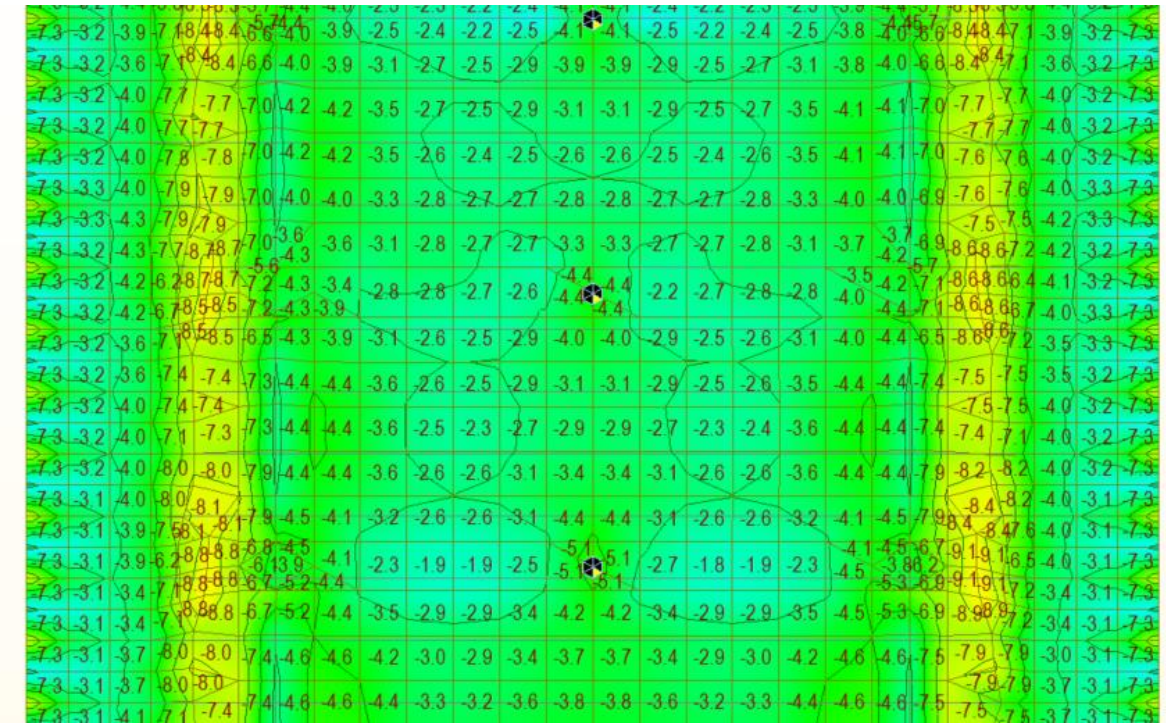

Figure 239 Bottom fiber stresses frequent combination Min [MPa]

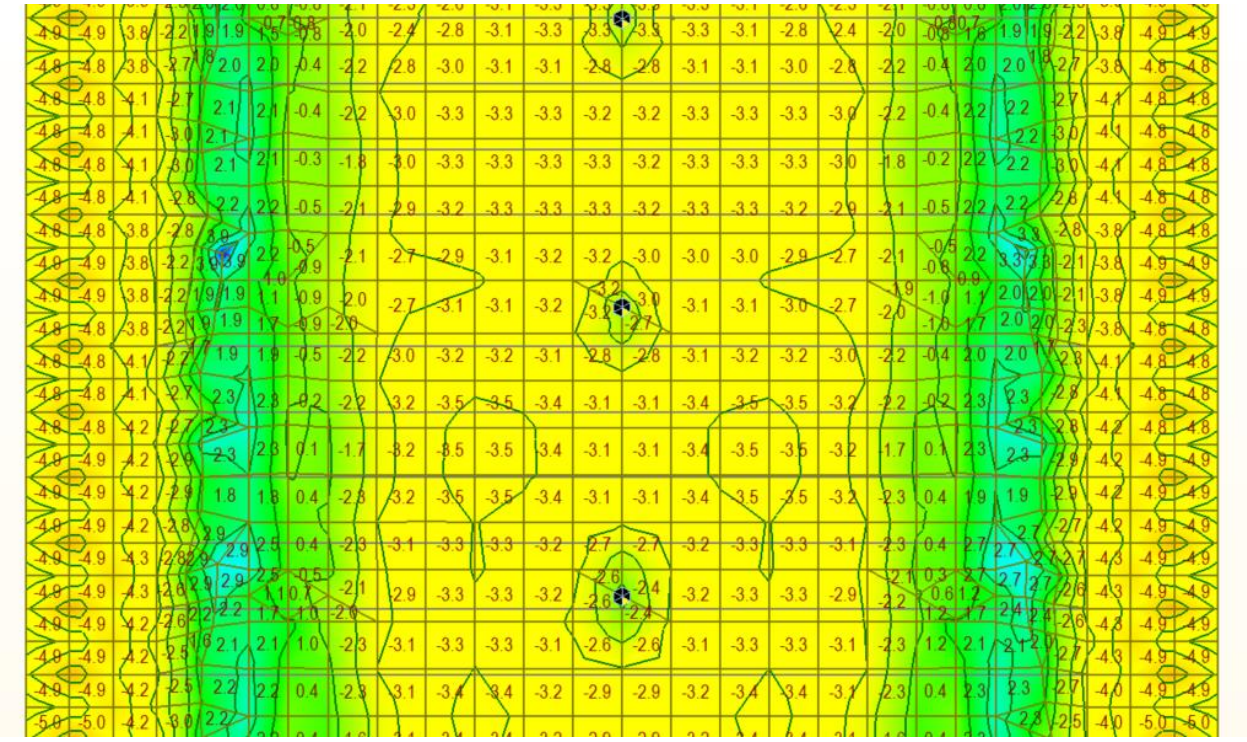

Figure 240 Top fibers stresses quasi-permanent Combination Max [MPa]

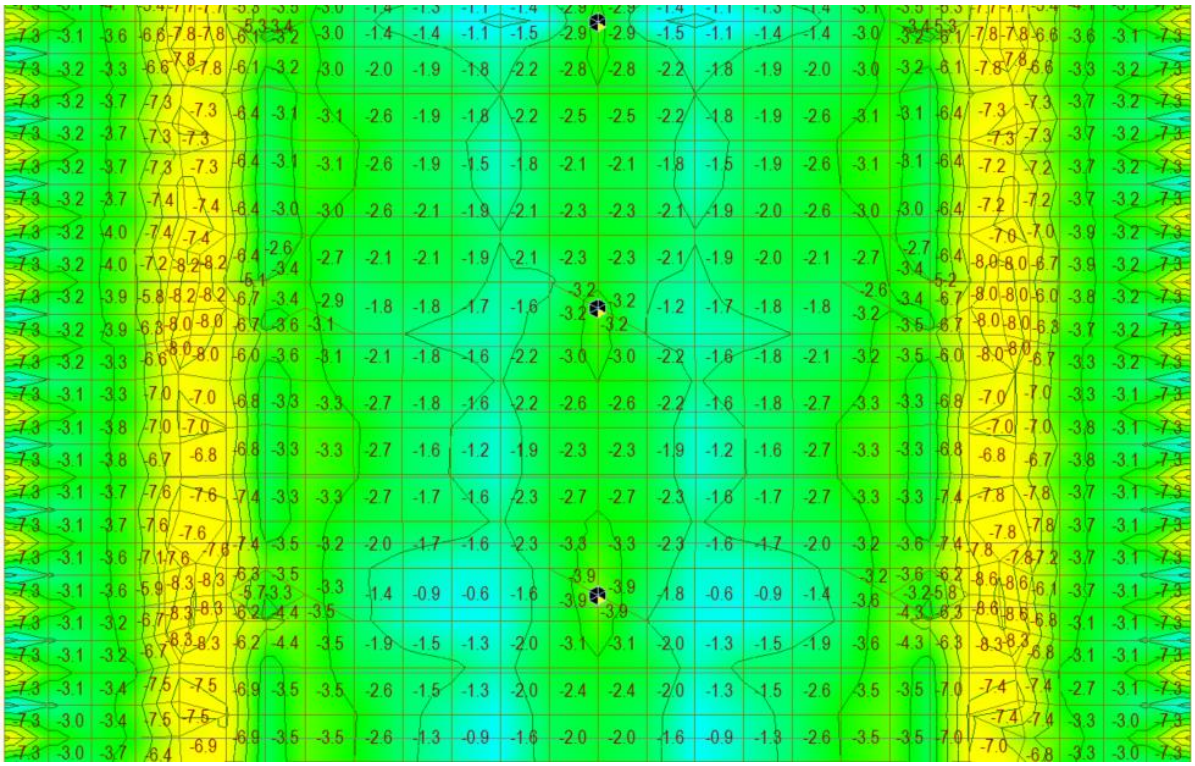

Figure 241 Bottom fiber stresses quasi-permanent Combination Max [MPa]

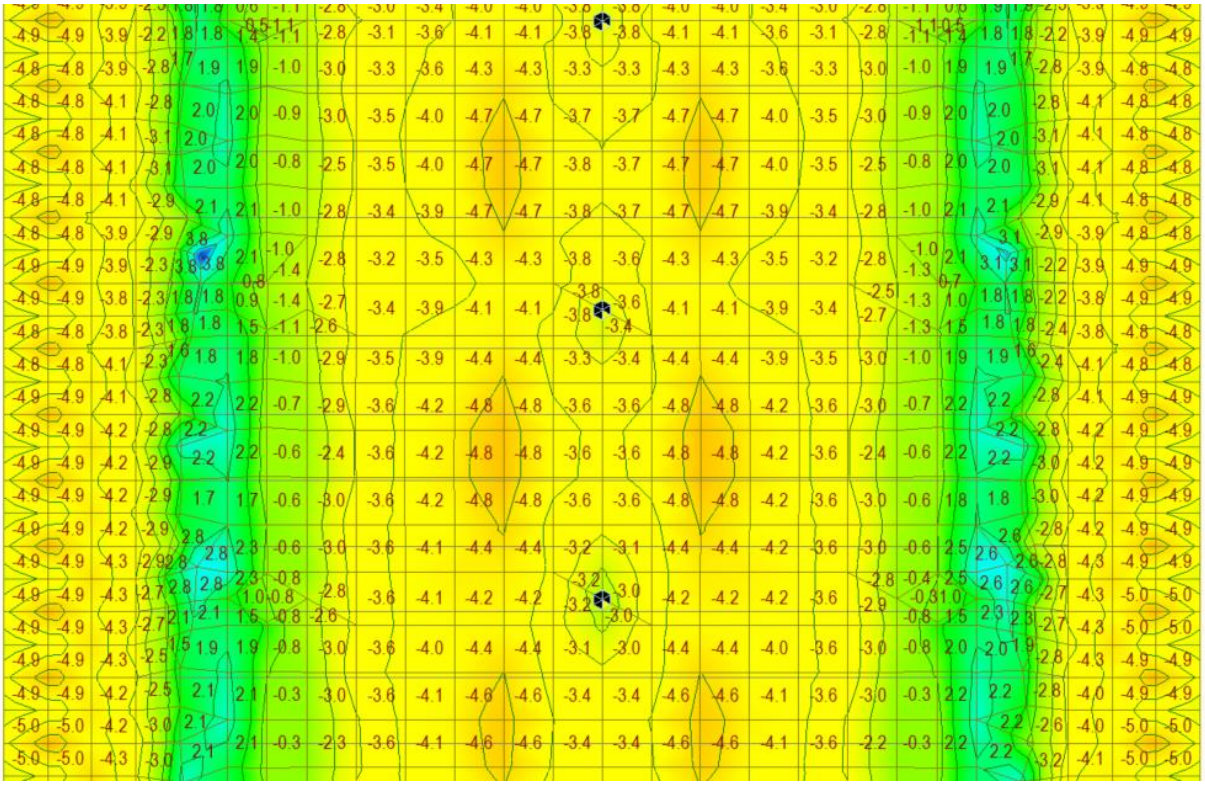

Figure 242 Top fibers stresses quasi-permanent Combination Min [MPa]

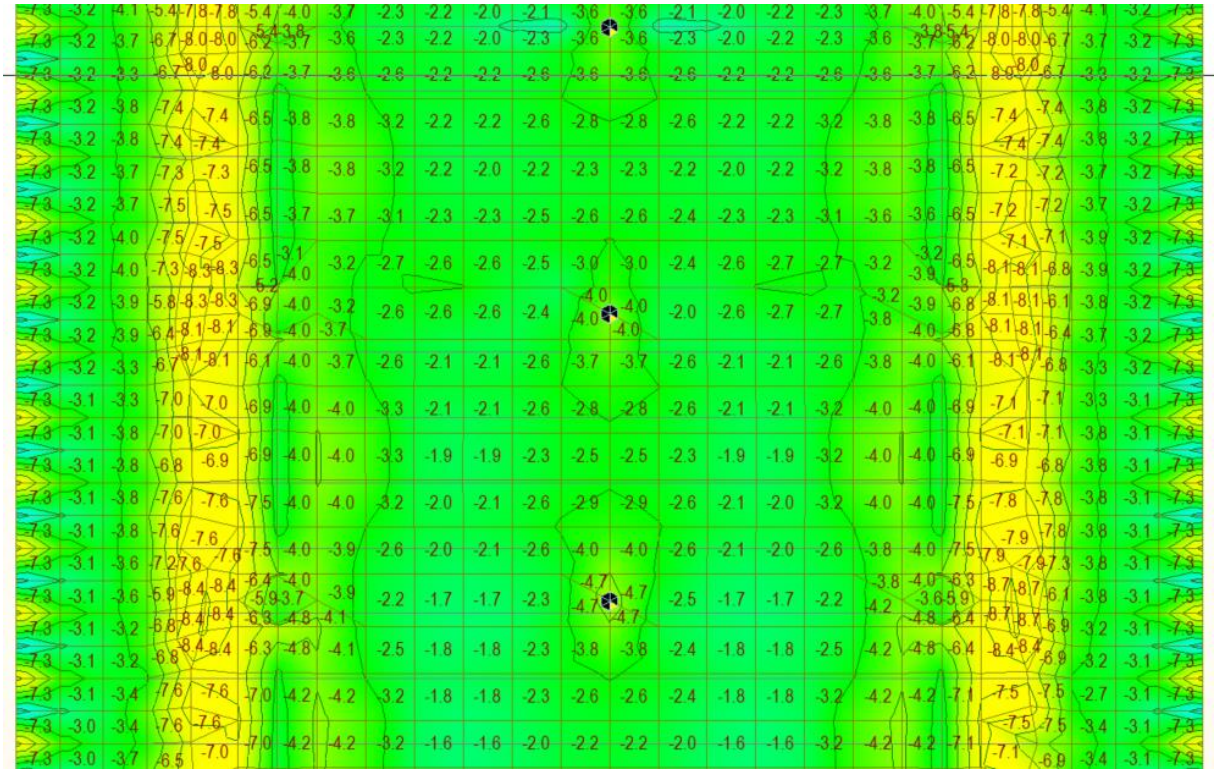

Figure 243 Bottom fiber stresses quasi-permanent Combination Min [MPa]

From the results, the stresses have not exceeded the limits and the tensile stresses have not exceeded the value of fctm =4.1 MPa. So, the section can be considered an uncracked section

9.3 Ultimate limit state

The max negative moment has been checked near the box girder walls (section 2) and the max positive moment has been checked between the box walls and the cable anchorage (section 1), the sections are shown below.

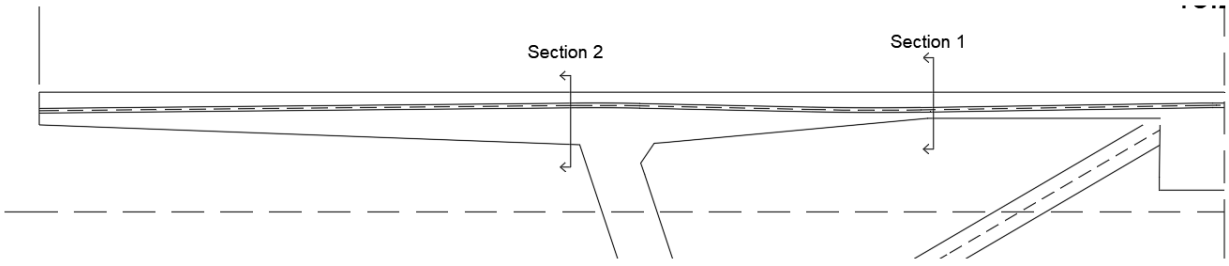

Figure 244 Transverse Cable profile

The section 1 and 2 are shown in the following figure.

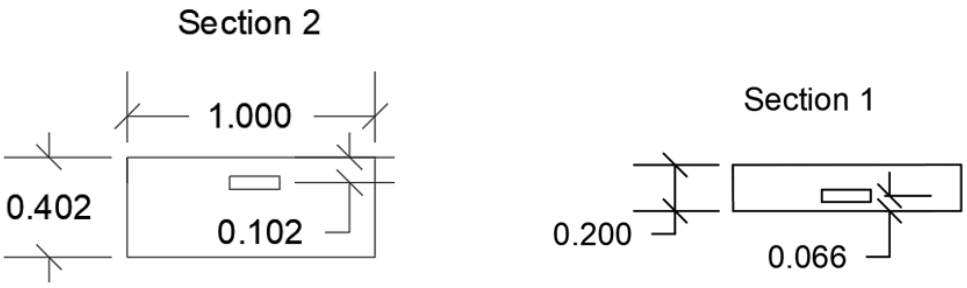

Figure 245 Section 1&2 in transverse analysis

9.3.1 Max positive moment

The results of the model for ULS are shown below.

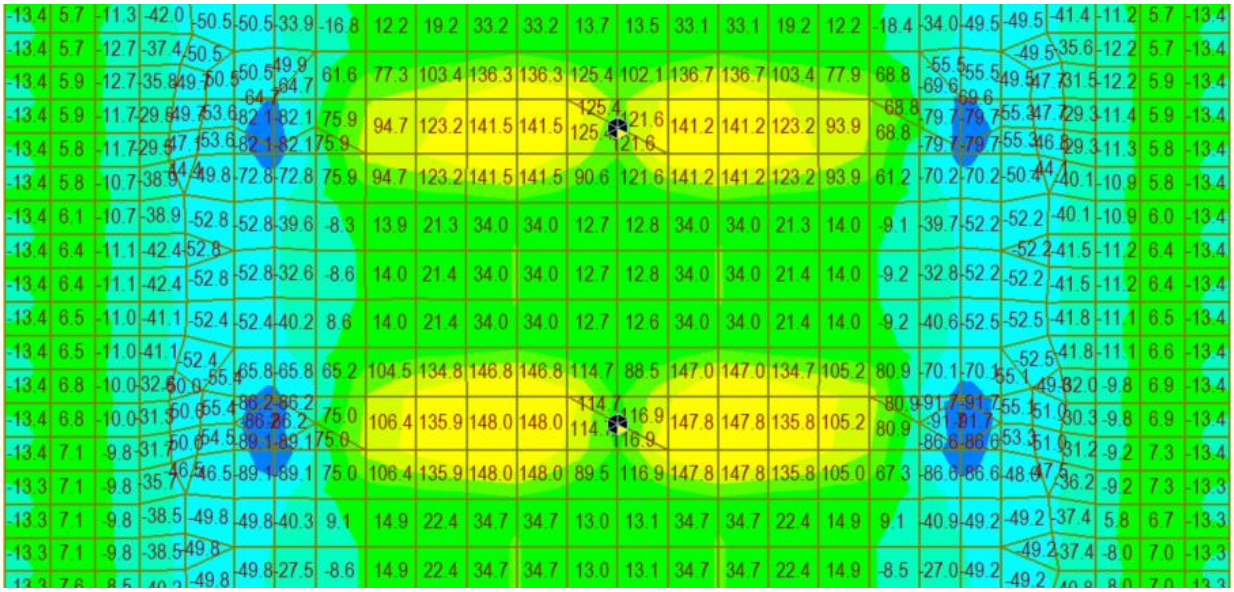

Figure 246Mxx ULS Max [KN.m]

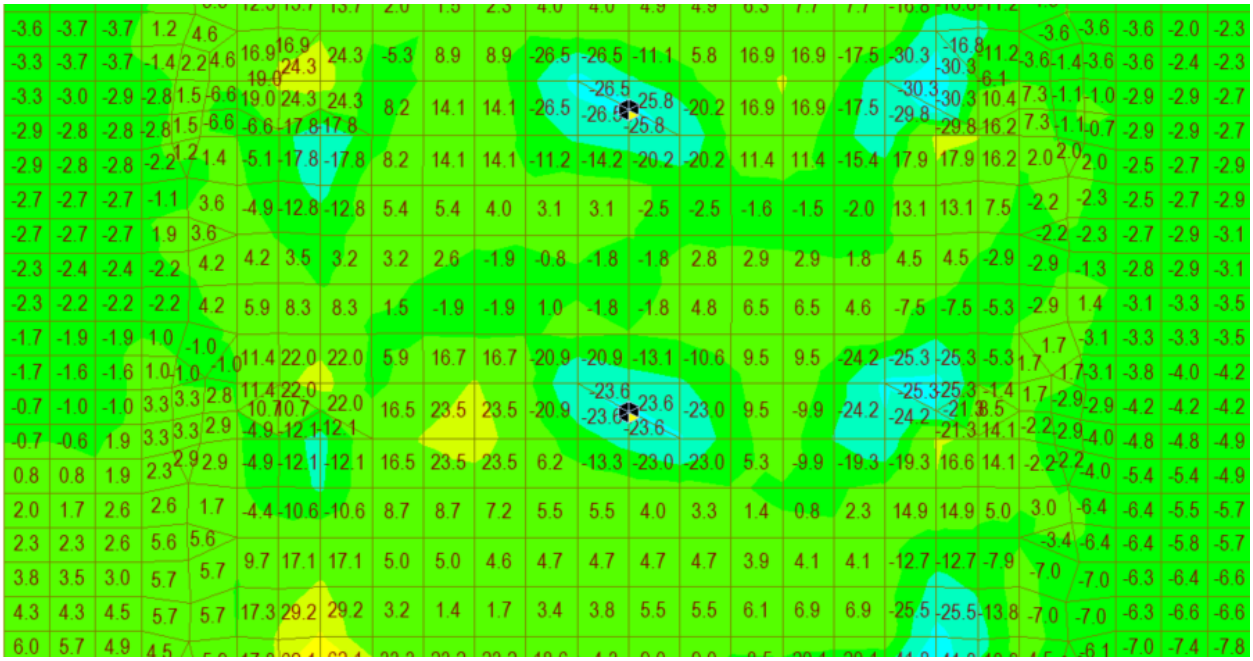

Figure 247 Mxy ULS Max [KN.m]

The design moment has been considered as the summation of the Mxx and Mxy (the longitudinal axis of the bridge is y-axis).

Mxx=148 KN.m

Mxy=23.5 KN.m

Med=148+23.5 = 171. 5KN.m

The section 1 has been designed to resist this moment.

The design of this section has been carried on an excel sheet, bottom and top reinforcement are considered ϕ16mm/200 mm.

For the prestressing cable, 3 components of the strain have been considered. εe0 which represents the strain in the cable due to effective prestressing forces after losses. The second component ε,ec represent the strain of the concrete at the location of the prestressing cable. The last component of the strain εp which is obtained from the strain compatibility of the cross-section (the relation between the prestressing effective depth and the x value). [4]

the forces in the section include the concrete compression force, the upper, lower ordinary reinforcement, and the cable force. The value of x has been obtained by iteration, so the sum of all forces equals 0. The following table represents the strain component in the cable at the ultimate state.

Table 36 Strain components at ULS in section 1

Parameter	ε_P	ε_e0	ε_ec	ε_tot	**stresses**	**Fp**	**check** εu=0.0315
Value	0.005582	0.005641	0.000148	0.011371	1425.218547	855.131128	0.360983

The design data and the moment resistant are including in the below table

Table 37 Moment resistance at Section 1

Parameter	Value	Unit	Parameter	Value	Unit	Parameter	Value	Unit
fy	434.000	MPa	E, cm	37278.000	Mpa	Eff, stresses	1100.000	Mpa
ey	0.002	-	ε_c3	-0.004	-	E, p	195000.000	Mpa
spacing Top steel	200.000	mm	dp prestress	134.000	mm	Ap, one strand	150.000	mm
spacing Bottom steel	200.000	mm	d	142.000	mm	No. of Strand in cable	4.000	
No. Top Bar/m	5.000		d'	58.000	mm	No. of tendon in lower	1.000	
No. bot Bar/m	5.000		x	51.642	mm	dp	134.000	mm
D of Top steel	16.000	mm	bf	1000.000	mm	Ap, bottom tendon	600.000	mm2
D of bottom steel	16.000	mm	fcd	33.300	Mpa	Ap, upper tendon	-	mm2
As Top/m	1004.800	mm2	FC concrete	-1375.733	KN	e, p	0.066	
As bottom/m	1004.800	mm2	As'	1004.800	mm2	P effect of prestress	-660.000	KN
h (section height)	0.200	m	As	1004.800	mm2	M effect of prestress	-22.440	KN.m
b (section width)	1.000	m	εs'	0.000	-	X/d	0.364	<0.45
A(area)	0.200	m2	εs	0.006	-	Check εs'/εut=0.025	0.017	Ok
I (moment of inertia)	0.001	m4	Fs' upper as	86.601	KN	Check εs/εut=0.026	0.245	Ok
Z, t top fiber	0.100	m	Fs lower as	434.000	KN	Med	171.5	KN.m
Z, b bottom fiber	0.100	m	Sum of forces	0.000	KN	Med/Mrd	0.985932134	Ok
			MRd	173.947	KN.m			

The following figure shows the forces in the concrete section (Prestressing force, top and lower ordinary steel forces, and concrete compression force)

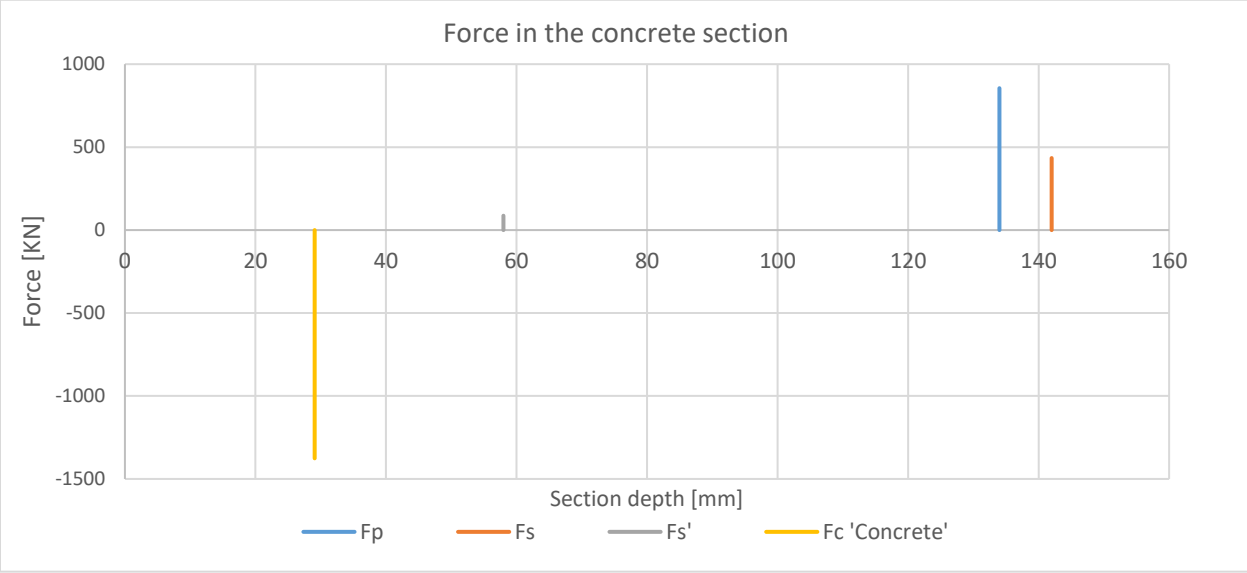

Figure 248 Forces in section 1

The state of prestressing cable at ULS is shown in the following figure.

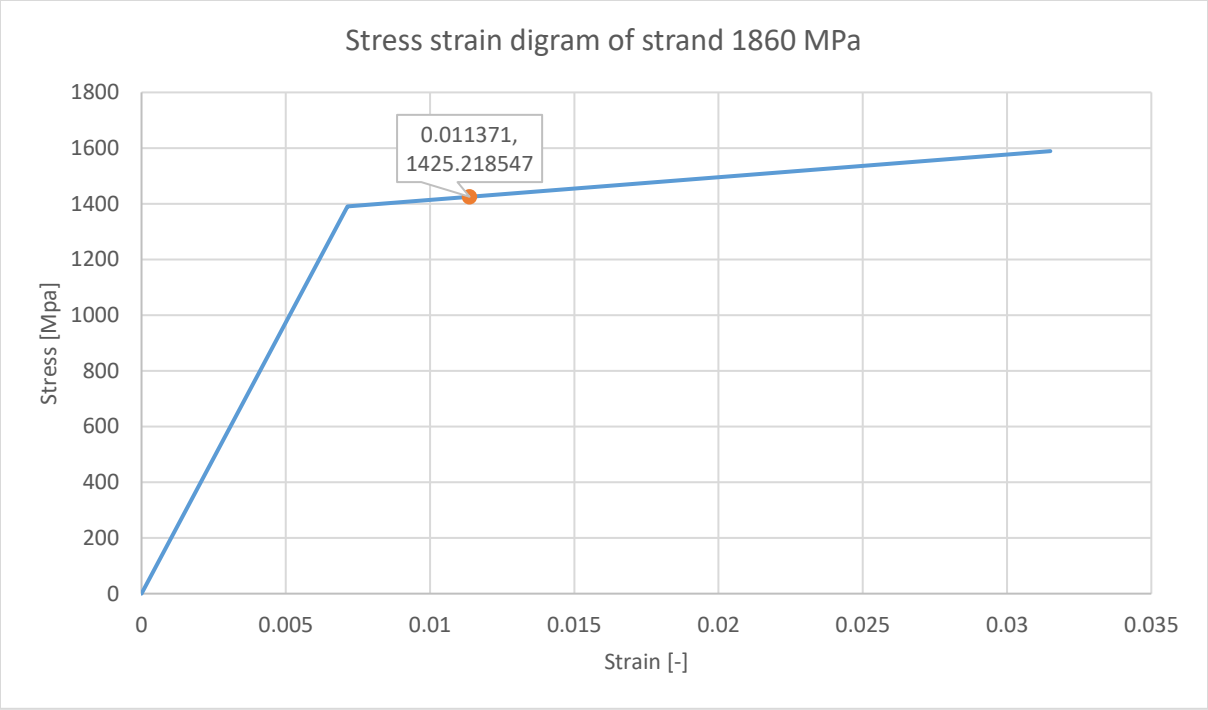

Figure 249 prestressing status in section 1

9.3.2 Max Negative moment

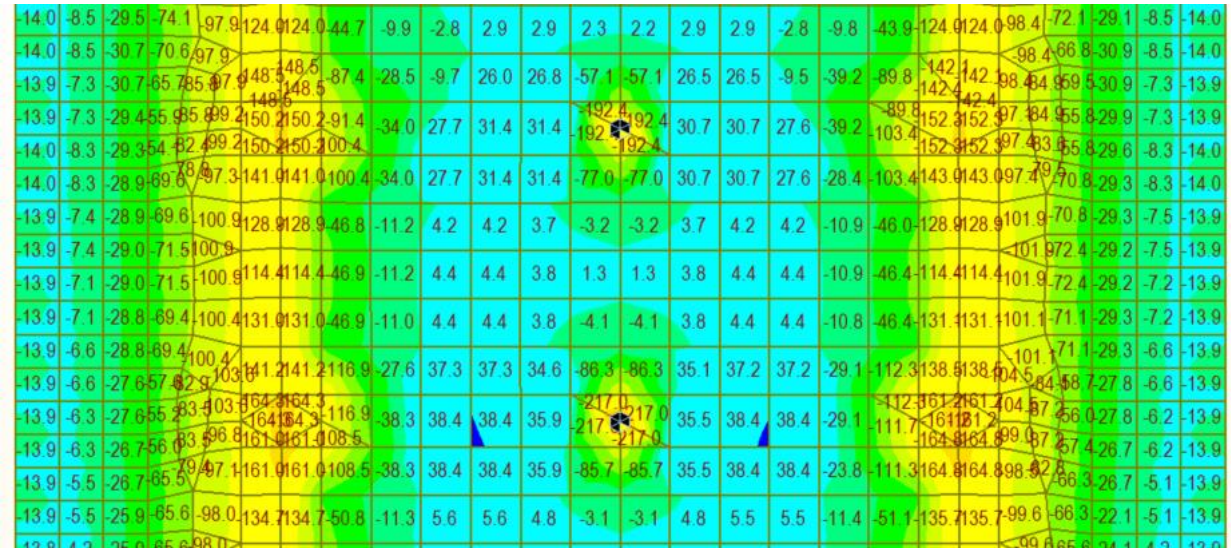

Figure 250 Mxx Min ULS [KN.m]

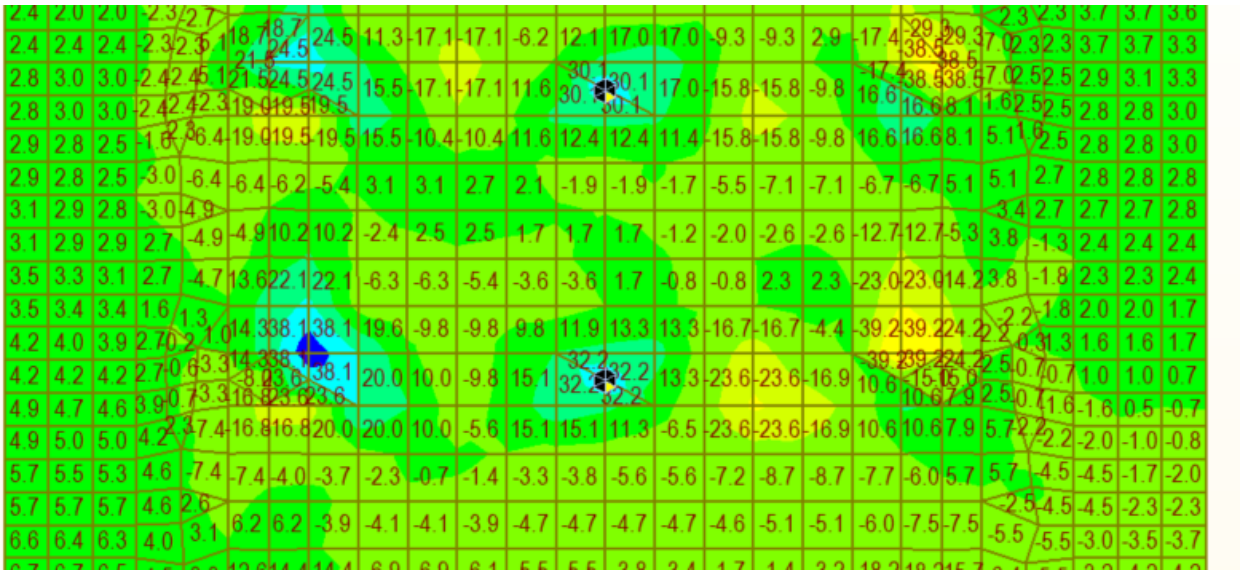

Figure 251 Mxy Min ULS [KN.m]

The design moment has been considered as the summation of the Myy and Mxy (the longitudinal axis of the bridge is y axis).

Myy=-164.4 KN.m

Mxy=-16.8 KN.m

Med=-164.4-16.8 = -181.2

The design has been done by excel, the following tables and figures shows the results (the same procedure of the design of the positive moment have been used).

Table 38 Strain components at ULS for section 2

Parameter	ε_P	ε_e0	ε_ec	ε_tot	**stresses**	**Fp**	**check** εu=0.0315
Value	0.016351	0.005641	0.000073	0.022065	1511.951095	907.170657	0.700492

Table 39 Moment resistance at Section 2

Parameter	**Value**	**Unit**	**Parameter**	**Value**	**Unit**	**Parameter**	**Value**	**Unit**
fy	434.000	MPa	E, cm	37278.000	Mpa	Eff, stresses	1100.000	Mpa
ey	0.002	-	e_c3	-0.004	-	E, p	195000.000	Mpa
spacing Top steel	200.000	mm	dp	300.000	mm	Ap, one strand	150.000	mm
spacing Bottom steel	200.000	mm	d	344.000	mm	No. of Strand in cable	4.000	
No. Top Bar/m	5.000		d'	58.000	mm	No. of tendon in lower	1.000	
No. bot Bar/m	5.000		x	52.893	mm	dp	134.000	mm
D of Top steel	16.000	mm	bf	1000.000	mm	Ap, bottom tendon	600.000	mm2
D of bottom steel	16.000	mm	fcd	33.300	Mpa	Ap, upper tendon		mm2
As Top/m	1004.800	mm2	FC	-1409.078	KN	e, p	0.066	

As bottom/m	1004.800	mm2	As'	1004.800	mm2	P effect of prestress	-660.000	KN
h (section height)	0.402	m	As	1004.800	mm2	M effect of prestress	-89.100	KN.m
b (section width)	1.000	m	es'	0.000	-	X/d	0.154	<0.45
A(area)	0.402	m2	es	0.019	-	Check εs'/εut=0.025	0.014	Ok
I (moment of inertia)	0.005	m4	Fs'	67.907		Check εs/εut=0.026	0.771	Ok
Z, t	0.201	m	Fs	434.000		Med	181.2	KN.m
Z, b	0.201	m	Sum of forces	0.000	KN	Med/Mrd	0.357541461	Ok
			MRd	506.794	KN.m			

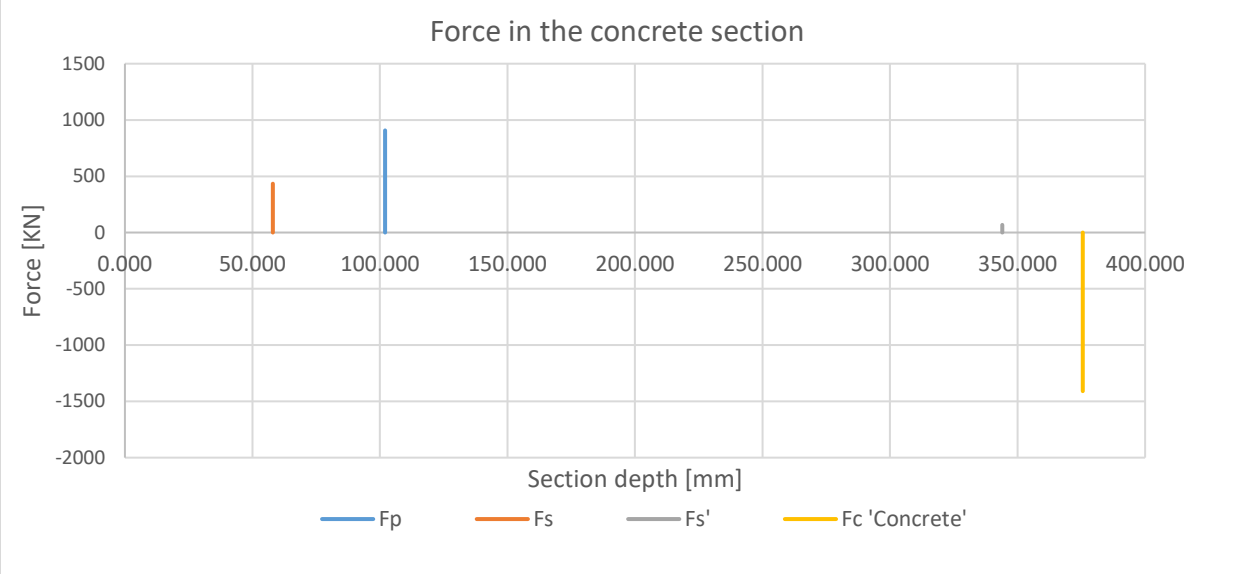

Figure 252 Forces in section 2

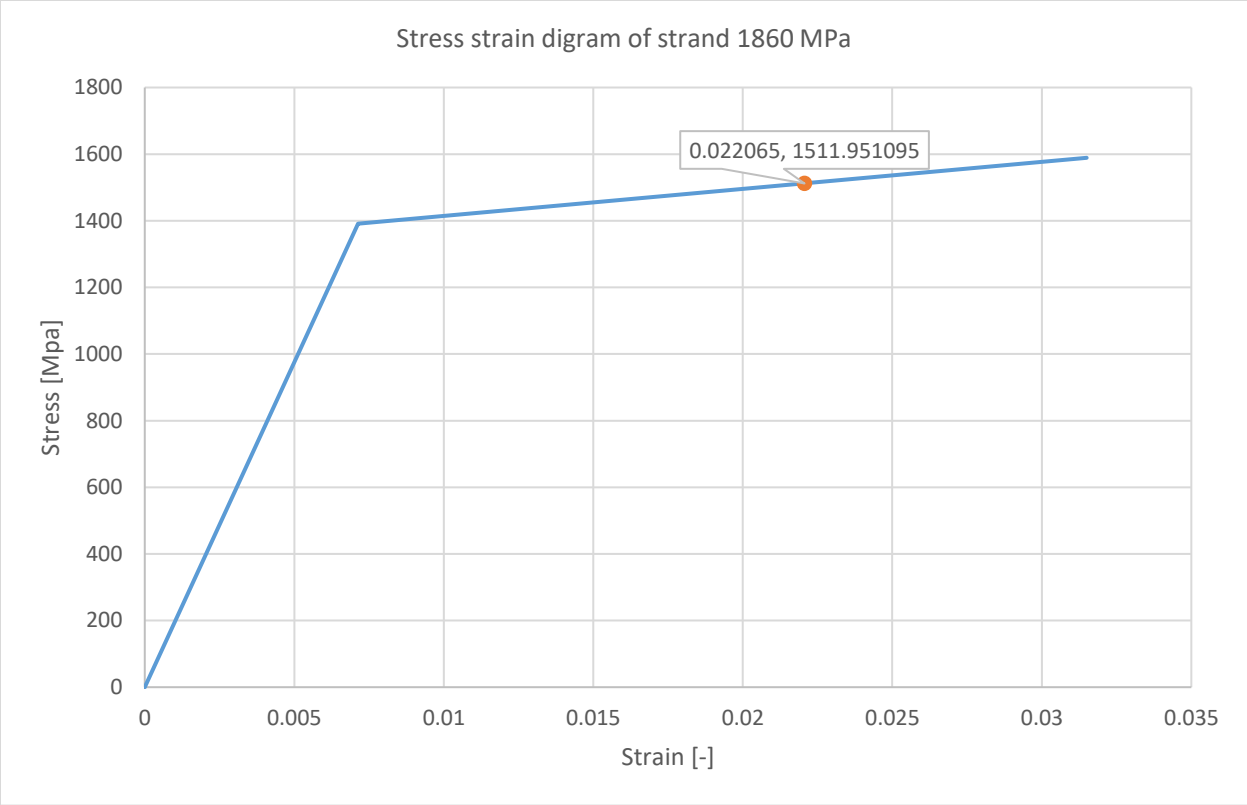

Figure 253 prestressing status in section 2

9.4 Design of concrete diagonal member.

The diagonal ties which help in disruption the cable forces to the entire box girder are one of the important parts which stiffen the entire cross section. The design of the ties has been done using plate model for transverse analysis. 12 members have been considered in the transvers analysis (6 pairs).

The design load for each member is shown in the following table also the results from the model are shown in the following figures.

Table 40 Design forces for diagonal members

Load	Ned, Max [KN]	Med, y Max(kN.m)	Med, z Max(kN.m)	Ned, Min [KN]	Med, y Min[kN.m]	Med, z Min(kN.m)
D1	1037.5	--11	131.5	716.3	-14.4	-65.1
D2	1038.9	-10.8	65.2	702.3	-14.4	-131.5
D3	887.0	-7.4	41.7	383.5	-12.8	-22
D4	869.3	-7.4	22	380.7	-12.9	-41.7
D5	1047.3	7.8	14	313.8	-14.5	-8.1
D6	1055.7	7.9	8.1	311.9	-14.6	-14
D7	917.2	-6.4	5.9	292.5	-13.1	-4.2
D8	921.6	-6.4	4.2	292.2	-13.1	-5.9
D9	1368.4	11.2	3.9	466.5	-17.9	-3.8
D10	1370.2	11.2	3.9	467.2	-17.9	-3.9
D11	1098.1	-8.4	3.5	477.0	-15	-4.1
D12	1098.6	-8.4	4.2	478.0	-15	-3.5

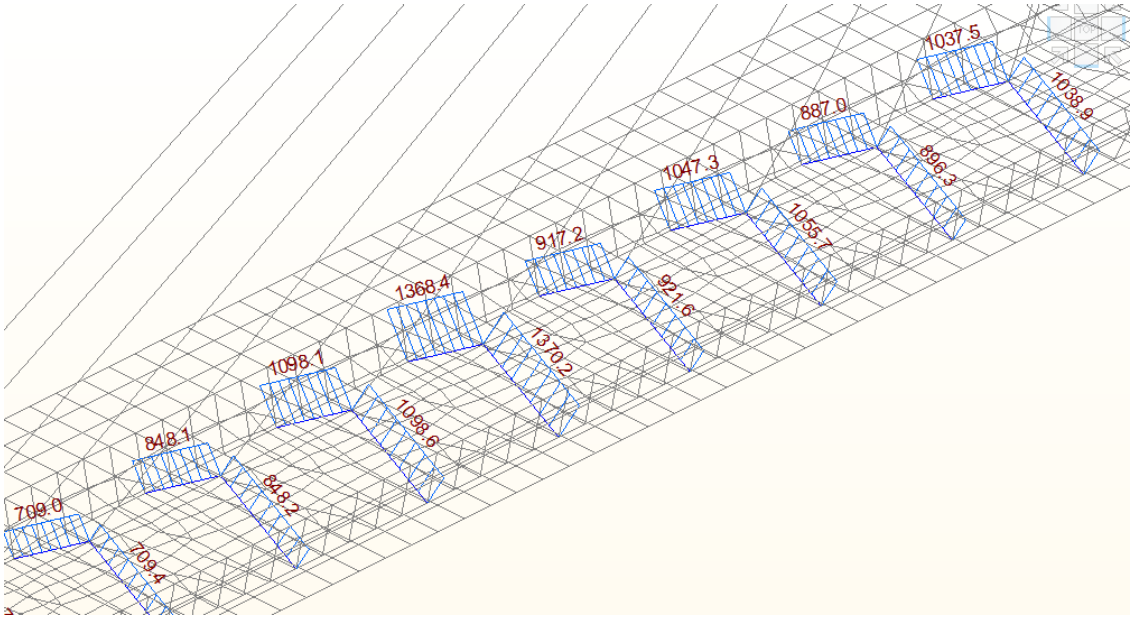

Figure 254 Ned Max ULS [KN]

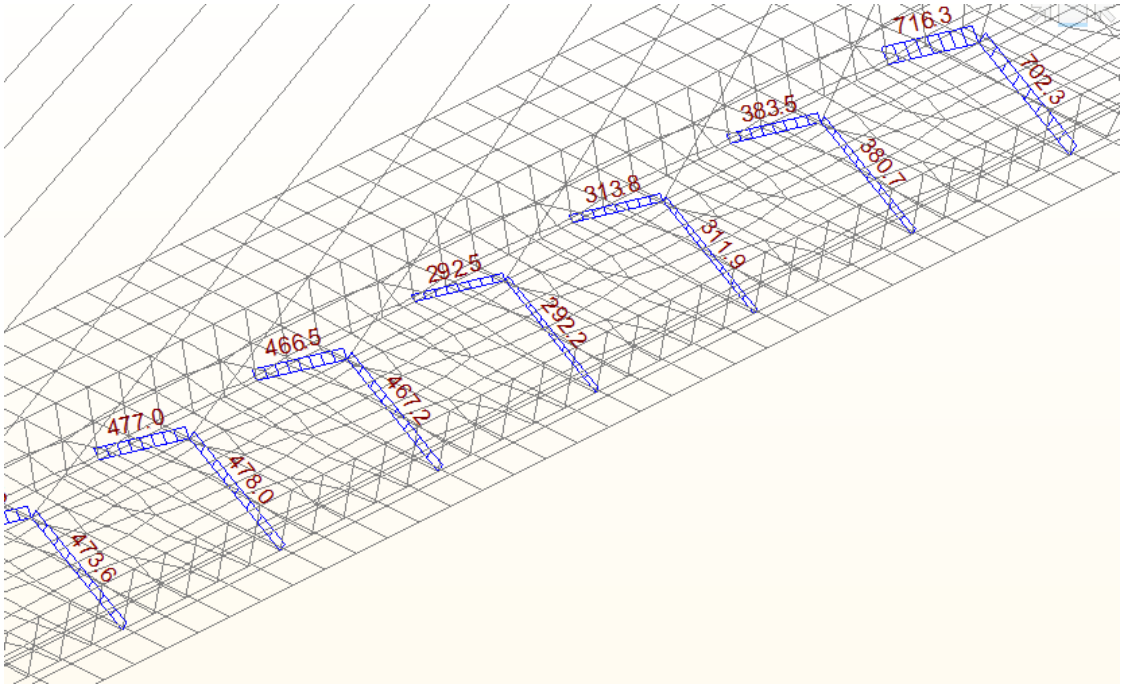

Figure 255 Ned Min ULS [KN]

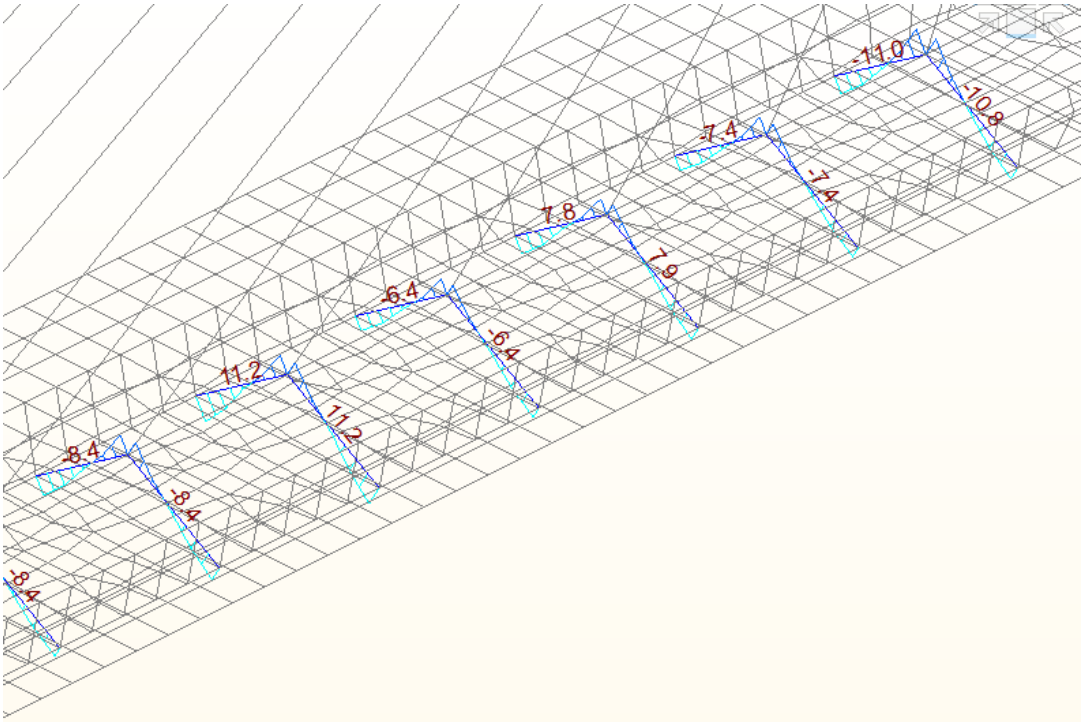

Figure 256 My,ed max ULS [KN.m]

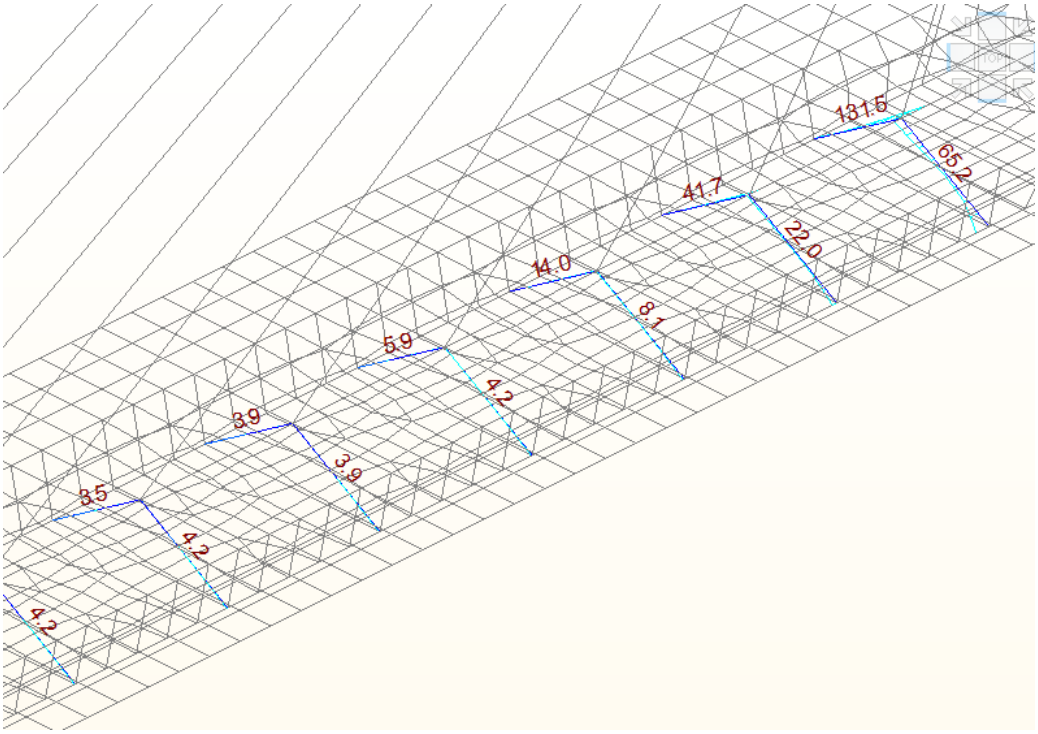

Figure 257 Mz,ed max ULS [KN.m]

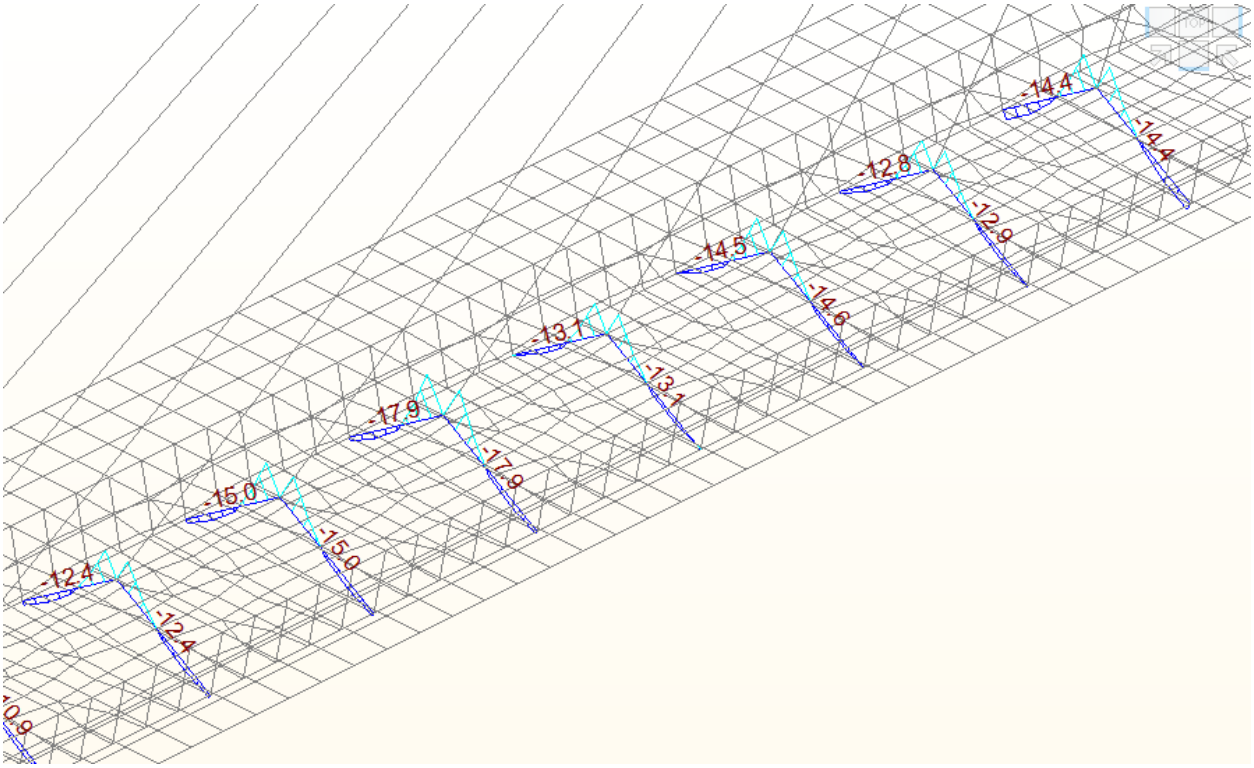

Figure 258 My,ed min ULS [KN.m]

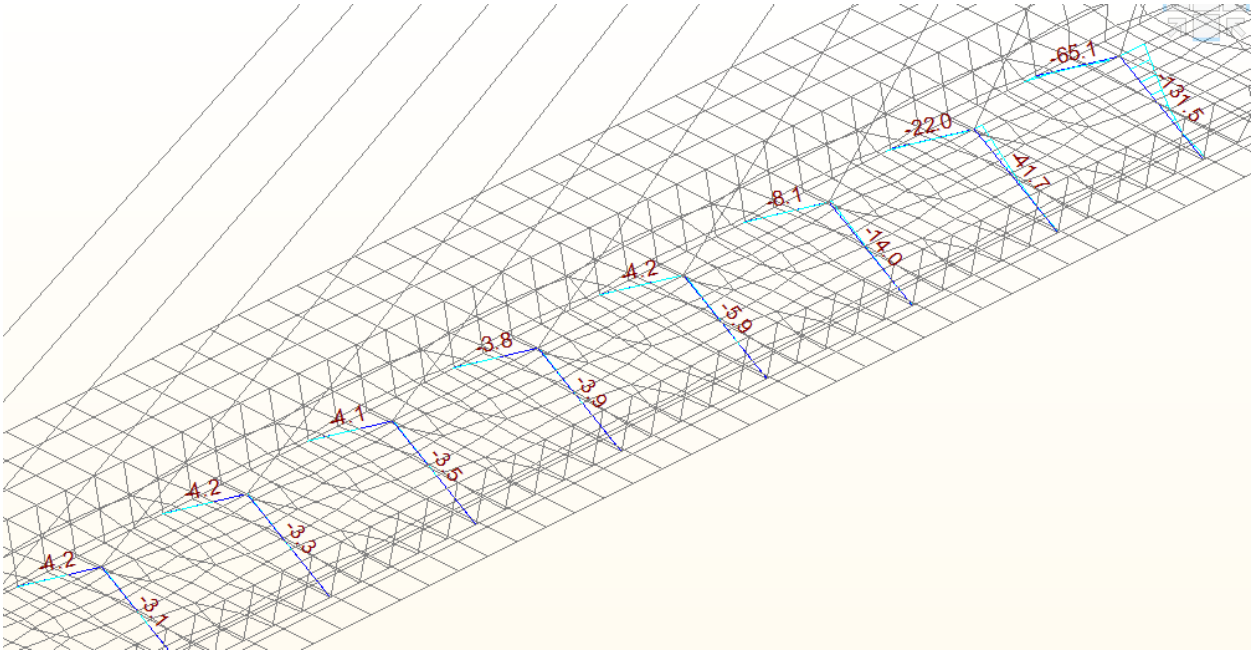

Figure 259 Mz,ed min ULS [KN.m]

The design of the longitudinal member has been carried by idea statica .

The members from D1 till D12 have been considered in the design by using an interaction diagram, the cross-section used is 35*35cm with 16ϕ20mm and 10mm stirrups at 2000mm and prestressed bar in the center ϕ40mm stressed by 970MPa and assuming 25% long-term losses, the results are below.

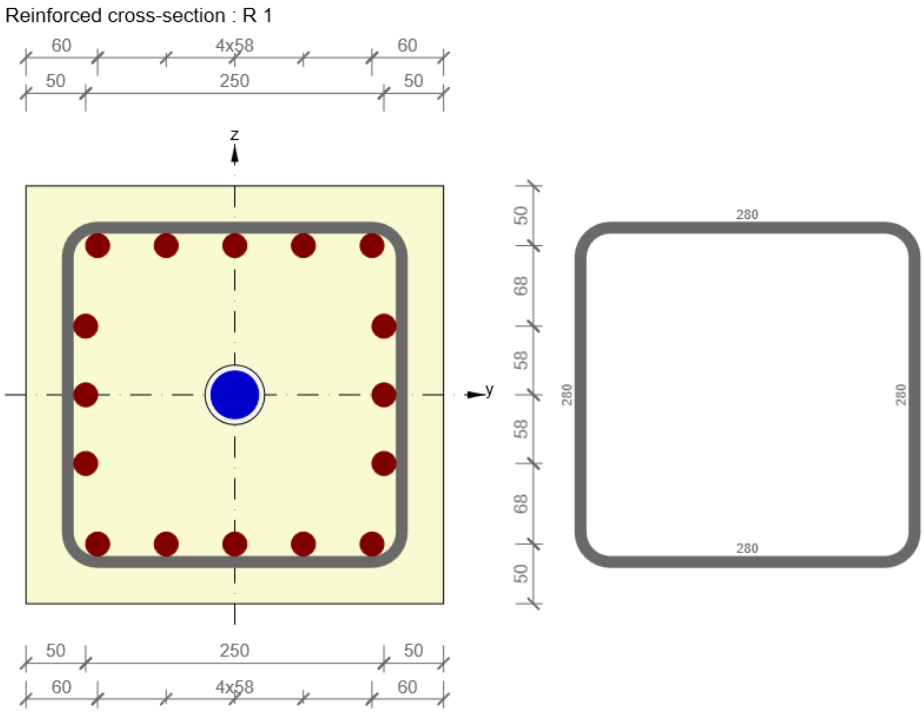

Figure 260 Cross section of the diagonal member

The interaction diagrams N-My & N-Mz with all assessed section are below

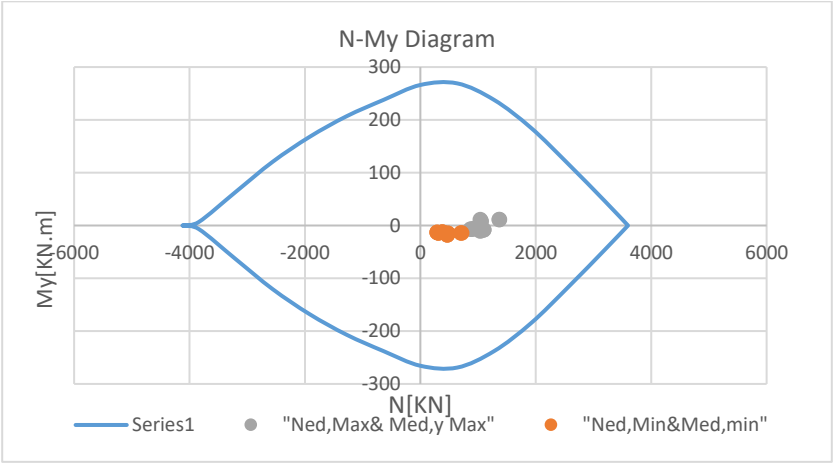

Figure 261 Interaction diagram N-My

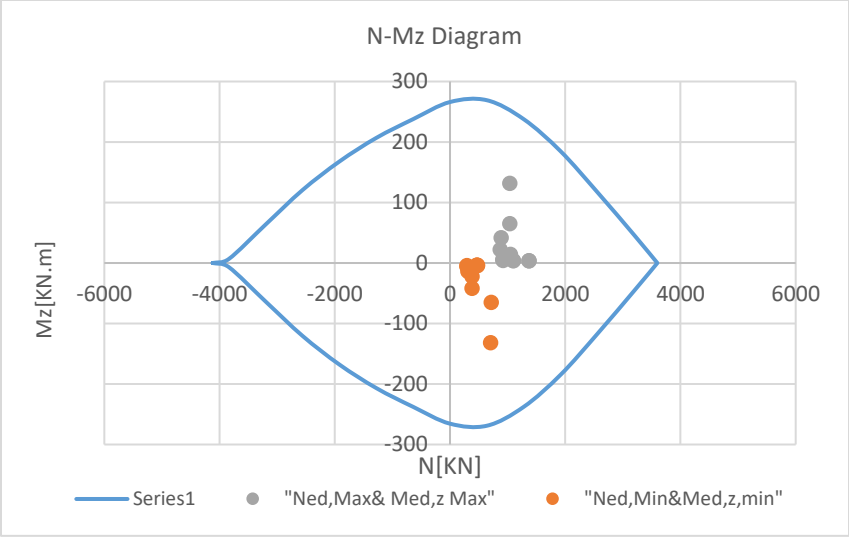

Figure 262 Interaction Diagram N-Mz

9.5 Diaphragm design

The diaphragm which is a very essential part of the superstructure has the role of transferring the superstructure load to the substructure. the load which is transferring to the substructure is mainly the vertical, horizontal, and torsional moments.

The diaphragms are one of the discontinuity areas in the structure which need particular care, the main aim of this master thesis is related to construction stage analysis

the design of the diaphragm has been introduced here using the idea statica software using the CSFM method.

The design load has been applied to the structure which includes the design shear forces and the shear flow which have been produced by the design torsional moment, this shear flow has been applied to the diaphragm clockwise and anti-clockwise.

The shear flow has been calculated based on the following formula.

Shear flow=Ted/(2*Ak) =11657.5/ (2*17.54) =332.31 KN/m.

The following figure shows the applied shear flow on the diaphragm.

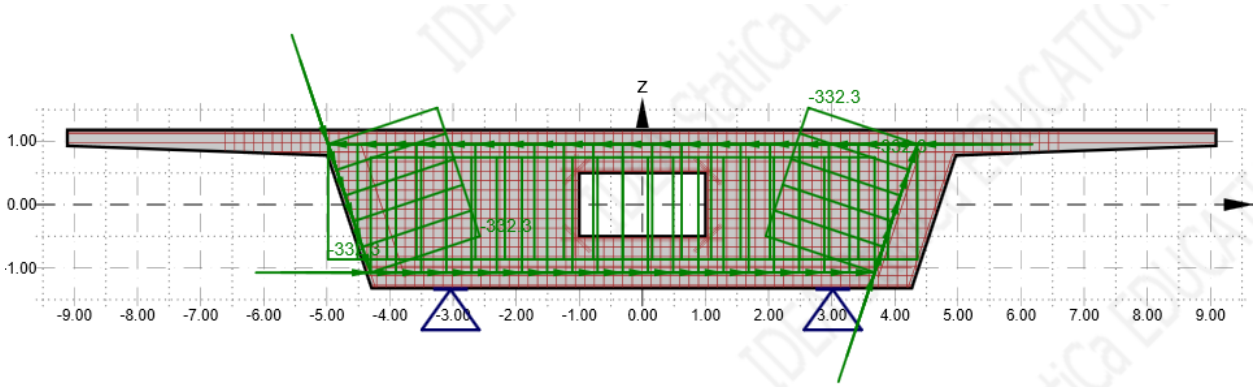

the topology of the forces is shown below for both combination (shear with torsion clockwise & shear with torsion anti-clockwise)

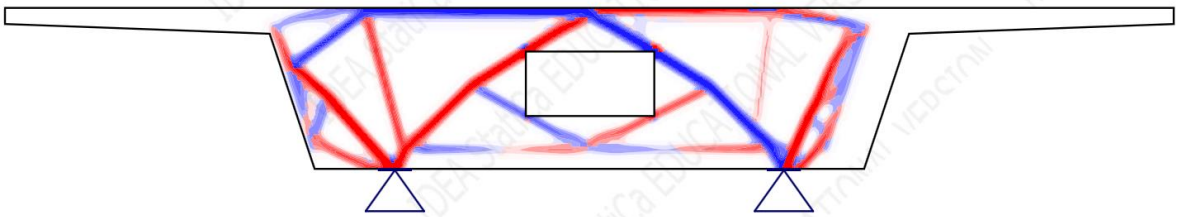

Figure 263 Topology (shear +Torsion anti-clockwise)

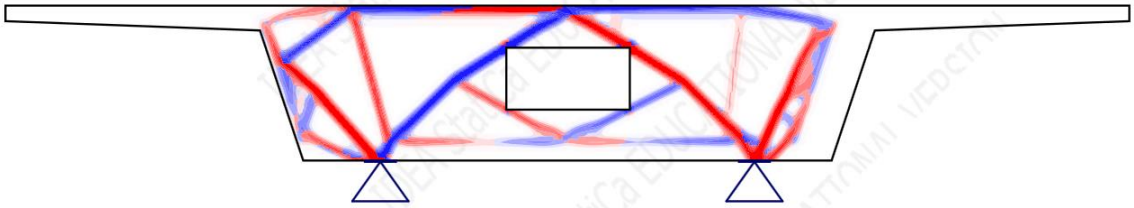

Figure 264 Topology (shear +Torsion clockwise)

The reinforcement has been modeled in the software, the top, bottom, and shear reinforcement are the same from the section design for a moment, shear, transverse, and minimum reinforcement.

In addition, a wire fabrics mesh has been applied (ϕ14mm @150 mm mesh with layer spacing 200mm) and 2 layers of 3ϕ8mm around the opening on all edges and diagonal near the corner.

The results are satisfied for strength check as shown below

Check item	Item	Utilization	
Strength of concrete	W1	σc/σc,lim: 99.4%	✓
Strength of reinforcement	WF1	εs/εs,lim: 55.8%, σs/σs,lim: 95.9%	✓
Anchorage length	RO1	τb/fbd: 100.0%	✓

Figure 265 Strength check for diaphragm

The following figure shows the utilization of the reinforcement (σs/σlim)

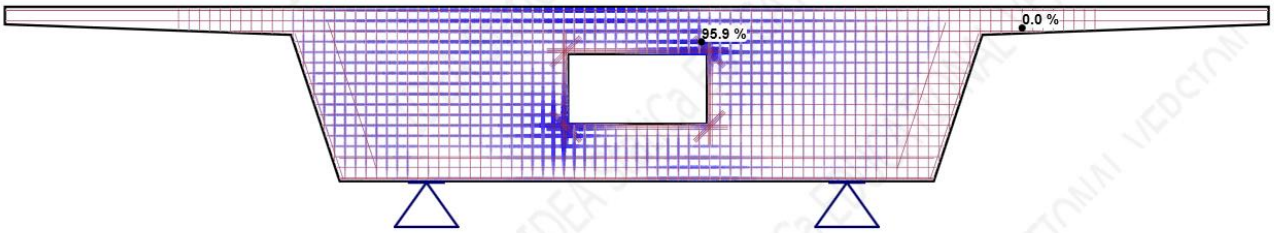

Figure 266 utilization of the reinforcement

The following figure shows the utilization of the concrete (σc/σlim)

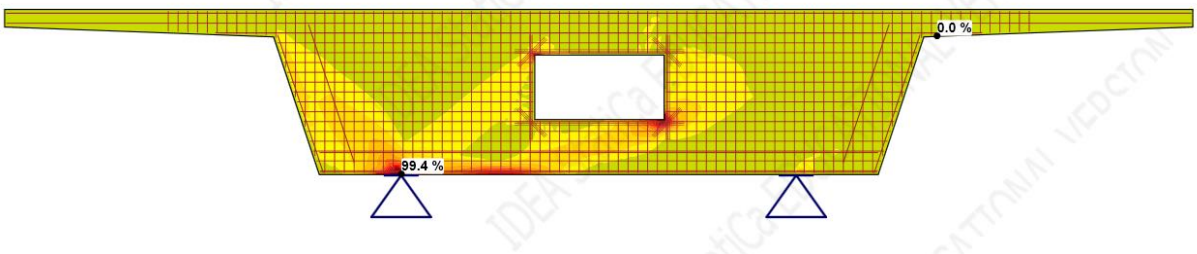

Figure 267 utilization of the concrete

The flowing figure shows the diaphragm reinforcement

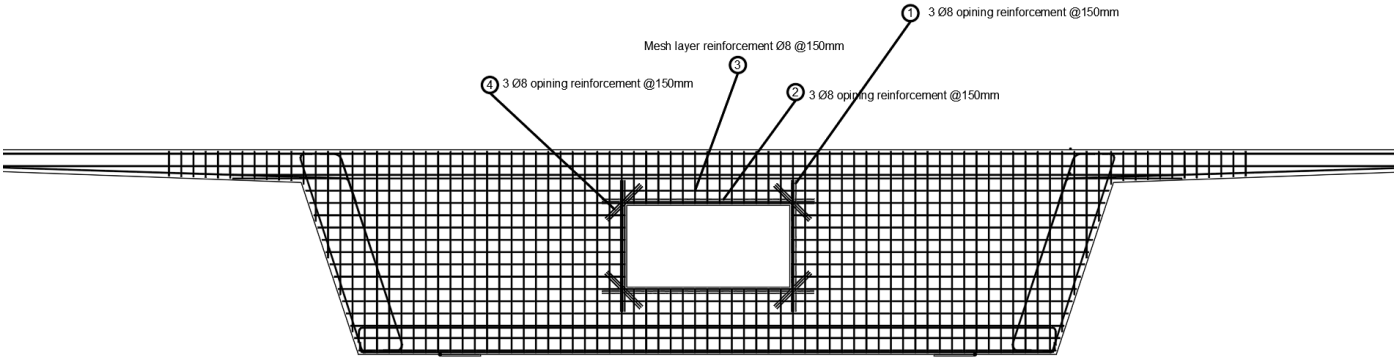

Figure 268 Reinforcement of diaphragm

10 Substructure Preliminary design

10.1 Pylon preliminary design.

The pylon is one of the main components of a cable-stayed bridge, the load applied to the pylon are mainly compression forces (from the vatical component of the cables) and horizontal force from the horizontal component of the cables, the traffic, self-weight of the deck, and other loads transfer to the pylon by the cables. The horizontal component of the cables will produce a moment in the pylon. The pylon is also considered fixed with the deck.

In the preliminary design of the pylon, the behavior has been considered as beam-column member with action of axial and bending moment, the assessment of the pylon was done by the Idea Statica using the interaction diagram.
The goal of this diploma thesis is to design the bridge for construction stages, so the pylon has been design just for the axial load from the cables, however in real design, the horizontal component of the cables should be designed so the walls of the pylon have to have a strength to transverse the horizontal component from one side to the other, such a solution require to have steel anchorage box inside concrete pylon, so the steel can carry the horizontal cable forces and also act with concrete as composite material to carry the vertical load of the cables. In this diploma thesis, this design has not been covered and the pylon has been assessed by interaction diagram just for axial load. In the figure below, it is shown the steel anchorage box which has been used in The Normandie Bridge, France. [18]

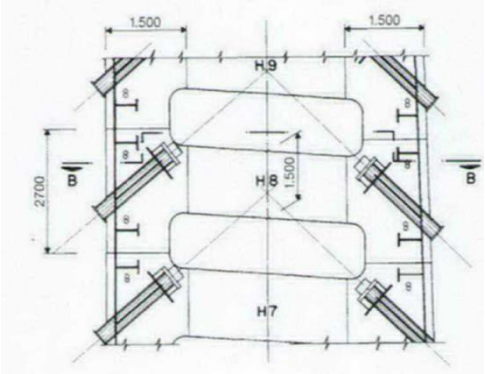

Figure 269 Steel anchorage box used for anchorage of the cables at the pylon [18]

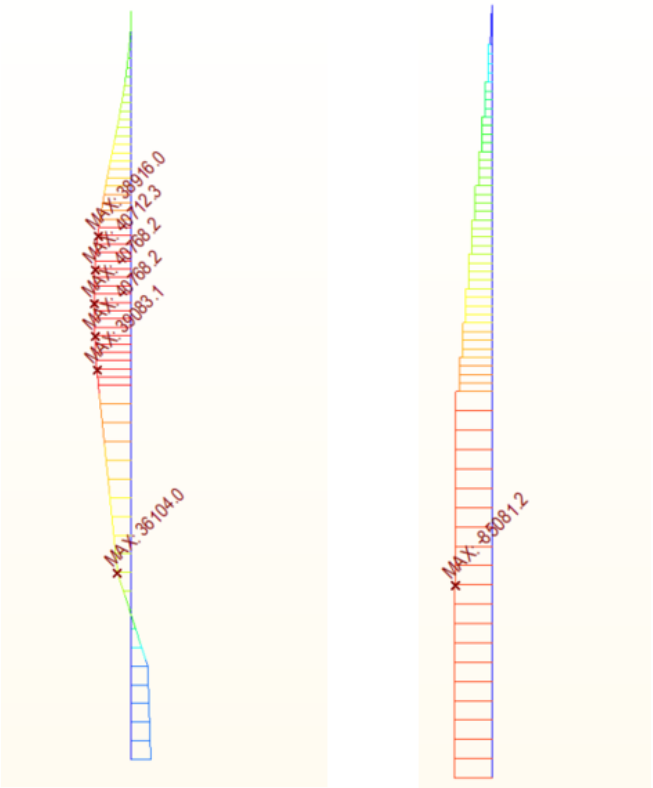

Figure 270 Inter design forces for pylon

The section of the pylon is 3x3m rectangle with wall thickness 0.5 m, the reinforcement is 134 ϕ 32 (As = 107468 mm2) (As, max>As=112594.65mm2>As, min) (As, min =max (0.002*Ac=5500, 0.1*Nc/Fyd = 19603.963), (As, max=0.04*Ac=110000mm2) and stirrups ϕ10 at S=200 mm as below. The pylon has been checked using interaction diagram as below

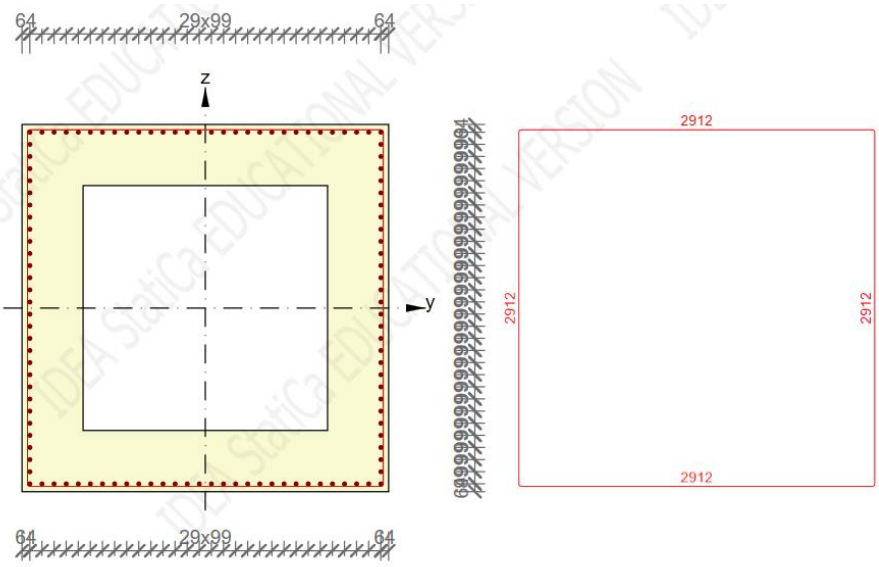

Figure 271 Pylon reinforcement

.

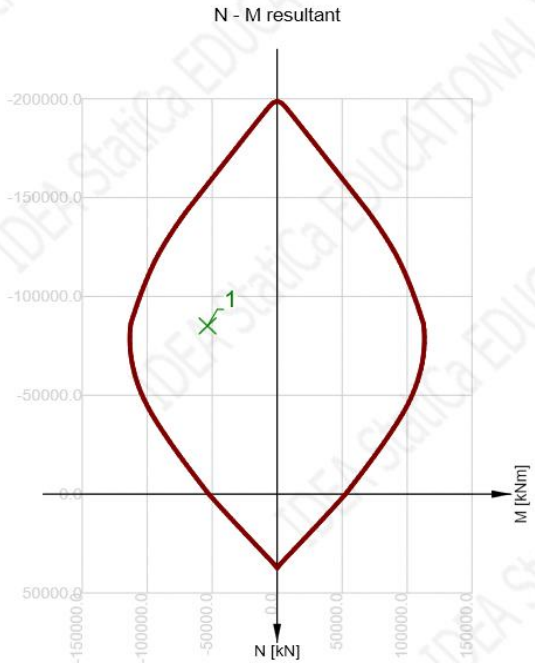

Figure 272 Interaction diagram for pylon

10.2 Pier preliminary design

The ultimate load applied to the pier Ned=96881.6 KN + the self-weight of the pier.

The horizontal load applied to the pier has been considered as the breaking and acceleration cables from the tram, the Czech load assume it to be % of the vertical load, the bridge carry 3 tram vehicles on each lane, the total vehicle has 8x120KN axial load, so the total vertical load is 5760KN and the breaking force equal 864KN which produce top moment equal to 864x2.5=2160 KN.m. The wind load in this preliminary design has not been included.

The section of the pier has been chosen as rectangle section 7.5x2.5 m

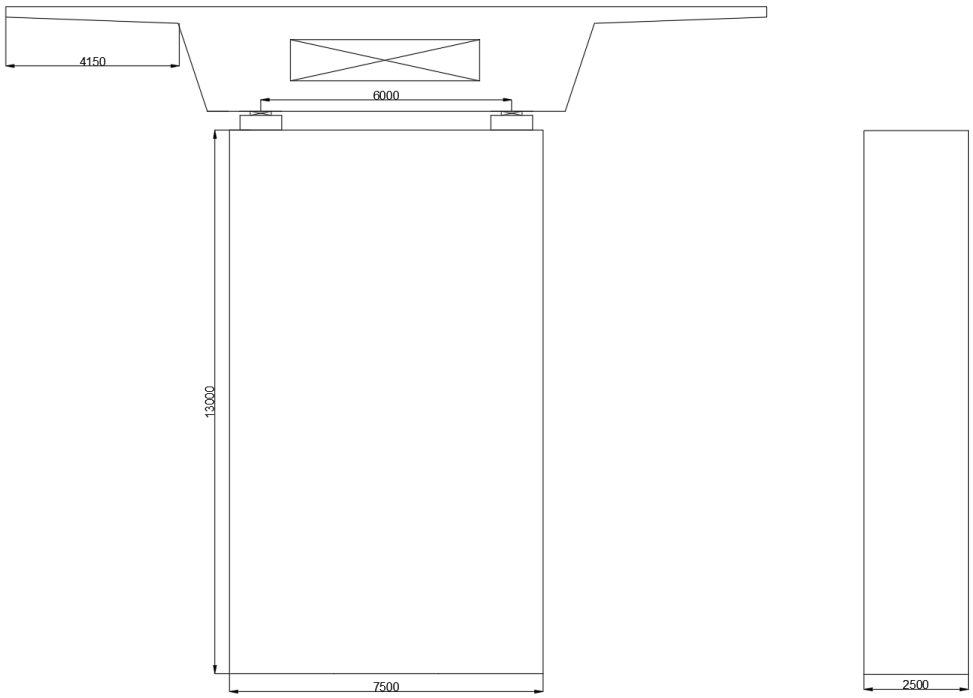

Figure 273 Pier & Pier cap

The design has been done by Idea Statice; the Pier behavior is the same as column. The design did not include the check for second order effect.

130ϕ32 have been uniformly distributed around the section (As, max>As=104552.2mm2>As, min) (As, min =max (0.002*Ac=37500, 0.1*Nc/Fyd = 2242.65), (As, max=0.04*Ac=750000mm2) and stirrups ϕ10 at S=200 mm as below.

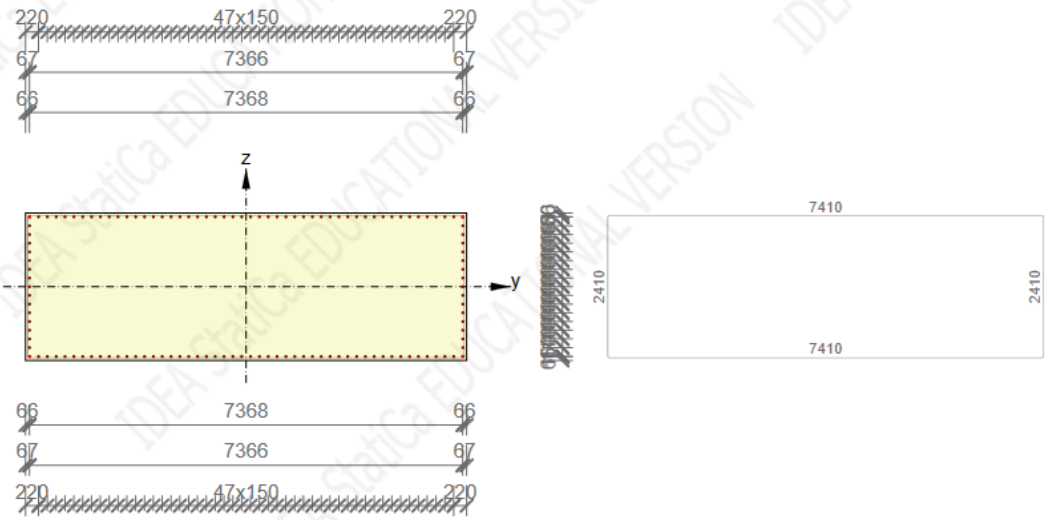

Figure 274 Pier reinforcement

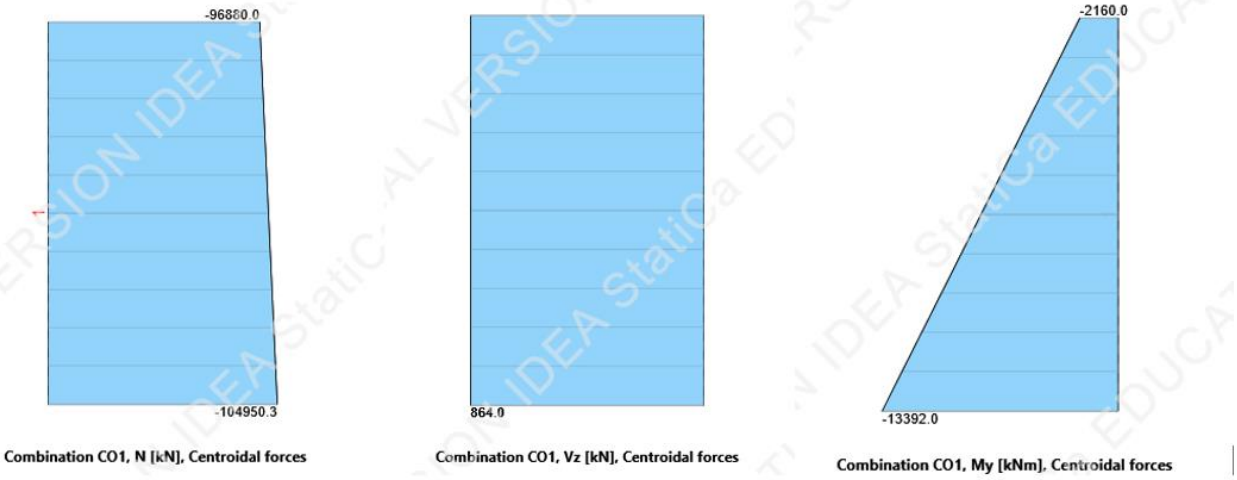

Figure 275 Design action used for pier

The following figure shows the interaction diagram for the pier.

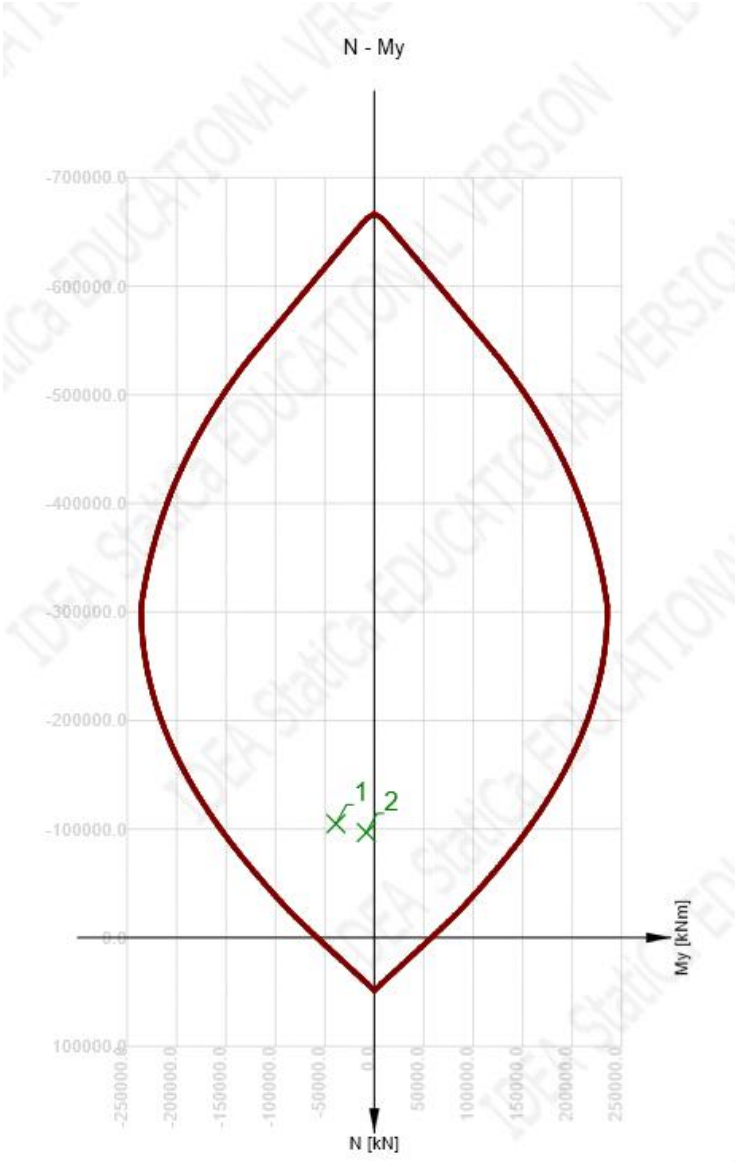

	Extreme	N [kN]	My [kNm]	Mz [kNm]
1	CO1(1)	-104950.3	-38799.0	0.0
2	CO1(1)	-96880.0	-8073.3	0.0

Figure 276 Pier interaction diagram

10.3 Bearing and expansion joint

Concrete bridges expand and contract with temperature changes, they shorten under the effects of concrete shrinkage and creep and they deflect under the effect of applied loads, prestress, and temperature gradients.

10.3.1 Design parameters

10.3.1.1 Temperature change

The value of expansion and contraction of the bridge due to the effect of thermal change has been obtained from the model from the result of the thermal load (see 3.2.2.1 Uniform temperature component)

$\Delta TN, exp$=31,5°

$\Delta TN, con$=−34°C

And by assuming T0=10°C and this temperature represents the temperature at the time of making the bridge to be structure indeterminate and in this project, it represents the time at construction the key segment).

The coefficient of expansion of concrete varies principally with the type of aggregate used, from about 12 × 10−6 per °C for gravel to about 7 × 10−6 per °C for limestone. The value of 12× 10−6 per °C has been assumed.

10.3.1.2 Shrinkage of concrete

The concrete gradually in volume with time, for the expansion joint design, the value of change of the bridge length has been obtained from the CS analysis model between the time of installation of the expansion joint(CS39) or bearing till the end life of service life of the bridge(CS41).

10.3.1.3 Creep of concrete

The creep is the delayed strain due to applied load (prestressing load) and the value of the shorting of the deck has been obtained from the model between the time of installation of the expansion joint or bearing (CS39) till the end life of service life of the bridge (CS41).

10.3.1.4 Elastic shortening under compression

This shorting has been considered just for bearing by assuming that the expansion joint has been installed after the prestressing of all tendons, the value has been obtained from CS analysis model at the time of prestressing (CS37).

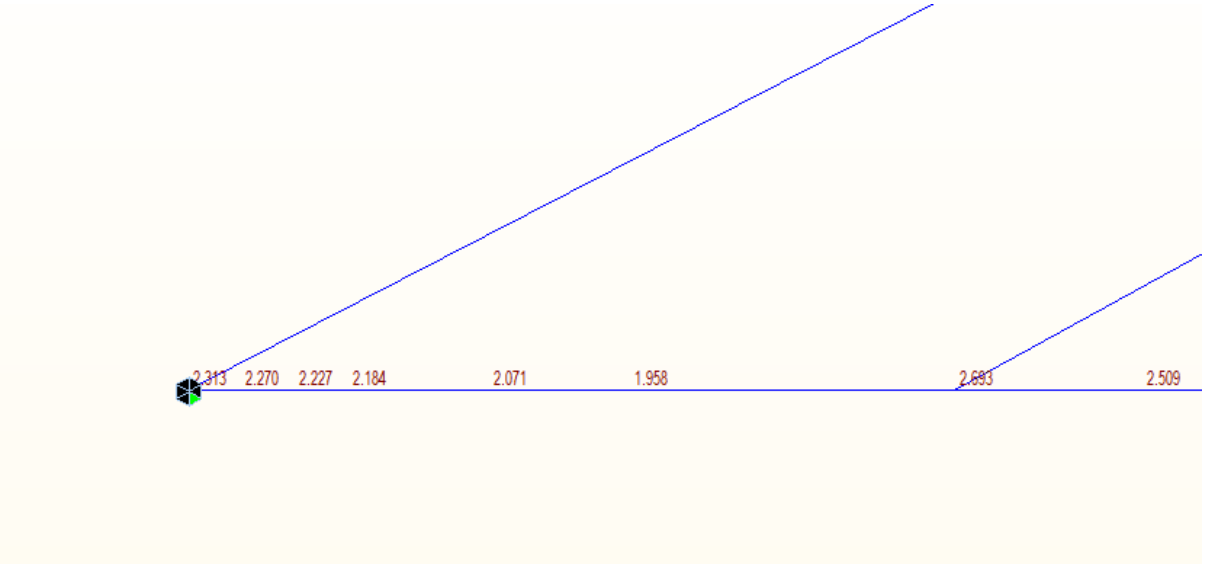

Figure 277 deformation in mm due to shrinkage at abutment A1 at CS39 (installation of expansion joint)

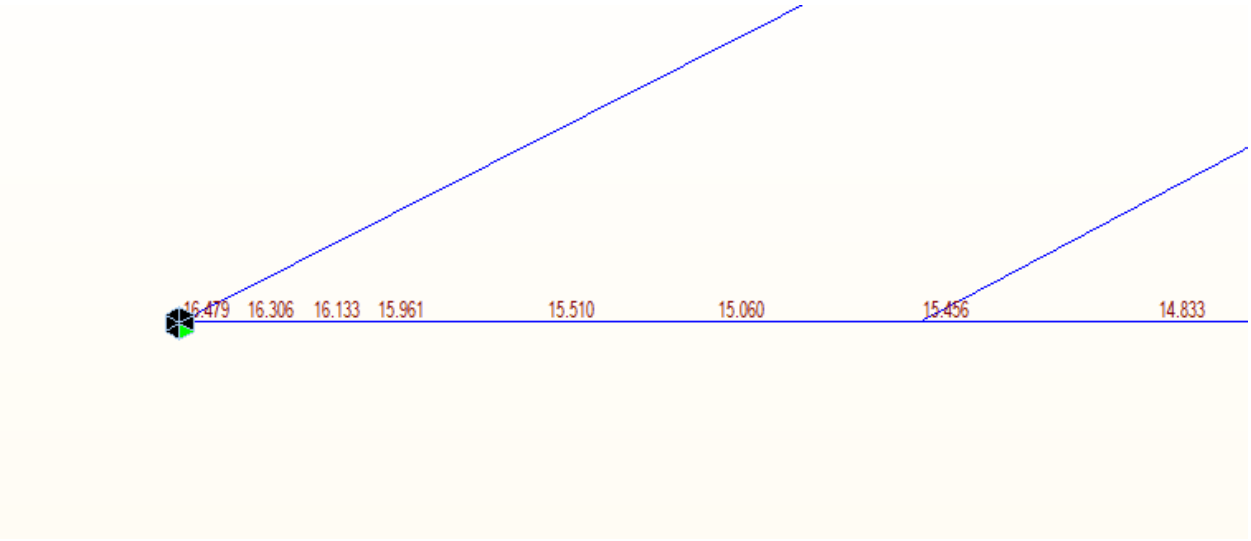

Figure 278 deformation in mm due to shrinkage at abutment A1 at CS41(end of service)

So, the deformation due to shrinkage at abutment A1 =16.479-2.313=14.166

The following table shows the deformation due to shrinkage, creep, elastic shortening and temperature.

Table 41 Movement in mm due to different action

Location	Load	Stage	DX (mm)	Stage2	DX (mm)3	Differance DX (mm)
A1	Elastic shortening	CS37	-5.95	-	-	-5.95
P1	Elastic shortening	CS37	0.00	-	-	0.00
P2	Elastic shortening	CS37	-14.09	-	-	-14.09
A2	Elastic shortening	CS37	-20.07	-	-	-20.07
A1	Creep Primary	CS41	-15.64	CS39	-5.57	-10.07
P1	Creep Primary	CS41	0.00	CS39	0.00	0.00
P2	Creep Primary	CS41	-29.89	CS39	-8.23	-21.66
A2	Creep Primary	CS41	-45.74	CS39	-13.96	-31.78
A1	Shrinkage Primary	CS41	-16.48	CS39	-2.31	-14.17
P1	Shrinkage Primary	CS41	0.00	CS39	0.00	0.00
P2	Shrinkage Primary	CS41	-31.08	CS39	-4.37	-26.71
A2	Shrinkage Primary	CS41	-47.17	CS39	-6.82	-40.35
A1	Tempre.uniform+	-	41.63	-	-	41.63
P1	Tempre.uniform+	-	0.00	-	-	0.00
P2	Tempre.uniform+	-	103.16	-	-	103.16
A2	Tempre.uniform+	-	153.08	-	-	153.08
A1	Tempre.uniform-	-	-44.93	-	-	-44.93
P1	Tempre.uniform-	-	0.00	-	-	0.00
P2	Tempre.uniform-	-	-111.35	-	-	-111.35
A2	Tempre.uniform-	-	-165.22994	-	-	-165.23

Table 42 Summation of the movements in mm at A1,A2, P1 &P2

Location	Elastic shortening	Creep Primary	Shrinkage Primary	Tempre.uniform +	Tempre.uniform-	Max movment(Expantion)	Min Movment (Contraction)
A1	-5.95	-10.07	-14.17	41.63	-44.93	41.63	-75.12
P1	0.00	0.00	0.00	0.00	0.00	0.00	0.00
P2	-14.09	-21.66	-26.71	103.16	-111.35	103.16	-173.81
A2	-20.07	-31.78	-40.35	153.08	-165.23	153.08	-257.43

Bearings provided from company Freyssinet have been used, the axial load has been obtained form the reaction of the 2-d model at the location of the pier or abutment divided by 2 + reaction from the torsional moment. Where

$$the\ torsional\ reaction = \frac{Ted}{spacing\ between\ the\ bearing} = \frac{11657.5}{6} = 1942.9\ KN$$

The following tables show the action on the bearing and the chosen type, for each location at the pier and abutment 2 bearings have been provided so the ultimate action has been divided by 2.

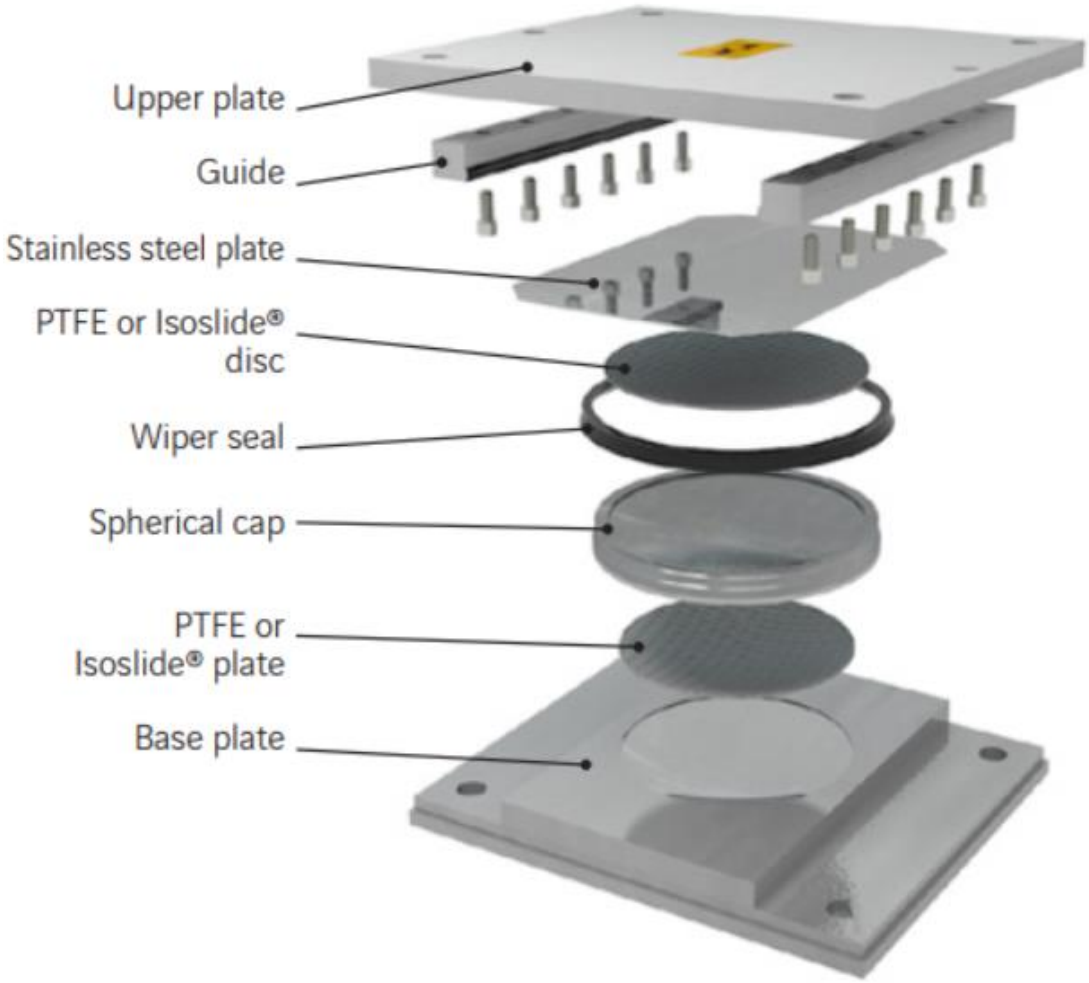

Figure 279 Tetron SB GG spherical bearings [19]

Table 43 Bearing table

Loacation	Fz,ed [KN]	Fz,ed/2 [KN]	Fz from torsion	Ned for bearing	1st bearing	2nd bearing
P1	96706.4	48353.2	1942.92	50296.12	special bearings	special bearings
P2	96885.16	48442.58	1942.92	50385.5	special bearings	special bearings
A1	7482.8	3741.4	1942.92	5684.32	GL 6,000 - 400 . 40	GG 6,000 - 1,800 . 400
A2	7511.6	3755.8	1942.92	5698.72	special bearings	special bearings

the location at P1, P2 need special bearing because the axial load is higher than the capacity of the available bearing, and the company Freyssinet provides this. Location A2 needs special bearing because the longitudinal displacement is higher than available (400mm , +-200mm). [19]

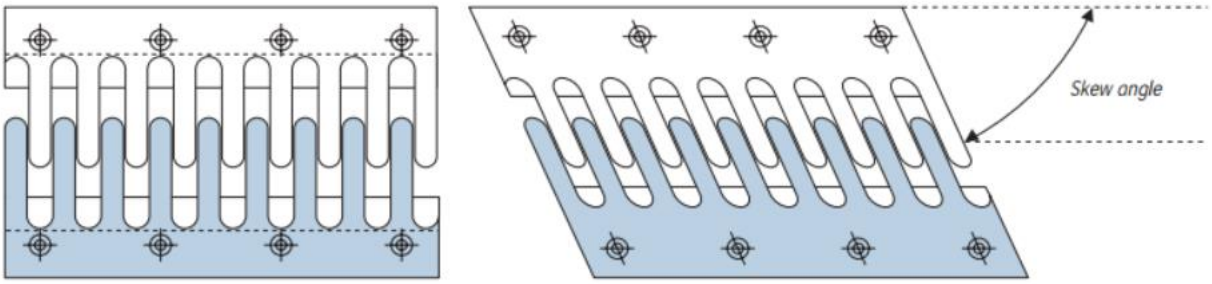

Figure 280 CIPEC WP Joint [19]

for the expansion joint, the expansion joint type WP450 provided by Freyssinet has been considered for abutment A2 which provides 450 mm movement, and WP160 for A1 which provides a 160mm movement range. [20]

.

11 Conclusion

The goal of this master thesis is to summarize the characteristic of the cable-stayed bridge and superstructure design of the cable-stayed bridge over the Vltava river, the bridge has been analyzed and designed during construction and at the final state.

The bridge consists of 3 spans (90,180,90) supported by 2 piers and 2 abutments. the deck and the pylon act as a frame.

The bridge will be loaded with pedestrian and public tram loads. The Box girder section has been chosen because of the high torsional resistance of such a section. the structure has been assessed in ULS and SLS. Cast in place concrete has been assumed in this project.

free cantilever method has been used for constructing the bridge. During construction, temporary post-tension bars have been used, and temporary fixed support at the location of the pier. After the abutment and key segment has been cast, post-tension cables have been stressed and the temporarily fixed supports at the pier have been replaced by the permanent support.

12 References

[1] H. Svensson, Cable-Stayed Bridges: 40 Years of Experience Worldwide, 2011.

[2] S. W. Chung C. Fu, Computational Analysis and Design of Bridge Structures, CRC Press, 2014.

[3] D. Huang and B. Hu, Concrete Segmental Bridges: Theory, Design, and Construction to AASHTO LRFD Specifications, CRC Press, 2020.

[4] C. H. a. D. Smith, Designers' Guide to EN 1992 Eurocode 2: Design of concrete structures. Part 2: concrete bridges, Thomas Telford Publishing; Reprint edition (January 1, 2007).

[5] M. T. H. G. a. H. G. J.-A. Calgaro, Designers' Guide to Eurocode 1: Actions on Bridges: EN 1991-2, Thomas Telford Publishing, 2010.

[6] "Limitní hodnoty podle vyhlášky č. 341/2002 Sb., o schvalování technické," [Online]. Available: www.policie.cz/soubor/prilohy-106-.

[7] I. Lucia, "NÁVRH NOSNÉ KONSTRUKCE EXTRADOSED MOSTU," 2019.

[8] N. R. Stránský J., Betonové mosty I – modul M01 – Základní principy navrhování.

[9] EN 1990: Eurocode - Basis of structural design.

[10] J.-A. C. (. M. H. (. Haig Gulvanessian (Author), Designers' Guide to Eurocode 0: Basis of Structural Design, 2nd edition, ICE Publishing; 2nd edition (, March 18, 2012).

[11] "midasoft," MIDASoft, Inc., November 12 2018. [Online]. Available: https://www.midasoft.com/bridge-library/session-7-advanced-3d-bridge-analysis-segmental-cable-stayed-1.

[12] V. Company, "Brochur named Post-Tensioning solutions," [Online].

[13] V. I. Ltd., "European technical assessment – VSL Post-Tensioning System," 20/06/2019.

[14] EN 1992-2: Eurocode 2: Design of concrete structures - Part 2.

[15] EN 1992-1-1: Eurocode 2: Design of concrete structures.

[16] J.-P. L. a. M. A. Hirt, Steel Bridges: Conceptual and Structural Design of Steel and Steel-Concrete Composite Bridges, EPFL Press; 1st edition (June 5, 2013).

[17] "European Technical Approval ETA-13/097VSLab® S system," June 2013.

[18] M. Virlogeux, "The Normandie Bridge, France:A New Record for Cable-Stayed Bridges," *Structural Engineeiing International,* vol. 4, no. 4, pp. 208-213, 1994-11.

[19] B. F. M. Bearings. [Online]. Available: http://www.freyssinet.com/freyssinet/fpc-italia_en.nsf/sb/products-and-solutions.bearings.

[20] F. E. Joints. [Online]. Available: http://www.freyssinet.com/freyssinet.

[21] EN 1991-1-1: Eurocode 1: Actions on structures.

13 List of figures

14 List of tables

15 List of used software:

- AutoCAD 2021 Student version
- Midas Civil Trial Version
- Idea Statica Student Version
- Microsoft office Student version
- PDF Reader

16 List of appendices:

- Longitudinal, plan, and cross-section
- Midspan section reinforcement
- Side-span section reinforcement
- Pier-section reinforcement
- Permeant post-tension
- Temporary post-tension